

https://dspace.org/

Chemical engineering modelling of a vegetated submerged reedbed for winery effluent treatment

Sheridan, Craig Michael

2014-02-25
http://hdl.handle.net10539/13942

Downloaded from a DSpace repository. https://dspace.org/

Chemical engineering modelling of a vegetated submerged reedbed for winery effluent treatment

Craig Michael Sheridan

A thesis submitted to the Faculty of Engineering and the Built Environment, University of the Witwatersrand, in fulfilment of the requirements for the degree of Doctor of Philosophy.

Johannesburg 2012

Declaration

I declare that this thesis is my own unaided work. It is being submitted for the degree of Doctor of Philosophy to the University of the Witwatersrand, Johannesburg. It has not been submitted before for any degree or examination to any other University.

Craig Michael Sheridan

10th day of June 2013

Summary

Environmental concerns for wineries in South Africa cover not only the conversion of effluent into more benign forms, but the reclaiming of water, a resource that is scarce and precious in a drought-prone country. However, not all waste treatment options are available to small wineries, because many are too sophisticated and expensive to be commercially viable. Accordingly, this study investigated the use of constructed wetlands in the form of Vegetated Submerged Reedbeds (VSR) as a practicable alternative for small-scale wine producers. Winery effluent is known to have a high chemical oxygen demand (COD) and low pH. In this study, effluent was extensively analysed from two cellars, including the temporal changes over the duration of a harvest and the duration of a year. It was found that for raw winery effluent, ethanol contributes approximately 85% to 90% of the COD, with acetic acid being the next significant contributor. The pH showed some dependence on the concentration of acetic acid. The concentration of sodium in the effluent is strongly dependent on the cleaning regime in place at the cellar, and the concentration of potassium has been shown to be linked to the spillage of juice, wine or lees.

It was also found that the hydraulic processes occurring within the VSR display significantly non-ideal behaviour. If the feed to the VSR was located on the surface the dead volume accounted for approximately 25% of the non-ideal behaviour of the system and bypass accounted for a further 6% of non-ideal behaviour. In the system studied, there was a preferential flow pattern within with the greatest flow occurring closest the surface and in the centre, and the least at the sidewalls. It was proposed that the flow profile can be conceptualised as being hull-shaped. We believe this hypothesis is correct and as far as we are aware this flow pattern has not been described previously. It was found that this profile was the same for irregularly shaped gravel and for spherically shaped gelatinous beads and it is therefore believed it is not dependent on the geometry of the VSR or the packing medium.

This study also investigated the use of three different methods for determining the rate constants for the degradation of winery effluent within a sub-surface flow constructed wetland (CW). These methods comprised using a dispersed plug flow (the Peclet) equation; a tanks-in-series (TIS) equation; and analysing the residence time distribution (RTD) directly. The last of these was called the Convolution Integral (CI) method. Within the CW studied, the principal constituent of the chemical oxygen demand (COD), ethanol, was always fully degraded by the time the flow reached the outlet. It was therefore possible to calculate the rate constant of degradation from the initial

eight metres of the CW. Self similarity of the RTDs was also demonstrated, which meant that in general the system's hydraulics were similar throughout the CW. This meant we could extrapolate the data so as to develop a more complete understanding of the hydraulic properties of the CW and examine how they affected the kinetics of degradation. It was found that whilst both the Peclet and the TIS equation were able to predict concentration within the CW accurately, this required multivariate optimisation. This rendered a result that was more of a modelling exercise than a useful design tool. The CI method, however, could be applied to predict system parameters effectively. This study used the CI to measure the rate constants of removal for both ethanol and potassium, which were found to be the key species that responded to the degradation/treatment of the effluent. The rate constant found for the biodegradation of COD was found to have significantly more uncertainty associated with it than the measurement of the rate of degradation individual components and it was therefore posited that it is better to describe the processes of degradation by tracking individual components rather than lumped parameters. In each chapter, a short abstract is provided in which results are given.

Acknowledgements

I wish to thank the following people for their very generous support and assistance:

- Professors David Glasser and Diane Hildebrandt for their excellent supervision;
- Pippa Lange for amazing help on developing a logical argument;
- Michelle Aucock and CLTD for helping me to develop a sense of perspective;
- The staff at the School of Chemical and Metallurgical Engineering;
- Professors Johann Rohwer and Jochen Petersen for their assistance;
- My family for their unfailing support; and most importantly
- Gill for always being there.

Table of Contents

1. Introduction ____ *18*

1.1. Thesis Structure ____ **20**

2. Background ____ *22*

2.1. A history on the use of CWs for effluent treatment ____ **22**

2.2. A description of the different types of CWs ____ **22**

2.2.1. Free Water Surface Wetlands ____ 22

2.2.2. Sub Surface Flow CWs (Vegetated Submerged Reedbeds) ____ 22

2.3. Uses of Constructed Wetlands ____ **23**

2.4. Some disadvantages and advantages of the use of CWs ____ **24**

2.5. How VSR CWs work ____ **25**

2.5.1. The water balance ____ 26

2.5.2. Reasons for non-ideal flow: dispersion, short circuiting, stratification and dead volumes ____ 28

2.5.3. Mechanisms of COD and BOD Removal ____ 30

2.5.4. Suspended Solids ____ 31

2.5.5. Nitrogen Removal ____ 31

2.5.6. Phosphorous Removal ____ 34

2.5.7. Other processes which have not been investigated in this work ____ 34

2.6. Modelling of vegetated submerged reedbeds (VSR) or subsurface flow constructed wetland (SSFCW) processes ____ **34**

2.6.1. Defining the reaction rate ____ 35

2.6.2. Measuring the reaction rate constant ____ 36

2.6.3. Kinetic equations for describing subsurface CWs ____ 37

2.6.4. Hydraulic equations for describing subsurface CWs ____ 39

2.7. Wetland plants for vegetated submerged reedbeds. ____ **47**

2.8. Research Objectives ____ **50**

3. On modifying the Arrhenius equation to compensate for temperature changes for reactions within biological systems ____ *52*

3.1. Abstract ____ **52**

3.2. Introduction ____ **52**

3.3. Methods and results of the investigation of the non-applicable temperature range of the MAF 54

3.4. Discussion of the modified Arrhenius equation 56

3.5. Conclusion 57

4. An Annual and Seasonal Characterisation of Winery Effluent in South Africa 58

4.1. Abstract 58

4.2. Introduction 59

4.3. Materials and Methods 60

4.3.1. Experimental techniques 60

4.4. Results and Discussion 61

4.4.1. Effluent composition 61

4.4.2. Annual monitoring of the effluent at Cellar 1 63

4.4.3. Seasonal monitoring of the effluent at Cellar 2 66

4.5. Discussion of the variation of winery effluent 69

4.6. Conclusions 71

5. Turning wine (waste) into water: Towards technological advances in the use of constructed wetlands for winery effluent treatment 73

5.1. Abstract 73

5.2. Introduction 74

5.2.1. Modelling Constructed Wetland Systems 77

5.3. Finding the internal age distribution and calculating some hydraulic parameters 82

5.4. Experimental Programme 84

5.5. Materials and methods 84

5.5.1. Description of the experimental rigs/apparatus 84

5.5.2. Conducting the impulse-response experiments 87

5.5.3. Sampling Protocol 88

5.5.4. Analytical Methods 89

5.6. Results 89

5.6.1. The calculation of hydraulic properties of the VSR 89

5.6.2. Calculation of the hydraulic properties of the laboratory-scale rig 97

5.7. Discussion of the results 100

5.8. Conclusions 101

6. Additional hydraulic experiments assessing the location of the dead volume ***103***

6.1. Introduction 103

6.2. Experimental Objective 103

6.3. Experimental method 104

6.3.1. Tracer experiments on the laboratory-scale rig 104

6.3.2. Sampling Protocol 105

6.4. Results 105

6.4.1. Residence Time Distributions 105

6.4.2. Photographic record of the experiments 107

6.5. Discussion 113

6.5.1. Changing the elevation of the outlet port 113

6.5.2. Changing the direction of the flow path 114

6.5.3. Increasing the number of outlet ports 114

6.5.4. Inserting a wedge to remove the dead zone 114

6.6. Conclusion 115

7. Estimating rate constants in constructed wetlands treating winery effluent: A comparison of three different methods. ***116***

7.1. Abstract 116

7.2. Introduction 117

7.3. Background: What is a reaction rate and what is a rate constant? 118

7.3.1. Defining the reaction rate 118

7.3.2. Measuring the reaction rate constant 119

7.3.3. Rate constants 120

7.3.4. Measuring the rate constants of lumped parameters 121

7.3.5. Deciding on a reactor equation in order to calculate the rate constants 122

7.3.6. Hypotheses 127

7.4. Materials and methods 127

7.4.1. Description of the winery supplying effluent to the CW 127

7.4.2. Description of the physical properties of the VSR at the ARC, Stellenbosch 128

7.4.3. Chemical Analyses 129

7.4.4. A study on the hydraulic processes occurring within the CW. 130
7.4.5. Experimental Method to calculate the rate constants of the processes of degradation 130
7.4.6. Average behaviour of the CW 132
7.4.7. Determining the rate constants using different techniques. 136
7.4.8. Verifying the rate constants found using the RTD directly (convolution integral), the TIS equation and the Peclet equation 140

7.5. Discussion of the measurement of rate constants 149

7.6. Concluding remarks and ramification for design 150

8. Discussion and Concluding remarks 152

8.1. Discussion 152

8.2. Concluding Remarks 156

9. References 158

10. Appendices 166

Table of Figures

Figure 2.1. Water balance for a CW 26

Figure 2.2. An example of increasing dispersion with increasing time/length in a reactor taken from Levenspiel (Levenspiel 1972) 29

Figure 2.3. An example taken from Levenspiel indicating that tracer may follow two parallel (independent) paths within a reactor. 29

Figure 2.4. An example of a concentration vs. time plot [C(t) curve] and its age distribution [E(t) curve (inset)] 41

Figure 2.5. Residence time distributions for N CSTR reactors in series taken from Levenspiel 44

Figure 2.6. A graphical depiction of the TIS model for N=4. 44

Figure 2.7. A plug flow reactor with dispersive forces at work. 45

Figure 2.8. A graphical depiction of the movement of tracer through a reactor taken from Levenspiel 46

Figure 3.1. A graph of the MAF to find the parameters for the Arrhenius Equation with regressed line shown 55

Figure 3.2. A comparison of the rate constants as calculated by the MAF and the Arrhenius equation showing differences at higher temperatures 56

Figure 4.1. Organic components (ethanol and acetic acid) overlaid on pH and COD at Cellar 1 63

Figure 4.2. Cationic components in winery effluent measured over a year at Cellar 1 66

Figure 4.3. Organic components (ethanol and acetic acid) overlaid on pH and COD at Cellar 2 67

Figure 4.4. Cationic components in winery effluent measured over a harvest season at Cellar 2 69

Figure 5.1. Variation of the outlet concentration for a given inlet concentration of 100mg/L COD for the correlations presented in Table 1. 80

Figure 5.2. Schematic diagram of the VSR showing a side and a top view 86

Figure 5.3. Laboratory apparatus used to test bed efficiency 87

Figure 5.4. Normalised age distributions showing the progression and dispersion of the pulse as it moves through the VSR (with lateral variation averaged). 90

Figure 5.5. Residence time distributions for sample ports at 32m and 40m with multimodal distributions 91

Figure 5.6. An analysis of the modes of distribution for the VSR 93

Figure 5.7. Hydraulic effectivity factor variation with length for each port within the VSR 94

Figure 5.8. Hypothetical flow regime showing the boat-shaped velocity profile of tracer dispersion within the VSR 96

Figure 5.9. RTD for the impulse-response laboratory experiment. 97

Figure 5.10. Photographs showing the flow patterns of tracer through the laboratory apparatus. 99

Figure 5.11. RTD for the impulse-response laboratory experiment with a well distributed feed and outlet. 99

Figure 5.12. Photographs showing the flow patterns of tracer through the laboratory apparatus. 100

Figure 6.1. The residence time distributions of the six experiments. 1. Connecting the inlet to the central inlet port and the outlet to the central outlet port; 2. Connecting the inlet to the lowest central port and the outlet to the highest central port; 3. Connecting the inlet and outlet to the central highest ports; 4. Connecting the inlet to the central lowest port and the outlet to all three highest outlet ports; 5. Connecting the inlet to the right lowest port and the outlet to the right highest port; and 6. Inserting a wedge in the location of the dead zone identified. 106

Figure 6.2. Experiment 1 - Connecting the inlet to the central inlet port and the outlet to the central outlet port 108

Figure 6.3. Experiment 2 - Connecting the inlet to the lowest central port and the outlet to the highest central port_ 109
Figure 6.4. Experiment 3 - Connecting the inlet and outlet to the central highest ports _____ 110
Figure 6.5. Experiment 4 - Connecting the inlet to the central lowest port and the outlet to all three highest outlet ports_____ 111
Figure 6.6. Experiment 5 - Connecting the inlet to the right lowest port and the outlet to the left highest port _____ 112
Figure 6.7. Experiment 6 – Inserting a wedge-shaped filler in the location of the dead zone identified _____ 113
Figure 7.1. Graphs showing the change in the shape in the RTD with increasing tanks taken from Levenspiel ($E\theta$ is described in this chapter) _____ 124
Figure 7.2. A graphical depiction of the TIS model for N=4. _____ 124
Figure 7.3. A plug flow reactor with dispersive forces at work._____ 124
Figure 7.4. A graphical depiction of the movement of tracer through a reactor (taken from Levenspiel, 1972)_____ 126
Figure 7.5. Schematic diagram of the VSR showing a side and a top view _____ 129
Figure 7.6. Daily flow characteristics (including the average flow, cumulative flow and a moving average) within the VSB_____ 131
Figure 7.7. Average concentration of propanol, propanoic acid and butyric acid for the entire harvest with increasing duration of flow along the length of the CW _____ 133
Figure 7.8. Average major organic components and COD concentration for the entire harvest at various locations along the length of the CW _____ 134
Figure 7.9. Average changes in concentration of sodium and potassium for the entire harvest as it travels along the CW _____ 135
Figure 7.10. Average concentration vs. t for the CW over the duration of the harvest season. _____ 140
Figure 7.11. Normalised age distributions for the middle sections of the CW _____ 140
Figure 7.12. Normalised age distributions for the initial and final sections of the CW _____ 141
Figure 7.13. Base case for comparison of the three different rate constant calculations (Pe equation rate constant k=7.85/hr, TIS equation rate constant = 0.088/hr and convolution integral k=0.804/hr) _____ 142
Figure 7.14. Optimised case for comparison of the three different rate constant calculations with Pe and N solved for minimum sum of squared errors (Pe equation rate constant k=7.85/hr, TIS equation rate constant = 0.088/hr and convolution integral k=0.804/hr). _____ 143
Figure 7.15. Second optimised case for comparison of the three different rate constant calculations with Pe and N solved for minimum sum of squared errors using the rate constant found via the convolution integral method. _____ 144
Figure 7.16. Base case for comparison of the three different rate constant calculations (Pe equation rate constant k=0.22/hr, TIS equation rate constant = 0.0049/hr and convolution integral k=0.037/hr) _____ 146
Figure 7.17. Optimised case for comparison of the three different rate constant calculations with Pe and N solved for minimum sum of squared errors (Pe equation rate constant k=0.22/hr, TIS equation rate constant = 0.0049/hr and convolution integral k=0.037/hr). _____ 147
Figure 7.18. Second optimised case for comparison of the three different rate constant calculations with Pe and N solved for minimum sum of squared errors, using the rate constant found with the convolution integral method (k=0.0374/hr). _____ 148

List of Tables

Table 2.1. Equations used for estimating rates of evapo-transpiration (ET) _____ *27*

Table 2.2. The Some different forms of the reaction rate _____ *36*

Table 2.3. A summary of aerial and volumetric BOD removal rate constants as given by the IWA _____ *38*

Table 2.4. Some emergent vegetation plant species which may be used in CWs _____ *48*

Table 3.1. Derivation of the MAF _____ *54*

*Table 3.2. Derivation of an Arrhenius Equation for use in biological systems*_____ *57*

Table 4.1. The composition of winery effluent at Cellar 2 as determined by an initial investigation at the beginning of the harvest season _____ *62*

Table 5.1. Regression equations for the removal of COD or BOD in CWs (adapted from (Kadlec, Knight et al. 2000)). _ *79*

Table 5.2. Different CW models presented as either being kinetic or hydraulic in method _____ *81*

Table 5.3. Engineering design specifications of the VSR _____ *85*

Table 5.4. Hydraulic parameters calculated for the VSB. _____ *92*

*Table 5.5. Hydraulic parameters for the laboratory apparatus*_____ *97*

*Table 5.6. Hydraulic parameters for the laboratory apparatus*_____ *99*

*Table 6.1. Hydraulic properties of the laboratory scale rig*_____ *107*

Table 6.2. Comparison Showing the effect of dead-zone reduction by inserting a wedge _____ *114*

*Table 7.1. Some different forms of the reaction rate*_____ *119*

Table 7.2. A summary of aerial and volumetric BOD removal rate constants as given by the IWA _____ *121*

Table 7.3. Engineering design specifications of the VSR _____ *128*

Table 7.4. A summary of the hydraulic parameters found for the CW _____ *130*

Table 7.5. The calculated rate constants (k/hr) using the TIS equation, the Peclet Equation and the Convolution Integral. _____ *137*

Nomenclature

r_i is the rate of reaction of component i

C^* is the background concentration

C_{Out} is the exit concentration

C_{In} is the inlet concentration

$C_{i,N}$ is the concentration of component i after N tanks

$C_{i,l}$ is the concentration of Component i at length l,

$C_{i,0}$ is the concentration of Component i initially

C_i is the concentration of the tracer at time i

L_{In} is the inlet organic load

L_{Out} is the exit organic load

$L_{\mathrm{Re}moved}$ is the load removed

X_i is the conversion of component i

$C(t)$ is the concentration time curve

t_i is the time i

$\bar{t}$ is the mean residence time for all components

θ is a dimensionless time, $t/\bar{t}$

E_i is the age at time i

Q is the cumulative concentration function

D is the dispersivity

$\tau_{effective}$ is the effective mean residence time

τ is the ideal mean residence time

$\bar{t}_m$ is the mean residence time

λ is the hydraulic efficiency factor

σ^2 is the second moment of the RTD, the variance

σ_θ^2 is the dimensionless or normalized variance

N is the number of tanks in a tanks-in-series model

P is the apparent number of tanks in the apparent tanks-in-series model

k_i is the rate constant for species i

$k_i(T)$ is the rate constant for species i as a function of temperature

$V_{\max}$ is the maximum rate of reaction

T is the temperature

R is the gas constant

A_E is the Arrhenius constant

A is the pre-exponential factor

θ is a temperature correction factor

b is a time-based retardation co-efficient

E_A is the activation energy

R is the Universal Gas Constant

l is the length of the bed

d is the depth of the bed

ϕ is the mean channel diameter

w is the width of the bed

V is the volume of the CW

ε is the void fraction of the gravel in the bed

ρ is the density of the liquid

μ is the viscosity of the liquid

K_{hyd} is the hydraulic conductivity of a porous medium

S is the slope of the saturated hydraulic zone

F is the volumetric flow rate

F_{Day} is the volumetric flow rate of the effluent during the experiment, on that day

F_{RTD} is the volumetric flow rate of the effluent during the tracer study

V_{Eff} is the ratio derived from the ideal residence time to the real residence time

Pe is the Peclet Number

Da is the Damkohler Number

Acronyms

PFR – Plug Flow Reactor (equation)

CSTR – Continuous Stirred Tank Reactor (equation)

TIS – Tanks in Series (equation)

STIS – Spatial Tanks in Series (equation)

PSTIS – Parallel Spatial Tanks in Series (model)

PTIS – Apparent Tanks in Series (model)

TDR – Time Dependent Retardation (model)

MAF – Modified Arrhenius Function

RTD – Residence Time Distribution

COD – Chemical Oxygen Demand

BOD – Biological Oxygen Demand

TDS – Total Dissolved Solids

TKN – Total Kjeldahl Nitrogen

TP – Total Phosphorous

SAR – Sodium Adsorption Ratio

EC – Electrical Conductivity

SS – Suspended Solids

SBR – Sequencing Batch Reactor

FWSCW – Free Water Surface Constructed Wetland

SSFCW – Sub-surface Flow Constructed Wetland

VSR – Vegetated Submerged Reedbed

ZDM – Zones of Diminished Mixing

EP – Pan Evaporation

ET – Evapo-transpiration

US EPA – United States Environmental protection Agency

IWA – International Water Association

WERF – Water Environment Research Foundation

1. Introduction

Winemaking in South Africa is primarily restricted to the winter rainfall and semi-arid areas of the Western and Northern Cape provinces. Geographically, these areas are characterised by low population densities (excepting the metropolitan area of Cape Town) and limited water resources. Farms often rely on farm-dam or spring water, the supply of which is highly variable. Those farms located near the Cape Town metropole can access municipal water from the Theewaterskloof Dam, which is situated within 100km of Cape Town, but this water is expensive, and farmers are competing with human and industrial consumption needs.

Winemaking is very similar to conventional chemical engineering. The process begins with a raw material (in this instance grapes). Some kind of beneficiation or size reduction process is conducted to speed up the rates of chemical reaction, which in winemaking is the conversion of glucose and fructose to ethanol. This yields a product—wine. As with all other industries, winemaking creates waste streams and as with all other chemical industries, this effluent has to be disposed of.

The water that enters the process that converts grapes into wine will leave as wastewater (since in South Africa it is illegal to add water to wine). The wastewater contains spillages from processing and handling, the residues of washing the tanks, intentionally drained wet waste products such as lees, and potentially other contaminants, such as agricultural manure. All wineries are expected to conform with legislation relating to the treatment or disposal of waste streams (Government Gazette 2009, Government Gazette 2001, Government Gazette 1998a, Government Gazette 1998b). Thus, if a winery discharges effluent into a sewer, it must ensure that it is under the maximum allowable limit on the COD (chemical oxygen demand) and the quantity of sodium it contains, as these are the criteria most relevant to winery effluent (Sheridan, Glasser et al. 2011a). The specific parameters applied will depend on the requirements of the municipality that manages the sewer. On the other hand, if the wastewater is to be released to the environment, the permissible strength of the chemicals in the waste will be governed by national rather than local legislation, although it will also depend on whether the environment in question is pristine or not.

Many wineries (46%) are small, and press less than 100 tons of grapes per annum (SAWIS 2012). Thus, using the method developed by Sheridan (Sheridan 2003) it can be assumed that just under half of all wineries in South Africa consume fewer than 1000 litres of water per day and produce a

corresponding quantity of effluent. These small wineries can be licensed to irrigate their wastewater to a pasture, provided both that the COD does not exceed 5000mg/L and that they irrigate less than 50m^3 per day (Government Gazette 1998b). The Department of Water Affairs discourages this practice, even by those who comply with the limit, because it is considered wasteful of water.

Because many wineries exceed the limits described above in terms of COD (Sheridan 2003), they are required to treat their wastewater by some form of processing before releasing it. Winery wastewater treatment techniques are diverse, but all have the same goal, which is to reduce the COD. Treatment technologies include using sequencing batch reactors (SBRs), aerobic digestion, anaerobic digestion, rotating biological contactors, settling ponds and constructed wetlands (CWs)(Sheridan 2003, Malandra, Wolfaardt et al. 2003). With the exception of the last, all these systems are capable of almost full effluent treatment. However, the technologies are costly, and require staff trained to operate and control them. The smaller wineries in particular cannot afford to employ such specialised kinds of personnel, and therefore cannot use these sophisticated systems reliably.

This is the reason why, in the research described here, we chose to investigate the last and most under-researched of the waste treatment options described above, in this case the use of vegetated submerged reedbed (VSR) type CWs. There are a number of reasons, apart from cost-saving and the relative simplicity of the technology involved, for believing that a CW offers the best option for small-scale wineries. Some of these are technical, for example:

- it is a low-maintenance treatment system;
- the treated water can be re-used; and
- preliminary tests indicate that CW plants can thrive in the effluent created by wineries.

However, a living treatment system is not only effective, but offers a number of benefits in a wider, environmental and social context, which include but are not restricted to:

- the aesthetic qualities of a constructed wetland;
- its production of biomass like cut flowers and thatching materials; and
- the potential use of this biomass to provide a means of livelihood to low-income farming communities (a significant factor in a developing country).

In South Africa, the use of CWs for winery effluent treatment is a very recent development. At present there are only a few such systems in existence. The design briefs for these systems are mostly heuristic, that is, they remain at the mathematical rules-of-thumb stage. This research was conducted on the basis of just such a CW, which had been constructed by the agricultural research council (ARC) at their Nietvoorbij Campus in Stellenbosch. Our aim was to conduct experiments to determine the properties of treatment process (listed below), and to use these to establish more rigorous design principles.

The initial research investigated the aspects of winery effluent treatment that in the context of this study were considered most significant.

1. The composition of winery effluent and its temporal variations: what does it consist of, how does it change over the duration of a harvest period, and how does it change over the course of the year? Answering these questions required analysis of the effluent over a full year.
2. The behaviour of effluent flowing through the CW: is there any bypass of flow or 'dead' volume within the CW that makes it less efficient? These data were obtained by running an impulse-response tracer experiment, by means of which we measured the mean residence time and the dispersion within the system. This method was also used to identify whether the CW behaved like a plug flow, stirred tank reactor or series of stirred tank reactors, or any combination thereof.
3. The rates at which the components of winery effluent are degraded. Answering this question required the use of the data obtained from both 1. and 2. above.

If points one to three were answered, it was believed that we could develop a model that would predict the behaviour of the system accurately. On the other hand, the possibility was recognised that the experimental results might indicate that the treatment process is too complex to make modelling possible. Even if the latter proved to be the case, it was reasoned that our findings would yield data that had not been considered before, such as the rates of decomposition of the winery effluent components. Both would be useful to designers of CWs.

1.1. Thesis Structure

This thesis has been dived into 8 Chapters. There is an introduction and an analysis of the literature in the first two Chapters. Following this there are four chapters, each of which has been written in the form of a paper, the intent being to publish as much of the work as possible. For

this reason, there is some degree of overlap between Chapter 2 (a discussion of the literature) and each Chapters' literature review and we request the readers' indulgence for this. If a chapter has been submitted to a journal, or has been published, it is indicated as such.

Chapter 3 presents a discussion on the use of the Modified Arrhenius Equation which is generally used to estimate rate constants at different temperatures in reacting biological systems. This work is presented up front in the thesis as it does not form the core of what was undertaken.

In Chapter 4 a paper detailing the composition of winery effluent and its temporal changes is presented.

In Chapter 5, a paper in which we investigated the hydraulic process occurring within a CW with a view to determining the correct hydraulic operating regime within the CW is presented.

In Chapter 6 the work in Chapter 5 was expanded and the results of additional experiments conducted with a view to completely characterising the hydraulic flow within the CW are given.

Chapter 7 is the central chapter of the thesis. A method is presented whereby the data and the findings from Chapters 4, 5 and 6 are used. The reactor equation is utilised to determine the rate constants of degradation in the CW treating the winery effluent. A comparison of three different methods is made and a discussion on the use thereof.

The final chapter is a discussion of the findings and conclusion to the work.

2. Background

2.1. A history on the use of CWs for effluent treatment

The use of wetlands specifically for the remediation of pollution can be traced back to the early 20th century. The earliest documented evidence of an engineered wetland system was patented in 1901 by Cleophus Monjeau (Wallace, Knight 2006). The first experiments, however, on the use of wetland plants were carried out in the early 1950's by Dr. Käthe Seidel in Germany (Vymazal 2006). Subsequent to this, the use of CWs for wastewater treatment has spread around the world. Subsurface Flow (SSF) CWs are more often used in Europe, whilst Free Water Surface (FWS) CWs are more often used in the USA and Australia (Vymazal 2006). To date, CWs have been used for effluent purification on all continents with the possible exception of Antarctica.

2.2. A description of the different types of CWs

CWs may be designed in a variety of different configurations. Flow is characterised as being either on the surface or below it. Surface-flow wetlands have primarily horizontal flow characteristics, whilst sub-surface flow wetlands (often referred to as vegetated submerged reedbeds [VSRs] if planted with reeds) may have either horizontal or vertical flow characteristics or a combination thereof. Subsurface flow constructed wetlands in particular may be hybridized into a combination of different configurations. These different systems have both advantages and disadvantages, and the choice of one over the other is often guided by the personal preferences of the designer as well as some objective design criteria.

2.2.1. Free Water Surface Wetlands

In these systems, water flows over the soil surface, from an inlet to an outlet point, and, in some cases, may vanish altogether either due to infiltration or evaporation. These systems have some similarity to facultative lagoons; however, they are often planted with emergent macrophytes including reeds, sedges, and floating plants such as water hyacinth. This type of wetland is most similar to a natural wetland and generally shows a healthy population of macro-organisms and micro-organisms. This type of wetland is most often used for polishing of the effluent from secondary treatment processes such as facultative ponds and lagoons (Wallace, Knight 2006).

2.2.2. Sub Surface Flow CWs (Vegetated Submerged Reedbeds)

These CWs are normally classified in two different categories depending on whether they have horizontal or vertical flow [(Kadlec, Knight et al. 2000) & (Wallace, Knight 2006)]. For horizontal subsurface flow, the CW is generally designed as a gravel bed, and the effluent is fed in on one side and removed on the other. The bed is normally lined with an impermeable membrane, filled with pea-gravel or another suitable matrix (Oliveira, Malva et al. 2006) planted with emergent macrophytes, and as the effluent trickles through this matrix, it is purified. These are most commonly used for small-scale applications (Wallace, Knight 2006).

For vertical sub surface flow CWs, the effluent is distributed uniformly over the surface and allowed to percolate down to a collection zone, where the purified effluent is drained. This design has the advantage that both nitrification and denitrification can occur during the different phases of operation, if nitrogen reduction is a requirement of the designer (Kadlec, Knight et al. 2000). If the system is operated with a cycle of loading, flooding and draining (these are called tidal CWs) aerobic and anaerobic conditions can be created and both nitrification and denitrification can be induced at different stages of the cycle. This can potentially remove much of the total nitrogen present (Austin, Wolf et al. 2006).

2.3. Uses of Constructed Wetlands

CWs are still primarily used to treat domestic or municipal wastewaters (Wallace, Knight 2006, Kadlec, Knight et al. 2000) as well as for combined sewer overflows and urban storm waters (Kadlec, Knight et al. 2000). There are a number of applications of their use for other types of effluent streams. They have been used to effectively treat non-point-source agricultural pollution (Kadlec, Knight et al. 2000), animal wastewaters (Kadlec, Knight et al. 2000), crop run-off (Kadlec, Knight et al. 2000), dairy wastewater (Cronk 1996, Dunne, Culleton et al. 2005, Marmiroli, Marmiroli et al. 2003, Tanner, Sukias et al. 1998, Wallace 2001a, Wallace 2001b), landfill leachate (Wallace, Knight 2006), petroleum wastewaters (Huddleston, Gillespie et al. 2000, Ji, Sun et al. 2007, Moore, Ross et al. 2000, Omari, Revitt et al. 2003, Pardue, Kassenga et al. 1999, Schnoor, Light et al. 1995, Wallace, Kadlec 2004), acid mine drainage (Wallace, Knight 2006, Kadlec, Knight et al. 2000, Batty, Younger 2004, Sheridan, Koller et al. 2012), heavy metal removal (Wallace, Knight 2006, Kadlec, Knight et al. 2000) and winery effluent (Wallace, Knight 2006, Masi, Conti et al. , Shepherd, Tchobanoglous et al. 2001) amongst others. Surface flow CWs are often used for secondary or tertiary treatment of municipal effluent, especially in the USA (Kadlec, Knight et al. 2000).

2.4. Some disadvantages and advantages of the use of CWs

Some of the disadvantages of CW use include a lengthy start up period and the inability to remove nitrogen efficiently without complicated modes of operation. CWs sometimes fail because the perception of 'low maintenance requirements' has the potential to result in no maintenance being done at all. They need occasional maintenance and this need should be stressed to the purchaser of such a system. Additionally, they can build up sludge and mosquitoes can colonise them (Borin, Tocchetto 2006). This is especially problematic in tropical areas where malaria, yellow fever and other mosquito-borne diseases occur.

CWs are also inherently unsuited for use in areas where land is at a premium, simply because they are often greater than one hectare. Some other disadvantages include:

- sensitivity of many plants to high COD levels;
- an incomplete understanding of the contribution of wetland micro-organisms and plants to the process of effluent biodegradation; and
- an incomplete understanding of the hydraulic processes occurring within constructed and natural wetlands.

CWs are similar to other technologies: as the technology matures, it becomes more complex. However, with increasing complexity, simplicity of operation may no longer apply (and CWs may have to compete with technologies such as aerobic and anaerobic digestion). This is illustrated in literature where it is reported that the nitrogen removal on their tidal CW was limited by process control inefficiency rather than biology (Austen, Maciolek et al. 2002). This should be considered if a tidal CW system is used to treat effluent in an area where skilled personnel are in short supply.

Possibly the greatest disadvantage of the use of CWs is the lack of an adequate design protocol which renders them prone to under-performance (US EPA 2000). Certain heuristic design methods exist, although these are often conservative and therefore land intensive, which means the CWs are sometimes prohibitively expensive. Current CW design is complicated by the different design configurations and modelling methods available (US EPA 2000). In one study, some of the available models were used to model the treatment of a specimen effluent to a given design specification and this approach gave results with orders of magnitude differences in the size (Rousseau, Vanrolleghem et al. 2004). For this design brief, the different models yielded CW designs with surface areas ranging from 0.1m^2 to 950 m^2.

The primary advantage of using CWs is that they are simple to operate and we believe this outweighs all the disadvantages listed above. For this reason, their use is often encouraged for small or rural communities where there may not be suitably qualified technical personnel to operate a complex wastewater treatment system (Sheridan, Glasser et al. 2011a). CWs may also be cheaper than conventional effluent treatment systems; operation and maintenance expenses are low, and they require only periodic on-site labour. They can tolerate flow fluctuations and they facilitate water re-use and recycling. This is of special importance in South Africa, due to the country being both drought prone and water scarce. They provide a habitat for wildlife species (especially birds and indigenous flora) through the creation of an environment suited to them and may be used for marketing or recreational purposes. An additional advantage of the use of these wetlands is their pleasing appearance.

2.5. How VSR CWs work

There are a number of simultaneous processes occurring within a CW. These include:

- solution transport which includes water flow (and the water balance), dispersion and short-circuiting of the effluent within the CW;
- chemical reactions which include Chemical Oxygen Demand (COD) removal which is directly linked to the degradation of organic matter for many effluents, removal of nitrogen through both nitrification and denitrification processes, stabilisation of effluent pH and cycling of sulphur amongst others; and
- physical separation processes which include removal of phosphorous, removal of suspended solids and the removal of pathogenic organisms.

Whilst this list is not exhaustive it represents some of the key processes that were examined within this study, as discussed below.

2.5.1. The water balance

The water balance is the primary mass balance of water through the CW. This can be applied for both surface and subsurface flow CWs and follows the same fundamental equation* which can be given as:

$$F_{in} + F_{precipitaton} + F_{\inf iltration} - F_{out} - F_{evapotranspiration} = Accumulation \qquad \text{Equation 2.1}$$

This mass balance is depicted in Figure 2.1.

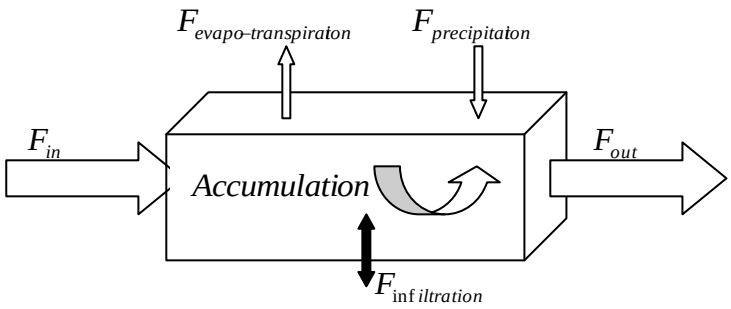


Figure 2.1. Water balance for a CW

At steady state the accumulation is zero. The precipitation term, $F_{precipitation}$, can be measured using a rain gauge or by consulting local meteorological records, and the rate of evapo-transpiration can be approximated. A list of correlations used to calculate evapo-transpiration terms from pan evaporation data is shown in Table 2.1 (adapted from (Wallace, Knight 2006)), where EP is rate of pan evaporation in mm/day and ET is rate of evapo-transpiration in mm/day, although pan evaporation data will not likely be as applicable as data accurately measured for VSRs. The relation found at Montana State University (Towler, Cahoon et al. 2004) is based on experimental methods and is used for determining the rate of evapo-transpiration for reedbeds planted with different plant species. It is possible to scale the equation by scaling the relation with the ratio of bare: covered areas within the reedbed.

* Throughout this thesis F is used to denote volumetric flow, since Q is used to denote the cumulative concentration function in the Tracer study, as denoted by Fogler (Fogler 2005)

Infiltration, listed in the equation as $F_{infiltration}$ can either add to or reduce the volume of water within the wetland. If the wetland is unlined and the system is permeable, groundwater may flow into the wetland at the base and increase the flow at outlet or the effluent may seep into the groundwater and reduce the quantity within the CW. Typically, subsurface flow CWs are lined with an impermeable liner, which means that this term is equal to zero, provided the liner is intact and undamaged.

Table 2.1. Equations used for estimating rates of evapo-transpiration (ET)

System	Relation (mm/day)	r^2†	Air Temp Range (°C)	Reference
Cattail and Gravel VSR	$ET = 1.128 \cdot EP + 0.072$	0.72	12 – 25	(Hammer 1989)
Bulrush and Gravel VSR	$ET = 0.948 \cdot EP - 0.027$	0.93	12 – 25	(Hammer 1989)
Jackson Meadow VSR	$ET = 0.929 \cdot EP + 0.313$	0.82	5 – 30	(Wallace, Nivala 2005)
Jones County Landfill VSR	$ET = 0.846 \cdot EP + 0.038$	0.83	4 – 27	(Wallace, Nivala 2005)
Montana State University Laboratory	$ET_c = K_c \cdot ET_o$ ‡	N/A	N/A	(Towler, Cahoon et al. 2004)

The flow within the wetland constitutes saturated flow through a porous medium and thus has been proposed to follow Darcy's law (Equation 2.2) under laminar flow conditions (Reynolds number <2000, Equation 2.3) (Shepherd, Tchobanoglous et al. 2001). In order for the residence time to be long enough for subsurface flow CWs to effect any remedial action upon an effluent, the flow must be low and laminar conditions prevail

† r is the Pearson product moment correlation coefficient, a dimensionless index that ranges from -1.0 to 1.0 inclusive and reflects the extent of a linear relationship between two data sets, often and experimental data set, and a modelled data set..

‡ K_c is the crop co-efficient for various species of wetland plants

Darcy's Law: $F = K_{hyd} \cdot d \cdot w \cdot S$ Equation 2.2.

where F is the volumetric flow, K_{hyd} is the hydraulic conductivity, d is the mean depth of the CW, w is the mean width of the CW and S is the slope of the saturated hydraulic zone within the CW.

Reynolds Number: $Re = \frac{\emptyset \cdot v \cdot \rho}{\mu}$ Equation 2.3

where $\emptyset$ is the mean channel diameter of the fluid flow through the matrix, v is the mean velocity through the channel; ρ is the density of the fluid and μ is the viscosity of the fluid and the latter two would usually be the same as that of water for most dilute effluents.

The choice of which flow model to use is usually dependent on the choice of the designer and the background discipline of the designer. If he/she is a civil engineer, Darcy's law is chosen, whilst if he or she is a chemical engineer, the equations of motion and continuity may be chosen. The chemical engineering transport equation governing the flow of fluid through a packed bed with reaction can be shown to be:

$$\frac{D_i}{uL} \cdot \frac{d^2 X_i}{dz^2} - \frac{dX_i}{dz} + k_i \tau \cdot C_{i0}^{n-1} \cdot (1 - X_i)^n = 0 \quad \text{Equation 2.4}$$

where $\frac{D_i}{uL}$ is equivalent to the dispersion number, D; X_i is the conversion of component i, C_{i0}^{n-1} is the initial concentration of component i, z is the dimensionless length of the reactor, τ is the ideal residence time of the system and n is the order of the reaction (Levenspiel 1972).

2.5.2. Reasons for non-ideal flow: dispersion, short circuiting, stratification and dead volumes

Subsurface flow CWs are similar to gravel bed filters (or trickle filters) and have been shown to have similar flow characteristics (i.e. non-ideal flow) due to a number of different factors (Małoszewski, Wachniew et al. 2006, Werner, Kadlec 2000). Non-ideal flow is mainly a result of dispersion and short circuiting.

Dispersion is a measure of the micro-mixing of a pulse of a tracer in the direction of flow which leads to the 'smearing' of the pulse. This occurs because the flow channels are not ideal and have different lengths and are orientated in different directions. The dispersion of an impulse of tracer is depicted in Figure 2.2.

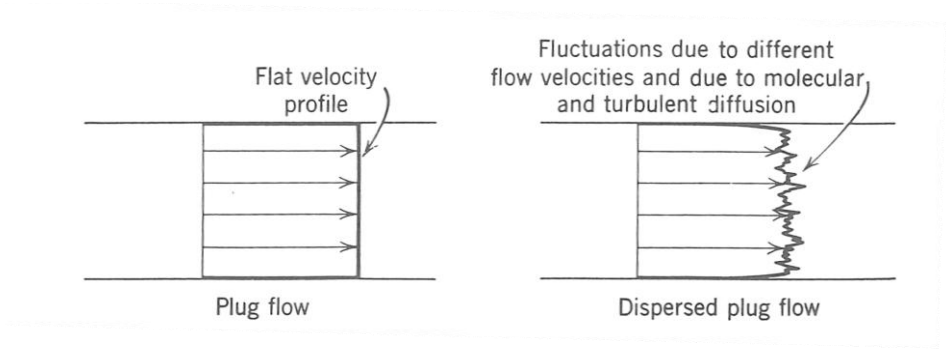


Figure 2.2. An example of increasing dispersion with increasing time/length in a reactor taken from Levenspiel (Levenspiel 1972)

Short circuiting is the process whereby some of the effluent bypasses the main flow channel following the path of least resistance and this parcel/stream of effluent passes through the CW in much less time than would be expected and is depicted in Figure 2.3.

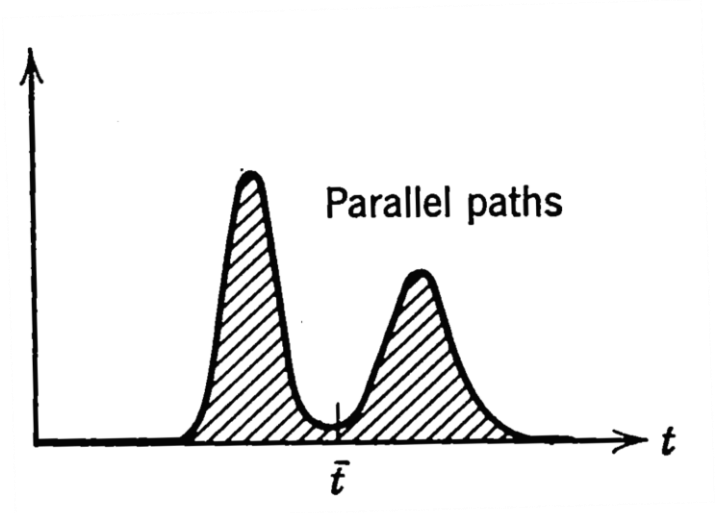


Figure 2.3. An example taken from Levenspiel indicating that tracer may follow two parallel (independent) paths within a reactor.

There may also be vertical stratification of the flow within a CW. This could potentially result in different rates of degradation occurring at different depths (Headley, Herity et al. 2005, Schmidt, Sliekers et al. 2002, Schmid, Hengl et al. 2004). This stratification has been shown to lead to preferential flow paths at the base of the CW for vegetated submerged beds. However, in one study in Australia, it was shown that there was no statistical difference in the reduction in concentration at different depths within a CW and thus the effect of this phenomenon remains under debate (Headley, Herity et al. 2005).

Another characteristic of the CWs is the occurrence of a stagnant or dead volume, a region within the CW which may have no or very low flow. These stagnant regions may significantly reduce the designed volume of a CW (Levenspiel 1972, Fogler 2005).

2.5.3. Mechanisms of COD and BOD Removal

Chemical Oxygen Demand (COD) is the quantity of oxygen, normally given in mg/L, which would be required to oxidise a sample of effluent completely. Biological Oxygen Demand (BOD) is a similar measure of the oxygen requirements for biological oxidation of an effluent stream, and this is sometimes quoted as a two or five day value. South African legislation focuses on COD as a removal parameter, and as such, BOD removal is not investigated within this study. COD and BOD are virtually equivalent for winery effluent (as found in this study) although they may be significantly different for other effluents. Both COD and BOD use is limited since they are both lumped parameters: they do not distinguish between those components which are readily oxidised and those which are not. This is important in the context of effluent treatment, because a recalcitrant effluent may require significantly more treatment than a more readily biodegradable effluent, with the same COD.

Within CWs, there are three primary mechanisms for the reduction of COD (Kadlec, Knight et al. 2000); these are:

- Filtration;
- Aerobic digestion; and
- Anaerobic digestion.

Filtration is responsible for the removal of some of the non-dissolved components contributing to the COD. In winery effluent, this would comprise grape skins, pips, and other colloidal or particulate cellular matter.

Aerobic degradation is responsible for the heterotrophic conversion of carbohydrates to carbon dioxide and water according to the following stoichiometrically balanced chemical reaction (Wallace, Knight 2006, Kadlec, Knight et al. 2000):

$$C_xH_yO_z + \frac{2x+\frac{1}{2}y-z}{2} O_2 \rightarrow xCO_2 + \frac{y}{2} H_2O$$

This relation can be used to calculate the contribution to the COD of any organic component if the values of x, y and z are known. The total COD calculated would be the sum of the CODs of all the individual components.

Anaerobic degradation is the primary removal mechanism in VSRs (Wallace, Knight 2006) due to the low oxygen transfer rates, and is a multi-stepped process (Kadlec, Knight et al. 2000) as follows (all equations unbalanced):

Sugar → Fatty Acid + H2

Sugar → Alcohol and CO2/ Fatty Acid + H2

Fatty Acid + Sulphuric Acid → CO2 + H2O + H2S

Fatty Acid + Hydrogen → CH4 + H2O

H2 + CO2 → CH4 + H2O

2.5.4. Suspended Solids

Suspended Solids (SS) can either be added to or removed from an effluent stream depending on the type of CW and the local conditions of the CW. Free water surface (FWS) wetlands remove SS primarily through sedimentation processes although the presence of aquatic animals may re-suspend these solids through actions such as digging in the sediments. VSR and other subsurface flow wetlands remove SS primarily through the processes of filtration and they are not normally re-suspended. Typically, these wetlands will remove 80% to 90% of the total SS (Kadlec, Knight et al. 2000). With time, however, the gravel or other submerged matrix will need to be removed and cleaned and/or replaced (depending on localised economics) to remove any sludge and other solid build-up.

2.5.5. Nitrogen Removal

Nitrogen is removed through a number of different physical, biological and chemical processes which are often interconnected. These processes are still a focus of current research despite recent gains in understanding (Wallace, Knight 2006). The main processes of removal are summarised below (and the stoichiometric relations presented are not necessarily balanced):

- Ammonia Volatilisation – this follows the equilibrium reaction between ammonium and ammonia, i.e. $NH_3(aq) + H_2O \leftrightharpoons NH_4^+ + OH^-$ which is a pH-dependent reaction. At high pH

values, the equilibrium shifts to the left, and volatilisation of ammonia may occur. It has been reported that if the pH is less than 8, this effect is not significant (Reddy, Patrick et al. 1984). It is only if the pH exceeds 9.3 that the removal of nitrogen via ammonia volatilisation is effective and significant.

- Ammonification – this is the process whereby organic N is transformed into inorganic N, primarily as NH4+ through physical processes. The rate is greatest in the oxygenated zone and is a function of temperature, pH, soil conditions, the presence of nutrients and the ratio of C:N.
- Nitrification – this is the process by which ammonia is bacterially oxidised to nitrite under aerobic conditions and generally follows the following equation:

  $NH_4^+ + 1.5O_2 \rightarrow NO_2^- + 2H^+ + H_2O$

  Recently, it has been posited that the protea-bacteria which perform this oxidative step may also have an anaerobic component to their metabolism in which nitrogen oxides have a complex role (Wallace, Knight 2006, Schmidt, Sliekers et al. 2002, Schmidt, Sliekers et al. 2003). This anaerobic step is shown in the following equation:

  $NH_4^+ + N_2O_4 \rightarrow 0.33NO_2^- + 1.33H^+ + 0.22N_2 + 2NO + 1.33H_2O$

  Aerobic nitrite oxidation normally follows the following reaction:

  $NO_2^- + 0.5O_2 \rightarrow NO_3^-$

  Recent studies indicate that anaerobic ammonium oxidation (Anammox®) is possible and is performed by bacteria of the order Planctomycetales of which three species which have been discovered to date. These bacteria oxidise ammonia by the following reaction (Wallace, Kadlec 2004, Jetten, Strous et al. 1998, Jetten, Wagner et al. 2001, Strous, Van Gerven et al. 1997):

  $$NH_4^+ + 1.32NO_2^- + 1.066HCO_3^- + 0.13H^+ \rightarrow 1.02N_2 + 0.26NO_3^- + 0.066CH_2O_5N_{0.15} + 2.03H_2O$$

- Denitrification – this is the first anoxic reaction to occur after oxygen is depleted and is normally the reduction of nitrate to molecular N2 gases. The reactions for this process are given as:

  $2(CH_2O) + 2NO_3^- \rightarrow 2HCO_3^- + NO_2(g) + H_2O$ and

  $5(CH_2O) + 4NO_3^- \rightarrow 2H_2HCO_3 + 4HCO_3^- + 2N_2(g) + 2H_2O$

  where the (CH2O) represents some organic matter (Wallace, Knight 2006, Kadlec, Knight et al. 2000)(Wallace, Kadlec 2004)(Wallace, Kadlec 2004)(Wallace, Kadlec 2004)(Wallace, Kadlec 2004)(Wallace, Kadlec 2004)(Wallace, Kadlec 2004). The presence of organic matter drives the process and in this way the reduction of N is concomitant with the reduction of COD. This

process is well understood (Wallace, Knight 2006, Vymazal 2006, Kadlec, Knight et al. 2000, Tanner, Sukias et al. 1998, US EPA 2000, Reddy, Patrick et al. 1984).

- Plant uptake is responsible for some nitrate removal, but the rate of uptake is limited because it is coupled to the growth rate of the plant (Kadlec, Knight et al. 2000). Because the economics of harvesting the above-ground plant biomass is often costly, this method of removal is generally not relied upon. It has been reported in literature that not more than 10% of the nitrogen is removed in this method (Gersberg, Elkins et al. 1984, Heshkowitz 1986, Vyamazal, Dusek et al. 1999). In the developing world, however, it may be feasible to harvest the biomass.
- Matrix adsorption – this mechanism is able to effect some removal of nitrogen, but it is not a long term sink, rather a short term adsorption. The Freundlich isotherm can be used to model both adsorption and desorption (Kadlec, Knight 1996).

In subsurface flow CWs (VSRs), there is normally little oxygen available away from the root zone causing a low rate of nitrification. Ways to introduce oxygen and thereby induce nitrification include forced aeration, or by inducing vertical flow and tidal flow (Austin, Wolf et al. 2006, Austen, Maciolek et al. 2002, Behrends 1999, Dufay 2000, Flowers 2002, Liehr, Kozub et al. 2000, Ouellet-Plamondon, Chazarenc et al. 2006). In a recent paper, a vertically reticulated flow system was reported to successfully overcome this problem (Tee, Lim et al. 2012, Wang, Gao et al. 2012). If organic carbon is the limiting factor in these systems, an alternative carbon source can be added (Whitehall 2003).

According to literature, the concentration of total nitrogen in winery effluent can range from 0mg/L to 142.8mg/L (for 21 different wineries in Spain (Bustamante, Pareded et al. 2005)). Within South African wineries this value has been found to be very low (<10mg/L) especially when compared to COD or organic carbon, which is normally three orders of magnitude greater (Sheridan 2003). Since legislation within South Africa for winery effluent specifically sets targets for sodium and COD but not for nitrogen, these were the parameters investigated in this body of work and the reduction of nitrogen was not examined. It is recognised that nitrogen removal is important, especially in the context of many other wastewater treatment systems and other types of effluents.

2.5.6. Phosphorous Removal

In general, phosphorous (in the form of phosphates) is not removed from the effluent in significant quantities unless the matrix has been specifically designed to do so. Phosphorous is normally adsorbed onto the matrix through ionic exchange mechanisms and the ion exchange capacity of the matrix material is the limiting factor (Wallace, Knight 2006, Kadlec, Knight et al. 2000). Once this capacity is exceeded, any further phosphorous removal is due primarily to deposition among the leaf litter at the base of the CW. VSRs remove little phosphorous (Wallace, Knight 2006, Kadlec, Knight et al. 2000). The removal of phosphorous by plants is limited by the plant growth rates and the concentration of nutrients within the plant tissue (Greenway 2003).

There has been considerable work conducted towards removing additional phosphorous through the use of matrix materials which have a greater sorption capacity. Light expanded clay aggregate is an example of such a material and is now a standard matrix material for VSR construction in Norway (Wallace, Knight 2006). There is also considerable research into the use of other materials such as metallurgical slags for CW matrices to enhance the adsorption of phosphorous (Chazarenc, Brisson et al. 2006, Asuman Korkusuz, Beklioğlu et al. 2007, Weber, Drizo et al. 2006).

Similarly to nitrogen, the concentration of phosphorous in winery effluent is low, especially in relation to COD (Sheridan 2003, Bustamante, Pareded et al. 2005)and the reduction thereof was not investigated in this study.

2.5.7. Other processes which have not been investigated in this work

There are a number of other processes which occur within CWs. These include pathogen removal (for disinfection of water), metal removal, treatment of acid mine drainage and the degradation of sulphate. These have not been investigated within this thesis as they are not relevant in the context of the winery effluent considered here. However, a detailed description of these can be found in literature [(Kadlec, Knight et al. 2000, Wang, Jawitz 2006), (Sheridan, Koller et al. 2012)]

2.6. Modelling of vegetated submerged reedbeds (VSR) or subsurface flow constructed wetland (SSFCW) processes

In chemical industries, the rate at which chemical components are converted is referred to as the ‘kinetics’ of a process (Fogler 2005). For physical chemists, the kinetics are important as a tool for understanding the nature of chemical interactions and bonds. For organic chemists, they are important because the mode of reaction provides information as to the nature of molecules. For

the microbiologist, the rates are important for determining if/when substrate limiting conditions occur. And finally, for the chemical engineer, the kinetics of a process are of importance for the design and sizing of equipment at a technical scale (Levenspiel 1972) since the speed of the reaction will often determine the size of a unit operation..

2.6.1. Defining the reaction rate

The reaction rate is defined as:

$$r_i = \frac{1}{V}\frac{dN_i}{dt} \qquad \text{Equation 2.5}$$

and is based on a unit volume of reacting fluid.

The reaction rate expresses the conversion of a chemical entity with respect to time and is be a function of the properties of the reacting materials or micro-organisms. It may be a linear or algebraic function of concentration. Linear rate laws (first order rates) have a rate that is proportional to the concentration and are the most common generally found, especially in unsaturated biologically reacting systems. Algebraic rate laws are proportional to concentration to some power, n, and generally include inhibitory effects or account for non-linear behaviour. For the general class of enzyme catalyzed reactions (Levenspiel 1972) the rate law is given as:

$$A \rightarrow products \qquad \text{Equation 2.6}$$

This class of reaction is classified as an Irreversible Unimolecular First-Order Reaction.

The Monod Equation (Monod 1949) is a special case of Michaelis Menton kinetics; and allows the rate equation to change from first to zero order if there is saturation of a substrate within a biological reaction. This occurs because the microbes reach their maximum metabolic rate and cannot uptake any additional molecules and the rate therefore becomes independent of concentration. Monod behaviour has been illustrated to be useful for the reduction of Chemical Oxygen Demand (COD) in a number of VSRs in the USA (Martinez, Wise 2003). Given that few VSRs operate beyond the conditions of saturation, it is reasonable to assume that we can use a linear reaction rate for CWs, where the rate is proportional to the concentration.

Some of the more common forms of the reaction rate for biological systems are shown in Table 2.2.

Table 2.2. The Some different forms of the reaction rate

Rate Equation	$\boldsymbol{A \rightarrow products}$
Linear	$-r_A = k \cdot C_A$
Algebraic	$-r_A = k \cdot C_A^n$
Monod	$-r_A = V_{max} \cdot \frac{C_A}{K_m + C_A}$
Other (Michaelis –Menton) of which the Monod equation forms a special case)	$-r_A = \frac{k_1 \cdot C_A}{1 + k_2 \cdot C_A}$

2.6.2. Measuring the reaction rate constant

From (Levenspiel 1972): Finding the reaction rate is normally a two step process. The concentration dependency is normally found at a fixed temperature. Following this, the temperature dependency of the reaction is found. The reaction rate is normally found in either a constant volume batch reactor or a flow reactor. (For a more detailed discussion on reactors please refer to (Levenspiel 1972) or (Fogler 2005)). Batch reactors are normally used for this because the reactor equation can be solved for first order reactions to yield:

$$C_i = C_{i0} \cdot e^{-k_i t} \qquad \text{Equation 2.7}$$

From this equation, the rate constant, k_i can be plotted and determined at a given temperature. Unfortunately, biological systems are not homogenous and the reactions are not always first order therefore this approach may not yield the correct data. Compared to a full-scale operating bioreactor, a smaller pilot-scale batch reactor may have fundamentally different rates of reaction, especially if the microbial consortia are different in the two reactors. In addition, large-scale systems tend to operate at a steady state, and thus the selective pressure on the micro-organisms will be significantly different to that found in a batch reactor, where the concentration is changing with time. As a result of this different behaviour, it was decided to determine the kinetics of the process of winery effluent degradation directly from our CW. In order to determine the kinetics, we needed to understand what was in the effluent, and the fundamental operating regime of the reactor.

By definition, the rate constant k_i should not be dependent on any other variable if the system is fully described by the rate equation. It may, however, require additional terms to account for process variables such as dynamic microbial populations or different catalysts if these are variables in a given system. For CWs which have been exposed to the same type of effluent for a number of years, where the microbial communities are stable, and if the temperature of the effluent feeding the system does not vary significantly, it is safe to assume that the rate constant, k_i is constant, for a single contaminant.

As discussed by Villaseñor et al (Villaseñor, Mena et al. 2011) the equations used to describe CWs can be broadly classified into two classes: kinetic or hydraulic. These two different classes are discussed below

2.6.3. Kinetic equations for describing subsurface CWs

Kinetic models can be defined as those models that seek to determine the rate constant with no prior knowledge of the hydraulic regime of the CW. Often the rate equation describing COD reduction or component removal is usually taken as linear, i.e. $-r_A = k \cdot C_A$. The IWA (Kadlec, Knight et al. 2000) cites an aerial rate constant (dependent on the surface only and does not include the depth) of $k = 0.1m/day$ with a standard deviation of 0.053 for Biological Oxygen Demand (BOD) reduction for free water surface constructed wetlands (FWSCWs). For VSRs a value of $k = 0.077m/day$ is given with a standard deviation of 0.053. It is important to note that for both these values, the standard deviation is of the same order of magnitude as the value. This indicates that there is substantial uncertainty with using such a datum. A summary of the different kinetic model rate constants is given in Table 2.3 with the original references (all for BOD removal). However, these rate constants are based on the rate of removal per unit surface area which can be a limitation if the same rate constant is being applied to wetlands with different depths. For this reason in our work the volume based rate constant was measured and used throughout as has been done before in literature (Shepherd, Tchobanoglous et al. 2001, Buchberger, Shaw 1995). In South Africa, the primary reporting parameter for legislative purposes is COD and thus SA does not focus on BOD. However, in the effluent investigated in this study, the COD was comprised primarily of ethanol (Sheridan, Glasser et al. 2011b) and thus the BOD and the COD are almost equivalent and are therefore relevant to this work.

Table 2.3. A summary of aerial and volumetric BOD removal rate constants as given by the IWA

Site	k (C*=0) (BOD)	Standard Deviation	Number of Wetlands	Reference:
Various within North America	0.077 m/day	0.053	38	(Kadlec, Knight et al. 2000)
Denmark	0.068 m/day	Not Specified	70	(Brix 1994)
Not specified	0.06m/day	Not Specified	Not Specified	(Cooper, Job et al. 1996)
USA	0.17m/day	Not Specified	14	(Kadlec, Knight et al. 2000)
USA	4.5/day	Not Specified	1	(Shepherd, Tchobanoglous et al. 2001)
USA	0.15m/day 0.46m/day	Not Specified	Not Specified	(Pardue, Kassenga et al. 1999)
Not Specified	0.1/day	Not Specified	Not Specified	(Buchberger, Shaw 1995)

2.6.3.1. Measuring the rate constants of lumped parameters

In most countries, including South Africa, legislative requirements relating to the release of effluent into the environment is normally given for lumped parameters (Sheridan 2003). There are exceptions for specific contaminants which are highly dangerous (such as for instance, Chromium) and these are separately specified in each country (Regional Screening Levels (RSL) for Chemical Contaminants at Superfund Sites in the US (US EPA Regional Screening Levels), and the Dutch Intervention Values (Interventiewaarden Gevaarlike Stoffen)). However, for sewage and more benign agricultural effluents such as that found in winery wastewater, the limits are mainly set for lumped parameters. COD is a good example of a lumped parameter. It is a measure of the oxygen requirement for complete oxidation of all oxidisable components in the effluent. In winery effluent, ethanol and acetic acid comprise approximately 85% to 90% of the effluent (Sheridan, Glasser et al. 2011b)). Other lumped parameters include total nitrogen (TN) or total phosphorous (TP). Since these lumped parameters are comprised of various components, it is difficult to measure a true rate of degradation or bioremediation. The individual components within the lumped parameters will have different rates of degradation and this can lead to the appearance of a non-constant rate constant for a simple first order equation; that is a rate constant which appears to vary with time. This has led to the development of a number of strategies to overcome

this problem such as developing a time-dependant rate constant (Shepherd, Tchobanoglous et al. 2001). The compartmental model (Wynn, Liehr 2001) which was developed further (Rousseau 2005) included additional parameters such as rapidly biodegradable COD and less rapidly biodegradable COD to accommodate the non-constant rate; and a modified tanks-in-series model (PTIS) included a k-value distribution rather than a lumped parameter rate constant (Kadlec 2003) as solutions to this problem.

2.6.4. Hydraulic equations for describing subsurface CWs

Much of the published work on measuring the kinetics of degradation within a CW relies on the first order plug flow equation (Equation 2.8), the residual plug flow model (Equation 2.9) or the perfectly mixed reactors (Equation 2.10).

$$C_{i,out} = C_{i,in} \cdot e^{-k \cdot \tau}$$ Equation 2.8

$$C_{i,out} - C^* = \left(C_{i,in} - C^*\right) \cdot e^{-k \cdot \tau}$$ Equation 2.9

where C^* is a residual concentration

$$C_{i,out} = \frac{C_{i,in}}{(1+k \cdot \tau)}$$ Equation 2.10

As a first design pass, many designers will usually assume the flow through a wetland is either ideally mixed or behaves as an ideal plug. For an ideal plug flow reactor (PFR), the assumption is made that there is a moving plug of liquid (essentially a small batch reactor moving down a pipe) and that this plug has no lateral mixing or diffusion in the direction of the flow. For perfectly mixed reactors, referred to as ideal continuous stirred tank reactors (CSTRs) the assumption is made that the liquid is perfectly mixed. This implies that the exit concentration should be the same as the concentration anywhere within the reactor. An inherent assumption with the use of these reactor equations is that the flow regime through the CW is ideal. It is believed this assumption is erroneous and that it leads to significant predictive uncertainty. In reality, few reactors are ideal, and phenomena such as dispersion, diffusion, dead zones and short circuiting of the fluid may occur (Fogler 2005). In addition to this, the flow regime may be such that the system has hydraulic characteristics which make it neither a PFR nor CSTR but a reactor with properties somewhere in between. This implies the time the reactants remain inside the reactor may be significantly different from the design brief. Thus, the first requirement for developing a

hydraulically correct model is to conduct either an impulse-response or a step change tracer experiment

2.6.4.1. The theoretical framework for determining Residence Time Distributions (RTDs) of subsurface flow constructed wetlands

The framework presented here is adapted from the texts of Levenspiel and Fogler ((Levenspiel 1972, Fogler 2005) and can be used for determining the hydraulic characteristics of reacting systems and calculating the moments of the associated RTD. This is presented as a step by step approach since some of the parameters (such as number of tanks, N, and mean of the residence time distribution, $\bar{t}_m$) are calculated and used throughout this thesis). Two experimental methods are available for calculating the RTD (and its parameters) – a step change experiment or an impulse-response tracer experiment. A step change experiment requires the inlet concentration to be changed from one set point to another instantaneously and the response of the outlet concentration is studied. This experiment requires rigid control of both flow and concentration. An impulse-response tracer experiment requires the addition of a known mass of a non-reacting component to be injected into the system, and the concentration of the pulse is measured at the outlet. For this method, only constant flow is required. The impulse-response tracer experiment is less accurate than a step change experiment because the tail of the resultant distribution normally requires estimation. However, for systems with non-constant feed composition or where the continuous addition of tracer to the inlet at a known concentration is not practicable, it is a preferable experiment. Due to wastewater often not having a uniform or controllable concentration, impulse-response tracer experiments are the norm for quantifying this effect.

In order to find the RTD, the concentration vs. time curve [the $C(t)$ graph] must be converted to an $E(t)$ graph, where $E(t)$ is defined as the age distribution. In order to find $E(t)$, Q needs to be calculated where:

$$Q = \sum C \cdot \Delta t \qquad \text{Equation 2.11}$$

which is essentially the area under the $C(t)$ curve. $E(t)$is defined as:

$$E = \frac{C}{Q} \qquad \text{Equation 2.12}$$

Thus for each concentration point, C_i an E_i can be calculated where:

$$E_i = \frac{C_i}{Q}$$ Equation 2.13

These parameters are depicted in Figure 2.4.

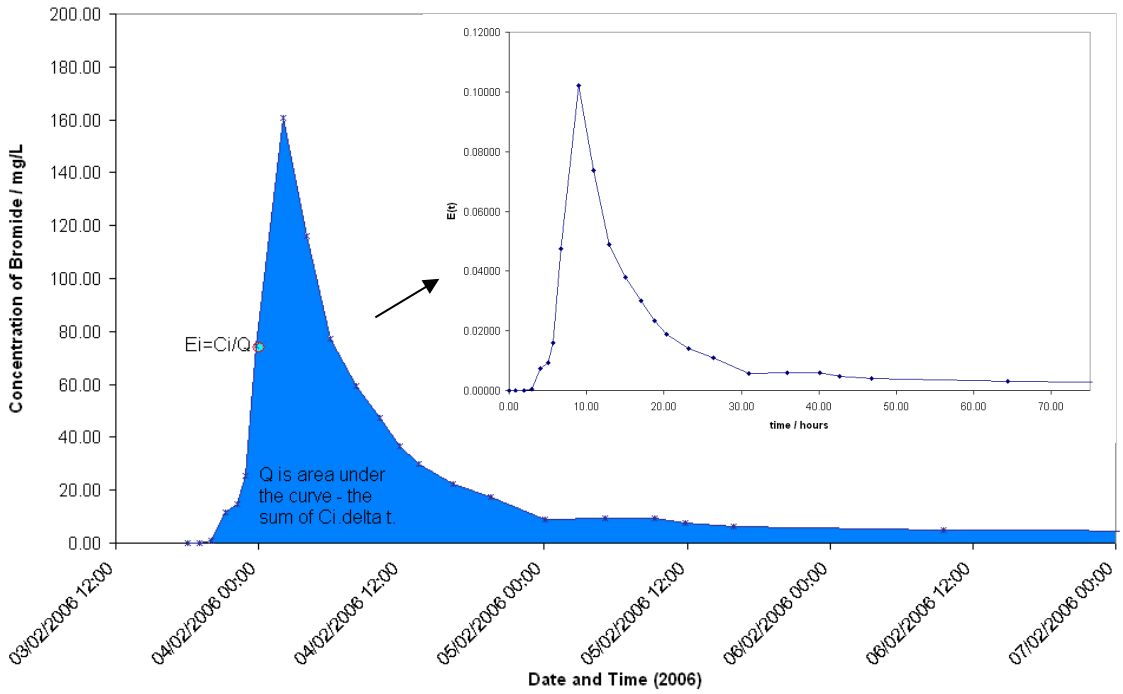


Figure 2.4. An example of a concentration vs. time plot [C(t) curve] and its age distribution [E(t) curve (inset)]

The following parameters are determined in order to calculate the moments of the resulting $E(t)$ distribution:

- The time multiplied by the age distribution multiplied by the change in time ($t_i \cdot E_i \cdot \Delta t$) or more specifically:

  $t_2 \cdot E_2 \cdot (t_2 - t_1)$ Equation 2.14
- The time squared multiplied by the age distribution multiplied by the change in time ($t_i^2 \cdot E_i \cdot \Delta t$) or more specifically:

  ${t_2}^2 \cdot E_2 \cdot (t_2 - t_1)$ Equation 2.15
- The mean of the distribution (the first moment and the mean residence time) is found by summing all the $t_i \cdot E_i \cdot (t_i - t_{i-1})$ terms and this is defined as:

  $\bar{t}_m = \sum_{i=1}^{n} t_i \cdot E_i \cdot (t_i - t_{i-1})$ Equation 2.16

- The second moment of the distribution can be calculated and this provides information on the degree of dispersion. The second moment (σ^2) is found through the following formula:

$$\sigma^2 = (\sum_{i=1}^{n} {t_i}^2 \cdot E_i \cdot (t_i - t_{i-1})) - \bar{t}_m \quad \text{Equation 2.17}$$

By normalising this moment, the dispersion number D can be calculated. The normalised second moment, σ_θ^2, may be calculated as follows:

$\sigma_\theta^2 = \frac{\sigma^2}{{\bar{t}_m}^2}$ where σ^2 and $\bar{t}_m$ have already been calculated in Equations 2.16 and 2.17.

The dispersion number, D, can be found iteratively from the normalised second moment of the RTD using Equation 2.18 as follows:

$$\sigma_\theta^2 = 2 \cdot D - 2 \cdot D^2 \cdot \left(1 - e^{-1/D}\right) \quad \text{Equation 2.18}$$

Sometimes researchers only require the mean residence time, $\bar{t}_m$, of the CW. If a Tanks-in-Series (TIS) or a Plug Flow Reactor (PFR) with dispersion model is used to describe the system, then the dispersion number (D) and number of tanks (N) may also be required. For a TIS model in particular, N can be found directly from this data:

$$N = \frac{1}{\sigma_\theta^2} \quad \text{Equation 2.19}$$

It is also possible to check the integrity of the calculations by means of Equation 2.19 since the value of N from Equations 2.19 and 2.20 must be the same, where:

$$N = \frac{{\bar{t}_m}^2}{\sigma^2} \quad \text{Equation 2.20}$$

An overview of the techniques for running tracer studies is presented in literature (Perrson, Somas et al. 1999). In that study the effective volume ratio is defined as a function of the length to width ratio given as:

$$V_{Eff} = \frac{\bar{t}_m}{\tau} \quad \text{Equation 2.21}$$

where $\tau = \frac{V}{Q}$ and is defined as the ideal residence time and is the volume divided by the volumetric flowrate. This is a ratio of the residence times, and not the volumes, because it is not possible to measure the dead volume directly. The authors also defined an hydraulic efficiency

factor, λ, by which it is possible to compare different designs of CWs. This hydraulic efficiency factor is given by Equation 2.22 where N is the number of tanks in the TIS model.

$$\lambda = V_{Eff} \cdot \left(1 - \frac{1}{N}\right) \qquad \text{Equation 2.22}$$

These parameters can be used to assess the extent of non-ideal behaviour within the CW.

Since the kinetic equations do not account for hydraulic processes occurring within the CW we chose to consider for this work three different equations/methods to determine the rate constant ensuring that non-ideal hydraulic behaviour within the CW was not neglected. These are:

- The tanks-in-series (TIS) equation, and solving for the rate constant;
- Using the plug flow with dispersion equation (the Peclet equation), and solving for the rate constant; and
- Using the residence time distribution directly, and solving the convolution integral to find the rate constant.

Each of these methods is discussed below.

2.6.4.2. The N tanks-in-series equation (TIS)

For certain types of residence time distributions the TIS equation is appropriate for describing the processes within a reacting system. In Figure 2.5 (Levenspiel 1972), the age distributions for various values of N are shown. It is noted that as $N \rightarrow \infty$ the RTD more closely resembles that of a plug-flow reactor. In this figure, for N=20 the RTD very closely resembles that of a PFR.

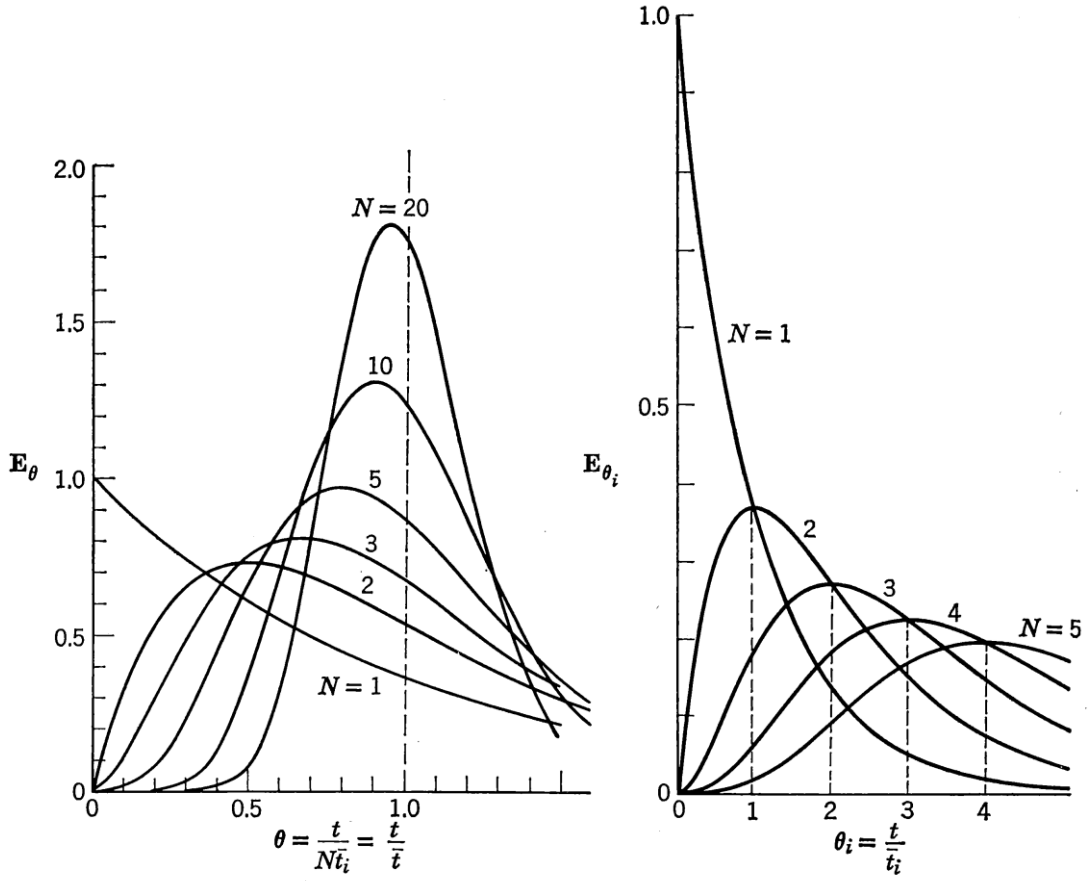


Figure 2.5. Residence time distributions for N CSTR reactors in series taken from Levenspiel

The physical representation of the TIS model is shown in Figure 2.6. In this case, N=4.

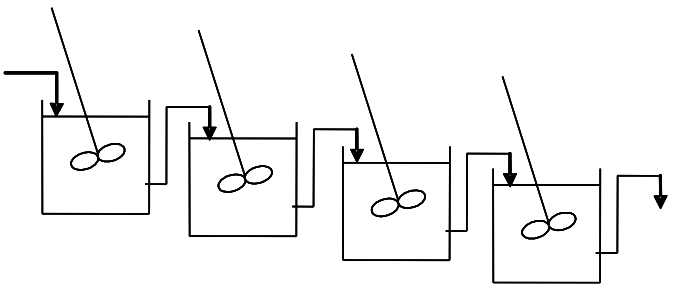


Figure 2.6. A graphical depiction of the TIS model for N=4.

The TIS equation is presented as Equation 2.23.

$$C_{i,N} = \frac{C_{i,0}}{\left(1 + k_i \cdot \tau_j\right)^N} \qquad \text{Equation 2.23}$$

The derivation of this equation can be found in Levenspiel, p 136 (Levenspiel 1972).

2.6.4.3. Peclet Equation (Dispersed Plug Flow Model)

The CW can also be considered to be behaving as a plug flow reactor displaying dispersive behaviour. This kind of system is shown in Figure 2.7.

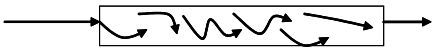


Figure 2.7. A plug flow reactor with dispersive forces at work.

For packed bed reactors (which is essentially what CWs are) the Peclet equation has been successfully solved for first order reactions (Levenspiel 1972). In terms of conversion, X, the rate constant, k, the Peclet Number, Pe, the length of the system, l, and the velocity of the impulse, u, the equation is given as:

$$X = 1 - \frac{4 \cdot q \cdot e^{\left(\frac{Pe}{2}\right)}}{(1+q)^2 \cdot e^{\left(\frac{Pe \cdot q}{2}\right)} - (1-q)^2 \cdot e^{\left(\frac{Pe \cdot q}{2}\right)}} \qquad \text{Equation 2.24}$$

Where: $q = \sqrt{1 + \frac{4 \cdot Da}{Pe}}$ Equation 2.25

and the Damkohler Number, $Da = \frac{l \cdot k}{u}$ Equation 2.26

From our investigation and others, it was found that it was possible to model the system using this Peclet Equation. The derivation of this equation is presented by Levenspiel, p.286, which is based on the work conducted by Wehner and Wilhelm (Wehner, Wilhelm 1956).

2.6.4.4. Convolution Integral

It is also possible to determine the conversion of a reactor (regardless of the degree of non-ideal behaviour) directly from the tracer information (what follows is largely adapted from Levenspiel, p 264 to 269). As an impulse of tracer passes through the reactor it will be modified into an output which will be a function of time. This is graphically depicted in Figure 2.8 (Levenspiel 1972).

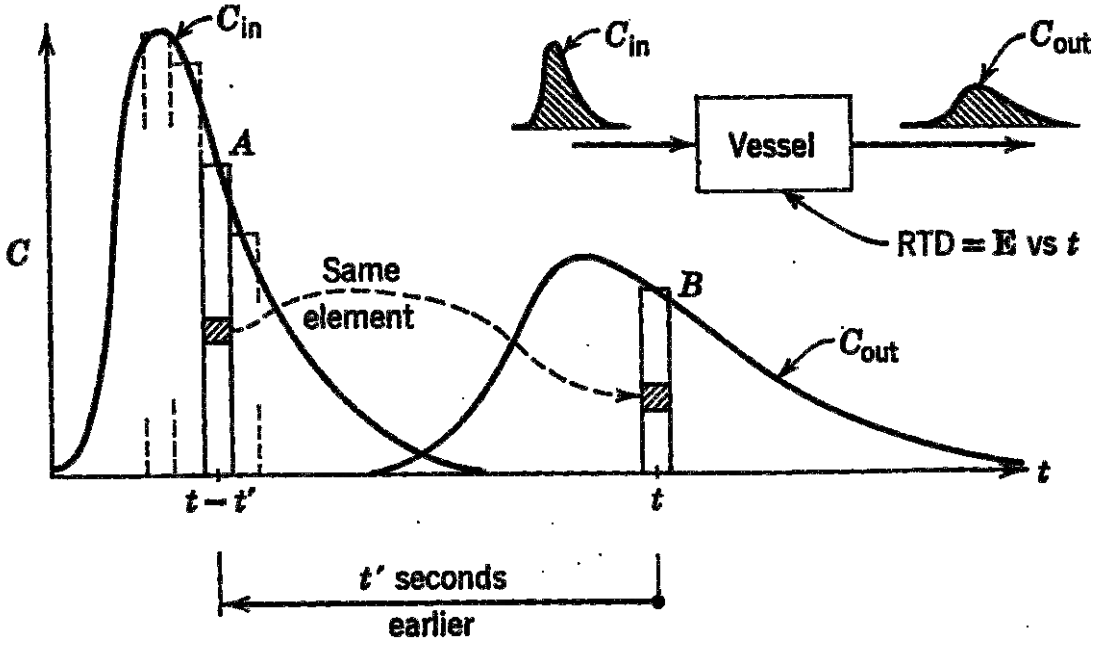


Figure 2.8. A graphical depiction of the movement of tracer through a reactor taken from Levenspiel

If the mass balance on the tracer is conducted on the tracer about to leave at time, t, it is found that

$$(tracer\ leaving\ in\ rectangle\ B) =$$
$$(all\ the\ tracer\ entering\ t'seconds\ earlier\ than\ t\ and\ staying\ for\ t'\ in\ the\ reactor)$$

Equation 2.27

The tracer which enters t' seconds earlier than t is shown as rectangle A. Therefore Equation 2.27 can be rewritten as:

$$(tracer\ leaving\ in\ rectangle\ B)$$
$$= \sum_{\substack{all\ rectangles\ A \\ which\ enter \\ before\ time\ t}} (tracer\ in\ rectangle\ A)(Fraction\ of\ tracer\ A\ which\ stays\ \ for\ t'\ seconds\ in\ the\ vessel$$

This can be rewritten as:

$$\boldsymbol{C_{out}} = \int_0^t \boldsymbol{C_{in}}(t-t')\boldsymbol{E}(t')dt' \qquad \text{Equation 2.28}$$

which is equivalent to:

$$\boldsymbol{C_{out}} = \int_0^t \boldsymbol{C_{in}}(t')\boldsymbol{E}(t-t')dt' \qquad \text{Equation 2.29}$$

or more elegantly;

$$\boldsymbol{C_{out}} = \boldsymbol{C_{in}} * \boldsymbol{E} \qquad \text{Equation 2.30}$$

Equation 2.30 can be used to describe the shape of the output (i.e. the response) at any given time. This can also be used to calculate the conversion directly as follows (for a first order reaction):

$$(mean\ concentration\ of\ reactant\ in\ the\ exit\ stream) = \sum_{\substack{all\ elements\ of \\ exit\ stream}} (concentration\ of\ reactant\ remaining\ in\ an\ element\ of\ age\ t\ to\ t+dt) \cdot (fraction\ of\ exit\ stream\ of\ age\ t\ to\ t+dt)$$

which can be rewritten as:

$$\overline{C_\iota} = \int_{t=0}^{\infty} C_{i,element} \cdot \boldsymbol{E} \cdot dt \qquad \text{Equation 2.31}$$

where $\overline{C_\iota}$ is the mean concentration of reactant in the exit stream

In this work each of these equations/methods to calculate the rate constant for the degradation of the components of winery effluent have been used.

2.7. Wetland plants for vegetated submerged reedbeds.

The choice of plants for use in CWs has received considerable attention in the literature. The IWA (Kadlec, Knight et al. 2000) lists some 32 species of emergent wetland plants that are tolerant of continuous water inundation. An adapted list is shown in Table 2.4.

Table 2.4. Some emergent vegetation plant species which may be used in CWs

Scientific Name	Common Name	Max Water Depth /m
Alternanthera philoxeroids	Alligator Weed	1.0
Canna spp.	Canna Lilies	0.25
Carex spp.	Sedges	0.25
Ceratophyllum spp.	Coontail	>3
Caladium jamaicense	Sawgrass	0.25
Colocasia esculenta	Wild Taro	0.5
Cyperus spp.	Sedges	0.5
Eleocharis spp.	Spikerushes	0.5
Elodea spp.	Waterweed	3
Glyceria spp.	Mannagrass	0.3
Hydrocloa caroliniensis	Watergrass	1.0
Iris spp.	Iris	0.2
Juncus spp.	Rushes	0.35
Lemna spp.	Duckweed	None
Ludwigia spp.	Water Primroses	0.5
Panicum hemitomon	Maidencane	0.3
Panicum repens	Torpedo grass	0.5
Peltandra spp.	Spoon flowers	0.25
Phalaris arundinacea	Reed canary grass	0.3
Phragmites australis	Common reed	0.5
Polygonum spp.	Smartweeds	0.25
Pontederia spp.	Pickerelweeds	0.25
Rhynchospora spp.	Beak-rush	0.5
Sagittaria spp.	Arrowheads	0.5
Saururus cernuus	Lizard's tail	0.2
Scirpus spp.	Bulrush	1.5
Sparganium spp.	Bur-weed	0.5
Sphagnum spp.	Sphagnum mosses	0.1
Thalia geniculata	Arrowroot	0.75
Typha spp.	Cattail	0.75
Zizania aquatica	Wild rice	1.0
Zizaniopsis milacea	Southern wild rice	1.0

With the exception of plant groups such as Carex, Phragmites, Scirpus and Typha, most of these plants are not indigenous to South Africa. Certain plants such as Canna are declared invader aliens (Government Gazette 1983) making their use inappropriate for the South African context.

In addition to the list given by the IWA, other plants have also been studied for their suitability of use within CWs. The difference in performance of two CWs, one planted with *Cyperus papyrus* and the other with *Miscanthidium violaceum* was investigated (Kyambadde, Kansiime et al. 2004) and it was found that Cyperus showed improved N and P removal. *Phragmites australis* and *Phalaris arundinacea* have been compared (Vymazal, Krőpfelová 2005) and it was found that Phragmites took four seasons to achieve maximum above ground biomass, which was twice as long as for the Phalaris. In another study the differences between eight different plants were assessed although no statistical differences were found between the different species for BOD removal (Tanner 1996). The use of *Zantedeschia aethiopica* (an ornamental plant referred to in literature as a Calla Lily, and in South Africa as an Arum Lily) was investigated for use in CWs (Belmont, Metcalfe 2003) and found to indeed reduce COD and Total Kjeldahl Nitrogen, although the unplanted reference CW reduced the COD by a statistically equivalent amount. Evaluating the potential effect of the plants is a subject of ongoing research.

The use of water hyacinth (*Eichornia crassipes*) for the removal of heavy metals was investigated in a different study and the plants were found to be effective (El-Gendy 2006). However, this is not recommended anywhere in Africa due to the invasive potential of this plant (which contributes to eutrophic conditions in lakes).

Nine different plant species were compared for removal efficiencies of BOD, N and P (Tomoko, Ping et al. 2006) Canna and *Cyperus papyrus* showed high removal rates of N, and Canna produced the lowest quantity of greenhouse gases (methane). However, in a review of 27 different studies in peer reviewed journals on the use of different plant selections it was found that no systematic rule exists that could guide which species to use because of significant differences both between studies and species (Brisson, Chazarenc et al. 2006). The authors listed at least 47 different species of plants. In this study, the aesthetics of using only one or two different species was been assessed and this study also investigated the use of twelve different ornamental plants; it was found that the BOD and COD removal were similar to that of the common reed, whilst sulphate removal was slightly reduced.

The US EPA lists the following criteria as important when choosing plants for a CW (US EPA 2000):

- Utilise indigenous flora;
- Use non-invasive species;
- Use species that are tolerant of high nutrient loads;
- Use species that can tolerate continuous flooding;
- Use species that are perennial rather than annual as this reduces the need for annual re-establishment;
- Use species that have wildlife benefits i.e. those species that provide shelter to animals;
- Choose a variety of species to improve diversity since monocultures are susceptible to insect or disease decimation.

These studies all indicate that there are many opportunities for choosing plants other than common reeds or cattails, especially if the major component of the effluent is COD. No studies were found that gave an indication of the maximum strength effluent that could be applied, which is especially important for systems that are treating effluents with COD levels as high as 8 000 mg/L such as winery effluent (Sheridan 2003).

2.8. Research Objectives

Within the context presented above, there were a number of broad research objectives for this study. The principal objective was to develop a mathematical model, for design or engineering purposes, that accounted for the hydraulic and kinetic processes occurring simultaneously within the VSR at the ARC. The objectives and tasks were:

- The principal objective of this thesis was to develop a mathematical model of a VSR for design or calibration purposes for the treatment of winery effluent, utilising the data obtained from the three points presented below. Within this objective, it was hypothesised that the specific components of the effluent should be used for the modelling of the process, rather than lumped parameters such as Chemical Oxygen Demand. It is hypothesized that tracking the degradation of key parameters is more accurate than by tracking the degradation of a lumped parameter.
- The characterisation of winery effluent. The principal goal of this task was to identify the main components of winery effluent and to quantify them within the effluent streams at the VSR investigated. This goal included identifying the primary constituents of COD, which is known to

be the most important of the lumped parameters normally used to characterise winery effluent as well as investigate some of the differences of the effluent during the harvest and the rest of the year.

- The measurement of the hydrodynamic properties of the VSR which would be utilised for modelling purposes. This required the measurement of the residence time distribution of the VSR and the calculation of the moments of the distribution. It was hypothesised that the assumption of ideal flow for modelling or design purposes is incorrect, and that the true residence time of the VSR is significantly different to the ideal residence time utilised in some of the current VSR models available.
- The calculation of the rate constants of the degradation of specific components of winery effluent. The specific components which were required for modelling purposes were defined by the data collected within the study. The calculation of these constants was measured in-situ, utilising the data measured from the hydraulic processes. This was done to reduce the error associated with scale-up/inaccuracies associated with the extrapolation of laboratory data to real systems.

3. On modifying the Arrhenius equation to compensate for temperature changes for reactions within biological systems

This Chapter presents a discussion in the use of the modified Arrhenius equation as noted in Chapter 1.1. The research does not use any measured data, but rather presents an alternative method to that which is currently used in literature and which is believed to be more accurate in warm climes.

This chapter was published in the Water SA, Vol. 38, No. 1, Jan 2012. This is an ISI listed Journal in the Web of Science and was peer reviewed prior to publication. The contribution of the co-authors towards the work is primarily that of supervision or collaboration and the work and write-up was conducted by the author of this thesis.

3.1. Abstract

In this communiqué, we discuss the use of the Arrhenius relationship to describe the temperature dependence of reacting biological systems such as those treating wastewater. We also discuss the use of the modified Arrhenius function, and those instances where its applicability is limited. It is shown that the error when using the modified relationship is 7% at 30°C, 15% at 40°C and 25% at 50°C. It is concluded that whilst the modified relationship is acceptable at lower temperatures, in those applications where higher temperatures are reached (above 25°C); the error with using the relationship may not be acceptable. We present an Arrhenius equation for use in biological systems, which is applicable for all temperature ranges.

3.2. Introduction

The kinetics of a process are related to temperature through the Arrhenius relationship (Fogler 2005). For a given catalytic or microbial system, with given chemical components, this relationship is shown in Equation 3.1 with the temperature given in Kelvin

$$k(T) = A \cdot \exp\left[\frac{-E_A}{R \cdot T}\right] \qquad \text{Equation 3.1}$$

Where: k(T) is the rate constant as a function of temperature

A is the pre-exponential factor

E is the activation energy in J/mol

R is the gas constant = 8.314 J/(mol.K)

T is the absolute temperature in K

This relationship is sometimes given in the differential form, as shown in Equation 3.2:

$$\frac{d(\ln k)}{dT} = \frac{E_A}{RT^2}$$ Equation 3.2

The kinetics of the degradation processes occurring within many reacting biological systems, including municipal wastewater treatment (Benefield, Randall 1980, Crites, Tchobanoglous 1998, Nitisoravut, Klomjek 2005), anaerobic lagoons (Oleszkiewicz, Koziarski 1986), facultative lagoons (Mashauri, Kayombo 2002) and constructed wetlands (Rousseau, Vanrolleghem et al. 2004, Nitisoravut, Klomjek 2005, Mashauri, Kayombo 2002, Marsili-Libelli, Checchi 2005, Andreottola, Oliveira et al. 2007, Kadlec 2009, Rodgers, Dunn 1995) are described using a modified form of this equation (denoted the Modified Arrhenius Function or MAF) given in Equation 3.3, with temperature, T, given in °C (Kadlec, Knight 1996, Benefield, Randall 1980, Haug 1993).

$$k = k_{20} \cdot \theta^{(T-20)}$$ Equation 3.3

The MAF is attractive as an experimental equation because of its ease of use; the temperature is given in °C and the temperature correction factor, θ, is measurable. The derivation of this form of the Arrhenius Equation is based on the assumption that the operating temperature is close to or below 20 °C (Table 3.1). In countries with hot climates such as South Africa, and especially those with high humidity where the effect of evaporative cooling is reduced, the MAF may not be applicable and could result in water treatment/other biological systems that do not perform to design specifications. For the temperature ranges where this assumption may not hold true, a new form of the Arrhenius Equation is proposed here that will not differ significantly from the current form of the MAF at lower temperatures, yet will follow the exponential form of the Arrhenius equation at higher temperatures.

Table 3.1. Derivation of the MAF

Integrating between T_1 and T_2 yields

$$\ln\left(\frac{k_2}{k_1}\right) = \frac{E \cdot (T_2 - T_1)}{R \cdot T_2 \cdot T_1}$$

Equation 3.4

If the process is carried out at or near 20 °C, the quantity for $\frac{E}{R \cdot T_2 \cdot T_1}$ is assumed constant, given as C. Equation 3. may be written as:

$$\ln\left(\frac{k_2}{k_1}\right) = C \cdot (T_2 - T_1)$$

$$\frac{k_2}{k_1} = \exp\left(C \cdot (T_2 - T_1)\right)$$

Equation 3.5

If e^C is substituted with a temperature coefficient, θ, Equation 3.5 yields:

$$\frac{k_2}{k_1} = \theta^{(T_2 - T_1)}$$

Equation 3.6

Since the rate constant is now a function of the temperature difference, it is no longer necessary to convert the temperature to Kelvin, and if 20°C is the reference temperature, Equation 3.6 can be solved to yield Equation 3.3

$$k_T = k_{20} \cdot \theta^{(T-20)}$$

The primary assumption to be considered when using the MAF is that the temperature is not much greater than 20°C. This assumption allows the conversion of an exponential function into a power function, which has different mathematical properties, which are more pronounced with increasing temperature.

3.3. Methods and results of the investigation of the non-applicable temperature range of the MAF

To assess applicable and non-applicable temperature ranges for the MAF, we have used θ values related to the design of constructed wetlands. For this assessment θ has been assigned a value of 1.06 as recommended by the IWA (Kadlec, Knight et al. 2000)and the value of k_{20} is taken as

1.104/day as specified by the US EPA (US EPA 2000), since the IWA does not recommend one single value. Using these parameters the rate constant can be calculated for a range of temperatures. If the log of Equation 3.1 is taken, the following relation can be obtained:

$$\ln(k) = \left(\frac{-\beta}{T}\right) + \alpha$$

Equation 3.7

where ln(A) is replaced by α and $\frac{E_A}{R}$ substituted by β

The value for k was calculated for the temperature range over which the data was most likely collected; i.e. 0°C to 20°C (273K to 293 K) using the MAF, and a plot of ln(k) vs. 1/T is shown in Figure 3.1. The points are essentially reproduced data, and this "data" has been regressed (the line through the points) to determine the constants in Equation 3.7.

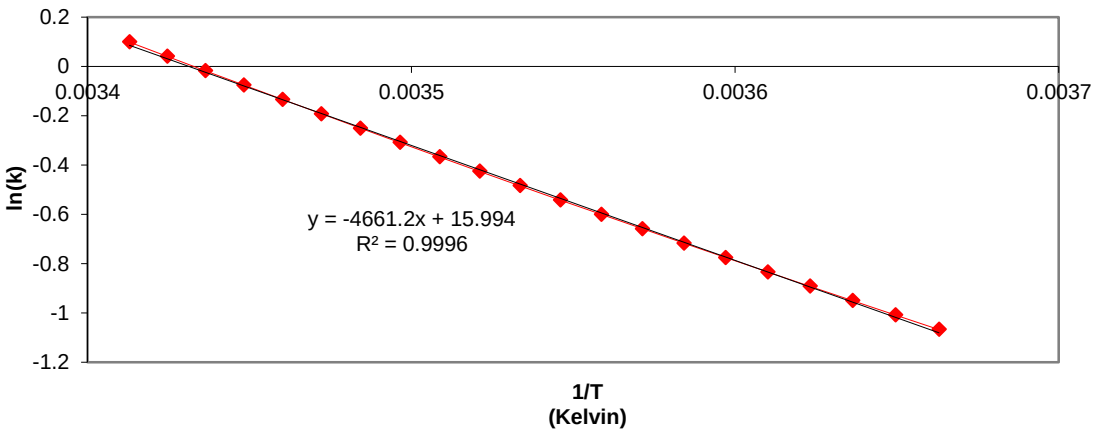


Figure 3.1. A graph of the MAF to find the parameters for the Arrhenius Equation with regressed line shown

The y-intercept and the x-intercept of this plot correspond to α and β in Equation 7. The twisting of the data around the regressed line is caused by the conversion of data found from a power function being presented as an exponential function.

These calculated values for α and β were then used to fit the Arrhenius function given by Equation 1, such that $A = 8.83 \cdot 10^6$ and $\frac{E_A}{R} = 4660$. Using these "data", a comparison of the Arrhenius equation and the MAF was performed and the results are presented in Figure 3.2.

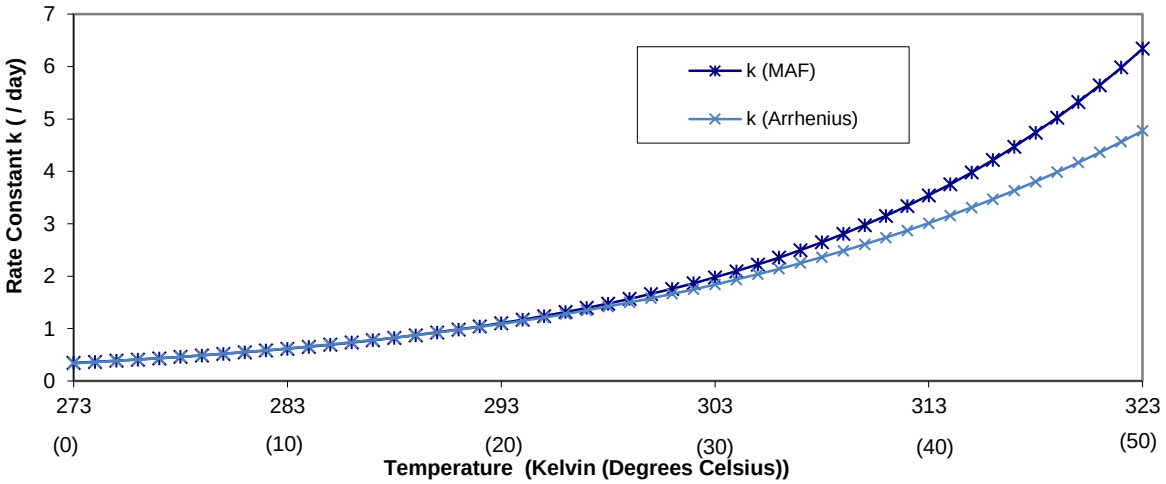


Figure 3.2. A comparison of the rate constants as calculated by the MAF and the Arrhenius equation showing differences at higher temperatures

This analysis indicates that the difference between the two forms of rate constant is 7% at 30°C, 15% at 40°C and 25% at 50°C. This difference would become greater at higher temperatures since the exponential law reaches an asymptote at the value for A at infinite temperature, whilst the MAF increases infinitely with increasing temperature. The analysis was halted at 50°C since there are few reacting biological process that will operate temperatures higher than this (although some bio-metallurgical operations may occur at temperatures higher than 60°C.

3.4. Discussion of the modified Arrhenius equation

In hot climes and for certain industries (such as distillery effluents) it is possible that the effluent temperature may rise above 30°C and thus the assumptions upon which the MAF is based may not be valid. It is with this in mind that a new functional dependence of k on temperature, given by Equation 3.7 is proposed (Derivation Box 2). In this derivation, the values of k_{20} as measured for the MAF will still be valid (shown as k_{293}). It is, however, a simple modification to change the temperature to °C.

Table 3.2. Derivation of an Arrhenius Equation for use in biological systems

Starting with Equation 1.

$$k(T) = A \cdot e^{\frac{-\beta}{T}}$$ Equation3.1

The rate constant expression can be solved at 20 ^{o}C (293 K):

$$k(293) = A \cdot e^{\frac{-\beta}{293}}$$

This can be solved for A, and substituted back into 1

$$k(T) = k(293) \cdot \frac{e^{\frac{-\beta}{T}}}{e^{\frac{-\beta}{293}}}$$ which can be solved as:

$$k(T) = k(293) \cdot \exp\left(\beta\left(\frac{T-293}{293 \cdot T}\right)\right)$$ Equation 3.7

3.5. Conclusion

Whilst the MAF is used substantially for the wastewater and other industries(Benefield, Randall 1980, Haug 1993) and is undoubtedly applicable to cooler and temperate climates, it should be used with caution at higher ambient or reaction temperatures since it may lead to the use of a rate constant which is greater than that which is occurring. At temperatures lower than 20°C, it is not important which equation is used, because the rate constants are small and the difference between the two functions is negligible. In countries with hot climates, and especially those with high humidity where the effect of evaporative cooling is reduced, the MAF may not be applicable and could result in systems that do not perform to design specifications. The MAF may also overestimate the rate constant required for designing systems to treat warm effluents, such as distilleries or for use in hot biological reacting systems such as composting or heap leaching. It should also be relatively easy to reassess existing literature to calculate the values for A and β and these could be used, with the published values for k_{20} to find the rate constant at any temperature.

4. An Annual and Seasonal Characterisation of Winery Effluent in South Africa

This Chapter presents an in depth investigation of the constituents of winery effluent. As discussed in the Research Objectives, it was hypothesized that the modelling of lumped parameters was not as effective for describing the processes of treatment of winery effluent. This required a thorough investigation into the individual components of winery effluent with a view to understanding what comprises the COD in particular. This study conducted a detailed investigation into the organic and inorganic components and also studied the COD. From this study, we have gained a deeper understanding of the nature of this effluent: that the COD is comprised primarily of ethanol and acetic acid, and that it contains substantial potassium and sodium. This Chapter also developed a correlation to link the organic components to the COD of the raw effluent, ex cellar. This data is critical for Chapters 5 and 6 where we consider the treatment of each of the components. The original data for this Chapter is presented in Appendices A and B.

This chapter was published in the South African Journal of Enology and Viticulture, S. Afr. J. Enol. Vitic., Vol. 32, No. 1, 2011. This is an ISI listed Journal in the Web of Science and was peer reviewed prior to publication. The contribution of the co-authors towards the work is primarily that of supervision or collaboration and the experimental work and write-up was conducted by the author of this thesis.

4.1. Abstract

Winery effluent is known to have a high chemical oxygen demand (COD) and low pH. In this study, we extensively analysed effluent from two cellars, and studied the temporal changes over the duration of a harvest and the duration of a year. It was found that for raw winery effluent, ethanol contributes approximately 85% to 90% of the COD, with acetic acid being the next significant contributor. The pH showed some dependence on the concentration of acetic acid. The concentration of sodium in the effluent is strongly dependent on the cleaning regime in place at the cellar, and the concentration of potassium has been shown to be linked to the spillage of juice, wine or lees. The data and correlations presented here could allow for an artificial effluent to be easily prepared for research purposes.

4.2. Introduction

The process of winemaking produces a large quantity of effluent; in the order of one million m^3 per annum in South Africa (Sheridan 2003). Historically, this effluent was irrigated onto a pasture, evaporated, or drained into the nearest river. In recent years, the Department of Water Affairs and Environment (DWAE) has made significant progress towards tightening SA water law, and in increasing water consumer compliance with this law. To this end, most wine makers and wineries have established some form of effluent treatment rather than simple disposal, even if that treatment is just irrigation of pasture. The current laws in place allow for disposal by irrigation, provided there is continuous measurement of effluent strength and of certain aspects relating to its composition. Under SA law (Government Gazette 2001), winery effluent is regarded as biodegradable industrial wastewater, and as such there are five parameters which must be reported: Chemical Oxygen Demand (COD), pH, Electrical Conductivity (EC), Sodium Adsorption Ratio (SAR) and Faecal Coliforms. If the effluent is released into a river, there are additional parameters that need to be measured, and the limits are stricter (Government Gazette 2001). In compliance with the law, these five measures of winery effluent are commonly reported. Any other chemical characteristics are rarely mentioned, however, and this can be a problem for the detailed design of an effluent treatment system.

A number of processes could be considered for the treatment of winery effluents, such as anaerobic digesters, aerobic digesters, sequencing batch reactors, rotating biological contactors amongst other. A quantitative description of such processes, especially modelling of the kinetics of various biodegradation processes, is needed for equipment design and process evaluation.

However, in order to achieve this additional information about the chemical composition of the effluent is required. Chemical Oxygen Demand (COD) and Sodium Adsorption Ratio (SAR), as lumped parameters, are not well suited to accurate modelling because they do not provide detailed information on what comprises them. For example, a certain quantity of glucose or lignin may have a similar COD, but the glucose is much more readily biodegradable than the lignin. Thus substantially different rate constants for the reduction of the COD would be found in each case. It is common practice in the literature to specify a biodegradation rate constant for the reduction of COD (or biological oxygen demand, BOD) for a given effluent (Shepherd, Tchobanoglous et al. 2001, Kadlec, Knight 1996, Wood 1995) and utilise these in process models for the design of effluent treatment technologies.

In this study, the effluent from two wineries was investigated. Effluent from the first winery (cellar 1) was characterized over the duration of a year. The winery is typical of the Stellenbosch region of South Africa. It is a small family business that presses approximately 700 tons per annum of various grape varietals. The process is traditional, with both open concrete fermenters and jacketed stainless steel tanks being used to produce both red and white wine.

The second winery (cellar 2) forms part of an experimental farm belonging to the Agricultural Research Council of South Africa (ARC). Red and white wines are produced in this cellar. Within this overlying research infrastructure, it was possible to sample the effluent on a daily basis and construct a profile of the effluent for the duration of a harvest season. In this case, the season was from the end of January 2005 to the end of March 2005. This harvest was particularly short (normally the harvest lasts for three months) and almost no rain fell in the two month period. This was advantageous as it allowed for accurate sampling because there was no dilution effect through rainwater mixing with the samples.

4.3. Materials and Methods

4.3.1. Experimental techniques

4.3.1.1. Sampling protocol

Cellar 1 is built on a slope and the various drains in the cellar exit the building at different locations. These drainage streams converge some distance from the cellar, and thus particular care was required to ensure samples were representative of the entire winemaking process. To achieve this, the samples were taken at a point at which all the effluent streams from the winery had been combined. Grab samples, comprising 500 mL aliquots were taken approximately every fortnight during the harvest season and monthly outside of the harvest season. These samples were analyzed for a number of different chemical constituents (see below).

For cellar 2, grab samples were taken daily, for the duration of the 2005 harvest (from 31st of January 2005 to 31st March 2005) with the exception of weekends and long weekends. The 500 mL aliquots were taken from a surge tank prior to treatment and were thus deemed to be representative samples.

4.3.1.2. Analytical methods for effluent characterisation

The COD was measured using a Merck COD Cell test (1.14555.001) and the Merck Spectroquant spectrophotometer. Metals in solution were measured by atomic absorption (AA) using a Varian SpectrAA flame spectrophotometer. Gas mixtures of acetylene/air were used for sample combustion and detection wavelengths for each of the metals identified are specified in the user's manual. Inorganic anions were analyzed using high performance liquid chromatography (HPLC) with a Waters IC-Pak (HR 4.6x75mm) Anion Column, using a conductivity detector (parameters used were: Column T = ambient, 1.5 mL per minute, mobile phase, 3.6 mM sodium carbonate). Some organic components were initially identified and quantified using the HPLC method described above. Thereafter, all organic components were identified using GC-MS, with a Restek RTX Capillary column (60m by 250µm), and T-initial of 70°C, ramped at 5°C per minute to 170°C, with a second ramp of 10°C per minute to 280°C. Routine analyses of those organic components identified as being the most abundant in the effluent were conducted using GC – FID with a J & W Scientific DB-Wax Column (60m by 250µm, T-initial of 40°C for 10 minutes, ramped at 10°C per minute to 160° C). The variance for this assay was 0.002 and the variance for the preparation of the samples was 0.046 (n=3). Total phenol concentration was measured using the Folin Ciocalteau method (Cheung, Cheung et al. 2003) measuring absorbance at a wavelength of 765nm.

4.4. Results and Discussion

4.4.1. Effluent composition

In an initial investigation, the composition of the winery effluent at Cellar 2 was determined at the beginning of the wine producing season, in order to identify the most significant components of winery effluent on the basis of concentration (Table 4.1) and their contribution to the COD. Na, K, Ca, Mg and Fe are the dominant metallic species and more specifically, Na and K were identified as being the most important metallic components in winery effluent based on prevalence. Although Ca is more abundant than Na, it was excluded because it occurred naturally in the groundwater at this site in similar concentrations. This is in agreement with data obtained by (Bustamante, Pareded et al. 2005) and (Sheridan, Bauer et al. 2005) who found these two components to be prolific in winery effluent.

No glucose was detected in any of the samples tested over the course of this study, although other authors (Malandra, Wolfaardt et al. 2003, Colin, Bories et al. 2005) found both fructose and

glucose in the effluent samples. A GC-MS analysis indicated the following components to be the primary organic constituents in the effluent study: ethanol, acetic acid (ethanoic acid), i-propanol, i-propanoic acid, i-butyric acid (iso-butanoic acid) and valeric acid (iso-pentanoic acid). These results are in agreement with data from Colin et al (2005) who found that ethanol was the main organic component of winery effluent.

The total polyphenol content of the winery effluent was measured (using the Folin Ciocalteau method) and was found to be between 17.72 ± 2.10 mg/L and 37.08 ± 10.29 mg/L (two separate samples taken on different days, 3 replications of each sample). This variation is likely due to the samples being taken on different days. These concentrations are in agreement with data presented by (Malandra, Wolfaardt et al. 2003) and (Petruciolli, Duarte et al. 2001). Relative to the dominant organic components, these levels are insignificant on the basis of concentration. Based on earlier studies (Sheridan 2003, Chapman 1996, Radford 2002) nitrogen and phosphorus are not significant components of winery wastewater, relative to the other compounds.

Using these preliminary findings, and based on their abundance, the following components were selected as being important components for the purpose of modelling the degradation of winery effluent: pH, Na, K, ethanol, propanol, acetic acid, propanoic acid and butyric acid. COD was also measured for comparison.

Table 4.1. The composition of winery effluent at Cellar 2 as determined by an initial investigation at the beginning of the harvest season

Component	Concentration (mg/L)	Standard Deviation (mg/L)	Method
Zn	0.71	0.00497	AA
Mg	12.3	0.0123	AA
Ca	59.3	0.5337	AA
Na	54.5	0.109	AA
K	82.9	0.1658	AA
Cu	0.03	0.00612	AA
Fe	21.35	0.06405	AA
Mn	0.29	0.00203	AA

Cr (Total)	Not Detected	Not Detected	AA
Pb	0.11	0.02541	AA
B	Not Detected	Not Detected	AA
As	Not Detected	Not Detected	AA
Glucose	Not Detected	Not Detected	HPLC
Fructose	Not Detected	Not Detected	HPLC
Citric acid	Not Detected	Not Detected	HPLC

4.4.2. Annual monitoring of the effluent at Cellar 1

The composition of the effluent has been plotted over the course of a year (Figure 4.1). Individual components of the effluent are discussed below.

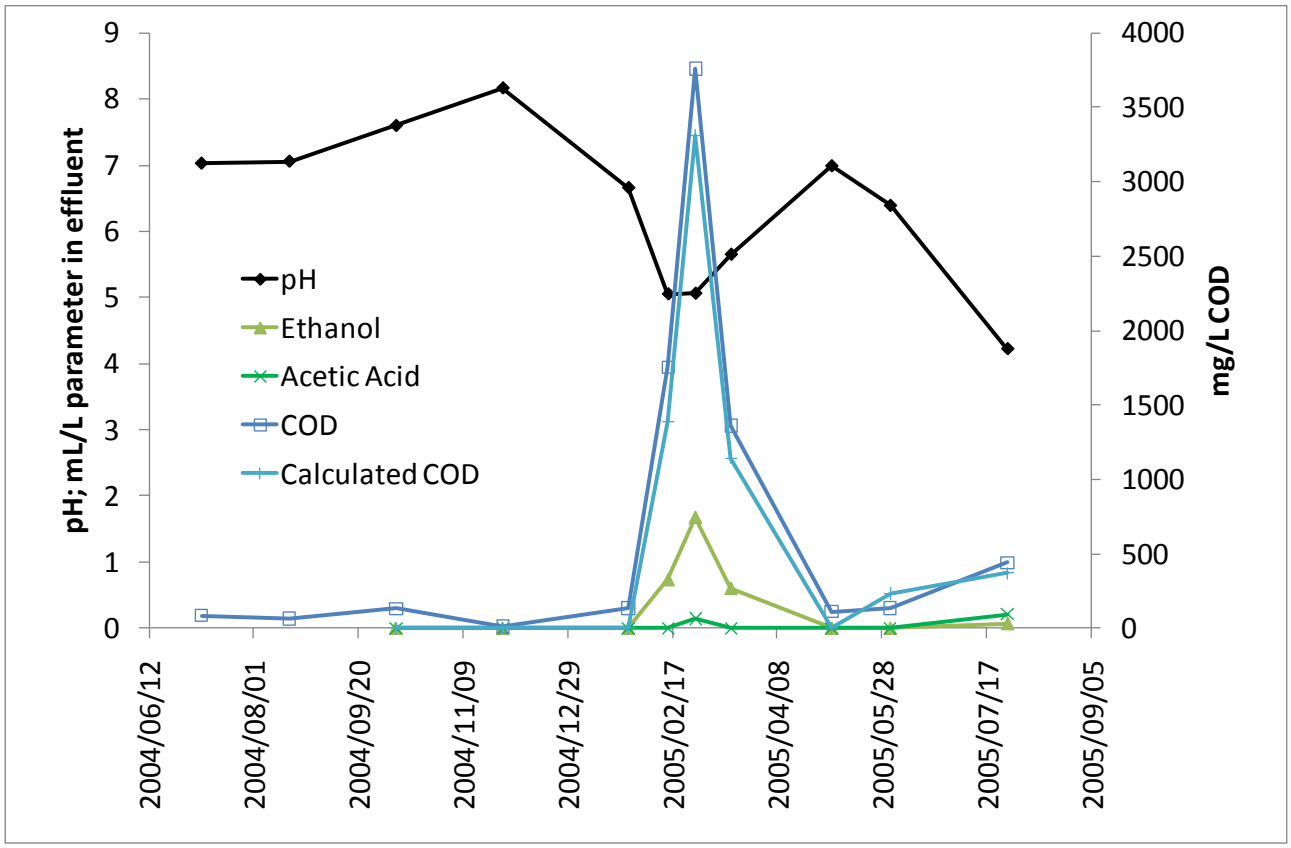


Figure 4.1. Organic components (ethanol and acetic acid) overlaid on pH and COD at Cellar 1

4.4.2.1. pH of the effluent (Cellar 1)

The pH was expected to be lower during harvest than at other times of the year due to the low pH of grape juice and wine (typically 3-4). The effluent was shown to have a pH of approximately 5 during the peak harvest period. The pH was unexpectedly low in August 2005, however, and this was ascribed to an observed once-off pulse of high strength effluent, which was not typical during this period and possibly due to wine handling operations (wine is naturally of a low pH and ethanol is degraded to acetic acid further reducing the pH).

4.4.2.2. Ethanol and propanol (alcohols) concentration (Cellar 1)

The ethanol concentration ranges from not detectable (indicated as 0 mL/L) to 1.7 mL/L which is approximately one third of that found by (Colin, Bories et al. 2005). Although propanol was defined as an abundant component based on the initial characterisation, for this particular winery effluent, it was not detected in any of the samples. This is indicative of the variability of the winemaking process.

4.4.2.3. Carboxylic acid occurrence (Cellar 1)

In most samples, the carboxylic acid levels were below detection and where found they rarely exceeded 0.2 mL/L. Propanoic acid and butyric acid are not shown in Figure 4.1 since their concentrations rarely exceeded 0.2mL/L. The contribution of carboxylic acids to the pH is significant which is shown by the peak in August 2005, which brought the pH of the effluent down to 4.2. Whilst acetic acid is relatively biodegradable, at these maximum observed concentrations it contributes to the environmental burden to the extent that the effluent is too acidic for general disposal under SA law (Government Gazette 2001). Propanoic and butyric acid are primarily important because they contribute significantly to the malodour of winery effluent. It was noted that the effluent had a particularly unpleasant odour in early June 2005, the same time that a pulse of propanoic acid was recorded.

4.4.2.4. Chemical oxygen demand (COD) (Cellar 1)

In Figure 1 the annual variation of the COD is shown as measured COD values and calculated COD values. COD is a measure of the oxygen that would be required to completely oxidise all constituents (organic and inorganic) of a given effluent. Thus for an effluent which is primarily ethanol and ethanoic acid (90% and more) Reactions 1 and 2 could be used to estimate the COD through calculating the stoichiometric oxygen requirements for complete combustion:

$$C_2H_6O + 3O_2 \rightarrow 2CO_2 + 3H_2O$$ Reaction 1

(ethanol oxidises to carbon dioxide and water)

$$C_2H_4O_2 + 2O_2 \rightarrow 2CO_2 + 2H_2O$$ Reaction 2

(ethanoic acid oxidises to carbon dioxide and water)

Thus, the volumetric concentrations of ethanol and ethanoic acid can be converted to molar concentrations, the molar quantity of oxygen required for complete oxidation can be calculated and this can be converted to a mass based oxygen requirement, relative to volume such as mg/L which is the norm for expressing COD. This is referred to as the calculated COD, as opposed to the measured COD, which utilises a reaction kit and is discussed in Methods. The COD of the effluent peaked in mid March (which is mid harvest) and decreased for the rest of the year; this is in common with the findings of others (Sheridan 2003, Malandra, Wolfaardt et al. 2003, Colin, Bories et al. 2005). The maximum concentration found (3800 mg/L) is also in the expected range for a cellar of this size (Sheridan 2003).

Because legislation primarily focuses on COD (with an upper legislative disposal limit of 5000mg/L) and not the specific organic components of the effluent, the calculated COD was compared to the measured COD. It was found that ethanol is the most important contributor to the effluent COD, and together with acetic acid, accounts for 86% of the measured COD (ethanol contributed 84% of the COD in this sample, and acetic acid 2%). This is in agreement with the findings of (Colin, Bories et al. 2005).

4.4.2.5. Metallic components of Cellar 1 effluent

Sodium and potassium were found to be the most prevalent metallic species in the initial effluent samples and were therefore investigated over the year. The results are shown in Figure 4.2, and clear trends can be observed.

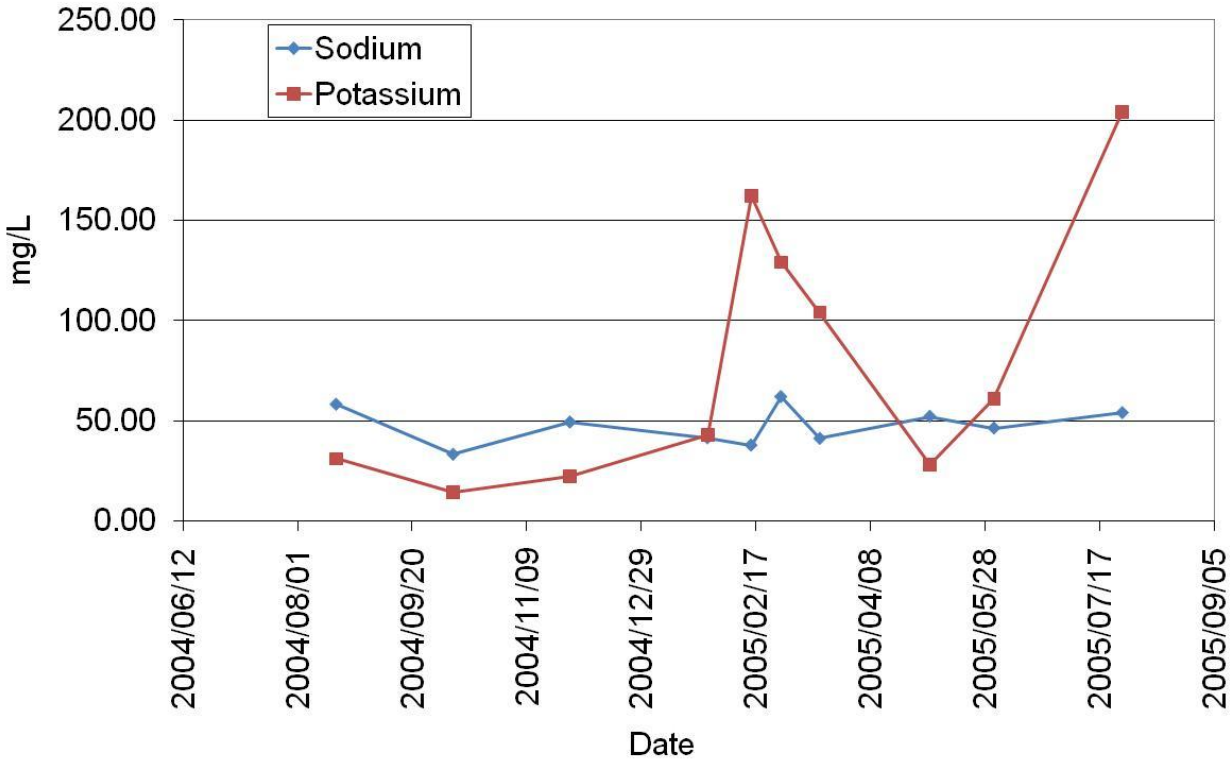


Figure 4.2. Cationic components in winery effluent measured over a year at Cellar 1

Potassium concentrations rose significantly during harvest and subsided to a base level after the harvest. Potassium is the primary cation in grapes, where it plays an important role for grapevine metabolism, and is the most important inorganic solute in plants (Marschner 1983). This explains the rise of potassium levels in the effluent during harvest period, and the subsequent drop once the juice and wine spillage ceased after harvesting. The sodium levels, however, remained relatively constant over the course of a year. At the winery investigated, the sodium concentration of the fresh water was 37.70 mg/L, and Na_2CO_3 is used for cleaning throughout the year. Since the same water source was used throughout the year, and the cleaning chemicals were also unchanged, there was no reason for the concentration of sodium to change. As was observed in the pH and levels of acetic acid, there was a spike of potassium in the effluent in August 2005, and all of these factors confirm a spill or release of wine (or possibly lees) just prior to sampling.

4.4.3. Seasonal monitoring of the effluent at Cellar 2

Since harvest time is the season of peak effluent strength, daily sampling of the effluent was conducted in order to gain an understanding of the daily variation at Cellar 2. The composition of

the effluent has been plotted in Figure 4.3 for the duration of a harvest season. Individual components are discussed separately below.

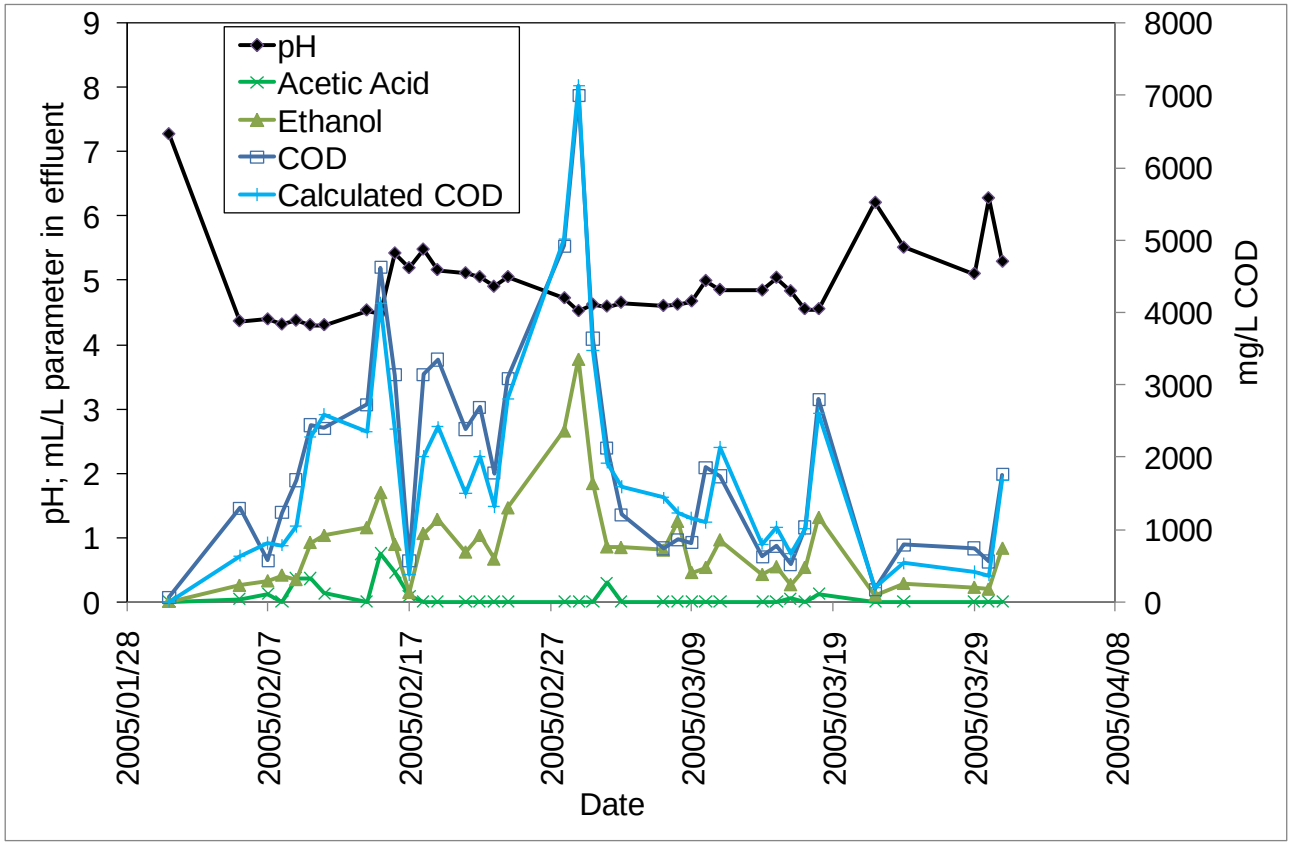


Figure 4.3. Organic components (ethanol and acetic acid) overlaid on pH and COD at Cellar 2

4.4.3.1. pH of the effluent (Cellar 2)

The data indicate that the pH was approximately constant and not dependent on the time of sampling within the harvest period. The average pH was 4.94 with a standard deviation of 0.61, in comparison to the fresh water at this cellar which has a pH of 7.63. The increase in pH at the end of March is related to the absence of harvesting over the Easter weekend, and the subsequent decline in activities towards the end of the harvest period.

4.4.3.2. Ethanol and propanol concentration (Cellar 2)

The concentrations of ethanol and propanol in the effluent were analyzed and the concentration of ethanol is shown in Figure 4.1 for the period running from early February to late March 2005. Propanol was detected occasionally with values reaching up to 0.2mL/L, but remaining mostly below the detection limit. The ratio of propanol to ethanol never exceeded 0.11 and was usually much lower, which implies that the quantity of propanol is insignificant in relation to the ethanol. The concentration of ethanol ranged from 0.2 mL/L to 3.75 mL/L. This was significantly more than

that found in Cellar 1 although (Colin, Bories et al. 2005) detected up to 4.9 g/L, which is approximately 50% more than that detected in this study. This variation can be explained by the differences between cellars pressing different tonnages of grapes and water handling practices.

4.4.3.3. Carboxylic acids (Cellar 2)

The concentration of acetic acid and ethanol in the effluent is shown in Figure 4.3. This data is inconclusive: where there was a significant amount of ethanol in the effluent, there was no corresponding significant quantity of acetic acid. It was expected that the levels of acetic acid in the effluent would be related to those of ethanol, but they follow no clear pattern. The concentration of propanoic acid and butyric acid was to be generally low; with a maximum of 0.2mL/L, but mostly below detection. As stated previously, these acids are not significant in terms of their contribution to the effluent COD, but they are significant environmentally because of their malodour. These findings are similar to those found in the effluent of Cellar 1 and also by Malandra, Wolfaardt et al. (2003).

4.4.3.4. Chemical oxygen demand (COD) (Cellar 2)

The COD of the raw effluent was assessed and is shown in Figure 4.3. The graph depicts the increase in COD from pre-harvest until the middle of the harvest, and the decrease from the middle to the end of the harvest. This trend was expected as the rate of processing increased from the start to the middle of the harvest and then decreased towards the end of the harvest. The calculated COD was found by calculating the stoichiometric oxygen requirements for the complete combustion of the organic components found in the effluent (as described earlier). The calculated COD includes the contributions from the organic components (ethanol, acetic acid, propanol, propanoic and butyric acid) and this method can account for approximately 91% of the COD of the raw effluent of Cellar 2. The implication is that the COD of the raw effluent from a winery can be calculated with reasonable accuracy if the ethanol and acetic acid concentrations of the effluent are known.

4.4.3.5. Metallic components of Cellar 2 effluent

Sodium and potassium were analyzed routinely, based on the initial effluent determination discussed above, with these two cations being the most abundant. The concentrations of sodium and potassium found in the effluent are shown in Figure 4.4.

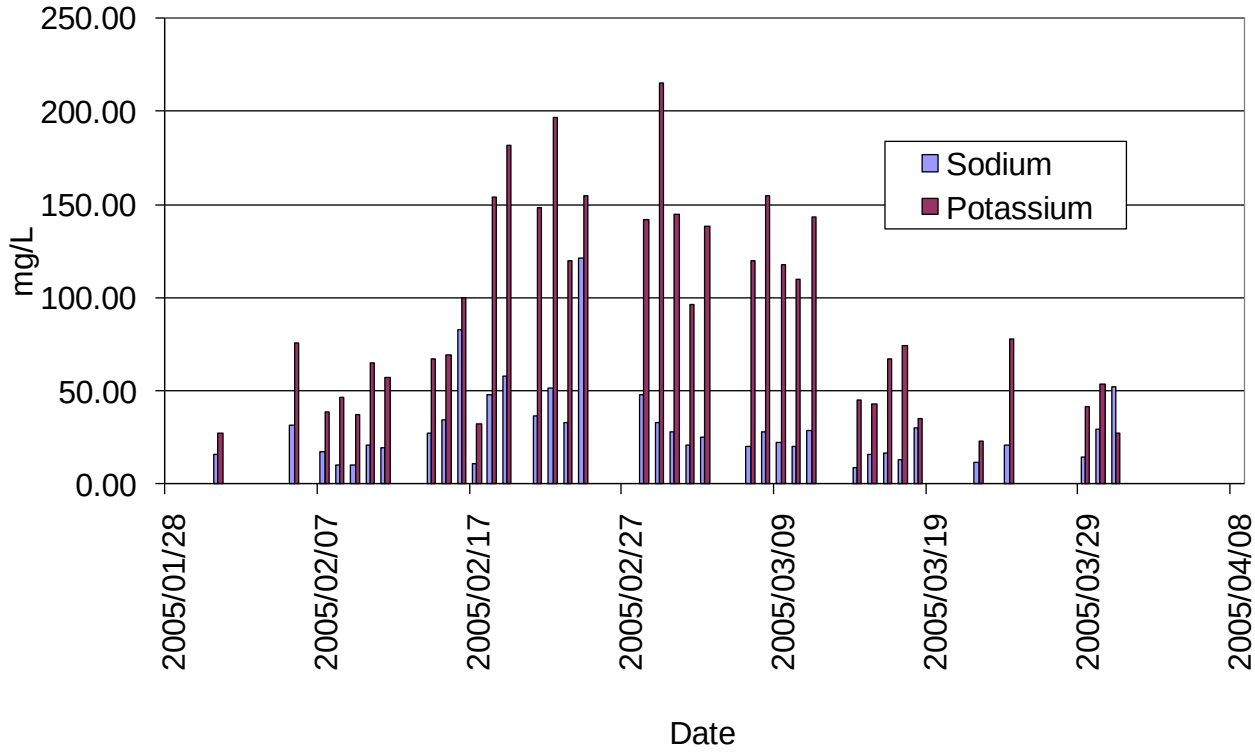


Figure 4.4. Cationic components in winery effluent measured over a harvest season at Cellar 2

Sodium was expected to arise in the effluent from cellar cleaning operations (caustic soda and sodium carbonate are used to clean dirty and stained tanks). Sodium levels varied widely from 8.9mg/L at the beginning of the harvest to a once off peak of 121mg/L at the height of the harvest and around 20 mg/L towards the end. The occasional spikes are consistent with cleaning activities in the cellar, which would occur on an ad hoc basis (as and when required). The average Na concentration over the harvest period was around 40 mg/L.

The potassium levels were strongly affected by the time of sampling within the harvest season. Potassium values rose from 22.9 mg/L to 225 mg/L at the peak of the harvest and then declined to background levels at the end of the harvest. This increase is consistent with the fact that potassium is a major inorganic constituent of grapes and hence grape juice and wine (Sheridan 2003). The potassium concentration range is within the range of values found by others (Malandra, Wolfaardt et al. 2003, Sheridan, Bauer et al. 2005).

4.5. Discussion of the variation of winery effluent

It was found that ethanol is the major constituent of winery effluent in Cellar 1, contributing 86% of the COD, with ethanol concentrations ranging from below detection to 2 mL/L in the effluent.

Acetic acid is the second organic component that contributes significantly to the COD of winery effluent and was found to occur at concentrations as high as 0.4mL/L. The maximum COD recorded was 3760mg/L. Similarly, for Cellar 2, ethanol was found to be the major constituent contributing approximately 91% of the COD and rising to concentrations as high as 3.75mL/L. Acetic acid was found to have concentrations as high as 0.75mL/L on certain days. The maximum COD of 7000mg/L found at cellar 2 is well within the normal range expected for a winery of this size (Sheridan, Bauer et al. 2005). The difference between cellars is due to the natural variance of the process, the degree of spillage, and due to the type of spillage; whether juice or wine was spilt. The data support the postulation that acetic acid would be the primary contributor to a decrease in pH and that ethanol is the primary component of the COD. In both cellars, the calculated COD was found to be similar to the measured COD, which is a valuable indicator of the accuracy of both the COD test, as well as the GC method.

For both cellars, the average pH of the effluent during the harvest period was approximately 4.9. This value is outside the lower limit for legal disposal without some form of treatment in South Africa (Government Gazette 2001). Since most of the acidic components of the effluent are readily biodegradable, chemical pH control would unlikely be required if the effluent was treated, by whatever method.

For both cellars the concentration of potassium in the effluent ranged from approximately 20mg/L to 220mg/L and was strongly dependent on the time of year and the intensity of the harvest season. The presence of potassium was very likely related to the natural quantities of potassium in grapes.

Sodium concentrations ranged from approximately 25mg/L to 80mg/L in the effluent from Cellar 1 and from approximately 10mg/L to 125mg/L in the effluent emanating from Cellar 2. The concentrations were roughly independent on the harvest and associated mostly with the background concentration of Na in the fresh water used in the cellar and the ad-hoc use of cleaning agents. The use of sodium based cleaning agents by wineries must be discouraged since the longevity of sodium cations in the environment is a concern, especially as it causes sodicity of the soil. Potash (potassium hydroxide) is as effective as sodium hydroxide for cleaning the precipitated tartrates from tanks, and potassium is also absorbed by the environment if it is released.

Whilst other components, such as longer (C_3, C_4, C_5) carboxylic acids, other organic acids and phenolic components, are present in winery effluent, they are not significant for determining/sizing a treatment method/plant. The peak of the effluent strength (maximum COD) occurred in the middle of the harvest period. This suggests that two weeks of intensive sampling on either side of the middle of the harvest period should be sufficient accurately characterize the peak effluent strength.

The winemaking process is inherently varied (Sheridan, 2003), and this variation is evident in the data presented here. Not all grape varietals ripen at the same time, and thus there are lulls within the harvest season. When this occurs, cellar washing is often made a priority, and on these days the quantity of effluent is greater, and the concentration of sodium is higher. On days when harvesting occurs, wine and juice transfer is most prevalent, and these are the days when the organic components of the effluent are likely to be the most significant. Since each winery has its own associated set of grape varietals, and its own unique climatic conditions, it may not be possible to extrapolate this data to other cellars.

4.6. Conclusions

The findings presented here profile the effluent from two different wineries over different periods of time. In the first section, the effluent is profiled for the duration of a year, and the peak effluent was found to occur during the harvest period. In the second section it has been shown that the peak of the harvest occurs approximately midway through the harvest.

Winery effluent poses a problem in terms of disposal without treatment because of the high concentration of ethanol present. This quantity of ethanol may indicate process inefficiencies (especially the loss of wine). If the final product from the winery is 13% ethanol and the effluent stream is 0.4% ethanol (both V/V) as measured in this study, a significant loss of product could have been incurred if a large quantity of effluent was produced. Without cleaner production strategies, or adherence to waste minimization programs, the ethanol (together with the other 10% of the COD of the raw effluent) will have to be treated before disposal.

Whilst the data generated in this study provides detailed information on the composition of raw winery effluent, they are also useful for determining those specific kinetic rate constants which need measurement in order to determine the degradation rate of winery effluent during treatment. However, the correlation between COD and ethanol concentration may no longer hold

once the process of effluent degradation has begun. The data and correlations presented here, are useful, however, to indicate trends as they occur over the course of a year, and could serve to inform the design of effluent treatment for the peak effluent periods of the year, as well as the likely composition and strength of that peak. The data could also be used for preparing an artificial effluent for research purposes.

5. Turning wine (waste) into water: Towards technological advances in the use of constructed wetlands for winery effluent treatment

In this Chapter an in depth investigation of the hydraulic behaviour of the VSR conducted the research on at the ARC Nietvoorbij VSR is presented.

This Chapter has been submitted for peer review and publication to the AIChE Journal. An abbreviated form of this Chapter was also presented at the 12 International Conference of Environmental Science and Technology, at Rhodes, Greece in 2011. A copy of the paper from the proceedings of this conference is presented in Appendix HHHH. The contribution of the co-authors towards the work is primarily that of supervision or collaboration and the experimental work and write-up was conducted by the author of this thesis. The original data for this experiment is presented in Appendices C to Y.

5.1. Abstract

Environmental concerns for wineries in South Africa cover not only the conversion of effluent into more benign forms, but the reclaiming of water, a resource that is scarce and precious in a drought-prone country. However, not all waste treatment options are available to small wineries, because many are too sophisticated and expensive to be commercially viable. Accordingly, the research presented in this Chapter describes an investigation into the use of constructed wetlands in the form of Vegetated Submerged Reedbeds (VSR) as a practicable alternative for small-scale wine producers. In this study, it was found that the hydraulic processes occurring within the VSR to display significantly non-ideal behaviour. It was also found that if the feed to the VSR was located on the surface that the dead volume accounted for approximately 25% of the non-ideal behaviour of the system and that bypass accounted for a further 6% of non-ideal behaviour. In the system studied, there was a preferential flow pattern within with the greatest flow occurring closest the surface and in the centre, and the least at the sidewalls. It is proposed that the flow profile can be conceptualised as being hull-shaped. It is believed this hypothesis is correct and as far as we are aware this flow pattern has not been described previously. This profile was found to be the same for irregularly shaped gravel and for spherically shaped gelatinous beads and therefore it is believed not to be dependent on the geometry of the VSR or the packing medium.

5.2. Introduction

Winemaking in South Africa is primarily restricted to the winter rainfall and semi-arid areas of the Western and Northern Cape provinces. Geographically, these areas are characterised by low population densities (excepting the metropolitan area of Cape Town) and limited water resources. Farms often rely on farm-dam or spring water, the supply of which is highly variable. Those farms located near the Cape Town metropole can access municipal water from the Theewaterskloof Dam, which is situated within 100km of Cape Town, but this water is expensive, and farmers are competing with human and industrial consumption needs.

Winemaking is very similar to conventional chemical engineering. The process begins with a raw material (in this instance grapes). Some kind of beneficiation or size reduction process is conducted to speed up the rates of chemical reaction, which in winemaking is the conversion of glucose and fructose to ethanol. This yields a product—wine. As with all other industries, winemaking creates waste streams and as with all other chemical industries, this effluent has to be disposed of.

The water that enters the process that converts grapes into wine will leave as wastewater (since in South Africa it is illegal to add water to wine). The wastewater contains spillages from processing and handling, the residues of washing the tanks, intentionally drained wet waste products such as lees, and potentially other contaminants, such as agricultural manure. All wineries are expected to conform with legislation relating to the treatment or disposal of waste streams (Government Gazette 2009, Government Gazette 2001, Government Gazette 1998a, Government Gazette 1998b). Thus, if a winery discharges effluent into a sewer, it must ensure that it is under the maximum allowable limit on the COD (chemical oxygen demand) and the quantity of sodium it contains, as these are the criteria most relevant to winery effluent (Sheridan, Glasser et al. 2011a). The specific parameters applied will depend on the requirements of the municipality that manages the sewer. On the other hand, if the wastewater is to be released to the environment, the permissible strength of the chemicals in the waste will be governed by national rather than local legislation, although it will also depend on whether the environment in question is pristine or not.

Many wineries (46%) are small, and press less than 100 tons of grapes per annum (SAWIS 2012). Thus, using the method developed by Sheridan (Sheridan 2003) it is assumed that just under half of all wineries in South Africa consume fewer than 1000 litres of water per day and produce a corresponding quantity of effluent. These small wineries can be licensed to irrigate their

wastewater to a pasture, provided both that the COD does not exceed 5000mg/L and that they irrigate less than $50m^3$ per day (Government Gazette 2001). The Department of Water Affairs discourages this practice, even by those who comply with the limit, because it is considered wasteful of water.

Because many wineries exceed the limits described above in terms of COD(Sheridan 2003), they are required to treat their wastewater by some form of processing before releasing it. Winery wastewater treatment techniques are diverse, but all have the same goal, which is to reduce the COD. Treatment technologies include using sequencing batch reactors (SBRs), aerobic digestion, anaerobic digestion, rotating biological contactors, settling ponds and constructed wetlands (CWs) (Sheridan 2003, Malandra, Wolfaardt et al. 2003). With the exception of the last, all these systems are capable of almost full effluent treatment. However, the technologies are costly, and require staff trained to operate and control them. The smaller wineries in particular cannot afford to employ such specialised kinds of personnel, and therefore cannot use these sophisticated systems reliably.

This is the reason why, in the research described here, we chose to investigate the last and most under researched of the waste treatment options described above, in this case the use of vegetated submerged reedbed (VSR) type CWs. There are a number of reasons, apart from cost-saving and the relative simplicity of the technology involved, for believing that a CW offers the best option for small-scale wineries. Some of these are technical, for example:

- it is a low-maintenance treatment system;
- the treated water can be re-used; and
- preliminary tests indicate that CW plants can thrive in the effluent created by wineries.

However, a living treatment system is not only effective, but offers a number of benefits in a wider, environmental and social context, which include but are not restricted to:

- the aesthetic qualities of a constructed wetland;
- its production of biomass like cut flowers and thatching materials; and
- the potential use of this biomass to provide a means of livelihood to low-income farming communities (a significant factor in a developing country).

In South Africa, the use of CWs for winery effluent treatment is a very recent development. At present there are only a few such systems in existence (personal knowledge). The design briefs for

these systems are mostly heuristic, that is, they remain at the mathematical rules-of-thumb stage. This research was conducted on the basis of just such a CW, which had been constructed by the agricultural research council (ARC) at their Nietvoorbij Campus in Stellenbosch. The aim was to conduct experiments to determine the properties of treatment process (listed below), and to use these to establish more rigorous design principles. The initial research investigated the aspects of winery effluent treatment considered most significant.

1. The composition of winery effluent and its temporal variations: what does it consist of, how does it change over the duration of a harvest period, and how does it change over the course of the year? Answering these questions required analysis of the effluent over a full year.
2. The behaviour of effluent flowing through the CW: is there any bypass of flow or 'dead' volume within the CW that makes it less efficient? These data were obtained by running a tracer impulse-response experiment, by means of which the mean residence time and the dispersion within the system were measured. This method was also used to identify whether the CW behaved like a plug flow, stirred tank reactor or series of stirred tank reactors, or any combination thereof.
3. The rates at which the components of winery effluent are degraded. Answering this question required the use of the data obtained from both 1. and 2. above.

If points one to three could be answered, it was hoped that we would be able to develop a model that would predict the behaviour of the system accurately. This could then be used to design new VSRs that treat winery effluent more efficiently than the existing models. On the other hand, it was recognised that the possibility that the experimental results might indicate that the treatment process is too complex to make prediction feasible. Even if the latter proved to be the case, it was reasoned that the findings would yield data that had not been considered before, such as the rates of decomposition of the winery effluent components. Both would be useful to designers of VSRs.

As indicated above, the research was broken into three segments. The first portion was an analysis of winery effluent. A report on this work has already been published (Sheridan, Glasser et al. 2011b), but to sum up our most significant results, it was found that in the winery effluent tested, ethanol comprised approximately 90% of the COD, and that ethanoic acid constituted most of the rest. (Other minor organic components of the effluent included propanol, propionic acid, and butanoic acid. The principal inorganic constituents of the effluent were sodium and potassium. Nitrate and phosphate were present, but in insignificant amounts.) The COD was

variable, and could be directly related to the number of tons of grapes harvested. However, COD concentrations higher than 7000 mg/L during this investigation were seldom encountered.

The second portion of the research involved an investigation into the hydraulic behaviour of the VSR, which forms the subject of this Chapter. To our knowledge, this is the first study of this kind on a CW system being used to treat winery effluent. The findings were of interest because they showed that the flow profile had a distinctive shape that suggested the presence of 'dead areas' in the movement of effluent through the VSR. Methods were therefore by means of which the flow rate (and with it the overall treatment capacity of the VSR) could be raised to optimal efficiency. In the third section the measurement and interpretation of the rate constants of the processes of degradation are presented. This topic too was presented in a separate Chapter.

The focus of the research experiment described in this chapter is threefold: to report on the data measured; to develop a hypothesis from the data obtained; and to test it. There are four components to the hypothesis.

- There is a preferential flow pattern within a VSR, with the greatest flow occurring closest the surface and in the centre, and the least at the sidewalls, if the flow is applied to the surface of the VSR at the feed position. This is conceptualised as a hull-shaped velocity profile.
- The hull shaped profile is formed irrespective of the shape of the packing medium.
- This hull-shaped profile can be reproduced in a laboratory-scale experiment using spherically shaped packing.

The profile can be changed by altering the location of the feed, and the dead volume can be significantly reduced by introducing a fully-distributed feed and outlet system.

5.2.1. Modelling Constructed Wetland Systems

For approximately a century, CWs have been used to provide biological treatment for wastewaters and effluents (Tchobanoglous, Burton et al. 2003). These constructions are typically packed with gravel, custom packing materials such as high-surface area media, or packing plates (Vohla, Kõiv et al. 2011). Vegetated trickle bed filters (also referred to as vegetated submerged reedbeds—VSR, or horizontal sub-surface flow constructed wetlands) are a type of trickle bed filter, which is colonised by macrophytes on the surface. VSRs can be successfully modelled using fundamental

chemical engineering theory (Sheridan, Glasser et al. 2011a, Rousseau, Vanrolleghem et al. 2004, Werner, Kadlec 2000, Martinez, Wise 2003, Villaseñor, Mena et al. 2011, Kadlec 2003, Suliman, Futsaether et al. 2006, Stein, Towler et al. 2006, Sheridan, Peterson et al. 2006, Carleton, Montas 2010). If the flow is assumed to be ideally mixed, the system can be modelled on that of a continuous stirred tank reactor (CSTR). If the flow is assumed to behave like an ideal plug, the system would follow the model of an ideal plug flow reactor (PFR). Other types of reactor model are described in the literature(Levenspiel 1972). In practice, few reactors are ideal, and phenomena such as dispersion, diffusion, dead zones and short-circuiting of the fluid are relatively commonplace (Fogler 2005). In VSRs, the flow regime may be typical of neither a PFR nor CSTR, but display characteristics of both. This implies that the time that the reactants remain inside the reactor may be significantly different from that envisaged in the design criterion. Therefore measuring the residence time distribution (RTD) of the reactor and determining the mean residence time are necessary for accurate model description.

5.2.1.1. Kinetic vs. hydraulic formulae as reactor models.

The literature on the subject describes different types of mathematical formulae for CWs, but these can be broadly broken into four types: empirical, kinetic, hydraulic, or a combination of kinetic and hydraulic.

Regression analysis has been used to model constructed wetlands at least since the early 1990s (Kadlec, Knight 1996, Wood 1995, Griffin, Bhattarai et al. 1999, Reed, Brown 1995, Vymazal 1998). Some of these correlations are given in Table 5.1. These relationships relate to either the load of the effluent applied to the CW or to the concentration of the effluent.

Table 5.1. Regression equations for the removal of COD or BOD in CWs (adapted from (Kadlec, Knight et al. 2000)).

Number	Equation	r^2
1	$C_{Out} = (0.11 \cdot C_{In}) + 1.87$	0.74
2	$C_{Out} = (0.33 \cdot C_{In}) + 1.4$	0.48
3	$C_{Out} = 502.2 \cdot e^{-0.111T}$	0.69
4	$C_{Out} = (0.099 \cdot C_{In}) + 3.24$	0.33
5	$L_{\mathrm{Re}moved} = (0.653 \cdot L_{in}) + 0.292$	0.97
6	$L_{Out} = (0.145 \cdot L_{in}) - 0.06$	0.85
7	$L_{Out} = (0.13 \cdot L_{in}) + 0.27$	0.57
8	$L_{Out} = (0.17 \cdot L_{in}) + 5.78$	0.73

As a thought experiment these equations have been used to calculate the outlet COD from a CW treating an influent of 100mg/L of COD. The outlet COD for this hypothetical CW is presented in Figure 5.1. It is clear from this plot that substantially different effluent degradation is predicted (±300%) by using the different regression correlations.

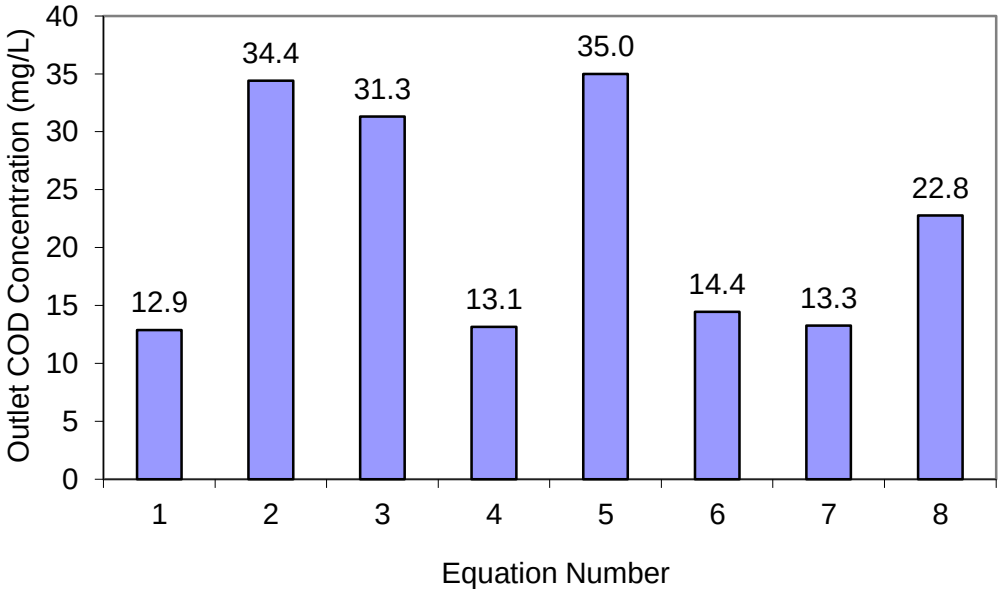


Figure 5.1. Variation of the outlet concentration for a given inlet concentration of 100mg/L COD for the correlations presented in Table 1.

Kinetic equations are used to describe the outlet concentration, usually as a function of the inlet concentration and the rate constant, k, which is sometimes expressed in different ways, for example the time-dependent retardation model (Shepherd, Tchobanoglous et al. 2001). Hydraulic equations are normally derived from investigation of the way in which the wastewater flows through the CW. Applying such a mathematical formula yields information on the mean residence time and the degree of dispersion, which can then be used to arrive at a conceptual reactor that determines the outlet concentration. This is a function of many variables such as inlet concentration, the length of the CW, the velocity of the rate at which the fluid passes through it, the rate constant and the degree of dispersion, D. Depending on the type of reactor described (a plug flow or tanks-in-series), the dispersion number can also be used to calculate the number of tanks, N. Finally, there are some reactors that require a component of kinetic and hydraulic modelling. An example of such a reactor is presented in this Chapter.

A summary of a number of these models is presented in Table 5.2, which is adapted from that drawn up by Villaseñor et al. (Villaseñor, Mena et al. 2011).

Table 5.2. Different CW models presented as either being kinetic or hydraulic in method

Hydraulic Model→ Kinetic Model ↓	Ideal Plug Flow	Plug Flow with Dispersion	Tanks-in-series
k-C	$\frac{C_{out}}{C_{in}} = e^{-kt}$	$\frac{C_{out}}{C_{in}} = \frac{4 \cdot q \cdot e^{\left(\frac{Pe}{2}\right)}}{(1+q)^2 \cdot e^{\left(\frac{Pe \cdot q}{2}\right)} - (1-q)^2 \cdot e^{\left(\frac{Pe \cdot q}{2}\right)}}$	$\frac{C_{out}}{C_{in}} = \frac{1}{(1+k\tau)^N}$
k-C*	$\frac{C_{out} - C^*}{C_{in} - C^*} = e^{-kt}$	$\frac{C_{out} - C^*}{C_{in} - C^*} = \frac{4 \cdot q \cdot e^{\left(\frac{Pe}{2}\right)}}{(1+q)^2 \cdot e^{\left(\frac{Pe \cdot q}{2}\right)} - (1-q)^2 \cdot e^{\left(\frac{Pe \cdot q}{2}\right)}}$	$\frac{C_{out} - C^*}{C_{in} - C^*} = \frac{1}{(1+k\tau)^N}$
Retardation (Shepherd, Tchobanoglous et al. 2001)	$\frac{C_{out}}{C_{in}} = \frac{1}{(1+bt)^{K_0/b}}$	N/A	N/A
Partial tanks in series (Kadlec 2003)			$\frac{C_{out}}{C_{in}} = \frac{1}{\left(1 + k_{app} \cdot \frac{\bar{t}}{P}\right)^P}$
Spatial tanks in series (Sheridan, Peterson et al. 2006)			$\frac{C_{out}}{C_{in}} = \frac{1}{\left(1 + k_i \cdot \frac{2}{3} \cdot \frac{l \cdot d \cdot w}{F \cdot N}\right)^N}$
ZDM (Werner, Kadlec 2000)	Zones of Diminished Mixing		
OTIS (Wynn, Liehr 2001)	One-dimensional Transport with Inflow and Storage		

where:

$$q = \sqrt{1 + \frac{4 \cdot Da}{Pe}} \qquad \text{Equation 5.1}$$

and the Damkohler Number, $Da = \frac{l \cdot k}{u}$ Equation 5.2

The kinetic formulae shown here which assume that the flow regime is ideal, introduce an error that may be significant under certain conditions. In addition, researchers using the retardation model, for example, seek to explain a change in the rate constant in terms of actual time spent in the reactor. (This should be distinguished from the mean residence time, which is the calculated average of the distribution of times for the entire contents of the effluent stream to pass through the reactor). We consider this approach misplaced, since lumped parameters (such as COD) will always display this type of behaviour. The change in rate of reaction is easily explained by observing that the more readily biodegradable substances in the COD (such as glucose) react quickly in comparison with the more recalcitrant substances it contains, like ligno-cellulosic materials. Believing that a more fruitful approach is to explain the effluent stream fully by characterising the components of lumped parameters, and to determine the different rate constants of the individual constituents, we have carried out the research and published our findings on the constituents of the effluent (Sheridan, Glasser et al. 2011b).

A kinetic or hydraulic model of a reactor can be used for describing the processes that occur in a CW. As noted the latter was chosen.

5.3. Finding the internal age distribution and calculating some hydraulic parameters

For a more detailed description of the methodology of conducting impulse-response tracer studies and the mathematical processing of the resulting data, the reader should refer to either Fogler (Fogler 2005) or Levenspiel (Levenspiel 1972). A tracer study needs to be done to determine the hydraulic parameters of any reacting system. Although this is normally conducted as an impulse-response tracer experiment, it can also be carried out as a step-change experiment. Both can be interpreted to provide mean residence times, degree of dispersion and so on. The internal age or residence time distributions (RTD) indicates the length of time that each molecule spends in the reactor. Some molecules will follow a short circuit from the feed to the outlet, whilst others will get caught up in dead volumes (that is, those parts of the VSR with zero flow). Both of these are discrepant from those that travel exactly as specified in the design brief. Because these particles take different paths, they spend varying amounts of time in the reactor. The distribution of these times can be plotted upon a graph (see Figure 5.4).

The shapes of the distribution presented in Figure 5.4 have significant statistical properties. The first moment of the age distribution is by definition the mean residence time, $\bar{t}_m$ (see Equation 5.3), and the second moment is notated as σ^2, which is calculated according to Equation 5.4. If the second moment is normalised, σ_θ^2 (Equation 5.5), it can be used to calculate the Peclet number (Pe), 1/Pe, which is the dispersion number (D) or the number of tanks, N, for a CSTR in series model.

$$\bar{t}_m = \sum_{i=1}^{n} t_i \cdot (t_i - t_{i-1}) \qquad \text{Equation 5.3}$$

$$\sigma^2 = [\sum_{i=1}^{n} {t_i}^2 \cdot E_i \cdot (t_i - t_{i-1})] - \bar{t}_m \qquad \text{Equation 5.4}$$

$${\sigma_\theta}^2 = \frac{\sigma^2}{{\bar{t}_m}^2} \qquad \text{Equation 5.5}$$

$${\sigma_\theta}^2 = 2 \cdot D - 2 \cdot D^2 \cdot \left(1 - e^{-1/D}\right) \qquad \text{Equation 5.6}$$

$$N = 1/{\sigma_\theta}^2 \qquad \text{Equation 5.7}$$

For packed-bed reactors (essentially plug flow with dispersion) the Peclet equation has been solved for first order reactions(Levenspiel 1972). In terms of conversion X, the rate constant is k; the Peclet number, Pe; the length of the system, l; and the velocity of the impulse, u, the Peclet equation is expressed as:

$$X = 1 - \frac{4 \cdot q \cdot e^{\left(\frac{Pe}{2}\right)}}{(1+q)^2 \cdot e^{\left(\frac{Pe \cdot q}{2}\right)} - (1-q)^2 \cdot e^{\left(\frac{Pe \cdot q}{2}\right)}} \qquad \text{Equation 5.8}$$

This equation has been used successfully by others (Werner, Kadlec 2000, Martinez, Wise 2003, Chazarenc, Merlin et al. 2003) to describe VSRs (since they are normally packed beds), and is shown in Table 5.2. VSRs are typified by a single-mode RTD with a characteristic long tail. The greater the value of D, the more non-ideal the flow within the system is.

Other methods for describing non-ideal flow have been reported in the relevant literature. (Perrson, Somas et al. 1999). Perrson *et. al.* in particular discusses the ratio of the measured residence time to the ideal residence time, and define an effective volume ratio as a function of the length to width ratio. This is given as:

$$V_{eff} = \frac{\bar{t}_m}{V/_F} \qquad \text{Equation 5.9}$$

This is a ratio of the residence times and not the volumes, because the authors felt that it was impossible to measure the dead volume directly. They also defined a hydraulic efficiency factor, λ, by means of which it is possible to compare different designs of reacting VSRs. This hydraulic efficiency factor is given by Equation 5.10, where N is the number of tanks in the TIS model.

$$\lambda = V_{eff} \cdot \left(1 - {}^{1}/_{N}\right) \qquad \text{Equation 5.10}$$

These parameters are used for comparison in this Chapter, to match against those used for our assessment of non-ideal behaviour.

5.4. Experimental Programme

In this study experiments were conducted in two stages. In the first, we investigated the existing VSR at the ARC Nietvoorbij in Stellenbosch, South Africa. An impulse-response tracer experiment was performed, the moments of the resulting distributions were analysed and used to develop an hypothesis on the flow characteristics of the system. This hypothesis was then tested by carrying out another impulse-response tracer experiment on a transparent laboratory-scale packed bed reactor, and analysing the moments of the resulting distribution. For testing our hypothesis, a glass reactor was built and filled with florists' polymer-based gelatinous balls that are roughly spherical in shape, approximately 10-15mm in diameter, and transparent. The rectangular glass reactor had nine dispersed inlet and outlet positions, and the inlet and outlet flows could be varied between using any one port and all ports simultaneously. The flow into the reactor was controlled, and the impulse was insertion by an injection of tracer into the feed line. The reactor setup allowed us to observe where the tracer was going, and to identify where the bypass and dead zones could be found. In both experiments, flow was observed to be laminar.

5.5. Materials and methods

5.5.1. Description of the experimental rigs/apparatus

5.5.1.1. Description of the physical properties of the VSR at the ARC, Stellenbosch

This VSR, which was built in about 2001, is a sub-surface flow constructed wetland 40m long, 4m wide and 1m deep. It was built on a slope with a gradient of approximately 2%, was lined with

black polyethylene pond-lining film, and filled with dolomite gravel ($CaMg(CO_3)_2$) with a mean particle diameter of 0.02m and a void fraction of approximately 40%.

The design specifications for the VSR are presented in Table 5.3.

Table 5.3. Engineering design specifications of the VSR

Design Specification	Value
Length	40m
Depth	1m
Width	4m
Lining	Plastic pond liner
Hydraulic Gradient	App 2%
Soil Matrix	Dolomitic Gravel
Average Matrix Particle Size	Approximately 20 mm
Matrix Void Fraction	40%

Fourteen sample ports constructed from a flexible PVC mesh were installed in the VSR for the purposes of this study. These flexible mesh strips were wrapped around a 100mm PVC pipe, joined and submerged vertically to a depth of 1m. The PVC pipes were then removed, leaving the mesh in place. Because it is inherently stable, the gravel did not collapse or force the closure of any sample ports at any time during the investigation. This feature of the design ensured that the sample ports did not impede the flow through the VSR. The grid of sampling ports was designed according to the published methodology given by Popek (Popek 2002). A schematic diagram showing the side and top views of the VSR is given in Figure 5.2. A photo of the system is given in Figure 5.2a. All the tailings were fed through sample port 5 into an open collection pond. Two meters were installed, a rain gauge and a water meter to measure the feed flow rate.

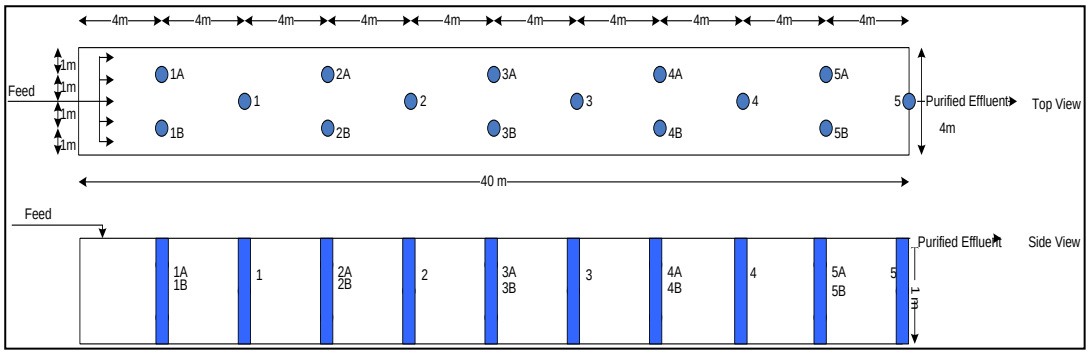


Figure 5.2. Schematic diagram of the VSR showing a side and a top view



Figure 5.2a. Photo showing the VSR

The VSR was originally planted sparsely with *Phragmites australis*, which partially colonised the surface as it grew. This planting also included a small number of ornamental plants, such as *Zantedeschia aethiopica*, *Chondropetalum tectorum* and *Cyperus papyrus*, on a trial basis. The

feed line was renovated to ensure the flow would be distributed as evenly as possible onto the surface at the entry-point end of the VSR.

5.5.1.2. Description of the laboratory-scale packed bed reactor

For this experiment we constructed a transparent glass reactor, 250mm high, by 250mm wide by 500mm long. The tank had nine inlet and nine outlet ports drilled into the sidewalls at the height to which the packing would fill the reactor. This would allow us to simulate any choice of flow pattern including flow along the top of the bed. Transparent polymer gel beads were used as the packing material. A sufficient number of the beads were placed in the tank to reach the height of the inlet ports—150mm, and these were hydrated in water. The tank had a total volume of 18.8L and the polymer beads had a measured void fraction of approximately 0.48. Thus the liquid volume was approximately 8.1L. A schematic of the apparatus is shown in Figure 5.3.

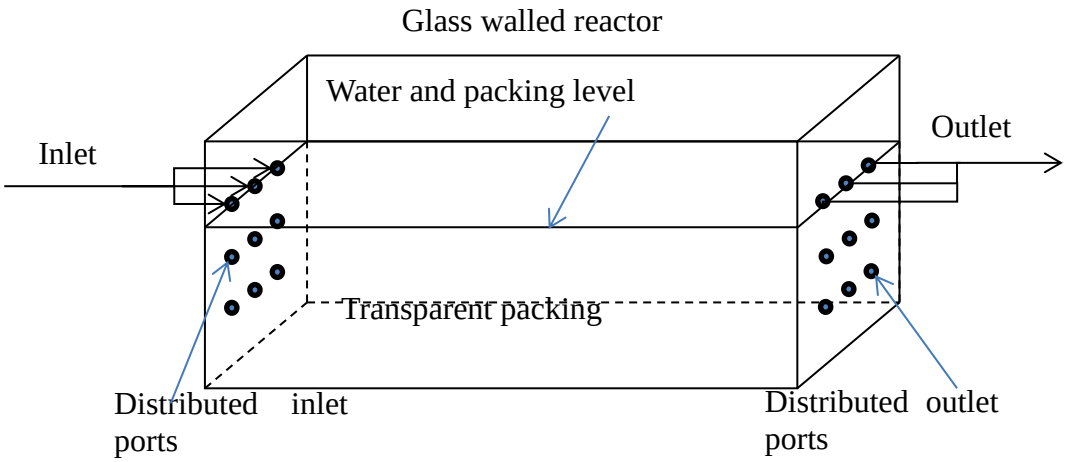


Figure 5.3. Laboratory apparatus used to test bed efficiency

5.5.2. Conducting the impulse-response experiments

5.5.2.1. Tracer experiments at the ARC VSR

A dose of potassium bromide was selected as the tracer to be pulsed through the VSR for the impulse-response experiment. The reasons for this choice were that bromide is highly soluble, is not adsorbed to or absorbed by the dolomitic matrix of the filter, is generally non-reactive, can be readily analysed and was an alien anion in the system studied. Before injecting the pulse, a reference sample at each port to record the environmental baseline was taken. Five kg of the

tracer was mixed with 20L of water and injected as an impulse into the feed line. During the experiment, water from a farm irrigation point was fed into the system in order to ensure the influent was as constant as possible. It is a recognised limitation of this experiment that the flow varied to some degree, because the water pressure was provided by a farm pump which had to meet competing demands. The data obtained were used to find the residence time distribution (RTD), which in turn made it possible for us to calculate the RTD, an age distribution ($E(t)$), for each of the sample ports.

5.5.2.2. Tracer experiments on the lab-scale rig

For this laboratory experiment, we chose FWT Red (Bright Dyes) as the tracer, since we were seeking to observe the flow patterns. A solution of 1 000mg/L of the dye was prepared and an impulse of 20mL of this solution was injected into the reactor. The flow was held constant at 7.3L/hour throughout this experiment. The results were used to determine the hydraulic properties of the system, in the same way as described in Chapter 5.5.2.1.

5.5.3. Sampling Protocol

5.5.3.1. Sampling regime at the ARC

The VSR was divided into a number of sample wells, as depicted in Figure 5.1. Sample aliquots of 500mL were taken from each sample point at intervals of approximately one hour for the first six hours; every two hours for the next 18 hours; and every four hours for the following 24 hours. A penultimate sample was taken at 64 hours, and a final sample at 200 hours.

5.5.3.2. Sampling regime on the lab-scale reactor

Samples for this experiment were taken at the point where the three outlet lines had converged, to smooth any lateral variation. The samples of 20mL aliquots were taken at irregular intervals, but were timed to ensure that the most valuable data was. In other words, many more samples were taken when significant change was most likely to occur. The final sample was obtained at 180 minutes.

5.5.4. Analytical Methods

5.5.4.1. Analysis of KBR samples taken from the VSR

The sample aliquots were analysed within 48 hours of being taken. Samples were analysed for bromide (Br-) using HPLC with a Waters IC-Pak (HR 4.6x75mm) anion column. The HPLC was fitted with a conductivity detector. During analysis the column was kept at ambient temperature, and used 1.5mL per minute of mobile phase containing 3.6nM of sodium carbonate. The resultant data were calibrated by applying pre-prepared standards.

5.5.4.2. Analysis of FWT red samples taken from the lab-scale reactor

The samples taken from the lab-scale reactor were not pre-treated in any way. They were transferred into plastic cuvettes, and analysed using a Merck Spectroquant at a wavelength of 550nm (according to the dye manufacturer's specification). The resultant data were calibrated according to pre-prepared standards.

5.6. Results

5.6.1. The calculation of hydraulic properties of the VSR

5.6.1.1. The calculation of the internal age distributions [E(t)] for the VSR at each sample port

An initial inspection of the breakthrough curves indicated that there was little difference between the left- and right-hand side (A and B) sample ports, which implies that there is little lateral variation of the flow across the width of the VSR. Therefore, the data for these locations (A and B ports) was averaged. The resultant data, shown in Figure 5.4, is a series of distributions. These illustrate the processes of dispersion (the long tail of the distribution) and short-circuiting (multi-modal distributions) of the effluent through the VSR. The mass balance recovery of tracer ranged between 11% and 24% at differing locations across the system. The presence of multimodal distributions indicates that some short-circuiting or bypass is occurring within the VSR.

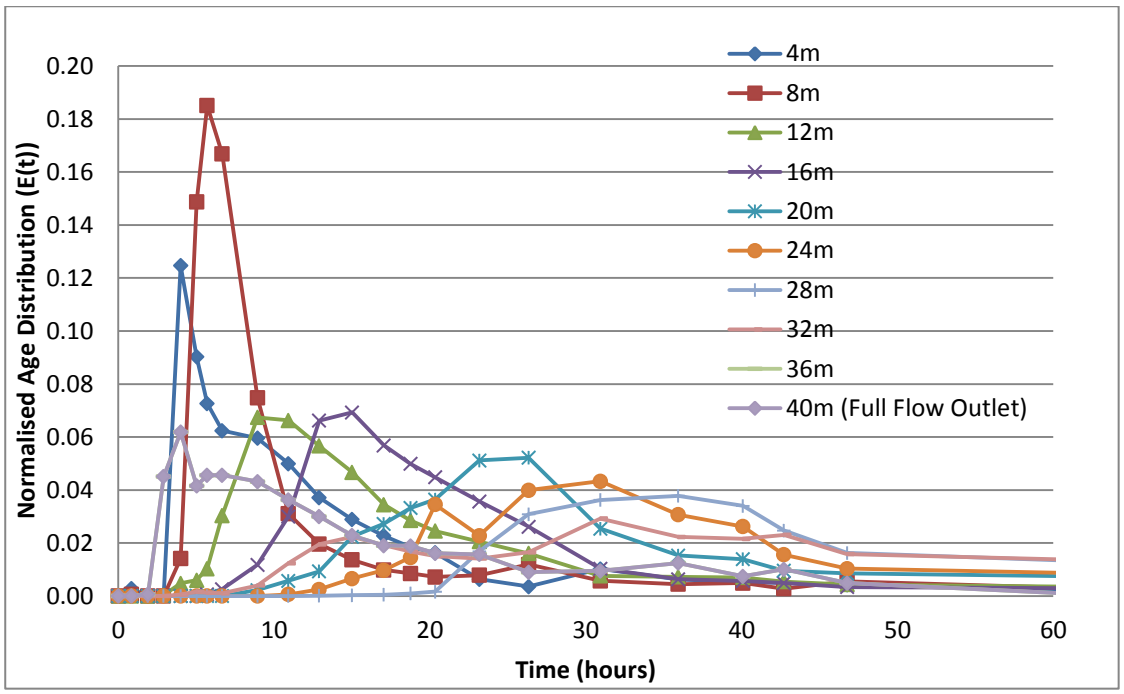


Figure 5.4. Normalised age distributions showing the progression and dispersion of the pulse as it moves through the VSR (with lateral variation averaged).

5.6.1.2. Calculation of hydraulic properties from the age distribution

The first moment of the normalised age distribution was used to calculate τ and V_{eff}, and the second moment to calculate the Peclet Number (Pe). The results of these calculations are presented in Table 5.4, as are the modes (the location of the peaks) of the distributions.

These data indicate that the pulse dispersed with increasing length, and that some degree of bypass occurred. The bypass (or short-circuiting) is indicated by multimodal distributions, and this is most clearly evident in sample port 5 (at 40m), through which the entire flow passed. The distributions of sample ports 4 and 5 (showing the greatest degree of bypass) are shown in Figure 5.5. The time for the pulse to pass, and concentration are represented by the peaks in this chart.

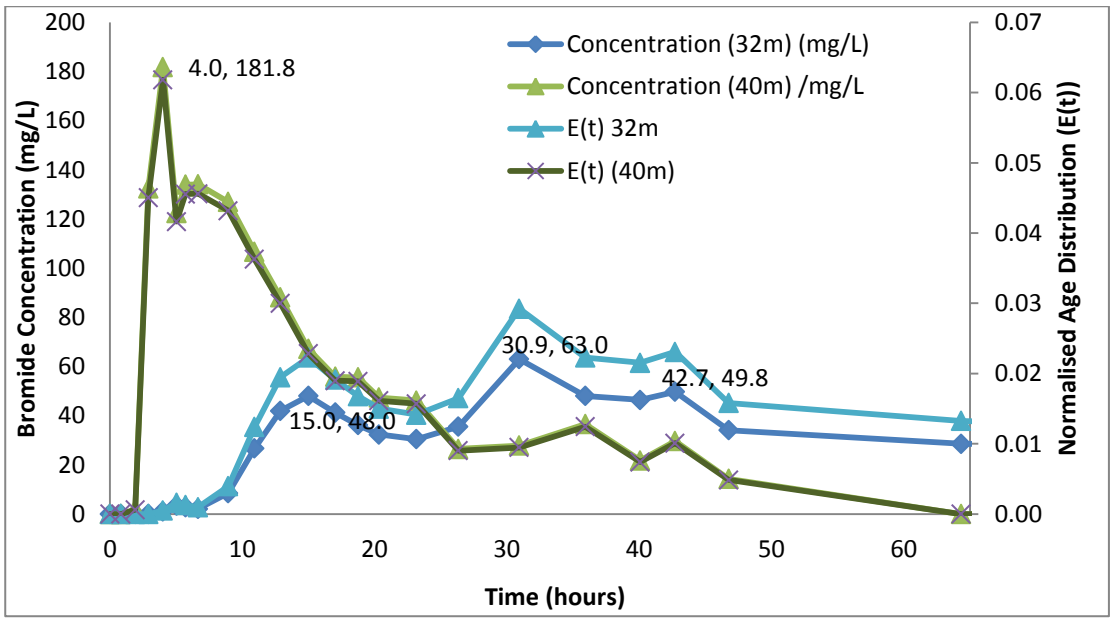


Figure 5.5. Residence time distributions for sample ports at 32m and 40m with multimodal distributions

The short-circuiting observed, particularly towards the end of the VSR, could be attributed to inadequate baffling at the sidewalls and bottom during construction, which would allow flow channels to be created. The effluent would use these channels to divert the flow to any location within the bed. It is, however, also possible that the bypass is caused by the pulse of KBr when it is not properly mixed, and therefore forms a pulse of liquid of a different density that typically travels along the base of the wetland. This effect has been described in various published works on pond experiments (Małoszewski, Wachniew et al. 2006, Schmid, Hengl et al. 2004, Chazarenc, Merlin et al. 2003), where vertical stratification was found. This was ascribed to the variations in the salinity of an assortment of tracers at different flow rates. This effect is particularly noticeable in Port 5, which has a residence time which is much lower than that which would be expected. This is shown in Table 5.4. This effect is discussed later.

Table 5.4. Hydraulic parameters calculated for the VSB.

Port Number	Length (m)	Pe	$\bar{t}_m$ (hours)	τ (hours) [V/Q]	Time for 1st Peak (hours)	Time for 2nd Peak (hours)	Time for 3rd Peak (hours)	Time for 4th Peak (hours)	V_{eff}
1A & 1B	4	0.01	15.03	8.70	4.00	30.93			1.73
1	8	0.01	14.61	17.39	5.70	26.33			0.84
2A & 2B	12	2.47	20.35	26.09	8.93				0.78
2	16	5.10	22.21	34.78	15.00				0.64
3A & 3B	20	7.76	31.55	43.48	26.33				0.73
3	24	12.63	36.13	52.18	20.33	30.93			0.69
4A & 4B	28	17.67	41.47	60.87	35.93				0.68
4	32	8.26	37.89	69.57	15.00	30.93	42.72		0.54
5A & 5B	36	24.57	49.70	78.26	26.33	42.72			0.64
5	40	1.67	22.36	86.96	4.00	6.67	35.93	42.72	0.26

5.6.1.3. Analysis of the hydraulic properties

An analysis of the modes of the distributions is presented in Figure 5.6. Theoretically, $\bar{t}_m$ must be directly proportional to length. The time taken for the peak of the RTD should also be directly proportional to the length of the VSR. This figure maps the progression of the peaks, that is, the time taken for the first peak and the ones that follow to pass. One can see that for the first peak there is a strong departure from linearity at the sample wells located at 24m, 32m, 36m and 40m. However, if other modes are examined together with the first peak, the appearance of a linear relationship returns. Thus, if the first peak (or mode) is plotted from 0m to 20m, the second peak for 24m, the third peak for 32m, the second peak for 36m and the fourth peak for 40 m, a linear relationship is observed ($r^2 = 0.94$) which is shown on the Figure. This means that the other modes of the age distribution for all sample ports can safely be assumed to represent bypass.

Within this figure, the Peclet number is also plotted with increasing distance. Since the system behaviour deviates strongly from ideal at 32m and 40m (based on the bypass encountered in these sample ports) these have been excluded from the analysis. The Pe number can be fitted with a second-order polynomial with a high level of confidence ($r^2 = 0.98$), which, since the Pe number must display a squared relationship to length as discussed in literature, confirms that the Peclet equation is applicable to this system (Levenspiel 1972).

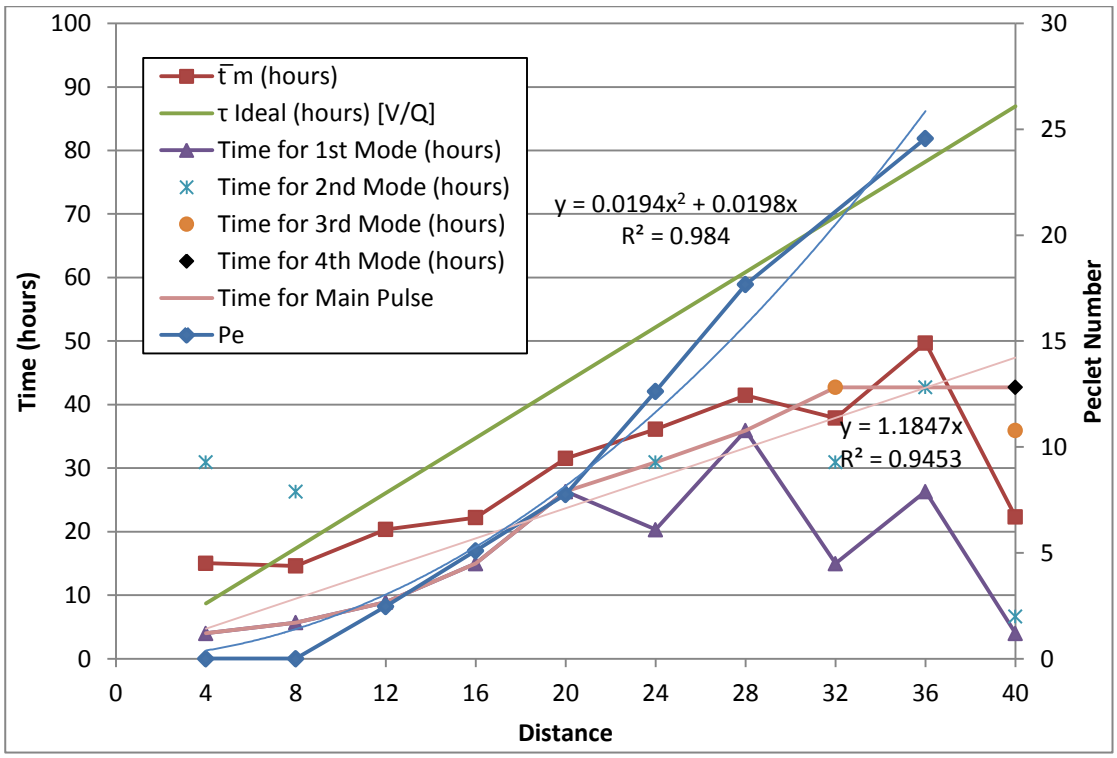


Figure 5.6. An analysis of the modes of distribution for the VSR

The breakdown of the pulses of tracer into 1st, 2nd peak and so on, and the examination of the time taken for a given pulse to pass through the bed correlate quite closely to the measured residence time, τ. This implies that the fitted line presented above correlates to the primary pulse of tracer, and hence the flow.

The effective volume for each of the sampling ports is presented in Table 5.4. Given the almost constantly scaled ratio between the V/Q and $\bar{t}_m$, it is reasonable to assume that the non-ideal behaviour of the system is primarily attributable to dead volume. A smaller degree of short-circuiting is evident during the initial stages (0 to 4m) and at the tail of the reactor (36m to 40m). This is shown by the deviation of linearity of $\bar{t}_m$ with respect to distance. The average effective volume calculated for this system was 75%. If the first 1m and the final 4m of the system are excluded, the average effective volume can be calculated at 69%. This implies that the short-circuiting is responsible for 6% and the dead volume for 25% of the non-ideal behaviour shown by the data. The implication is that approximately 30% of the designed volume of the reactor is not utilised.

In order to test our calculations we used the methodology of Perrson et al (Perrson, Somas et al. 1999) to provide a comparison. Their equation was used to calculate hydraulic effectivity, as shown in Figure 5.7. For this VSR, the maximum hydraulic effectivity was calculated to be 0.64 or

64%. Hence, at most the system used 64 % of its volume for effluent degradation purposes, while the remaining volume was essentially static or dead-zones. This correlates reasonably well with our calculated effective volume of 69%.

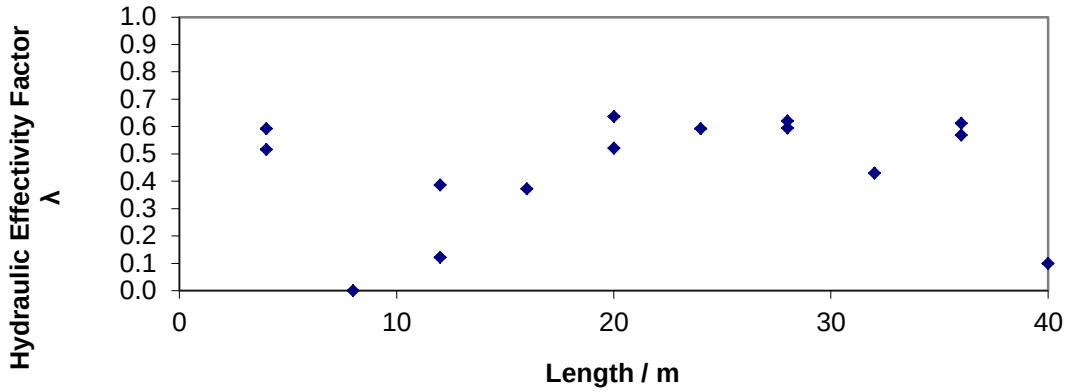


Figure 5.7. Hydraulic effectivity factor variation with length for each port within the VSR

5.6.1.4. Hypothetical reactor volume

From the RTD curves the initial stages of the VSR have a Gaussian-type distribution with a long tail, as discussed by Levenspiel (Levenspiel 1972) and also reported by others (Tanner, Sukias et al. 1998, Werner, Kadlec 2000, Marsili-Libelli, Checchi 2005, Kadlec 2009, Giraldi, de'Michieli Vitturi et al. 2009) for VSRs and packed bed filters. This behaviour indicates that the VSR can be represented using the Peclet model with dead zone(s) or as a series of tanks with dead-volumes. It was found that as the distance through the VSR increased, the bromide pulse became steadily degraded as other processes interfered with it. There were possible density effects from the impulse (which were attributed to poor mixing with the effluent as a result of differences in salinity and density, and/or bypass towards the end of the filter—sample port 5). It was postulated that this was probably an effect of the density currents, which would be encountered only in the tracer experiment, and not in a well-mixed effluent stream arriving at the filter.

The experiment also showed that the behaviour of the VSR deviates significantly from the ideal. This evidence includes the Figures showing the difference between $\bar{t}_m$ and τ, the relationship of the Peclet number with increments in length, the increase in residence time with length and the hydraulic effectivity as a function of length. For this system, the inactive volume of the VSR was found to be approximately 25%. It was hypothesized that the dead zones can, especially in this case, be explained by investigating the location of the inlet and outlet port. In this filter the outlet port is marginally lower than the inlet port. Since the filter was full of liquid with no free surface

runoff, the only way for the fresh influent to reach the bottom layers would be through deflection and diffusion. This would create preferential flow, with the greatest amount of flow occurring nearest the surface and in the centre, and least flow occurring at the sidewalls and at the bottom. This is conceptualised as a hull-shaped velocity profile, which is shown in Figure 5.8.

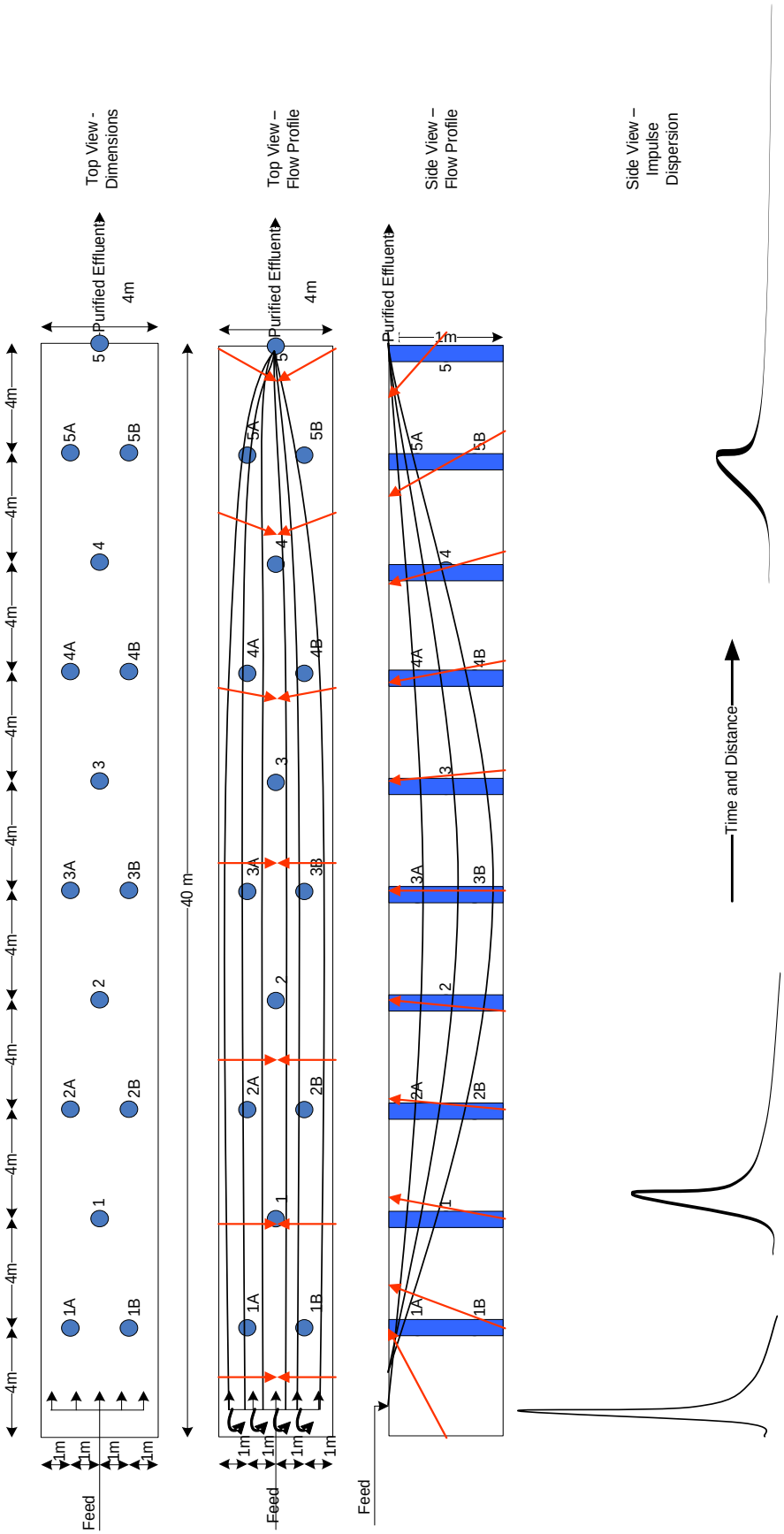


Figure 5.8. Hypothetical flow regime showing the boat-shaped velocity profile of tracer dispersion within the VSR

5.6.2. Calculation of the hydraulic properties of the laboratory-scale rig

5.6.2.1. Simulation of the large-scale CW – flow top to top.

The RTD for the laboratory reactor is shown in Figure 5.9. The RTD displays the typical behaviour of a packed bed, as described above. This is the same type of behaviour that was found for the VSR discussed earlier in this chapter, which implies that the systems are operating according to a fundamentally similar hydraulic regime.

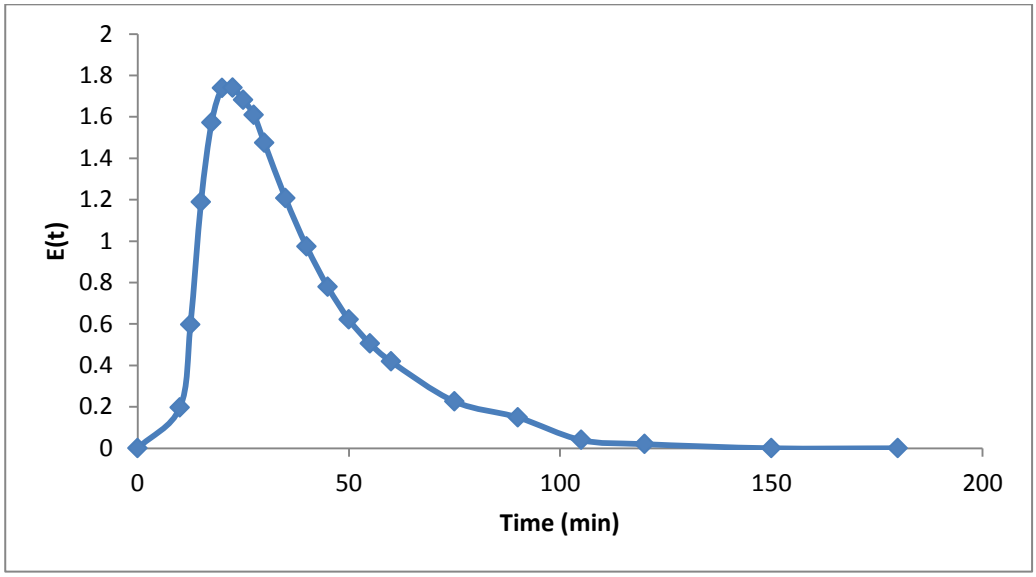


Figure 5.9. RTD for the impulse-response laboratory experiment.

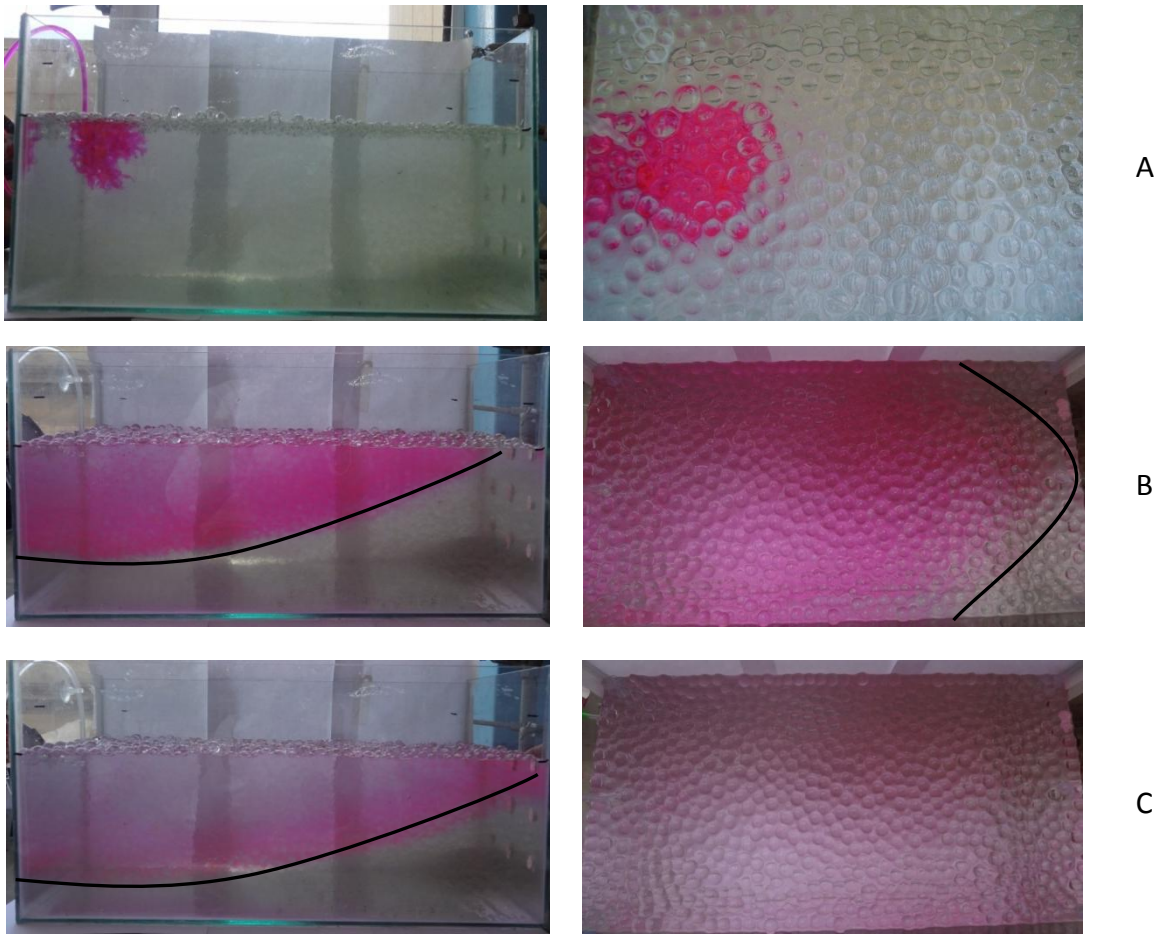
A summary of the calculated hydraulic parameters for the laboratory reactor is presented in Table 5.5.

Table 5.5. Hydraulic parameters for the laboratory apparatus

Parameter	Value
$\bar{t}_m$ (hours)	0.616
τ (hours) [V/F]	1.233
Time for 1st Peak (hours)	0.375
V_{eff}	0.500
Pe	4.753

The laboratory reactor was calculated to have a Peclet number of approximately 4.8. This indicates that there are significant dispersive forces at work, and that the lab reactor is operating similarly to the VSR, although because of its shorter length, there is a significantly greater dead volume.

Having established mathematically that the laboratory apparatus is operating in a fundamentally similar manner to the VSR, it was proposed that the hypothesis posited earlier for the VSR is valid for the laboratory apparatus. (In summation: there is a preferential flow, with the greatest flow occurring nearest the surface and in the centre, and least flow occurring at the sidewalls and at the bottom; and that the flow can be conceptualised as a hull-shaped velocity profile.) Having used a transparent reactor and packing medium, it was possible to photograph the tracer as it passed through the apparatus bed presented in Figure 5.10. Photograph A was taken during injection of the impulse of tracer; and Photograph B after 10 minutes as the tracer began to exit the apparatus. The distinctive hull-shaped profile of the dispersed tracer is clear, and has been accentuated in Photo B. Photograph C was taken after approximately an hour, and shows a new hull-shaped profile of clear liquid visibly replacing the dye.



A

B

C

Figure 5.10. Photographs showing the flow patterns of tracer through the laboratory apparatus.

5.6.2.2. Experiment to test if the hull-shaped profile could be reduced by distributing the feed and the outlet.

The aim of this experiment was to test if it was possible to reduce dead volume by distributing the feed and outlet fully. In this experiment, the feed entered the rig via all nine inlet holes and exited through all nine outlet ports. The RTD for this experiment is shown in Figure 5.11.

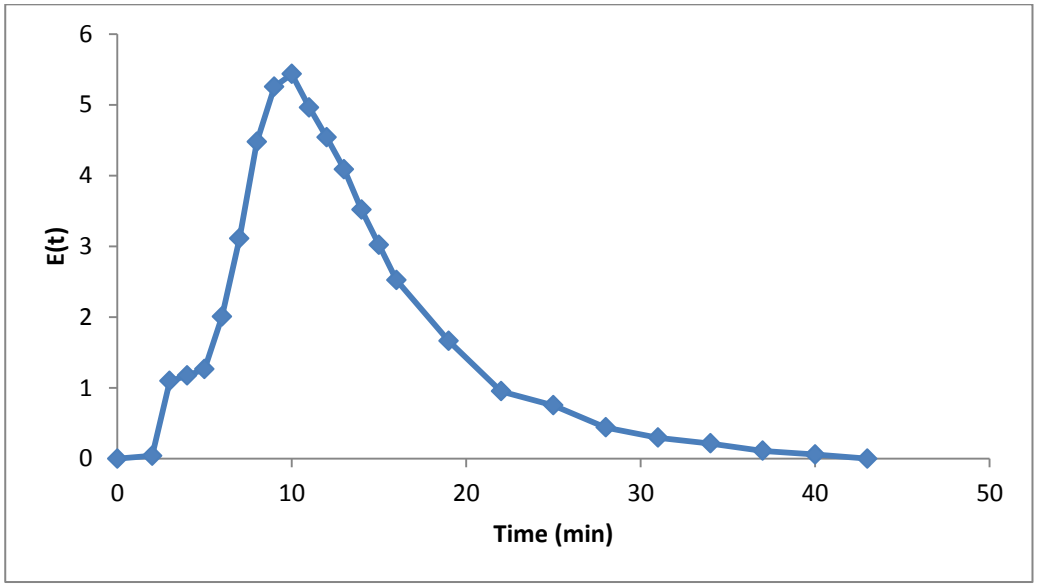


Figure 5.11. RTD for the impulse-response laboratory experiment with a well distributed feed and outlet.

A summary of the calculated hydraulic parameters for the laboratory reactor is presented in Table 5.6.

Table 5.6. Hydraulic parameters for the laboratory apparatus

Parameter	Value
$\bar{t}_m$ (hours)	0.223
τ Ideal (hours) [V/F]	0.308
Time for 1st Peak (hours)	0.166
V_{eff}	0.724
Pe	6.667

The laboratory reactor was calculated to have a Peclet number of approximately 6.7 for this experiment (i.e. Pe=4.67). This value is significantly greater than that found in the experiment with feed and outlet located upon the surface. There was also a significant reduction in the dead volume in comparison to the experiment discussed in Section 3.2.1 from 50% to 37.6%. This implies that the dead volume can be significantly reduced by distributing the feed and outlet lines. A photographic record of the experiment is presented in Figure 5.12. It is quite clear from this photo that the hull shaped profile no longer exists.

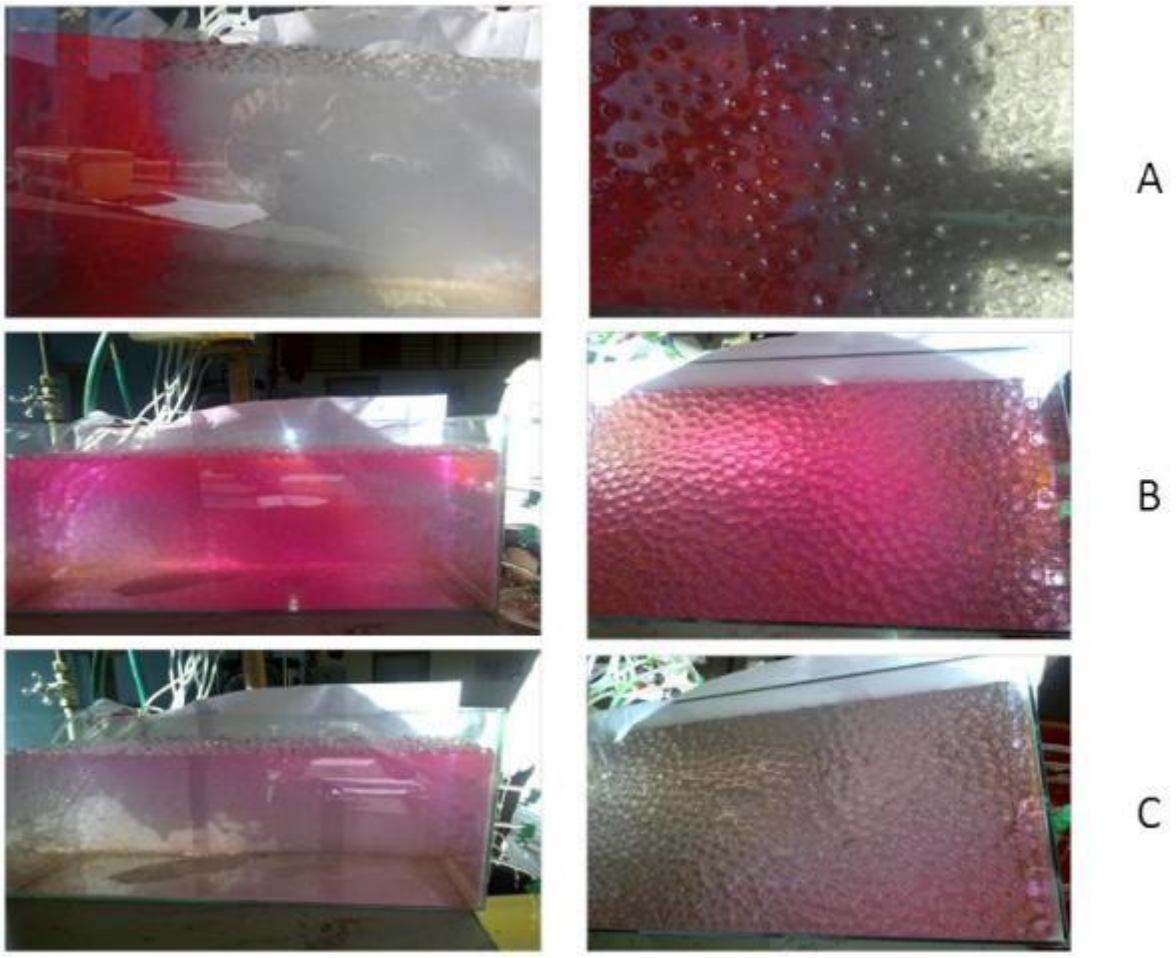


Figure 5.12. Photographs showing the flow patterns of tracer through the laboratory apparatus.

5.7. Discussion of the results

Based on the data collected in this study, it is believed that our hypothesis is indeed correct, that the flow in a VSR or any other packed bed reactor has the following two properties; that it will carry on trying to go in the direction it started with some degree of dispersion that increases over distance; and that if the flow to such a system is upon the surface, and the outlet is also near the surface, the profile will be hull-shaped. It is noted that the location of the inlet and outlet positions

could also have a significant effect on the shape of this profile (as found by other researchers (Suliman, Futsaether et al. 2006), or could even reduce the dead zone.

What remains to be done in this research investigation (to estimate what effect the flow properties have on the effectiveness of the water treatment) will be the subject of the next chapter. The results of this stage of our work have indicated where the current design of the VSR can be improved from the hydraulic point of view, but we also require sufficient data to assess what chemicals remain in the treated water when the conventional VSR design is followed. Only when these results are combined can we come up with an optimal design for a VSR.

5.8. Conclusions

As discussed, the focus of the research experiment described in this Chapter was threefold: to report on the data measured; to develop a hypothesis from the data obtained; and to test it. In summary the four components of the hypothesis included:

1. That there is a preferential flow pattern within a VSR, with the greatest flow occurring closest the surface and in the centre, and the least at the sidewalls, if the flow is applied to the surface of the VSR at the feed position. This is conceptualised as a hull-shaped velocity profile. It is believed this hypothesis is correct and as far as we are aware this flow pattern has not been described previously.
2. This profile is not dependent on the shape of the packing medium. The laboratory experiment confirms (at least with spherical packing materials) that the profile is not dependent on the packing if it is randomly distributed or if spherical packing materials are used in a VSR.
3. This hull-shaped profile can be reproduced in a laboratory-scale experiment using spherically shaped packing. It was found that it was possible to induce the hull shaped flow profile.
4. The profile can be changed by altering the location of the feed, and can be significantly reduced by introducing a fully-distributed feed and outlet system. It was found that it was possible to change the profile by modifying the feed and outlet distribution of the lab-scale rig, and that by doing so, the dead volume could be significantly reduced and thus the performance of the system substantially increased.

To conclude, hydraulic processes should be taken into account (that is, not discounted or assumed to be ideal) in VSR calculations, and that the mean residence time is significantly different from the ideal residence time. This has significant consequences for any model which assumes that the

hydraulic process occurring within the system are ideal. The data measured indicate that for the optimal design of a bioreactor such as a VSR, the feed should be evenly distributed, and, even more important, the inlet and outlet from the VSR must be sufficiently well positioned to encourage flow through what in the experiments was identified as having the potential to be dead volume.

The design of a VSR that is efficient and relatively simple to maintain will fill the gap that exists at present between extremely sophisticated and expensive effluent treatment systems, and the more affordable low-technology wetland model. The water reclaimed can be used for irrigation, and the scale and effectiveness of the VSR design will be well suited to the needs of small-scale wineries.

6. Additional hydraulic experiments assessing the location of the dead volume

6.1. Introduction

This Section is important in the context of this thesis since it tested the additional hypothesis, not presented in Chapter 5. From that Chapter: "The profile can be changed by altering the location of the feed, and can be virtually eliminated by introducing a fully-distributed feed pattern. This hypothesis was yet to be tested for the submission of Chapter 5 to the Journal. Here this idea is explored a little further, and the data indicate that the feed distribution can change the profile. We acknowledge Ms Lindsay Westraadt from the School of Civil and Environmental Engineering, University of the Witwatersrand and her two fourth year students, Ms Shona Pepper and Mr Werner Pieters for their assistance with the experimental work presented here. The data is given in Appendices Z to EE.

6.2. Experimental Objective

In Chapter 5, it was hypothesised that the flow regime in the ARC VSR was hull shaped and an attempt to explain the dead zones in terms of this shape was made. Unfortunately, gravel is opaque, and the tracer, potassium bromide is transparent. This meant that it was not easy to test the existence of the hull shape flow profile using this system. Therefore, we decided to run an additional experiment, utilising a laboratory-scale rectangular bed. This apparatus needed to be made of glass, and the packing of this apparatus needed to be transparent, in order to visually observe the path of the tracer through the bed. The purpose of this experiment was thus:

- To test and determine if there was a hull shaped profile, and
- To assess if changing the distribution of inlet and outlet ports had any impact on changing the shape of the dead zones within this packed bed;
- To assess if the dead volume could be reduced by adjusting the shape of the system slightly; and
- To assess if the dead volume could be reduced by distributing the inlet and outlet to the system.

To test these four objectives, seven separate experimental runs were conducted:

- connecting the inlet to the central inlet port and the outlet to the central outlet port;

- connecting the inlet to the lowest central port and the outlet to the highest central port;
- connecting the inlet and outlet to the central highest ports (this data was presented in chapter 5)
- connecting the inlet to the central lowest port and the outlet to all three highest outlet ports;
- connecting the inlet to the right lowest port and the outlet to the right highest port; and
- inserting a wedge in the location of the dead zone identified as discussed in chapter 5.
- connecting the feed to all nine inlet ports and the outlet to all nine outlet ports (this data was presented in Chapter 5 and is hence not presented here).

The experimental apparatus is shown in Figure 5.3. As discussed in Chapter 5, the rig was filled with florists' gel balls.

6.3. Experimental method

6.3.1. Tracer experiments on the laboratory-scale rig

For this laboratory experiment, FWT Red (Bright Dyes) was chosen as the tracer, since we were seeking to observe the flow patterns. A solution of 1 000mg/L of the dye was prepared and a 20mL pulse was injected into the reactor. The inlet flow was held constant at 7.3L/hour throughout this experiment. The results were used to determine the hydraulic properties of the system, in the same way as described in Chapter 5. The matrix used as a proxy for the gravel was florists' gelatinous balls. These were prepared by soaking them overnight in water in order for them to be fully saturated. The tank was prepared by placing a white neutral background behind and below it in order to make the dye more visible in photographs. The inlet position(s) of the specified experiment were noted and a suction cup attached to those position(s). The inlet pipe (4mm diameter) was then attached to the sucker and aligned correctly. The outlet position(s) were noted and prepared by inserting the necessary exit piping (4mm diameter) and sealing them correctly. The tank was filled with the gelatinous balls and water was added until the correct level was obtained (corresponding to a specific reactor volume). The rate of flow was set and the system was allowed to stand for 10 minutes in order to ensure that it was operating at steady state i.e. the water level of the system was not rising or falling. Following this, the tracer was inserted by injecting it as an impulse into the feed line. Front and plan view photographs were taken at the same time that samples were taken, until the tracer was no longer detectable.

6.3.2. Sampling Protocol

Samples for this experiment were taken at the point where the three outlet lines had converged, to average any lateral variation. The samples of 20mL aliquots were taken at irregular intervals, but were timed to ensure the most valuable data was obtained. In other words, many more samples were taken when significant change was most likely to occur. The final sample was obtained at 180 minutes.

6.3.2.1. Analysis of FWT red samples taken from the lab-scale reactor

The samples taken from the laboratory-scale rig were not pre-treated. They were transferred into plastic cuvettes and analysed using a Merck Spectroquant at a wavelength of 550nm (according to the dye manufacturer's specification). The resultant data were calibrated according to pre-prepared standards.

6.4. Results

6.4.1. Residence Time Distributions

The result of the impulse-response tracer experiments on the apparatus is presented in Figure 6.1.

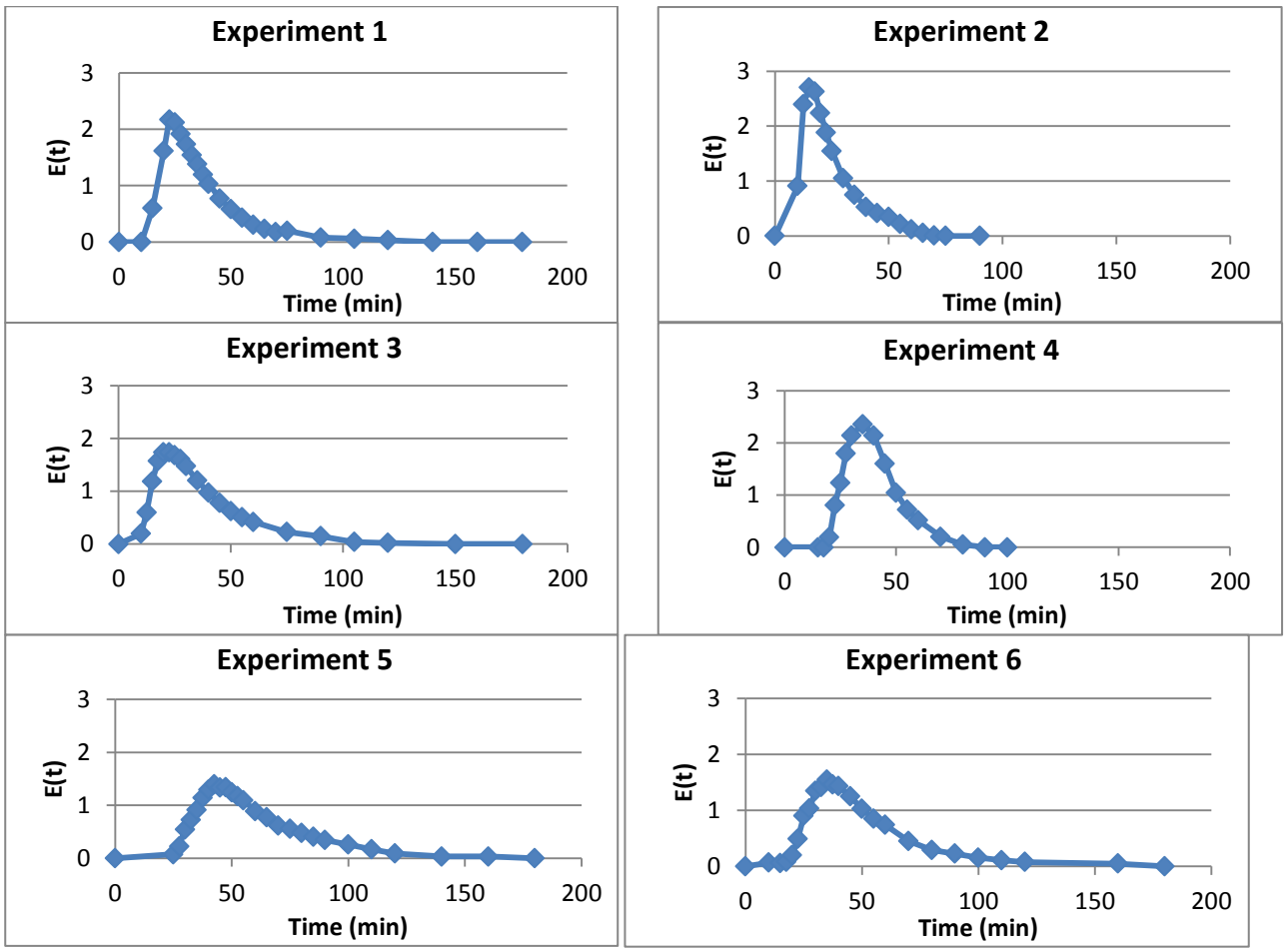


Figure 6.1. The residence time distributions of the six experiments. 1. Connecting the inlet to the central inlet port and the outlet to the central outlet port; 2. Connecting the inlet to the lowest central port and the outlet to the highest central port; 3. Connecting the inlet and outlet to the central highest ports; 4. Connecting the inlet to the central lowest port and the outlet to all three highest outlet ports; 5. Connecting the inlet to the right lowest port and the outlet to the right highest port; and 6. Inserting a wedge in the location of the dead zone identified.

As can be seen in the RTDs, the laboratory-scale reactor displayed the characteristic age distribution for a packed bed reactor, namely a single mode and a long tail. It is noted that the median of the residence time changed between experiments. A summary of the calculated hydraulic parameters is presented in Table 6.1.

Table 6.1. Hydraulic properties of the laboratory scale rig

Experiment	Mean Residence Time, $\bar{t}_m$ (min)	Normalized Variance (σ_ϑ^2)	Effective Volume, V_{Eff} (%)
1	36.51	0.287	50.7
2	23.11	0.288	32.1
3	36.95	0.333	50.0
4	40.33	0.085	56.0
5	60.42	0.184	62.9
6	53.75	0.301	79.8

The data indicate that the reactor was displaying highly non-ideal behaviour since the mean of the RTD is significantly different to the ideal; i.e. $V_{Eff} \neq 1$. The effective volume was particularly low in the first three experiments, including the simulation of the ARC wetland (i.e. from top to top; experiment 3).

6.4.2. Photographic record of the experiments

A photographic record of each experiment is shown in Figures 6.2 to 6.7. The photographs were taken with the intent of observing the passage of tracer through the experimental apparatus and more specifically with the intent of observing the appearance or lack thereof of the hull shaped flow profile. The sequence of numbers indicates the passage of time, i.e. picture 1 was taken first and picture 6 was taken last.

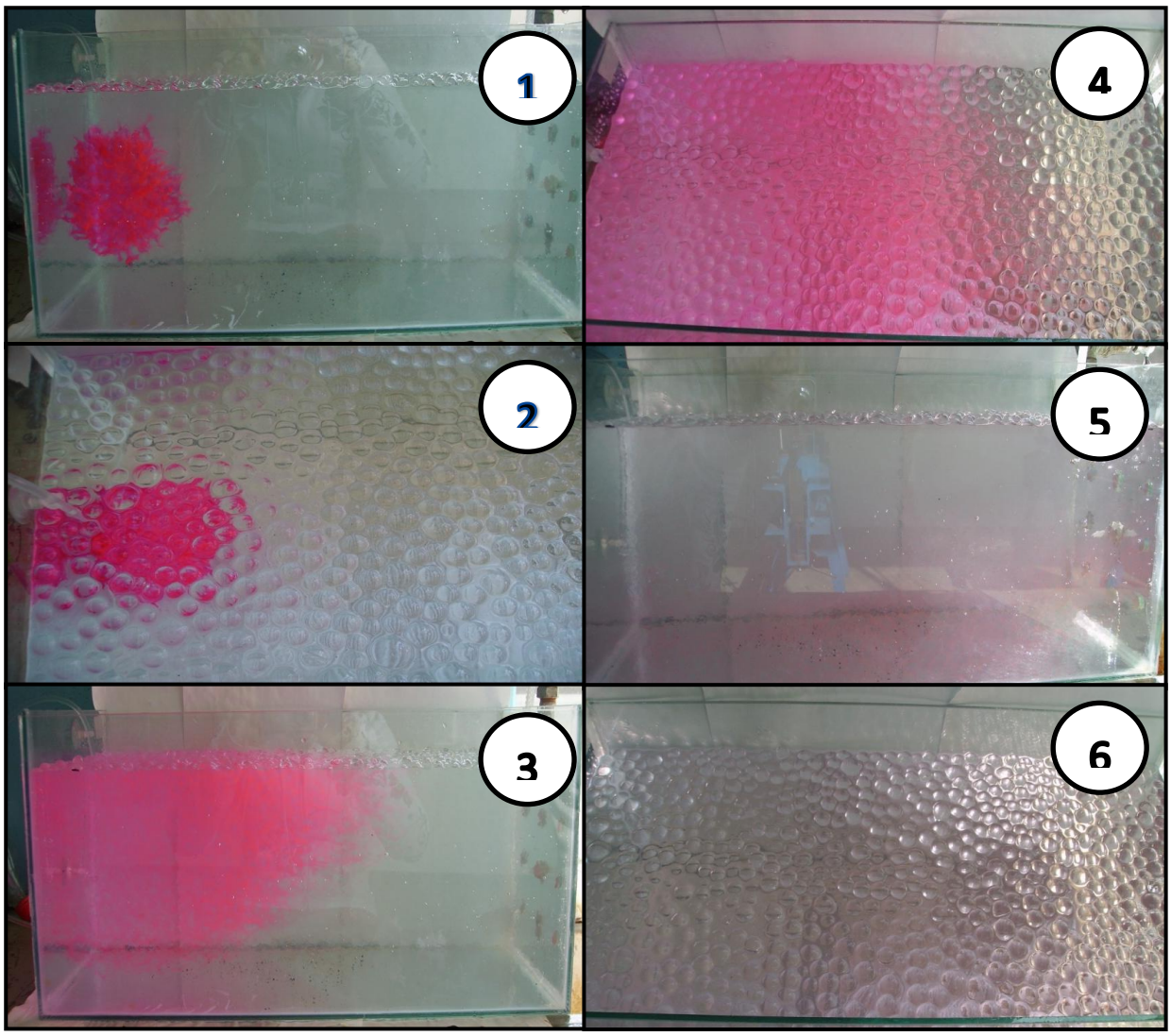


Figure 6.2. Experiment 1 - Connecting the inlet to the central inlet port and the outlet to the central outlet port

In this experiment there was some formation of a hull shaped profile although this primarily occurred below the lowest outlet port.

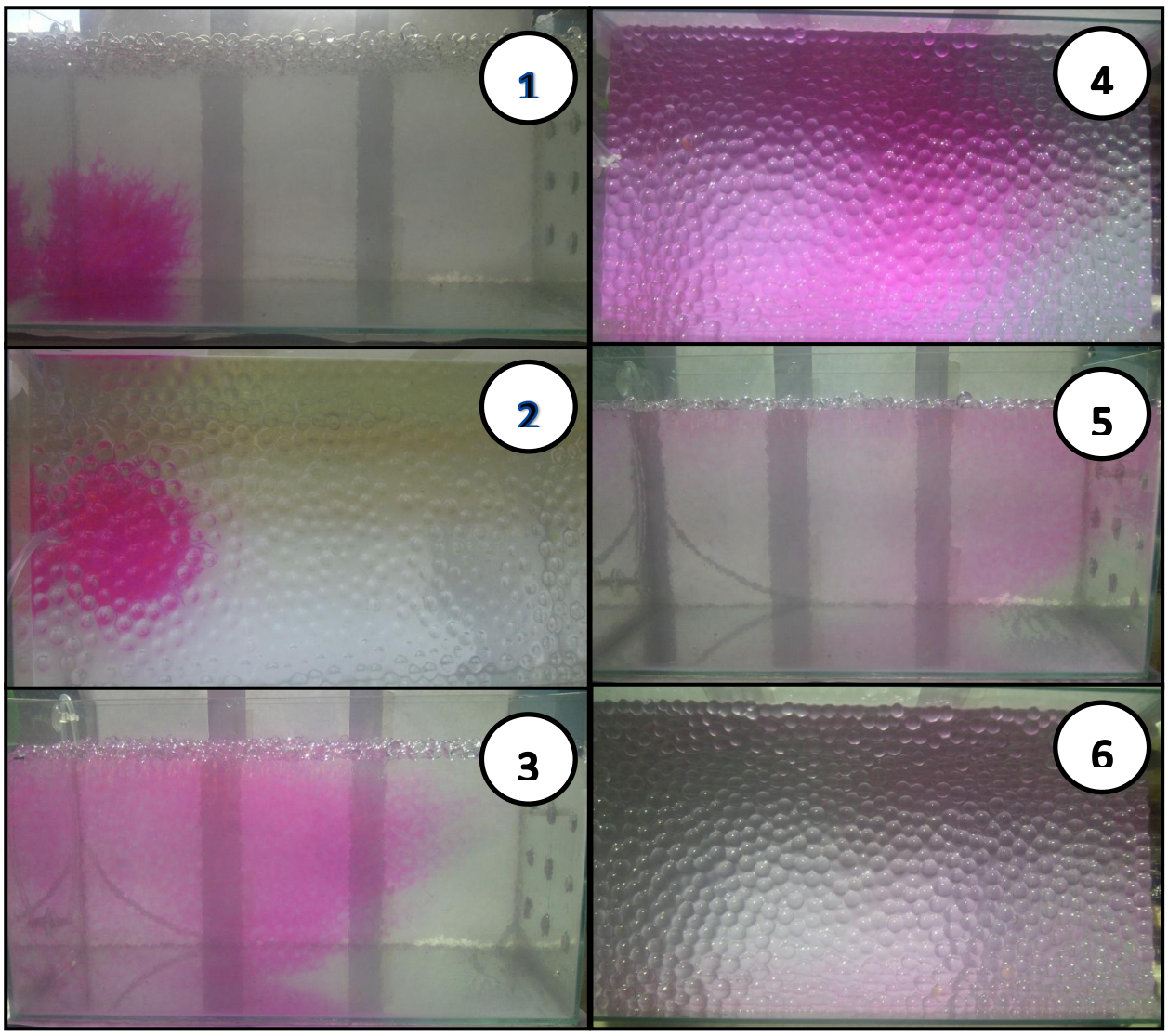


Figure 6.3. Experiment 2 - Connecting the inlet to the lowest central port and the outlet to the highest central port

In this experiment there was a pronounced hull formed as a result of the large space between the outlet and the base of the tank.

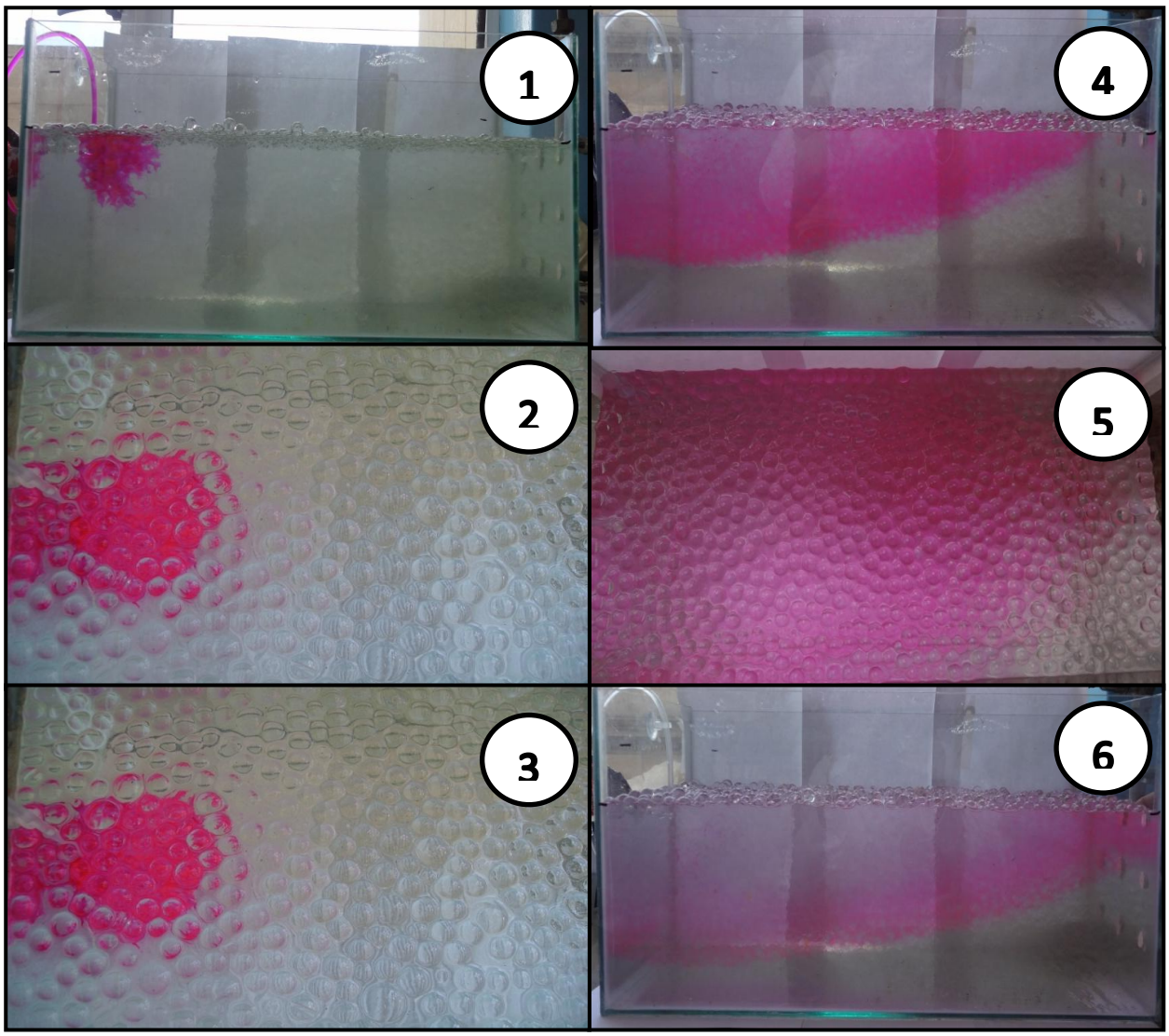


Figure 6.4. Experiment 3 - Connecting the inlet and outlet to the central highest ports

In this experiment, which most closely resembled the large-scale CW that we were trying to model, the most clear evidence of the hull-shaped flow profile can be seen.

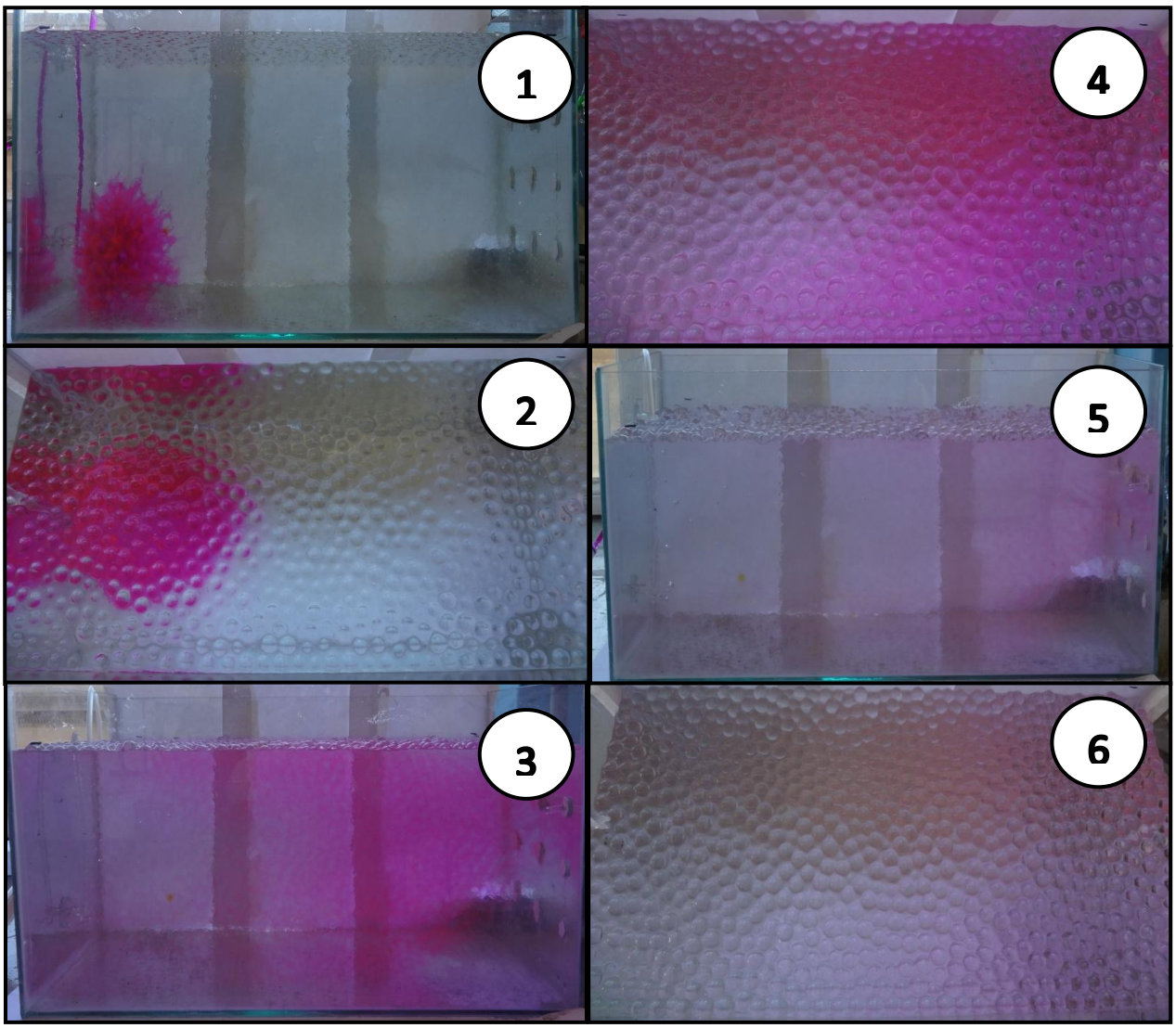


Figure 6.5. Experiment 4 - Connecting the inlet to the central lowest port and the outlet to all three highest outlet ports

Again, the dead volume is visible beneath the outlet ports, and in side view, a hull-shaped profile can be observed. There is no tapering to the point of the hull of a result of the three outlet locations.

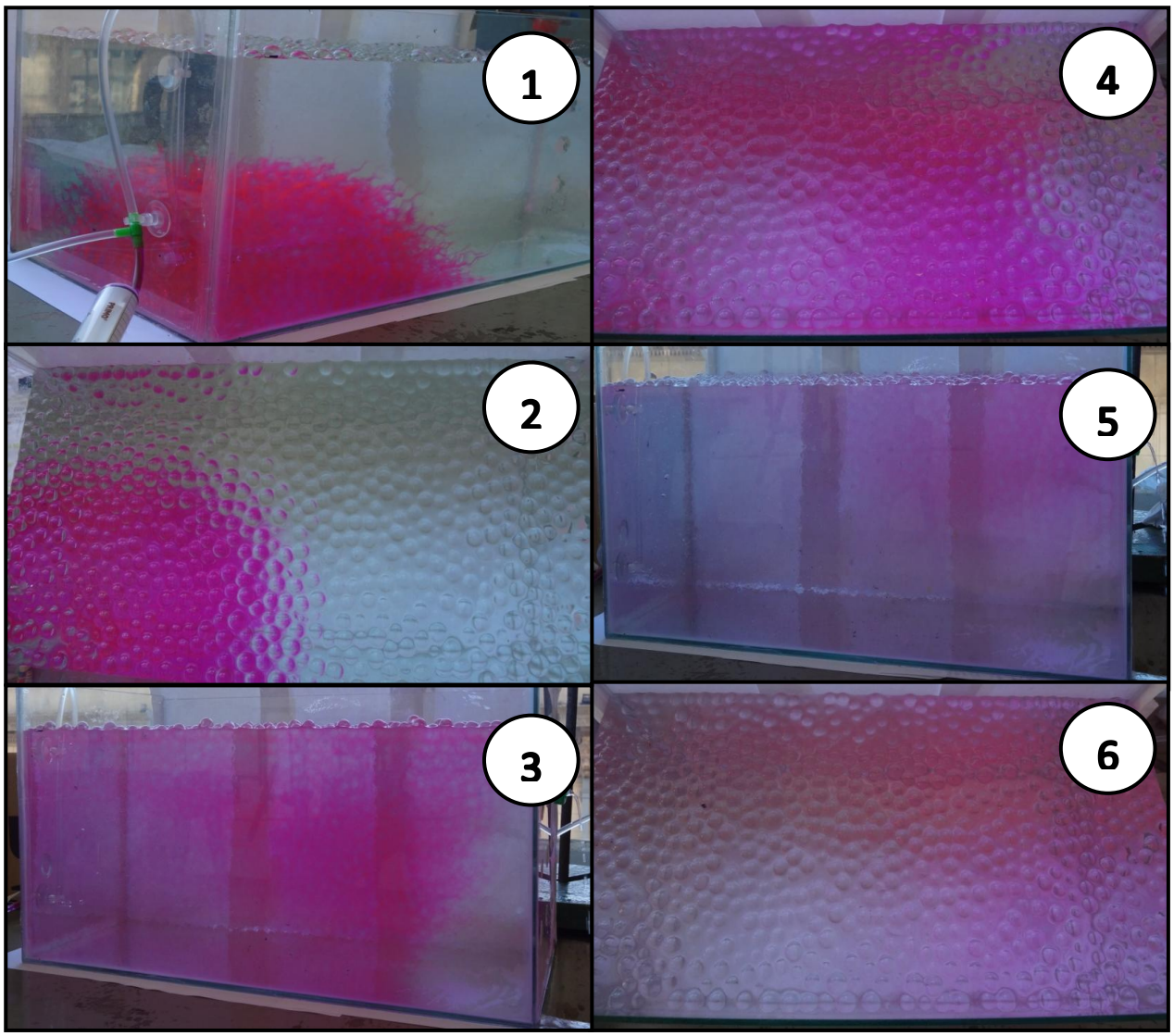


Figure 6.6. Experiment 5 - Connecting the inlet to the right lowest port and the outlet to the left highest port

In this experiment it was sought to see the impact of inducing a diagonal flow. The flow profile is no longer hull-shaped, yet the dead volume occurs in the same location, i.e. beneath the outlet ports.

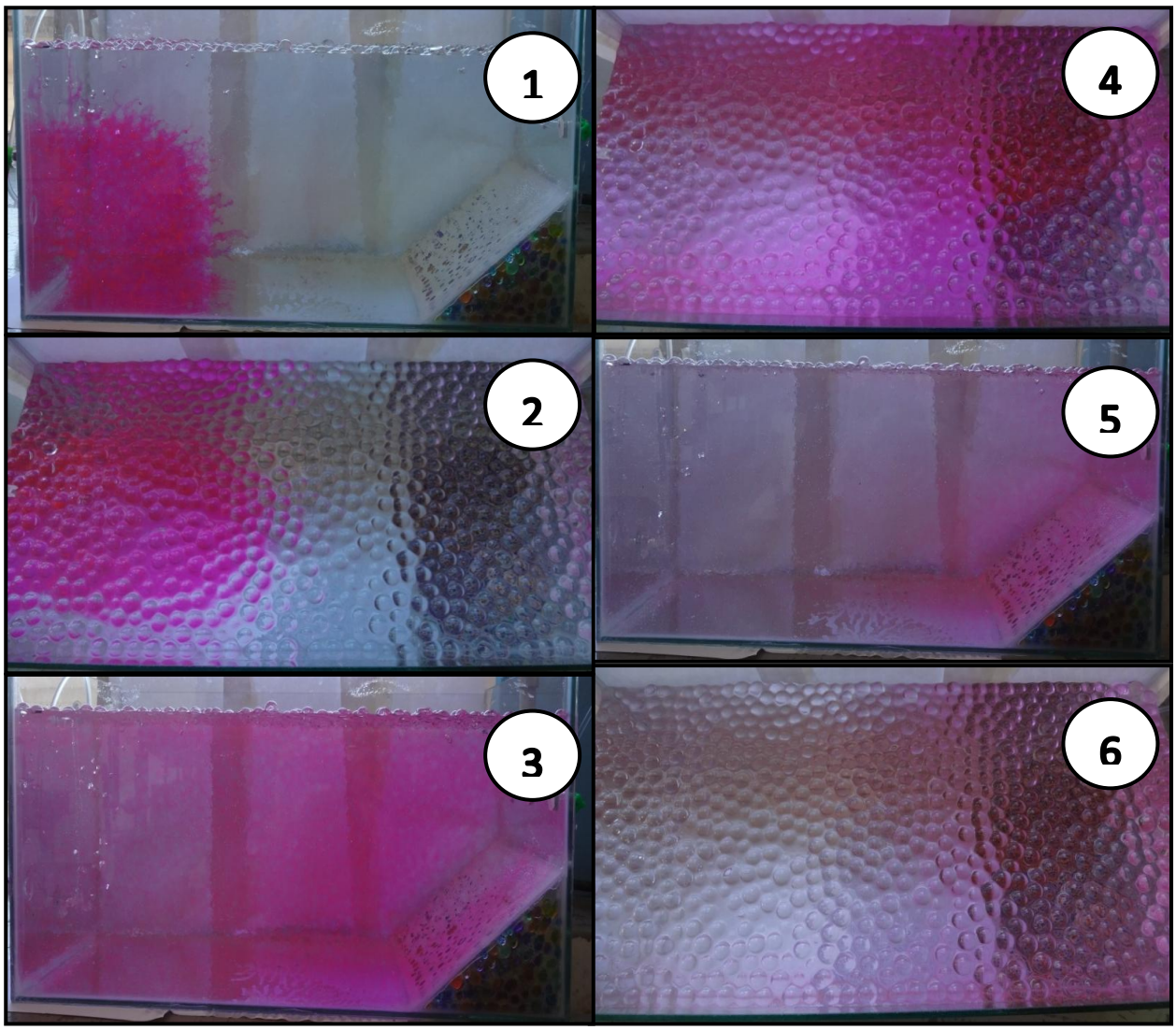


Figure 6.7. Experiment 6 – Inserting a wedge-shaped filler in the location of the dead zone identified

In this experiment the dead volume was removed, and there was a consequent improvement in the hydraulic process – i.e. the measured and the ideal residence time were much closer.

6.5. Discussion

In Table 6.1 the moments of the RTD obtained for each experiment are compared. These are the most important values which determine the hydraulic efficiency of the system.

6.5.1. Changing the elevation of the outlet port

When comparing the results of Experiments 1 and 3 no see significant difference is seen in the calculated properties or in the visual results. Due to the elevation change of the outlet port it was expected to see better performance in experiment 1 than 3. This was not the case as experiment

three showed a 1.2% increase in residence time, a 16.0% increase in normalized variance but a decrease of 1.38% in the effective volume. Even though these two experiments vary very little they are both inefficient in terms of the mean residence time and effective volume.

6.5.2. Changing the direction of the flow path

A comparison of Experiments 2 and 5 show more interesting results. Both of these experiments were designed in an attempt to increase the mean residence time by forcing the tracer to flow against gravity. In Experiment 2 we forced the tracer along a straight path whereas Experiment 5 forced the tracer along a diagonal route. The diagonal path increased $\bar{t}_m$ by 162% and the σ_θ^2 decreased by 57%. The effective volume was found to be increased by 96% thus indicating that inducing the diagonal flow pattern improved the hydraulic efficiency of the reactor.

6.5.3. Increasing the number of outlet ports

It was noted that by increasing the number of outlets a substantial increase in the effective volume was obtained. This can be seen by comparing results of Experiments 2 and 4. The increase in V_{Eff} was found to be 74.5%. That implies that the mean residence time has also increased by the same amount.

6.5.4. Inserting a wedge to remove the dead zone

In Table 6.2 a comparison of results found when we inserted a wedge into the system at the location of the dead volume is shown.

Table 6.2. Comparison Showing the effect of dead-zone reduction by inserting a wedge

Experiment	Tank Volume (l)	Mean Residence Time, $\bar{t}_m$ (min)	Normalized Variance (σ_θ^2)	Effective Volume, V_{eff} (%)
4	25	40.33	0.085	56.0
6	23.4	53.75	0.301	79.8
Percentage Increase	-6.4	33.3	255.1	42.4

The data clearly indicate that there is a significant improvement in the efficiency of the system, which was caused simply by changing the system geometry.

6.6. Conclusion

In conclusion, it was found that the location of the feed and outlet location to a CW had a significant effect on the system performance. It was noted that by adding feed to the surface and removing outlet from the surface (which is how many CWs are currently designed and operated) caused the worst system performance and that by distributing the inlet and outlet pipes led to the greatest efficiency. It was also noted that the efficiency of the CW could be greatly improved by altering the geometry of the CW. These effects all have significant impact on the efficiency of design but the solutions are simple to implement.

7. Estimating rate constants in constructed wetlands treating winery effluent: A comparison of three different methods.

In this chapter a method for determining the rate constants for the processes of degradation of winery effluent occurring within the VSR is presented. As with the other chapters, this too has been written in the form of a paper. We intend to submit this Chapter for publication in the Chemical Engineering Journal. The original measurements of the concentrations through the CW at each day is presented in Appendices FF through OOO. The spreadsheets with the calculations for the different models presented are given in Appendices PPP to GGGG.

7.1. Abstract

In this Chapter the use of three different methods for determining the rate constants for the degradation of winery effluent within a sub-surface flow constructed wetland (CW) are investigated. These methods comprise using a dispersed plug flow (the Peclet) equation; a tanks-in-series (TIS) equation; and analysing the residence time distribution (RTD) directly. The last of these is described by the Convolution Integral (CI).

Within the CW studied, the principal constituent of the chemical oxygen demand (COD), ethanol, was always fully degraded by the time the flow reached the outlet. Therefore the rate constant of degradation was calculated from the initial eight metres of the CW. The date also demonstrated the self similarity of the RTDs, which meant that in general the system's hydraulics were similar throughout the CW. This meant it was possible to extrapolate the data so as to develop a more complete understanding of the hydraulic properties of the CW and examine how they affected the kinetics of degradation. It was found that whilst both the Peclet and the TIS equation were able to predict concentration within the CW accurately, this required the optimisation of more than one variable. This rendered the result that was more of a modelling exercise than a useful design tool. The CI method, however, could be applied to predict system parameters effectively. There the CI was used to measure the rate constants of removal for both ethanol and potassium, which were found to be the key species that responded to the degradation/treatment of the effluent. Acetic acid, on the other hand, did not degrade within the system. This implies that the CW operates aerobically. The concentration of sodium increased very slightly, indicating that it is not

bioremediated/removed and that there are some minor evapotranspirative effects. The rate constant found for the biodegradation of COD was found to have significantly more uncertainty associated with it than the measurement of the rate of degradation individual components and it is therefore posited that it is better to describe the processes of degradation by tracking individual components rather than lumped parameters.

7.2. Introduction

Vegetated submerged reedbeds (VSRs) or constructed Wetlands (CWs) are used in a range of diverse applications. These uses include treating storm-water run-off (Kadlec, Knight et al. 2000); remediating acid mine drainage (Wallace, Knight 2006, Kadlec, Knight et al. 2000, Batty, Younger 2004, Sheridan, Koller et al. 2012); polishing the effluent from sewage treatment plants (Kadlec, Knight et al. 2000); and removing toxic chemicals from agricultural effluent amongst others (Kadlec, Knight et al. 2000). In this study, the research was conducted on the use of CWs to treat winery effluent. Within the South African context very little research has been done on such systems, although a few publications on the subject have been published in other countries [(Masi, Conti et al. , Shepherd, Tchobanoglous et al. 2001)(Wallace, Knight 2006)].

This Chapter is the last of a series of three papers. In this series the properties of the effluent (Chapter 4) and the CW treatment processes (Chapter 5) were determined. The work was split into three broad sections (listed below) that covered the most significant aspects of the research.

A. Determining the composition of winery effluent and its temporal variations. What does it consist of? How does it change over the duration of a harvest period? How does it change over the course of the year? Answering these questions required analysis of the effluent over a full year. A description and analysis of this research has been published in the *South African Journal of Oenology and Viticulture*.
B. Investigating the behaviour of effluent flowing through the CW. Was there any bypass of flow or 'dead' volume within the CW that made it less efficient? The required data was obtained by running a tracer impulse-response experiment that enabled us to measure the mean residence time and the dispersion within the system. This method was also used to identify whether the CW behaved like a plug flow, a stirred tank or a series of stirred tank reactors, or any combination thereof. The Chapter devoted to this stage of the investigation, and an interpretation of results, has been submitted to the AIChE Journal for publication.

C. Finding the rates at which the components of winery effluent are degraded. Answering this question required the use of the data obtained from both A and B above, and is the subject of this Chapter.

7.3. Background: What is a reaction rate and what is a rate constant?

In chemical industries, the *rate* at which chemical components are converted is referred to as the 'kinetics' of a process (Fogler 2005). For physical chemists, the kinetics provide an important tool for understanding the nature of chemical interactions and bonds. For organic chemists, they are equally valuable, because the mode of reaction provides information on the nature of molecules. For the microbiologist, the rates are essential to determining if/when substrate limiting conditions occur. And finally, for the chemical engineer, the kinetics of a process are significant aids in the design and sizing of equipment at a technical scale (Levenspiel, 1972).

7.3.1. Defining the reaction rate

The reaction rate of component i is related to the change in moles of component i as an ideal batch reactor of constant volume by:

$$r_i = \frac{1}{V}\frac{dN_i}{dt} \qquad \text{Equation 7.1}$$

and is based on a unit volume of reacting fluid.

The reaction rate expresses the conversion of a chemical entity with respect to time, and is a function of the properties of the reacting materials or micro-organisms. It may be a linear or some other algebraic function of concentration. Linear rate laws (first-order reaction rates) have a rate that is proportional to the concentration and are those most commonly found. They are also generally well-suited to biological systems in which the concentration of a particular nutrient is not saturated. Algebraic rate laws are proportional to concentration to some power, *n,* and usually include inhibitory effects or account for non-linear behaviour.

For the general class of enzyme catalyzed reactions, the rate law is given as (Levenspiel 1972):

$$A \rightarrow products \qquad \text{Equation 7.2}$$

This class of reaction is classified as an Irreversible Unimolecular First-Order Reaction.

The Monod Equation (Monod 1949) is a special case of Michaelis-Menton kinetics. It allows the rate equation to change from first to zero-order if there is saturation of a substrate within a biological reaction. This occurs because the microbes reach their maximum metabolic rate and cannot take up any additional molecules. The rate therefore becomes independent of concentration. Monod behaviour has been shown to be useful for the reduction of Chemical Oxygen Demand (COD) in a number of VSRs in the USA (Martinez, Wise 2003). Given that few VSRs operate beyond the conditions of saturation, it is reasonable to assume that one can use a linear reaction rate for CWs, where the rate is proportional to the concentration.

Some of the more common forms of the reaction rate for biological systems are shown in Table 7.1.

Table 7.1. Some different forms of the reaction rate

Rate Equation	$\boldsymbol{A \rightarrow products}$
Linear	$-r_A = k \cdot C_A$
Algebraic	$-r_A = k \cdot C_A^n$
Monod	$-r_A = V_{max} \cdot \frac{C_A}{K_m + C_A}$
Other (Michaelis-Menton, in which the Monod forms a special case)	$-r_A = \frac{k_1.C_A}{1 + k_2 \cdot C_A}$

7.3.2. Measuring the reaction rate constant

According to Levenspiel (Levenspiel 1972), finding the reaction rate is normally a two-step process. The concentration dependency is usually found at a fixed temperature, which enables the researcher to identify the temperature dependency of the reaction. The next step is more complex, and depends to some degree on the reactor used. Although the reaction rate can be found in either a constant volume batch reactor or a flow reactor, the former are commonly used because the reactor equation can be solved in first-order kinetics to:

$$C_i = C_{i0} \cdot e^{-k_i t} \qquad \text{Equation 7.3}$$

Using this equation, the rate constant, k_i can be plotted and determined at a given temperature.

Unfortunately, biological systems are not homogeneous, and therefore this approach may not yield the correct data for a biologically catalysed system. Compared to those of a full-scale operating bioreactor, the rates of reaction in a smaller pilot-scale batch reactor may be fundamentally different, especially if the microbial consortia are dissimilar. In addition, large-scale systems tend to operate at a steady state, and thus the selective pressure on the micro-organisms will differ significantly from that in a batch reactor, where the concentration is changing over time. Because of these discrepancies in behaviour, it was decided to determine the kinetics of the process of winery effluent degradation directly from our CW, operating under harvest-time conditions. In order to do so, it was necessary to understand what was in the effluent and the fundamental operating regime of the reactor. This information is presented in Chapters 4, 5 and 6.

The rate constant, *k*, should not be dependent on any other variable if the system is fully described by the rate equation. It may, however, require additional terms to account for process variables such as dynamic microbial populations or different catalysts if these are variables in a given system. For CWs which have been exposed to the same type of effluent for a number of years, where the microbial communities are stable, and if the temperature of the effluent feeding the system does not vary significantly, it is reasonable to assume that the rate constant, *k*, remains the same for a single contaminant.

7.3.3. Rate constants

For CWs the rate equation describing COD reduction or component removal is usually taken as linear, that is, $-r_A = k \cdot C_A$. The International Water Association cites an aerial rate constant (dependent on the surface only, and therefore not including the depth) of $k = 0.10 m/day$ with a standard deviation of 0.053 for biological oxygen demand (BOD) reduction for free water surface constructed wetlands (FWSCWs) (Kadlec, Knight et al. 2000). For VSRs a value of $k = 0.077 m/day$ is given with a standard deviation of 0.053. It should be noted that the standard deviation is of the same order of magnitude as the value, which suggests these data do not provide reliable information.

In Table 7.2 a summary of the different rate constants found for BOD removal is presented. Because these rate constants are based on the rate of removal per unit of surface area this can be of limited use if the same rate constant is being applied to wetlands with different depths.

Accordingly, in our research work we measured the volume-based rate constant and used it throughout, a choice that previous researchers in the field have made.

In South Africa, the primary reporting parameter for legislative purposes is COD, which is why our primary focus was not on BOD. However, in the effluent investigated, the main constituent of COD was ethanol and thus the BOD and the COD are almost equivalent.

Table 7.2. A summary of aerial and volumetric BOD removal rate constants as given by the IWA

Site	k (C^*=0) (BOD)	Standard Deviation	Number of Wetlands	Reference:
Various within North America	0.077 m/day	0.053	38	(Kadlec, Knight et al. 2000)
Denmark	0.068 m/day	Not Specified	70	(Brix 1994)
Unspecified	0.06m/day	Not Specified	Not Specified	(Cooper, Job et al. 1996)
USA	0.17m/day	Not Specified	14	(Kadlec, Knight et al. 2000)
USA	4.5/day	Not Specified	1	(Shepherd, Tchobanoglous et al. 2001)
USA	0.15m/day 0.46m/day	Not Specified	Not Specified	(Pardue, Kassenga et al. 1999)
Not Specified	0.1/day	Not Specified	Not Specified	(Buchberger, Shaw 1995)

7.3.4. Measuring the rate constants of lumped parameters

In most countries, including South Africa, legislative requirements relating to the release of effluent into the environment normally relates to a number of different parameters lumped together (Sheridan 2003). There are exceptions for specific contaminants that are highly dangerous (such as chromium). These are individually specified in each country (US EPA Regional Screening Levels, Interventiewaarden Gevaarlike Stoffen). However, for domestic wastewater

treatment and the more benign agricultural effluents such as that found in winery wastewater, the limits are mainly set by lumped parameters, of which those relating to COD are a good example. COD is a measure of the oxygen requirement for complete oxidation of all oxidisable components in the effluent. In winery effluent, ethanol and acetic acid comprise approximately 85–90% of the COD. Other parameters include total nitrogen (TN) and total phosphorous (TP). Since these lumped parameters cover various components, it is very difficult to measure a true rate constant for their degradation because the individual components will have different rates of degradation. This can lead to an apparent non-constant rate constant, that is, a rate constant that seems to vary over time.

A number of strategies have been adopted to overcome this problem, for example the development of a time-dependent rate constant (Shepherd, Tchobanoglous et al. 2001). The compartmental model presented by Wynn and Liehr (Wynn, Liehr 2001), which was extended further by (Rousseau 2005) included additional parameters. One was making a distinction between two kinds of COD (the rapidly and the less rapidly biodegradable) to accommodate the non-constant rate. Another was the use of a modified tanks-in-series model (PTIS) that involved a k-value distribution rather than a lumped parameter rate constant (Kadlec 2003). These solutions met with varying degrees of success. It is considered that this approach is misplaced, for reasons that will be set out in this Chapter.

7.3.5. Deciding on a reactor equation in order to calculate the rate constants

Much of the published work on measuring the kinetics of degradation within a CW relies on the first order plug flow equation (Equation 7.4) or that for the residual plug flow model (Equation 7.5).

$$C_i = C_i^o \cdot e^{-k \cdot t} \qquad \text{Equation 7.4}$$

$$C_i - C^* = (C_i^o - C^*) \cdot e^{-k \cdot t} \qquad \text{Equation7.5}$$

An inherent assumption of most of the researchers working in this field using these reactor equations is that the flow regime through the CW is ideal thus the above equations cannot directly be used to describe a CW. Since it was found that the flow through our reactor was significantly non-ideal, we believe that this approach leads to inaccuracies in the design. These errors are shown and discussed in Chapter 5. However, this does not mean that the ideal flow assumption has not been successfully used. We have chosen not to enter into this debate because the

empirical data we collected using our CW clearly indicate that the ideal flow model is not appropriate to our calculations.

In this study, three different methods to calculate the rate constant that account for the non-ideal flow were chosen:

- the tanks-in-series equation;
- the Peclet equation (plug-flow with dispersion); and
- the residence time distribution as directly measured, and use of the convolution integral to determine the rate constant.

Each of these methods is discussed below.

7.3.5.1. The N tanks-in-series equation (TIS)

For certain types of residence time distribution the TIS equation is appropriate for describing the processes within a reacting system. In Figure 7.1, adapted from Levenspiel, the age distributions for various values of N (or number of tanks in series) are shown. It is noted that as $N \rightarrow \infty$ the RTD more closely resembles that of a plug-flow reactor.

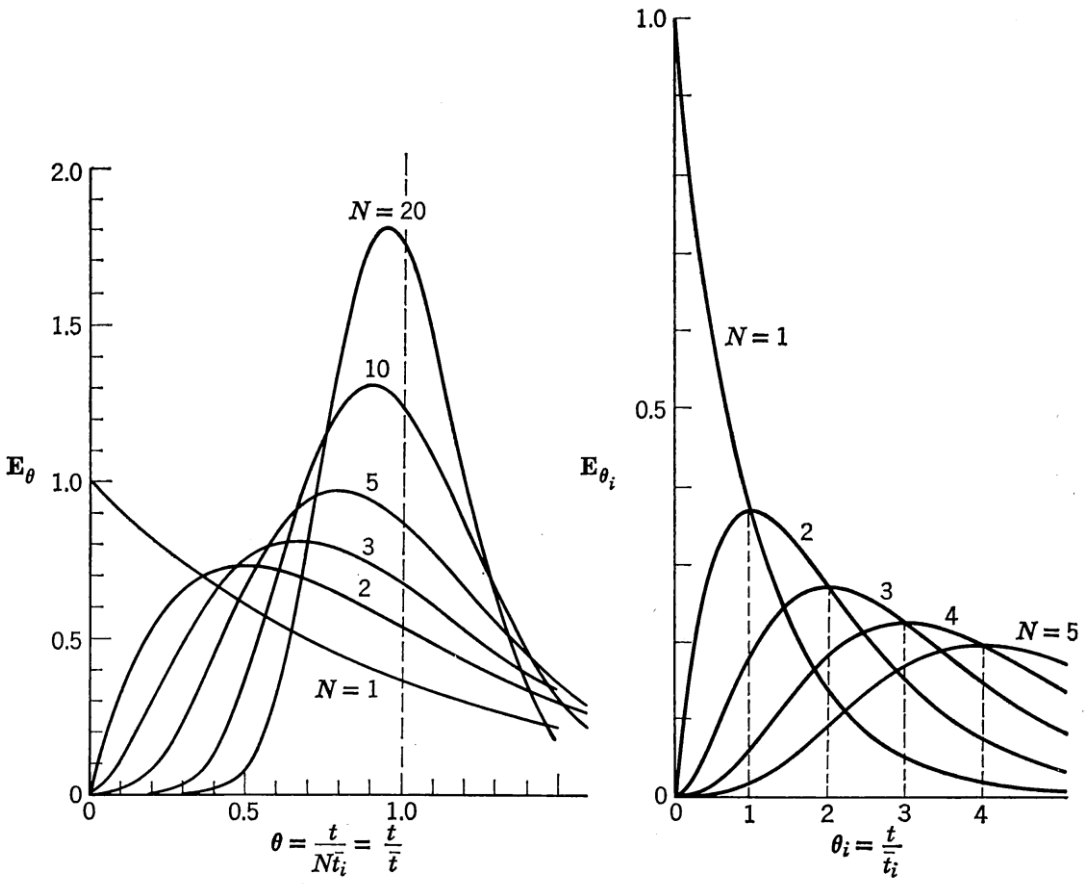


Figure 7.1. Graphs showing the change in the shape in the RTD with increasing tanks taken from Levenspiel (E_ϑ is described in this chapter)

A physical representation of the TIS model is shown in Figure 7.2. In this case, N=4.

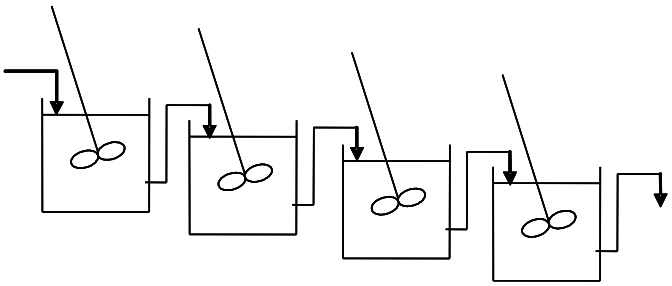


Figure 7.2. A graphical depiction of the TIS model for N=4.

The TIS equation is presented as Equation 7.6, the derivation thereof can be found in Levenspiel, p. 136 (Levenspiel 1972).

$$C_{i,N} = \frac{C_{i,0}}{\left(1 + k_i \cdot \tau_j\right)^N} \qquad \text{Equation 7.6}$$

where $C_{i,N}$ is the concentration of the *i*th component leaving tank *N* in a series of *N* tanks or residence time, τ_j each and assumes first order kinetics and constant density.

7.3.5.2. Peclet Equation (Dispersed Plug Flow Model)

The CW can also be considered as behaving like a plug flow reactor displaying dispersive behaviour. This kind of system is shown in Figure 3.

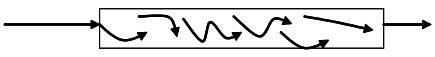


Figure 7.3. A plug flow reactor with dispersive forces at work.

The Peclet equation has been successfully used for first-order reactions in packed bed reactors (Levenspiel 1972), to which category CWs belong. In terms of conversion, *X*, the rate constant, *k*,

the Peclet Number, *Pe*, the length of the system, *l*, and the velocity of the impulse, *u*, the equation is given as:

$$X = 1 - \frac{4 \cdot q \cdot e^{\left(\frac{Pe}{2}\right)}}{(1+q)^2 \cdot e^{\left(\frac{Pe \cdot q}{2}\right)} - (1-q)^2 \cdot e^{\left(\frac{Pe \cdot q}{2}\right)}} \qquad \text{Equation 7.7}$$

$$\text{where: } q = \sqrt{1 + \frac{4 \cdot Da}{Pe}} \qquad \text{Equation 7.8}$$

$$\text{and the Damkohler Number, } Da = \frac{l \cdot k}{u} \qquad \text{Equation 7.9}$$

From our investigation it was found that it was possible to model the system using the Peclet Equation derived from Levenspiel who in turn based his work on that conducted by Wehner and Wilhelm (Wehner, Wilhelm 1956).

7.3.5.3. Convolution Integral

It is also possible to determine the conversion of a reactor (regardless of the degree of non-ideal behaviour) directly from the tracer information for first order reactions. The description of the process that follows is largely an adaptation of Levenspiel's (pp. 264-269). As an impulse of tracer passes through the reactor, it will be modified into an output which will be a function of time. This is graphically depicted in Figure 7.4.

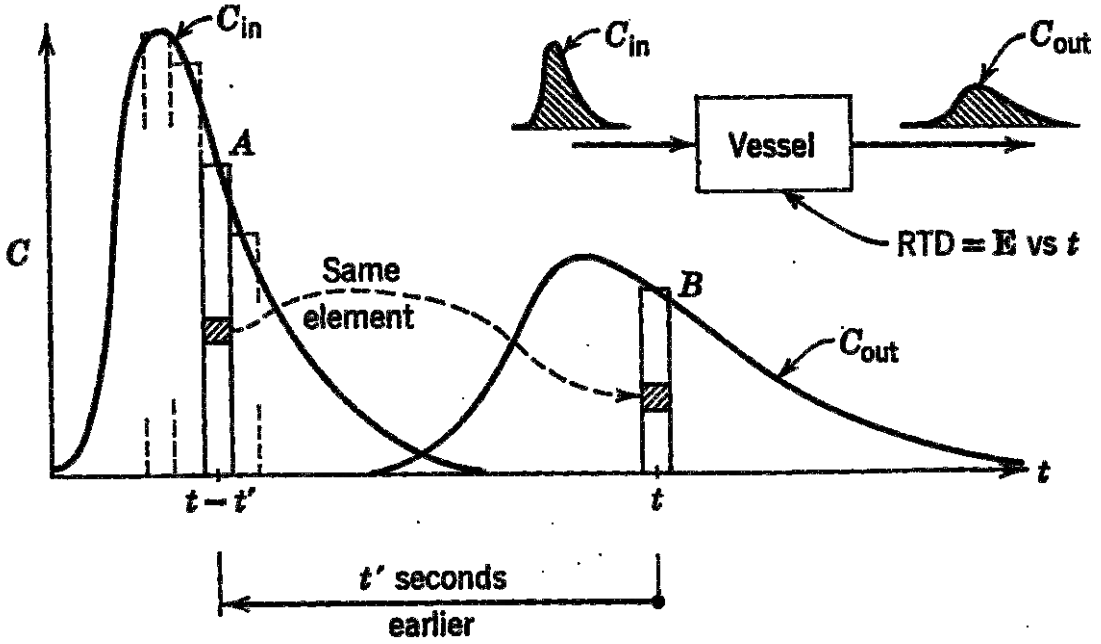


Figure 7.4. A graphical depiction of the movement of tracer through a reactor taken from Levenspiel (Levenspiel 1972)

If we conduct a mass balance analysis of the tracer about to leave at time, t, we find:

$$(tracer\ leaving\ in\ rectangle\ B) =$$
$$(all\ the\ tracer\ entering\ t' seconds\ earlier\ than\ t\ and\ staying\ for\ t'\ in\ the\ reactor)$$

Equation 7.10

The tracer which enters t' seconds earlier than t is shown as rectangle A. We can thus rewrite Equation 7.10 as:

$$(tracer\ leaving\ in\ rectangle\ B)$$
$$= \sum_{\substack{all\ rectangles\ A \\ which\ enter \\ before\ time\ t}} (tracer\ in\ rectangle\ A)(Fraction\ of\ tracer\ A\ which\ stays\ \ for\ t'\ seconds\ in\ the\ vessel$$

Equation 7.11

This can be rewritten as:

$$\boldsymbol{C_{out}} = \int_0^t \boldsymbol{C_{in}}(t - t')\boldsymbol{E}(t')dt'$$

which is equivalent to:

$$\boldsymbol{C_{out}} = \int_0^t \boldsymbol{C_{in}}(t')\boldsymbol{E}(t - t')dt'$$

or, more elegantly:

$$\boldsymbol{C_{out}} = \boldsymbol{C_{in}} * \boldsymbol{E}$$ Equation 7.12

Equation 7.12 can be used to describe the shape of the output (the response) at any given time. This can also be used to calculate the conversion directly (for a first-order reaction):

$$(mean\ concentration\ of\ reactant\ in\ the\ exit\ stream)$$
$$= \sum_{\substack{all\ elements\ of \\ exit\ stream}} (concentration\ of\ reactant\ remaining\ in\ an\ element\ of\ age\ t\ to\ t + dt) \cdot (fraction\ of\ exit\ stream\ of\ age\ t\ to\ t + dt)$$

which can be rewritten as:

$$\overline{C_i} = \int_{t=0}^{\infty} C_{i,element} \cdot \boldsymbol{E} \cdot dt$$ Equation 7.13

For each of these methods (the TIS equation, the Peclet Equation and the Convolution Integral), we have calculated the rate constant for the degradation of the components of winery effluent.

7.3.6. Hypotheses

The focus of the research experiment described in this chapter is threefold: to report on the rate constants measured and to develop hypotheses from the data obtained; to test the hypotheses; and to identify the best method for determining the rate constants, i.e. to estimate the rate based on different models and then check which fits the data best.

There are three components to the hypothesis.

- It is possible to find the rate constants for the degradation of the primary components of winery effluent using the methods and/or equations described above;
- The degradation of lumped parameters will be modelled less accurately than the degradation of individual components; and
- If the rate constants of individual components are very different the most accurate method of determining them is by using the measured experimental data directly via the convolution integral as this does not require a model for the flow of the reactor.

7.4. Materials and methods

7.4.1. Description of the winery supplying effluent to the CW

The winery forms part of an experimental farm belonging to the Agricultural Research Council of South Africa (ARC). Red and white wines are produced in this cellar. Given the research infrastructure that already exists, it was possible to sample the effluent on a daily basis for the duration of a harvest season, and use the data to construct a profile of the effluent. In this case, the season lasted from the end of January 2005 to the end of March 2005. This was a particularly short period (normally the harvest lasts for three months), and almost no rain fell during this time.

This allowed for accurate sampling because there was no dilution effect through rainwater mixing with the samples.

7.4.2. Description of the physical properties of the VSR at the ARC, Stellenbosch

The VSR, which was built in about 2001, is a sub-surface flow constructed wetland 40m long, 4m wide and 1m deep. It was built on a slope with a gradient of approximately 2%, was lined with black polyethylene pond-lining film, and filled with dolomite gravel ($CaMg(CO_3)_2$) with a mean particle diameter of 0.02m and a void fraction of approximately 40%.

The design specifications for the VSR are presented in Table 7.3.

Table 7.3. Engineering design specifications of the VSR

Design Specification	Value
Length	40m
Depth	1m
Width	4m
Lining	Plastic pond liner
Hydraulic Gradient	App 2%
Soil Matrix	Dolomitic Gravel
Average Matrix Particle Size	Approximately 20 mm
Matrix Void Fraction	40%

Fourteen sample ports constructed from a flexible PVC mesh were installed in the VSR for the purposes of this study. Each of these flexible mesh strips were wrapped around a 100mm PVC pipe, joined and submerged vertically to a depth of 1m. The PVC pipes were then removed, leaving the mesh in place. Because it is inherently stable, the gravel did not collapse or force the closure of any of the sample ports at any time during the investigation. This feature of the design ensured that the sample ports did not impede the flow through the VSR. The grid of sampling ports was designed according to the methodology given by Popek (Popek 2002). A schematic diagram showing the side and top views of the VSR is given in Figure 7.5. All the tailings were fed

through sample port 5 into an open collection pond. Two meters were installed, a rain gauge and a water meter, to measure the feed flow rate.

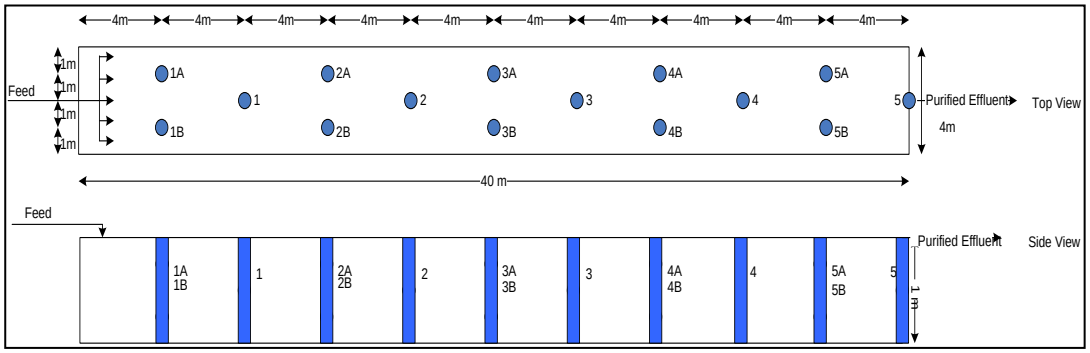


Figure 7.5. Schematic diagram of the VSR showing a side and a top view

The VSR was originally planted sparsely with *Phragmites australis*, which partially colonised the surface as it grew. This planting also included a small number of ornamental plants, such as *Zantedeschia aethiopica*, *Chondropetalum tectorum* and *Cyperus papyrus*, on a trial basis. The feed line was renovated to ensure the flow would be distributed as evenly as possible onto the surface at the entry-point end of the VSR.

7.4.3. Chemical Analyses

The COD was measured using a Merck COD Cell test (1.14555.001) and a Merck Spectroquant spectrophotometer. Metals in solution were measured using a Varian SpectrAA spectrophotometer. Gas mixtures of acetylene/air were used for sample combustion, and detection wavelengths for each of the species were as specified in the User's Manual. Inorganic anions (including bromide for the tracer study) were analysed using HPLC with an Anion Column, using a conductivity detector (the parameters used were: Column T = ambient, 1.5 mL per minute, mobile phase, 3.6 mM sodium carbonate). Organic components were identified using GC-MS – Restek RTX Capillary column (60m by 250µm), T-initial of 70 °C, ramped at 5 °C per minute to 170 °C, second ramp of 10 °C per minute to 280 °C. The routine analyses of those organic components identified as being the most significant were conducted using GC – FID; J & W Scientific DB-Wax Column (60m by 250µm, T-initial of 40 °C for 10 minutes, ramped at 10 °C per minute to 163 °C). A complete chemical analysis of this effluent was made by the authors and is presented in press (Sheridan, Glasser et al. 2011b).

7.4.4. A study on the hydraulic processes occurring within the CW.

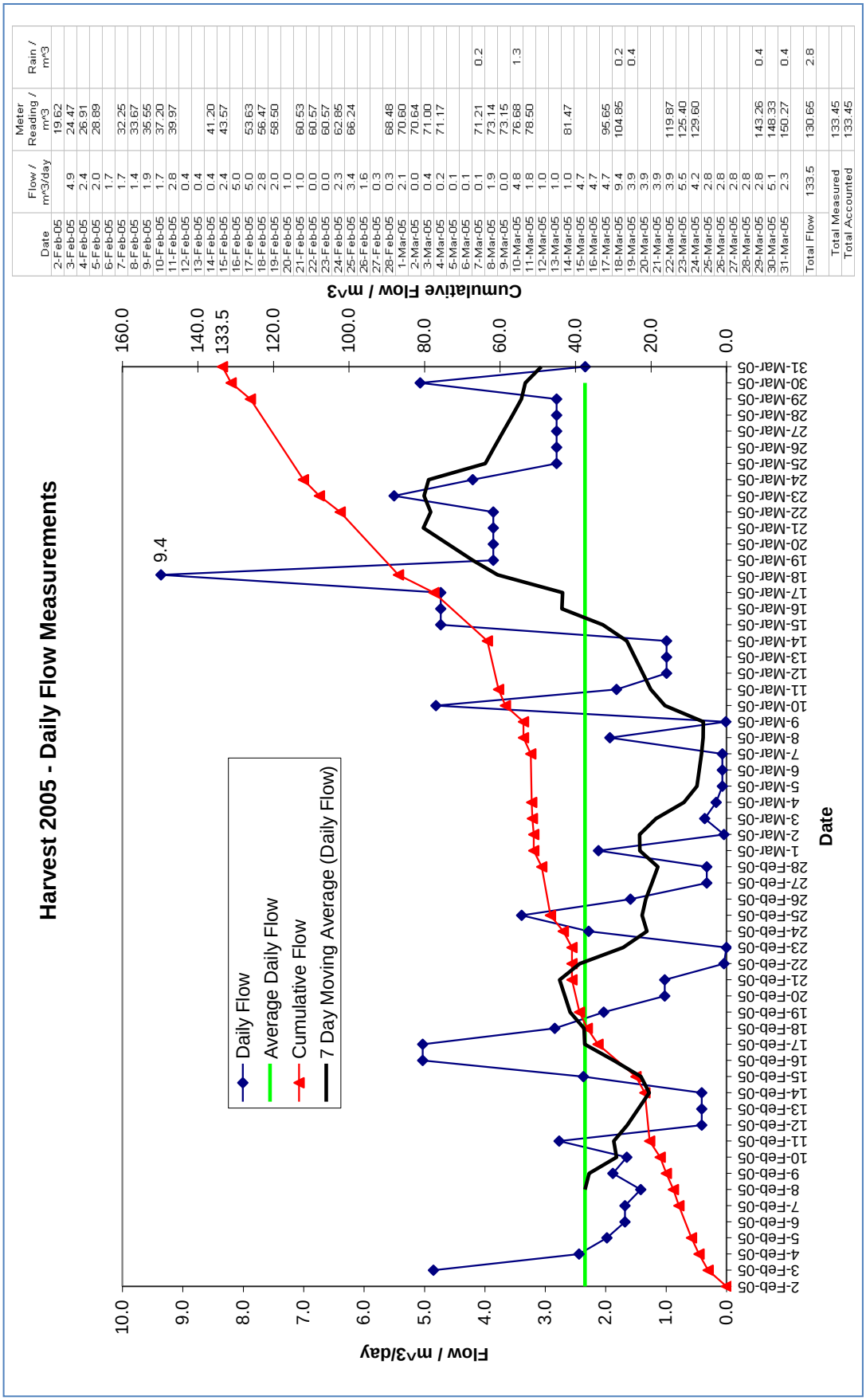
A full study of the hydraulic behaviour of the VSR was conducted, and the results were written up and discussed in Chapter 5. Table 7.4 below records the parameters used.

Table 7.4. A summary of the hydraulic parameters found for the CW

Port Number	Length (m)	Pe	τ (hours)	τ_{Ideal} (hours) [V/Q]	Time for 1st Peak (hours)	Time for 2nd Peak (hours)	Time for 3rd Peak (hours)	Time for 4th Peak (hours)	V_{eff}
1A & 1B	4	0.01	15.03	8.70	4.00	30.93			1.73
1	8	0.01	14.61	17.39	5.70	26.33			0.84
2A & 2B	12	2.47	20.35	26.09	8.93				0.78
2	16	5.10	22.21	34.78	15.00				0.64
3A & 3B	20	7.76	31.55	43.48	26.33				0.73
3	24	12.63	36.13	52.18	20.33	30.93			0.69
4A & 4B	28	17.67	41.47	60.87	35.93				0.68
4	32	8.26	37.89	69.57	15.00	30.93	42.72		0.54
5A & 5B	36	24.57	49.70	78.26	26.33	42.72			0.64
5	40	1.67	22.36	86.96	4.00	6.67	35.93	42.72	0.26

7.4.5. Experimental Method to calculate the rate constants of the processes of degradation

The flow rates for the entire harvest period are shown in Figure 7.6. Since this was not a laboratory system but a CW that belongs to an operational farm, the flow was variable, because of process pulses and blockages in the effluent stream. Rainfall was measured which was accounted for within the fluid mass balance. However, rates of evapo-transpiration were not measured and are therefore not included in the calculation of the rate of degradation. There are no locally derived data for evapo-transpiration, so a rate of evapo-transpiration was found using the formula presented in Table 2.1 with data derived from the Jackson Meadow subsurface flow CW (Wallace, Nivala 2005). This correlation provided a rate of evaporation of 10mm/day, which is equivalent to a calculated loss of effluent of 1536L/day. However, the CW was never observed to dry up, even on days when the flow was as low as 100L/day for three days. It was therefore assumed that since the vegetative cover for this VSB is so sparse, the pan evapo-transpiration correlations do not apply, and evapo-transpiration was negligible. Any evapo-transpirative effects (however insignificant) can be taken as inherent to the measurement of the rate constants.



Date	Flow / m^3/day	Meter Reading / m^3	Rain / m^3
2-Feb-05		19.62	
3-Feb-05	4.9	24.47	
4-Feb-05	2.4	26.91	
5-Feb-05	2.0	28.89	
6-Feb-05	1.7		
7-Feb-05	1.7	32.25	
8-Feb-05	1.4	33.67	
9-Feb-05	1.9	35.55	
10-Feb-05	1.7	37.20	
11-Feb-05	2.8	39.97	
12-Feb-05	0.4		
13-Feb-05	0.4		
14-Feb-05	0.4	41.20	
15-Feb-05	2.4	43.57	
16-Feb-05	5.0		
17-Feb-05	5.0	53.63	
18-Feb-05	2.8	56.47	
19-Feb-05	2.0	58.50	
20-Feb-05	1.0		
21-Feb-05	1.0	60.53	
22-Feb-05	0.0	60.57	
23-Feb-05	0.0	60.57	
24-Feb-05	2.3	62.85	
25-Feb-05	3.4	66.24	
26-Feb-05	1.6		
27-Feb-05	0.3		
28-Feb-05	0.3	68.48	
1-Mar-05	2.1	70.60	
2-Mar-05	0.0	70.64	
3-Mar-05	0.4	71.00	
4-Mar-05	0.2	71.17	
5-Mar-05	0.1		
6-Mar-05	0.1		0.2
7-Mar-05	0.1	71.21	
8-Mar-05	1.9	73.14	
9-Mar-05	0.0	73.15	
10-Mar-05	4.8	76.68	1.3
11-Mar-05	1.8	78.50	
12-Mar-05	1.0		
13-Mar-05	1.0		
14-Mar-05	1.0	81.47	
15-Mar-05	4.7		
16-Mar-05	4.7		
17-Mar-05	4.7	95.65	
18-Mar-05	9.4	104.85	0.2
19-Mar-05	3.9		0.4
20-Mar-05	3.9		
21-Mar-05	3.9	119.87	
22-Mar-05	3.9		
23-Mar-05	5.5	125.40	
24-Mar-05	4.2	129.60	
25-Mar-05	2.8		
26-Mar-05	2.8		
27-Mar-05	2.8		
28-Mar-05	2.8		
29-Mar-05	2.8	143.26	0.4
30-Mar-05	5.1	148.33	
31-Mar-05	2.3	150.27	0.4
Total Flow	133.5	130.65	2.8
Total Measured		133.45	
Total Accounted		133.45	

Figure 7.6. Daily flow characteristics (including the average flow, cumulative flow and a moving average) within the VSB

7.4.6. Average behaviour of the CW

Because this system was used at an operational winery with no control over the effluent entering it, there are large fluctuations in the data. The winemaking process and the effluent it produces has been discussed at length in Chapter 4, but in summary our findings were that the effluent quantity and strength varies considerably:

- from day to day;
- diurnally; and
- seasonally, with a peak occurring towards the middle of the harvest period.

As a consequence of this temporal variation, it is difficult to induce trends from daily data. Thus, in order to determine which components of the effluent are degraded within the system, we took an average of the concentration of each component in each location in the CW over the entire harvest season. These averages are presented in Figures 7.7 to 7.9.

The change in concentration of the minor organic components of the effluent observed as it passed further down the length of the CW are shown in Figure 7.7. In each case (propanol, propionic acid and butyric acid) the concentrations were very low, and thus were not described or modelled. It is, however, interesting to observe their characteristic profiles, because they contribute to an understanding of the behaviour of the whole system. In each case, the concentration of these minor components increases above that of the raw effluent fed into the CW, reaches a maximum and then starts to decrease. It is most probable that this is the result of metabolites released by the microbial consortia as they utilise the ethanol that is fed to the CW. The concentration of each of these components is two orders of magnitude less than the ethanol and acetic acid (which are major components of the effluent) thus do not add significantly to the COD. Therefore it was considered it unnecessary to calculate a rate of (either) production or consumption in order to predict variations in the COD.

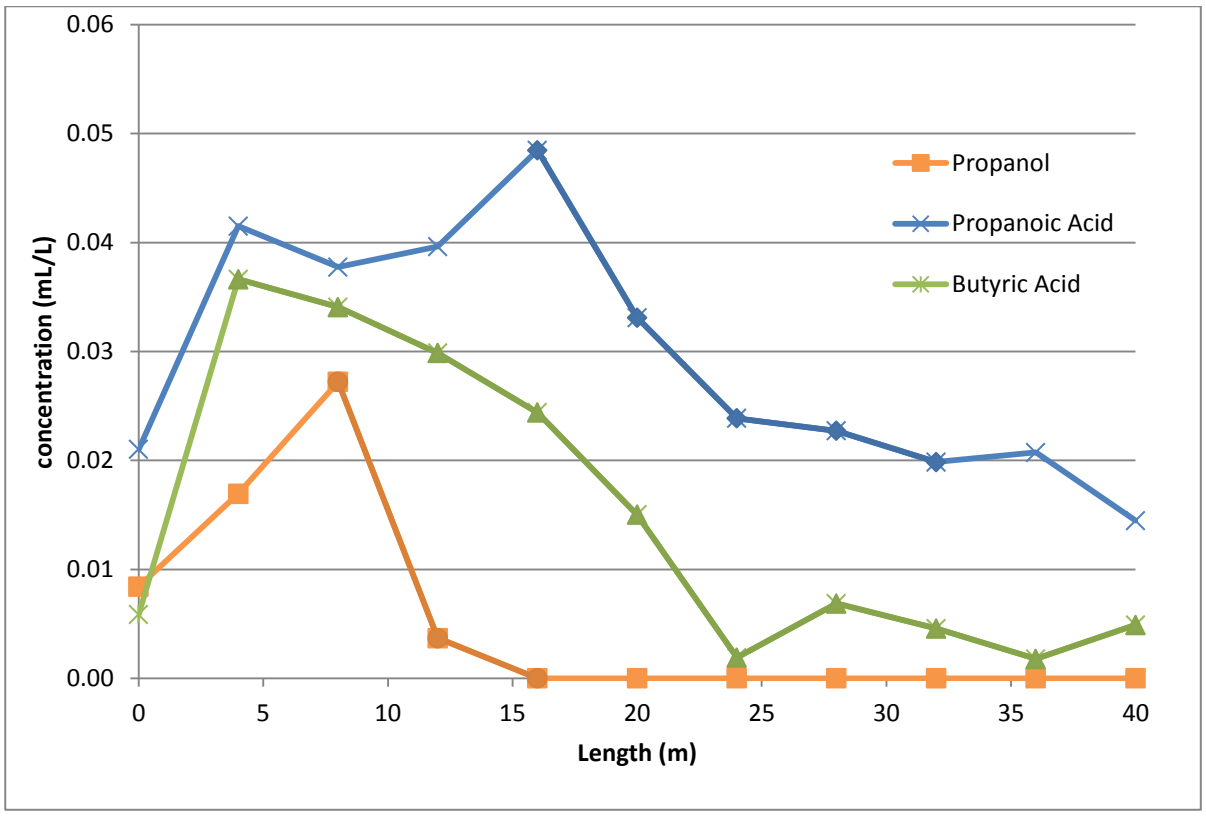


Figure 7.7. Average concentration of propanol, propanoic acid and butyric acid for the entire harvest with increasing duration of flow along the length of the CW

The change in the concentration of the major organic components and COD of the effluent as it moves further down the CW are shown in Figure 7.8. These data indicate that the concentration of ethanol and COD decrease approximately exponentially as the effluent reaches the end of the CW.

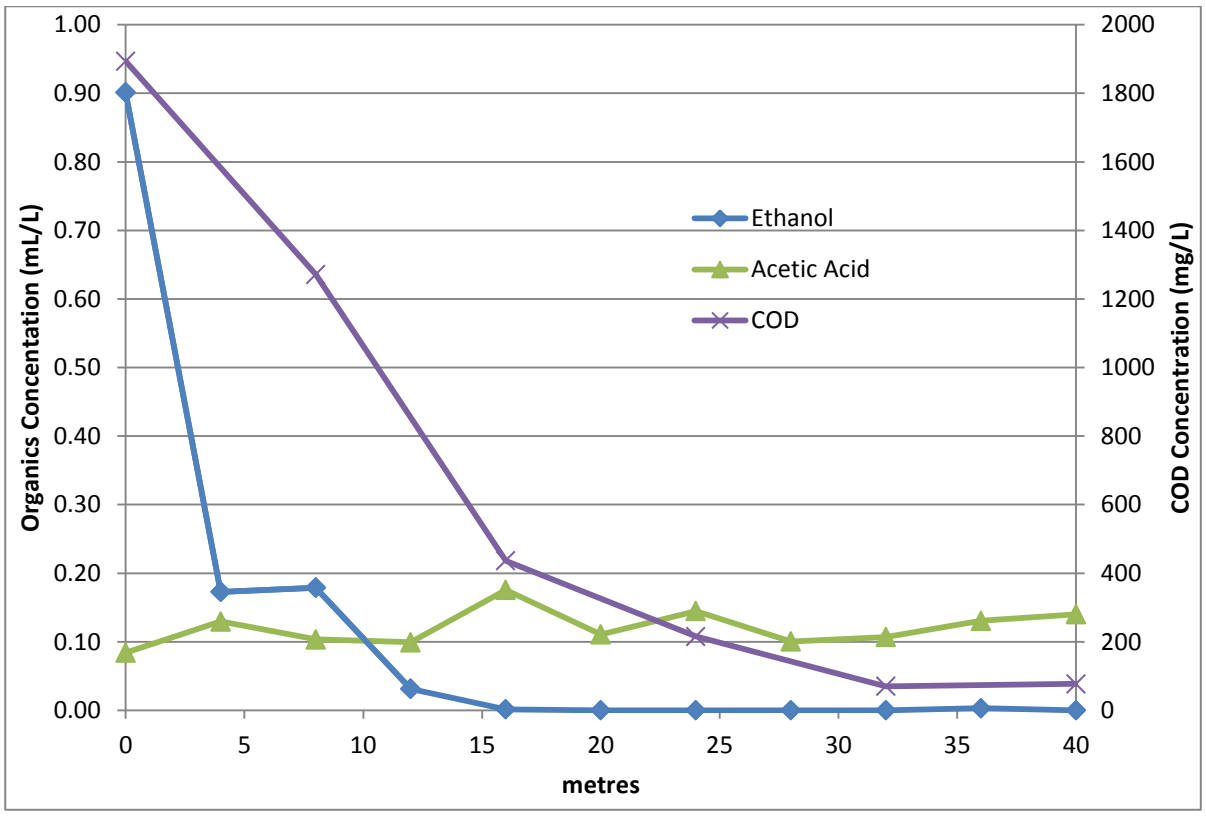


Figure 7.8. Average major organic components and COD concentration for the entire harvest at various locations along the length of the CW

From this data the following can be inferred:

- Although the COD is readily biodegradable, there appears to be a residual amount of 75mg/L at the outlet of the CW.
- The ethanol, which is the principal component of the effluent, is fully biodegradable.
- The acetic acid within the effluent does not appear to be degraded within the CW and remains constant, with a concentration of approximately 0.1 mL/L.

These inferences are very interesting, because they can be used to explain some of the behaviour of the system. The degradation of ethanol appears not to be affected by the concentration of acetic acid, although it was initially assumed that the principal path of ethanol degradation would be through oxidation to acetic acid. However, given that there is almost no increase in the concentration of acetic acid it is much more probable that the ethanol is degraded directly to CO_2, and that the microbes within the system are utilising the ethanol as a food source. The roughly constant concentration of acetic acid of 0.1mL/L corresponds to a COD of 112mg/L. This is very similar to our statistical COD average found in the CW at the outlet of 77mg/L. It is therefore reasonable to assume that (within the bounds of experimental error and the statistical analysis

conducted) that the residual COD is comprises primarily acetic acid. Also, it was observed that the pathway for bio-degradation of acetic acid is anaerobic (acetic acid is converted to methane through methanogenesis (Strong, McDonald et al. 2011)). Thus, if no reduction in the concentration of acetic acid was observed, either the rate of production is equal to the rate of consumption, or there is no bioremediation of acetic acid. It was hypothesized earlier (Chapter 5) that the flow in this CW was primarily at the surface or within the shallow "hull", which would be located mostly in the upper layers and within the root zone (aerobic and anoxic layers). Consequently, there would be little flow into the deeper anaerobic layers, which would make it unlikely that any degradation of acetic acid could be expected. These findings lend support to our early hypotheses, which were based purely on the examination of the hydraulic performance of the CW. In other words, the chemical data support the hypotheses grounded in the hydraulic data.

In Figure 7.9 the change in concentration of the major ionic components of the effluent as it progresses through the length of the CW is shown.

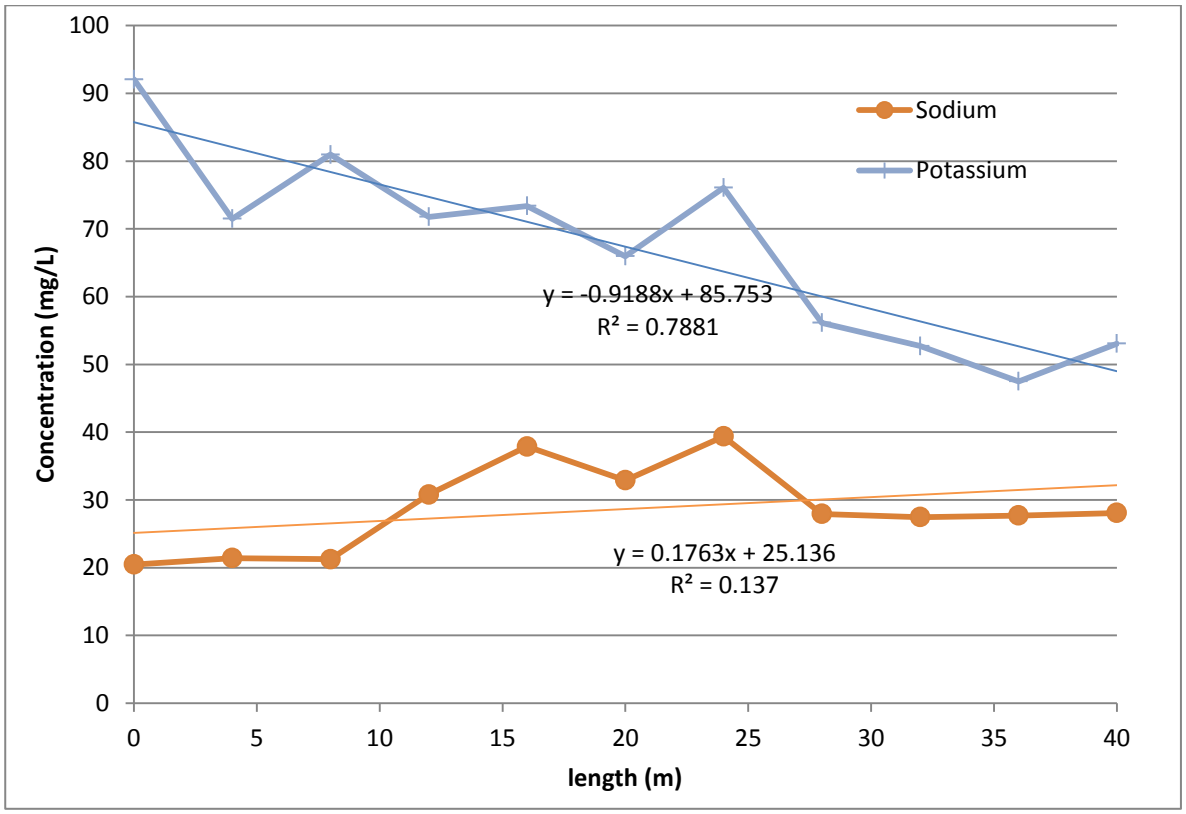


Figure 7.9. Average changes in concentration of sodium and potassium for the entire harvest as it travels along the CW

Since the CW was not planted with halophytes, there were no plant-based mechanisms in the system to remove (excess) sodium ions. In addition, the matrix of dolomite has no sorptive

capacity for sodium, and the microbial need for sodium would be minimal. Accordingly we did not expect any decrease in the concentration of sodium, and our observations confirmed this. The slight increase could be a result of evapo-transpiration. However, given the very low correlation coefficient it would be difficult to defend any explanation of this increase. It can be seen in Figure 7.9 that the concentration of potassium diminishes at a consistent rate as the effluent flows through the CW through its entire length and over an increasing duration, with a fairly good coefficient of correlation (0.79). This is consistent with the idea that potassium is a major plant cation that can be utilised by the plants growing within the CW (Marschner 1983). As with sodium, the matrix has no sorptive capacity for potassium, and thus the average decrease from 86mg/L to 49mg/L (a 43% drop) is probably due to plant uptake and, to a lesser extent, microbial consumption.

This data was applied in developing the techniques outlined below for determining the rates of degradation of components in the effluent entering this CW. It is suggested that these techniques can be used successfully for the degradation of any component, provided that the kinetics of the removal processes are similar — that is, first order. This is not an unreasonable suggestion for any linear (no production, only removal) bio-degradation process, because all typically follow Monod kinetics.

7.4.7. Determining the rate constants using different techniques.

Following our thorough investigation of the hydraulic processes occurring within the CW it is believed that it is possible to justify three different modelling techniques to assess the rate constants. These three techniques involve using:

- a tanks-in-series equation;
- the Peclet equation, which is essentially a plug-flow with diffusion equation; and
- the RTD directly to apply the conversion data.

The data supporting the calculations is presented in Appendices PPP through GGGG.

For all three methods, the degradation of our chosen components was modelled from 0m–4m and from 0m–8m.

The TIS model for 0m–4m has a theoretical number of tanks, N, of 1.26, and from the feed–8m, the value for N is 1 (in other words, the system is modelled as a single CSTR for this region).

Despite these values for N being close to 1, given Figure 5.4, the RTD is significantly different to a single RTD and thus N=1 is not a good approximation of the system behaviour.

For the Peclet model, the built-in module "solver" in MS Excel was used to determine the value for k, since it was known what the conversion (X) was for each "reactor" — that is, from 0m–4m and from 0m –8m. For the convolution integral technique, the solver was used to find a value for k, such that the calculated conversion was the same as the measured conversion. The results showing the rate constants and associated uncertainty are presented in Table 7.5.

Table 7.5. The calculated rate constants (k/hr) using the TIS equation, the Peclet Equation and the Convolution Integral.

TIS Model	**Feed to 4m**			**Feed to 8m**		
Component	k /hr	Std Dev	Std Dev %	k /hr	Std Dev	Std Dev %
Ethanol (mL/L)	-0.0889	0.190	214%	-0.0877	0.179	204%
K (mg/L)	-0.00392	-0.00455	116%	-0.00577	0.00692	120%
COD (mg/L)	N/A			-0.0111	0.0276	249%
Peclet Model	**Feed to 4m**			**Feed to 8m**		
Component	k /hr	Std Dev	Std Dev %	k /hr	Std Dev	Std Dev %
Ethanol (mL/L)	-12.113	25.700	212%	-3.578	6.061	169%
K (mg/L)	-0.312	0.388	124%	-0.127	0.195	154%
COD (mg/L)	N/A			-0.517	1.506	291%
Convolution Integral	**Feed to 4m**			**Feed to 8m**		
Component	k /hr	Std Dev	Std Dev %	k /hr	Std Dev	Std Dev %
Ethanol (mL/L)	-0.2459	0.1910	78%	-0.2052	0.0987	48%
K (mg/L)	-0.0386	0.01720	45%	-0.0262	0.0201	77%
COD (mg/L)	N/A			-0.0599	0.0653	109%

The TIS equation gives almost the same rate constant for each section (the feed–4m and the feed–8m) for ethanol, with a value of -0.088/hour. However, the uncertainty with this value is large: in both cases, the standard deviation is more than twice the calculated value. For potassium, the rate constant was calculated to be -0.0039/hr for the feed–4m sample port and -0.0058/hr for the feed–8m. In both cases the standard deviation was high, although not as high as that found for ethanol. This is a result of the poor fit of the RTD by the equation.

The Peclet equation gives a rate constant for ethanol removal of -12.19/hr for the feed–4m and a rate constant of -3.58/hr for the feed–8m. In both calculations the uncertainty associated with this value is less but remains considerable at greater than 160%. For potassium, the rate constant for the feed-4m was found to be -0.31/hour and from the feed - 8m was found to be -0.13/hr. In both these cases the standard deviation was of similar magnitude to the value found. For both ethanol and potassium, this equation gives us rate constants that vary by more than 300%, which is clearly not good enough for design purposes. Similarly to the TIS equation, this is a result of the poor fit of the equation to the RTD. For both the TIS and the Peclet equations, because they do not fit the RTD well, there was no expectation that they would predict the system accurately.

The convolution integral method gave a rate constant for the feed–4m of -0.246/hr for ethanol and for the feed–8m a rate constant of -0.205/hr. However, in this instance the standard deviation was significantly lower than the value for both sections. The results calculated for potassium were similar: a rate constant of -0.0386/hr for 0m–4m and 0.0262/hr for 0m–8m. In each case, the standard deviation was significantly less than the value. Using this method, similar values were found for the two reacting regions with lower standard deviations, which is why there is greater confidence in using this method and these rate constants.

The three different methods for determining the rate constant gave very different results. Clearly we needed a value which was correct, and which could be used for potential design or description purposes. Given that these three values have orders of magnitude differences between them, a strategy had to be developed to determine both the most accurate value, and the most exact method for determining the rate constant. It was believed that because of the non-ideal nature of the flow within the first 8m, our calculation of the hydraulic processes occurring in the CW was not as accurate as that calculated for the sample ports located further along the CW. This was indicated in Figure 5.6, where the Peclet Number was not well correlated with length/duration in this region. However, in general it was found that by 8m most of the ethanol had degraded.

Therefore when there was good hydraulic data, there clearly was no degradation since it was primarily complete, and when there was good data for determining the kinetics there was poor hydraulic data. Our solution to this conundrum was to show self-similarity of the RTDs. We did this since the RTD found at each port did not represent the entire system, but rather the flow through that particular location. Self-similarity can be demonstrated by plotting $E(\theta)$vs. θ where $\theta = {}^{t}/_{\bar{t}}$. If the graphs appear similar, then self similarity would hold, and once self similarity was established it would be able to extrapolate backwards or forwards (that is, the hydraulic information from the regions towards the end of the CW could be used to determine a rate constant in the regions near the beginning). This was important because sample port 5, located at the outlet of the CW, could be used for modelling, since all the effluent flowing into the CW also exited through this port. It was therefore possible to scale the port 5 RTD to any location within the CW and use it to calculate a rate constant based on the measurement of the concentration of all the components at that specific location. These concentrations are shown in Figure 7.10, where the correlation developed in Chapter 5 is used to convert distance (as shown in Figure 5.6) into mean residence time, $\bar{t}$, and the concentrations found at various lengths are presented in terms of $\bar{t}$. By using this graph, the different methods for calculating the conversion are compared with the values actually found within the system.

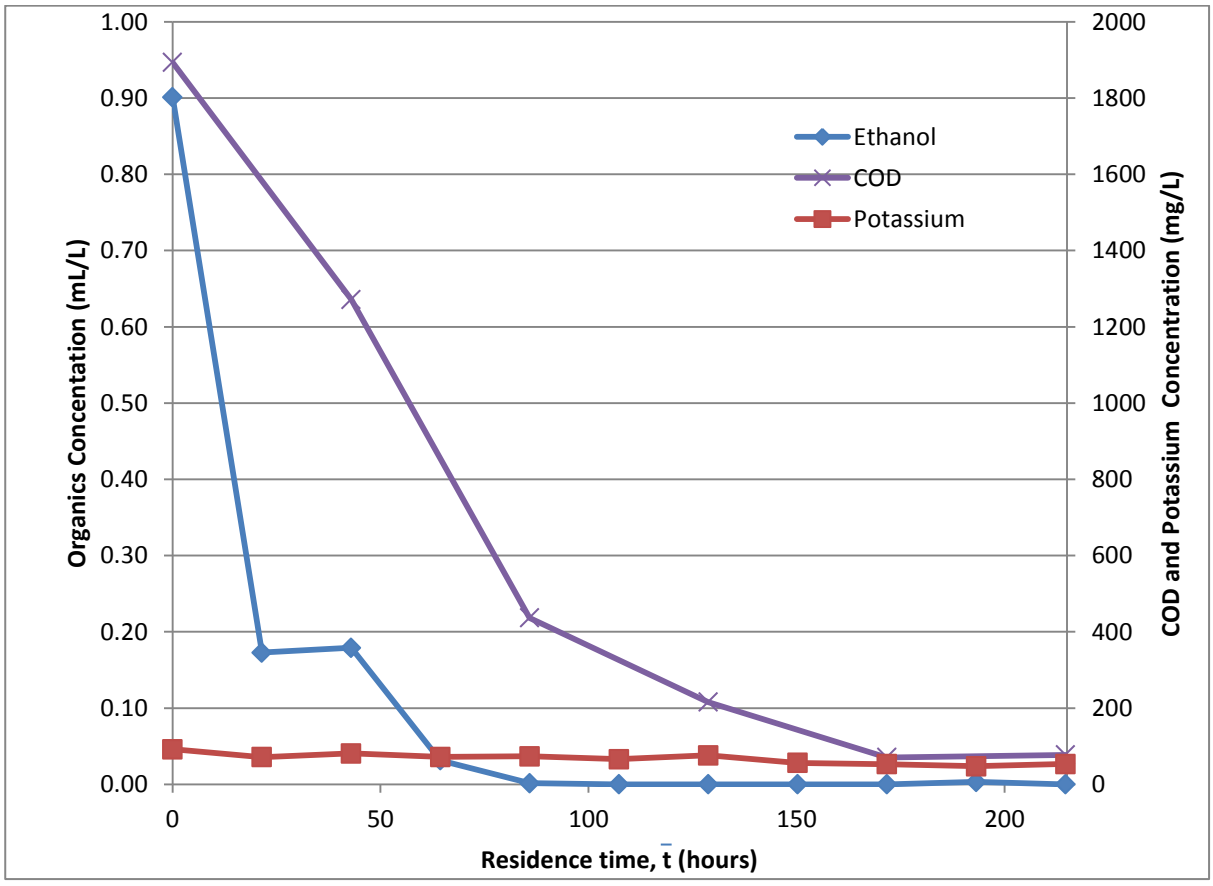


Figure 7.10. Average concentration vs. $\bar{t}$ for the CW over the duration of the harvest season.

7.4.8. Verifying the rate constants found using the RTD directly (convolution integral), the TIS equation and the Peclet equation

7.4.8.1. Demonstrating self similarity of the reactor

As mentioned earlier, showing self similarity of the RTDs is required for our demonstration that our proposed approach works. Initially, $E(\theta)$vs. θ for all sample ports was plotted, but it became evident that there were three regions of self similarity. These three regions are plotted on two separate graphs, which are seen in the figures below.

The graph in Figure 7.11 shows the RTDs for sample ports 12m–32m, and demonstrates clearly that within the middle sections, where there is little disturbance, the RTDs are self similar.

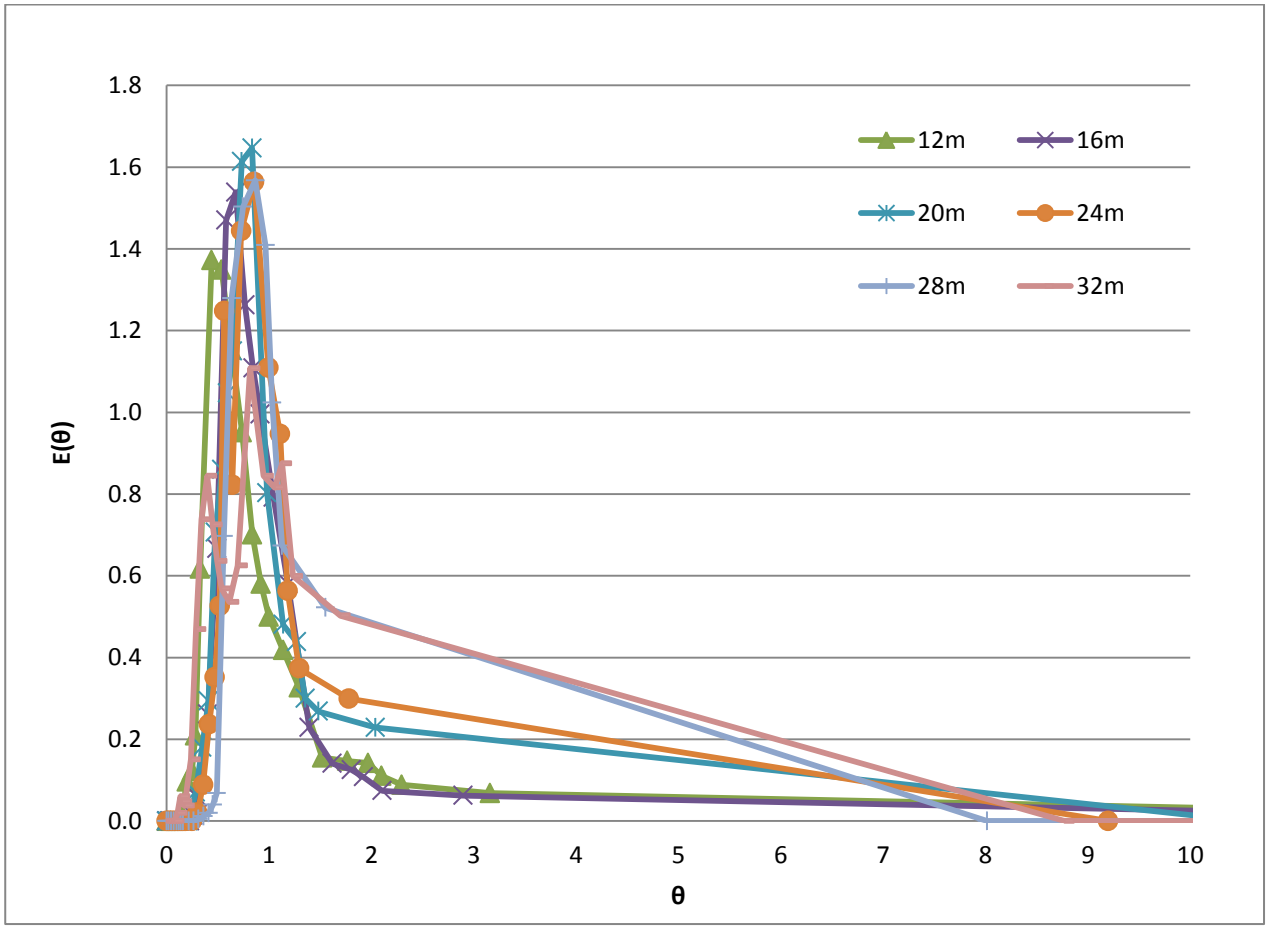


Figure 7.11. Normalised age distributions for the middle sections of the CW

In Figure 7.12, the normalised RTDs for the first two and the final two sample ports are presented. Here the similarity can be seen between the first two ports and the last two ports.

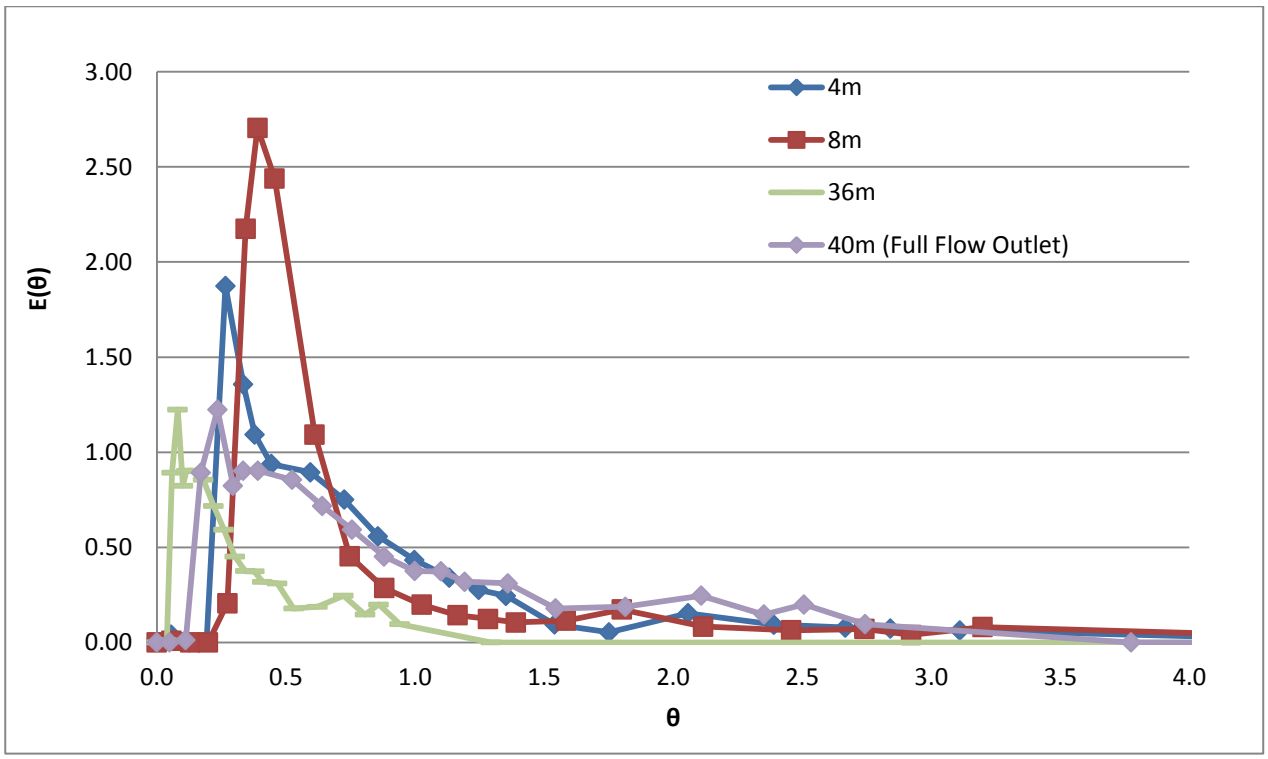


Figure 7.12. Normalised age distributions for the initial and final sections of the CW

Following the concept of self similarity, the analysis of the CW was divided into three clearly separate regions: the front end, the mid region and the back end. In the front end, non-ideal behaviour in the flow rate could be seen, possibly due to back mixing and the establishment of the flow profile, namely the hull. In the mid-region, which occupies the bulk of the reactor, fairly similar and consistent behaviour was observed with increasing dispersion as the effluent travelled further down the length of the CW. At the final two sample ports, increasingly non-ideal behaviour was noticed, which is ascribed to the tapering of the streamlines into the apex of the hull as the full flow in the CW passed through this point (the outlet). Bypass was also observed, especially in port 5 (at the end of the CW) as separate yet distinct mode of the distribution. This is because the entire flow of the CW passes through this location. Thus, despite there being three regions in the CW, on the whole, the system is self similar. It is therefore not unreasonable to extrapolate the RTD between different locations within the CW.

7.4.8.2. Modelling the ethanol degradation using Port 5; the outlet of the reactor.

The hydraulic properties found for Port 5 are presented in Table 7.4. Although ethanol was not detected in the outlet of the CW (at Port 5) an assumed residual concentration was needed in order to determine a rate constant (a zero concentration implies an infinitely large rate constant). A conversion of 99% was assumed, which gave an outlet concentration of 0.01mL/L. This value

was chosen because it was below the lower detection limit for ethanol on our analytical apparatus. In Figure 7.13, the base case is presented, the TIS equation with N calculated for port 5 and average k as found in Port 1A/B and Port 1. This is compared to the Peclet model, with D as calculated for Port 5 and average k as calculated from Port 1a/b and Port 1. The RTD is also utilised directly, as discussed earlier, with an average rate constant. In this case, θ was scaled as the same as the overall average (from 0m–40m, which is equivalent to 0 hours–215 hours). The rate constant found and the RTD from Port 5 was used to calculate the conversion for each time (or distance).

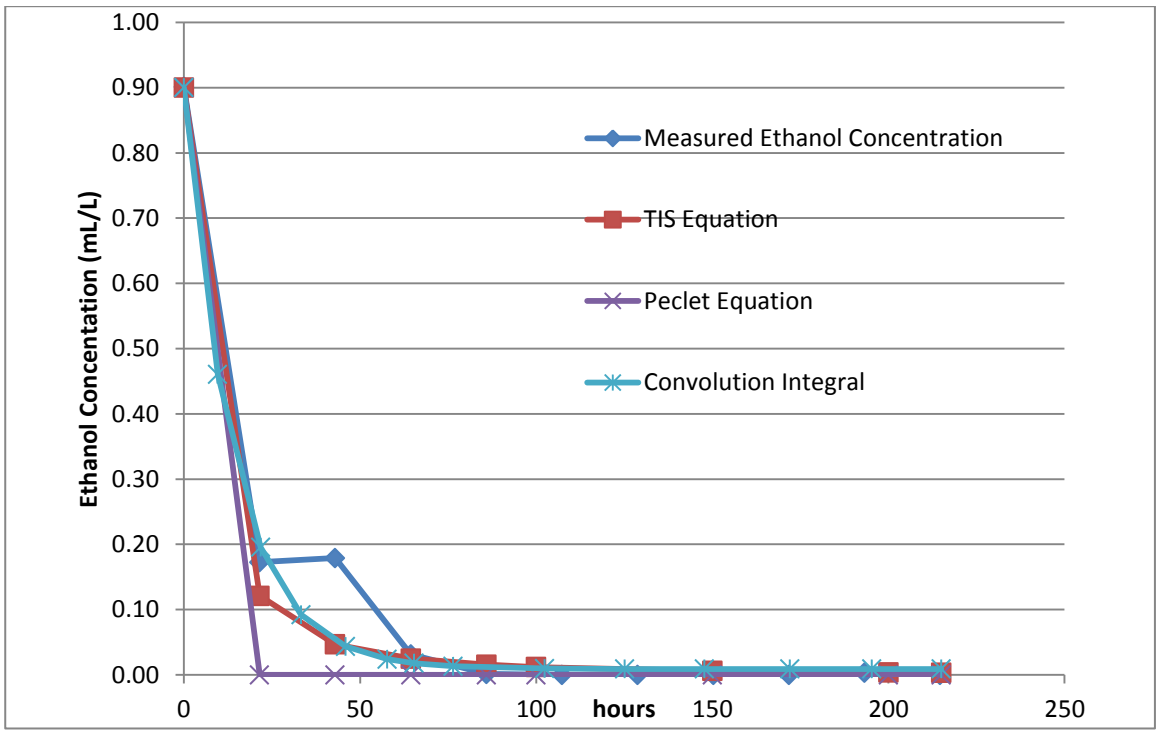


Figure 7.13. Base case for comparison of the three different rate constant calculations (Pe equation rate constant k=7.85/hr, TIS equation rate constant = 0.088/hr and convolution integral k=0.804/hr)

It was then chosen to optimise the Peclet and the TIS equations. An error was defined as the measured concentration subtracted from the calculated concentration. The square of the errors was summed and the MS Excel built-in Solver Module to minimise the sum of the squared errors by varying the Pe number for the Peclet equation and the number of tanks, N, for the TIS equation, using those rate constants found in the base case presented above. The results of this optimisation are shown in Figure 7.14. The convolution integral is not optimised, since it is representative of what is occurring within the reactor. For this case the Pe number was found to be 0.014, and N 1.425.

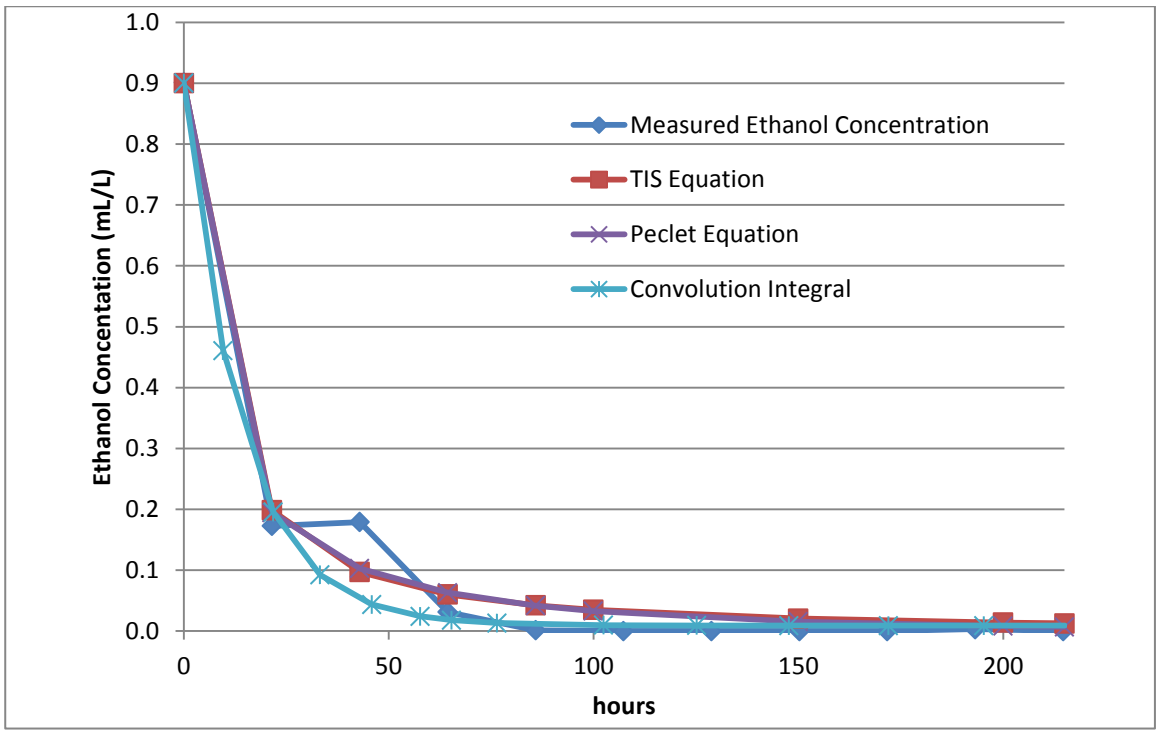


Figure 7.14. Optimised case for comparison of the three different rate constant calculations with Pe and N solved for minimum sum of squared errors (Pe equation rate constant k=7.85/hr, TIS equation rate constant = 0.088/hr and convolution integral k=0.804/hr).

It is evident that this approach allowed us to achieve a calculated value that is closer to the measured value than for the base case, and it also appears that the Peclet and TIS equations give the same result, albeit with vastly different rate constants. This is attributable to the similarity between the Peclet and the TIS models. It can be shown that the two are equivalent under certain conditions (an infinite number of tanks in series is exactly the same as a plug flow reactor).

The data found led to an ambiguous result: a rate constant was needed for the model, but the three different methods for determining the rate constant gave us results which were orders of magnitude apart and with large standard deviations. Therefore, it was assumed, based on standard deviation and the close fit to the data found in the base case, that the convolution integral method gave us the correct rate constant. This can be justified on the grounds that when the CI was used to solve for the rate constant, the data is being used directly, rather than getting the data, fitting an equation and using the results arrived at.

A second optimisation was therefore attempted in which the rate constant found using the convolution integral method (k=0.804/hr), and optimised for Pe and N was used. This case is shown in Figure 7.15.

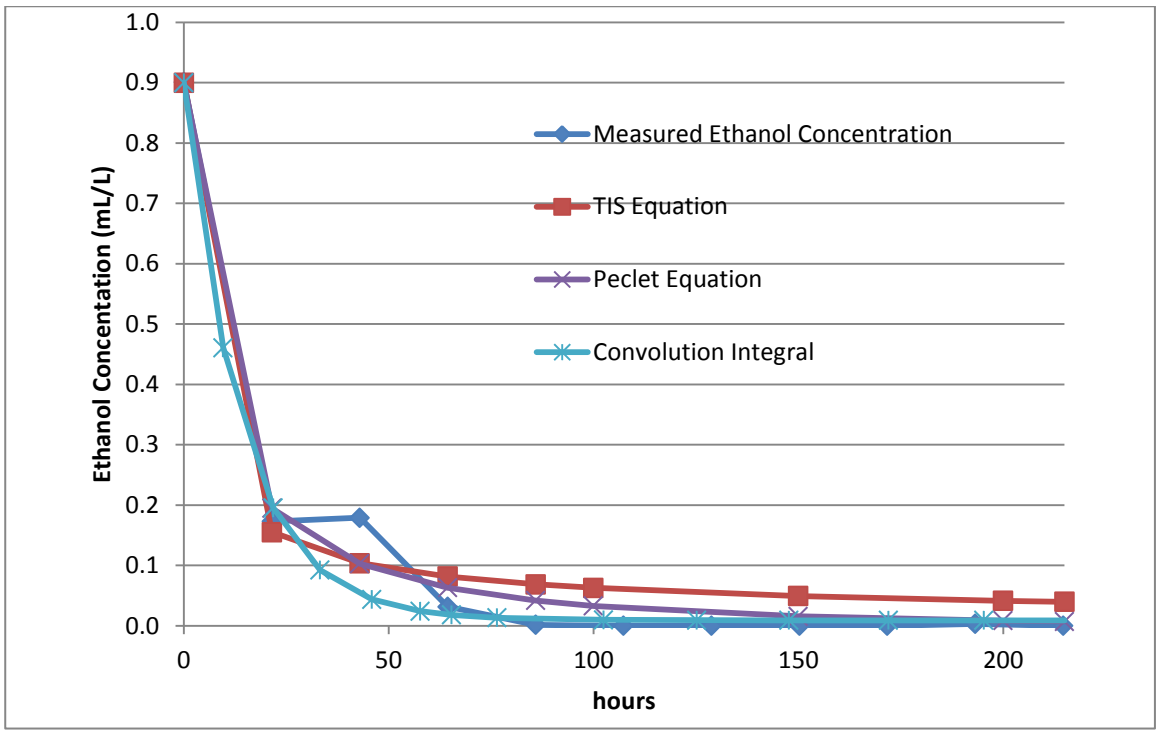


Figure 7.15. Second optimised case for comparison of the three different rate constant calculations with Pe and N solved for minimum sum of squared errors using the rate constant found via the convolution integral method.

In this case, the calculated concentrations are reasonably accurate. However, the calculated value for N is 0.6055 and the calculated Pe number is 0.014. These are significantly different to those calculated for sample port 5 from the RTD.

On the basis of the graphs, and the ambiguity caused by using models, it is believed that the convolution integral method is the most appropriate for the in-situ measurement of rate constants in CWs. It is, however, fortunate in that we measured the RTD for each port, since this gave us an understanding of at what point (that is, how far down the CW) individual components would be fully degraded. It is this information that enabled us to determine the rate constants. It is therefore concluded that whilst it is possible to fit the data using the Peclet or TIS equation, they are not particularly good for use in design or scale-up. For this purpose it would be preferable to use the convolution integral. A statistical analysis was conducted on the three cases, the results of which are presented below:

Ethanol Modelling		P -value	T value
Base Case	Convolution Integral	0.1199	-1.74
	CSTR	-0.3155	1.07
	Peclet	0.1297	1.69
Optimised case	Convolution Integral	0.1199	-1.74
	CSTR	0.2094	-0.852
	Peclet	0.46	-0.77
Optimised with rate constant found using CI	Convolution Integral	0.1199	-1.74
	CSTR	0.1618	-1.541
	Peclet	0.4635	-0.77

7.4.8.3. Modelling the potassium removal using Port 5; the outlet of the reactor.

On average, the conversion (X) of potassium was 42% (a decrease from 92.06mg/L - 53.07mg/L) as it passed through the CW. Accordingly, when the potassium degradation was modelled, measured data was used rather than assuming any outlet value. In Figure 7.16, the base modelling case is depicted, the TIS equation with N calculated for port 5, and the average k found in Port 1A/B and Port 1. This is compared with the Peclet model, with D as calculated for Port 5 and average k as calculated from Port 1a/b and Port 1. Lastly, the RTD is shown directly. In exactly the same way used for modelling ethanol concentration, θ was scaled to match the overall average (from 0m–40m, which is equivalent to 0 hours–215 hours), and the rate constant found from Port 5 and the RTD was to calculate the conversion for each time (or distance).

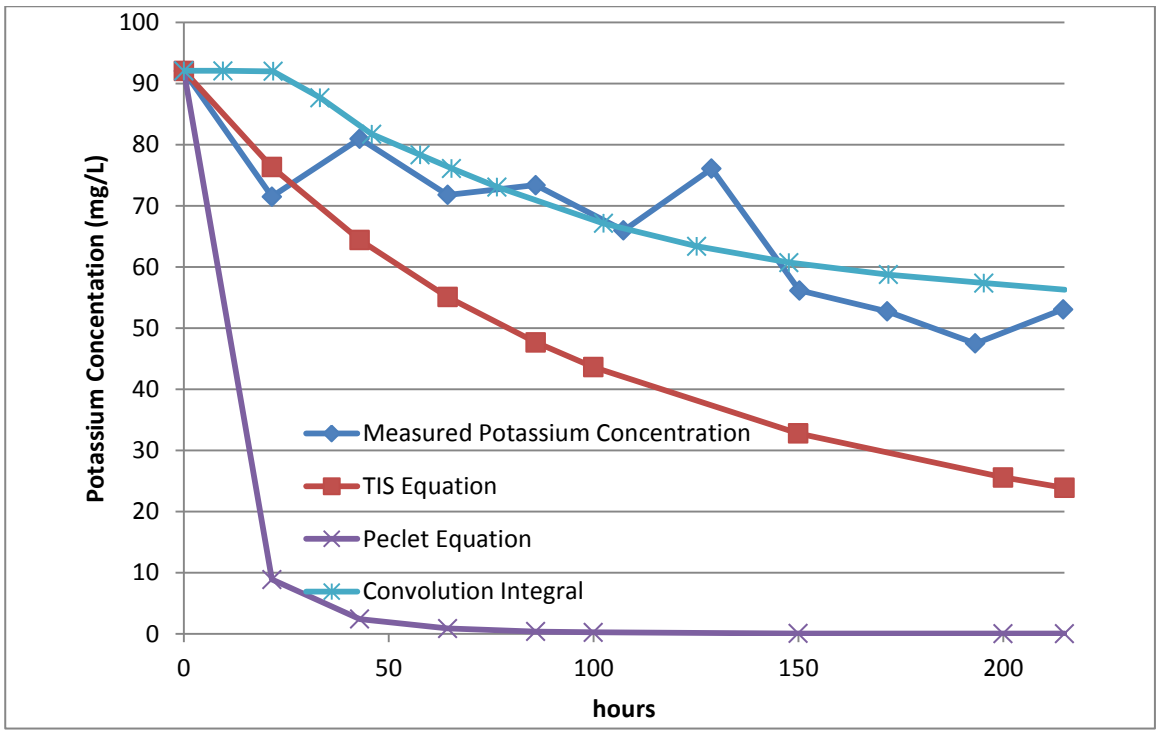


Figure 7.16. Base case for comparison of the three different rate constant calculations (Pe equation rate constant k=0.22/hr, TIS equation rate constant = 0.0049/hr and convolution integral k=0.037/hr)

We then chose to optimise the Peclet and the TIS equations. As described earlier in the calculations we used for ethanol, MS Excel Solver was used to minimise the sum of the squared errors by varying the Pe number for the Peclet equation and the number of tanks, and N for the TIS equation, using those rate constants found in the base case presented above. The results of this optimisation are plotted in Figure 7.17. The convolution integral was not optimised, and in this case the Pe number was 0.004 and N was 0.70.

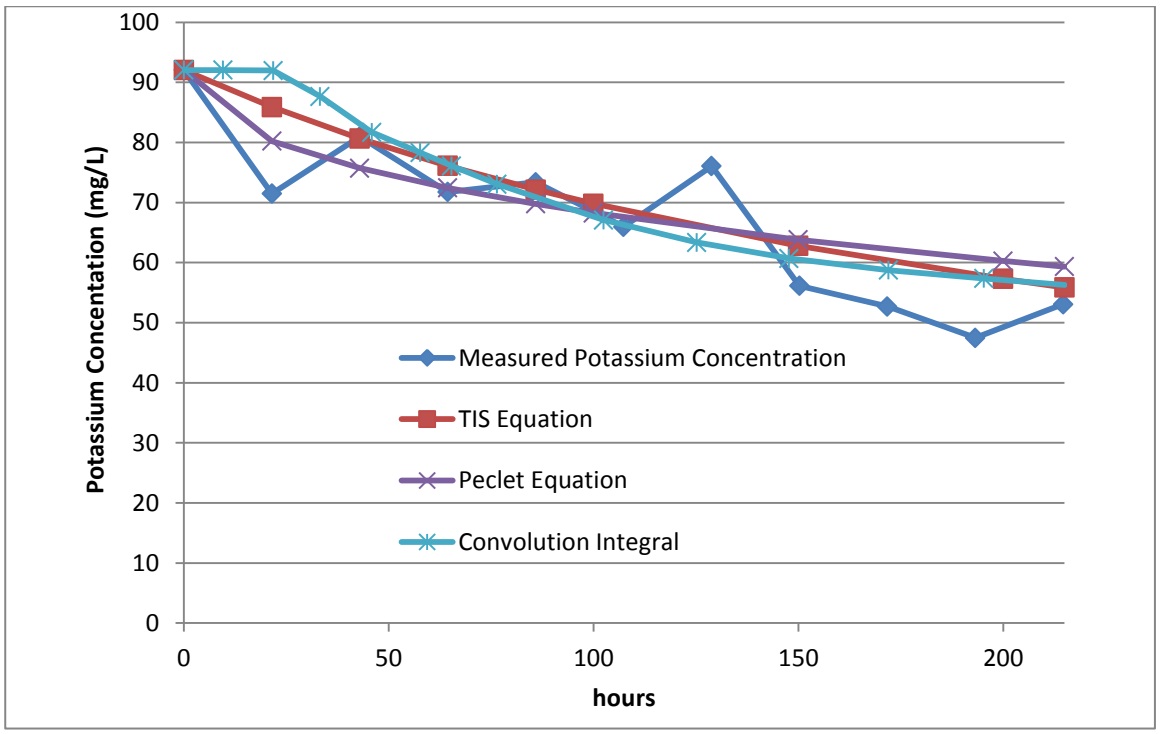


Figure 7.17. Optimised case for comparison of the three different rate constant calculations with Pe and N solved for minimum sum of squared errors (Pe equation rate constant k=0.22/hr, TIS equation rate constant = 0.0049/hr and convolution integral k=0.037/hr).

Whilst this process of optimisation leads to fairly accurate modelling, the values found for Pe and N are no longer sensible. As with ethanol, the same ambiguity was encountered: a rate constant for the model was needed, but the three different methods for determining the rate constant gave us results that were orders of magnitude apart and had massive standard deviations. Therefore, basing our assessment on standard deviation and the close fit with the data in the base case, it was assumed that the convolution integral method gave us the correct rate constant. This was also justified on the grounds that when the convolution integral was used for the base case, a very good fit for the latter was seen, in comparison with those derived from the Peclet and TIS equations.

Again, as with regard to ethanol modelling, a second optimisation was conducted in which the rate constant found using the convolution integral method, and optimised for the values of Pe and N was used. This case is shown in Figure 7.18.

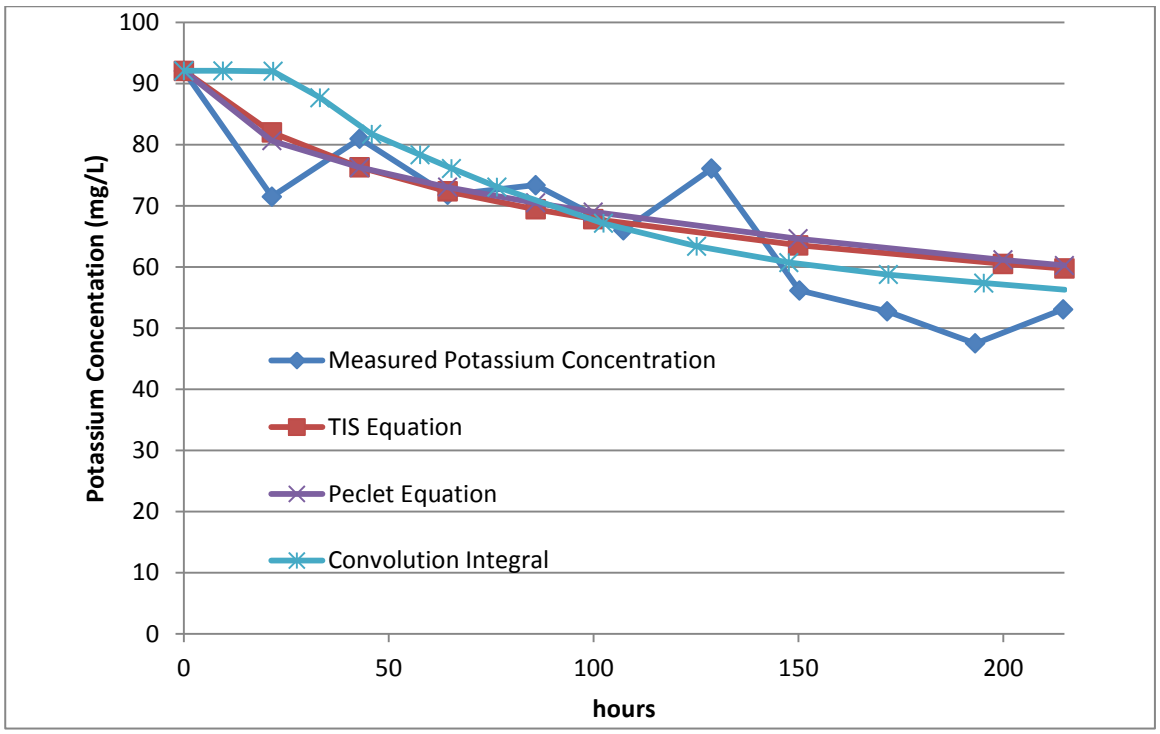


Figure 7.18. Second optimised case for comparison of the three different rate constant calculations with Pe and N solved for minimum sum of squared errors, using the rate constant found with the convolution integral method (k=0.0374/hr).

In each instance, the calculated concentrations are reasonably accurate. However, the value for N arrived at is 0.2, while the Pe number is 0.0039. These differ significantly from those calculated for sample port 5 from the RTD, and can be dismissed as unreasonable.

The results obtained for the modelling of the reduction in potassium support those found for ethanol, and additional weight to the finding that the convolution Integral method is the most appropriate for the in-situ measurement of rate constants in CWs. A statistical analysis was conducted on the three cases, the results of which are presented below.

Potassium Modelling		P -value	T value
Base Case	Convolution Integral	0.09	-1.89
	CSTR	0.004	3.97
	Peclet	$7.25x10^{-5}$	7.45
Optimised case	Convolution Integral	0.09	-1.89
	CSTR	0.19	-1.48
	Peclet	0.94	-0.07
Optimised with rate constant found using CI	Convolution Integral	0.09	-1.89
	CSTR	0.88	-0.15
	Peclet	0.73	-0.35

7.5. Discussion of the measurement of rate constants

The convolution integral method was found to be the most accurate of the three considered for determining the rate constants of degradation. The TIS and the Peclet equations can be used, but the need for multivariate optimisation to fit the data implies that using either of these equations yields not much more than a fitting exercise. The convolution integral does not require optimisation, and thus it is believed that the rate constants found using this method are correct and should produce the best results when determining the extent of biodegradation of the effluent within a CW system.

The rate constant for ethanol degradation was calculated and found to be almost 3.5 times that of the COD. Since the uncertainty associated with the rate constant for ethanol degradation is an order of magnitude less than that for COD, it is suggested that when modelling the processes of biodegradation within an effluent treatment system such as this, it is appropriate to use the specific rate constants of the individual components rather than lumped parameters. Given that acetic acid was not observed to degrade, it would not have been possible to make this observation had we been applying a number of parameters lumped together. However, one must bear in mind that there is a reservation, because this method rests on the assumption that every time such an exercise is carried out, the full range of effluent components and their rates of production and reduction are known (which is not normally the case). This is why it is cautioned that when scientists apply the method presented here, they should take care when using the rate constants

for different effluents. An effluent could have two primary components that may have antagonistic effects on overall degradation. For instance, component A may inhibit the degradation of component B, such that B may degrade only after A has been fully broken down. An example of this phenomenon occurs during the fermentation processes during which sugar is converted into ethanol, which has an inhibitory effect upon further fermentation processes). The type of approach to measuring kinetics described in this Chapter may not apply in such a system. Other disadvantages of this approach include lack of control over the degradation processes, the weather and the temperature.

The rate constants for many of the minor components of the effluent in the experimental CW were not determined, since they were deemed negligible relative to the concentration of ethanol and acetic acid. This does not, however, mean that these components are not important. Whilst propanoic and butanoic acid contribute very little to the effluent COD, they are important in terms of odour, since they have an offensive smell (rotten cheese and rancid butter respectively) which is perceptible to the human nose even at very low concentrations. Malodorous wastewater treatment plants tend to be offensive to communities living nearby. Therefore, while it is possible to exclude these components from consideration for modelling purposes, they form an important criterion in CW design. The necessary precaution is to check the levels of these acids in the specific effluent that is being treated, and ensure that they occur in low concentrations, especially in comparison with the other components of the wastewater.

As far as the cationic components of the effluent were concerned, sodium was not degraded (by ab/adsorption) but the quantity of potassium was reduced by approximately 42%, probably as the result of plant metabolism and uptake (Marschner 1983). This indicates that caustic chemicals should be used sparingly in the winemaking process, or that a switch should be made to KOH (potash) as a cleaning agent since the CW has an ability to remove it somewhat.

7.6. Concluding remarks and ramification for design

Ethanol and potassium were found to be the key species that degraded in the experimental CW. The rates of degradation were determined using three different techniques. Acetic acid did not degrade within the system, a finding which lends very strong support to our investigation of the hydraulic patterns in the CW, which led to the discovery of a hull-shaped flow profile in which most of the flow remained in the aerobic regions. The concentration of sodium increased very slightly, indicating that it is not bioremediated or removed and that there are some minor

evapotranspirative effects. The rate constant found for the biodegradation of COD has significantly more uncertainty associated with it than the measurement of the rate of degradation of individual components. Accordingly, it was posited that it is better to describe the processes of degradation by tracking individual components than to lump them all together. Thus, the hypothesis, which stated: "The degradation of lumped parameters will be modelled less accurately than the degradation of individual components" was found to be true for this body of work.

From the data obtained, it appears that TIS/Peclet equations may be inappropriate for describing dynamic, very complex reacting systems such as a CW. It was found, on the other hand, that it is possible to measure the rate constants of degradation directly from the RTD, provided that the kinetics of the degradation are linear. This is a reasonable assumption for unsaturated biological systems displaying Monod kinetics. Thus our hypothesis, which was: "It is possible to find the rate constants for the degradation of the primary components of winery effluent using the TIS equation, the Peclet equation and the Convolution integral" was disproved; instead it was found that the convolution integral was the best method for calculating rate constants *for this system.*

There are various ramifications of these findings that bear on CW design. It would appear that it is not possible to design a large-scale CW for the treatment of an effluent without first preparing a pilot plant in which the kinetics can be measured. In addition, the pilot plant should be designed/constructed in such a way to reduce potential dead zones and other disruptions of the flow. If not, the residual COD may be larger than required, as components of the effluent that require specific aerobic conditions may not be met. The result would be that the system might not perform optimally.

8. Discussion and Concluding remarks

8.1. Discussion

This chapter provides a summary of the findings of this thesis, and relates these findings to the research objectives discussed in Chapter 2.8, *viz*.:

- A complete analysis of what constitutes winery effluent and how this changes over the duration of a harvest season and how this changes over the course of a year was completed;
- An extensive hydraulic analysis of the CW was conducted; and
- Both of these experiments were used to determine the rates of treatment of winery effluent within a constructed wetland.

The initial objective was to characterise winery effluent. The principal goal of this task was to identify the main components of winery effluent and to determine the concentration of these components within the winery effluent. This objective included identifying the primary constituents of COD, which is known to be the most important of the lumped parameters which are normally used to characterise winery effluent. The results are summarised below:

- Ethanol was found to be the primary organic constituent of winery effluent and was found to comprise between 85% and 91% of the COD, and was found in concentrations as high as 3.75mL/L. This quantity of ethanol indicates that the process of winemaking is inefficient. If the final product from the winery is 13% ethanol and the effluent stream is 0.4% ethanol (both V/V) a significant loss of product is being incurred by the winery.
- Ethanoic acid was found to be the second largest contributor to the COD and concentrations as high as 0.75mL/L were encountered. i-Propanol, propanoic acid, butanol, butanoic acid, and pentanoic acid were also found but at concentrations low enough to exclude from the modelling process.
- The organic loading of the effluent peaked during mid harvest, although subsequent peaks were encountered throughout the year whenever processing operations led to a spill.
- The peak of the effluent strength (maximum COD) occurred in the middle of the harvest period, which suggests that two weeks of intensive sampling on either side of the middle of the harvest period should be sufficient to accurately characterize the peak effluent strength for modelling or other purposes. The maximum COD found at this cellar was 7 000mg/L.

- The pH of the effluent during the harvest period was approximately 4.9 and was relatively constant with respect to whether or not grapes were harvested.
- Potassium and sodium were identified as the two main cationic constituents of winery effluent on the basis of concentration. The quantity of potassium in the effluent was strongly dependent on the time of year and the intensity of the harvest season whilst sodium concentrations in the effluent were less dependent on the time of the year. It was found that the maximum sodium concentration was approximately 150mg/L and a maximum potassium concentration of approximately 225mg/L was found. The use of sodium (hydroxide or carbonate) by wineries as a cleaning agent is discouraged. Potash (potassium hydroxide) is as effective as sodium for cleaning the precipitated tartrates from tanks and is more benign if released into the environment than sodium compounds.

The second principal objective of this study was to understand how the effluent travelled through the CW. Therefore an impulse-response tracer experiment was performed on the large-scale CW. The result of this experiment gave substantial data and also provided some insight into how the effluent flows within the CW. Specifically, the following was found:

- The residence time distributions were found to be Gaussian-like, with long drawn out tails, and this was an expected result for flow through for gravel bed filters;
- In the impulse-response experiment, the error was possibly increased due to the tracer not mixing with the water as a result of significant density differences or because there was significant bypass to the end of the CW (sample port 5). This was indicated by the mean residence time for that sample port was half that of the sample wells immediately before it. It is postulated that this is more likely due to the density currents than short circuiting, which would only be encountered in the tracer experiment and not in a well mixed effluent stream arriving at the CW. However, it was not possible to distinguish between the two in the context of this experiment; and
- It was calculated that the true residence time was approximately 75% of the ideal residence time. This supports the hypothesis that the assumption of ideal flow is incorrect, and that the true residence time of the CW may be significantly different from the ideal residence time. It was determined from this experiment that by feeding the effluent to the surface of the CW and by taking the outlet off at the surface a hull-shaped flow profile is induced which dramatically reduces the effectiveness of the CW. This hull-shaped profile induced a dead-volume of approximately 25% of the CW and in the laboratory-scale experiments it was found

that this dead volume could increase to as much as 50%. To the best of our knowledge, no-one has ever observed or described such a flow pattern and this is therefore a novel finding. It was also found that it was possible to reduce the dead zone and eliminate the hull-shaped flow profile by introducing a distributed feed and outlet. Various combinations were tried, but a fully distributed inlet and outlet were found to be the best. The presence of a hull-shaped flow profile also implied that the flow in the CW was primarily in the upper layers which are well oxygenated. This implied that little anaerobic degradation within the CW would be observed and thus it was expected that acetic acid should not be degraded since this requires an anaerobic pathway.

Based on the hydraulic and chemistry data we sought to determine the kinetics of the processes of removal or degradation within the CW by using a sophisticated non-ideal flow model. The TIS equation and the plug flow with diffusion (Peclet) equations were chosen as these are both recommended for flow in packed beds. The RTD of the outlet was used directly through the convolution integral method. Again, interesting observations were made.

It was found that potassium was removed and this was explained as being caused by plant metabolic uptake. Conversely, sodium was found to increase in concentration slightly. This indicated no plant uptake and that there was some small degree of evapo-transpiration.

It was found that ethanol was not being oxidised to acetic acid, but was being utilised as a substrate and appears to have been degraded directly to CO2. It was also determined that acetic acid was not degraded within the CW. This finding strongly supported the hypothesis of a hull-shaped flow profile and the location of the dead-zones and the lack of movement of effluent into the anaerobic regions of the CW. The outlet COD also corresponded quite well to the outlet acetic concentration.

It was found that the CW displayed significant non-ideal behaviour at the feed and outlet. This can be explained by the location of the feed ports on the surface and the non-ideal processes involved in setting up the flow paths. The non-ideal outlet conditions were explained as occurring due to the outlet seeing bypass as well as the tapering of the hull to a point. The mid-sections of the CW were however shown to be operating stably and in a very similar manner. This finding is also to

the best of our knowledge never been described before. It is very useful finding for design which is discussed below.

The rate constants for the degradation of ethanol, potassium and COD were calculated. There were two significant outcomes from this calculation. The first was that the calculation of degradation of a lumped parameter has substantially more uncertainty associated with it than calculating the rate constant for the degradation of a single parameter since there is more than one process of degradation, thus one rate constant will not fit either process at the same time. This was observed by comparing the standard deviation of the rate of degradation of COD with that of ethanol. It was also found that neither the Peclet nor the TIS equation were particularly good for calculating the kinetics. Indeed, both equations could be optimised to very closely describe the conditions within the CW, but that this was due to the models being multivariate. This meant that describing the CW with either model was more of an exercise than particularly useful. The RTD and the convolution integral method were however found to be quite accurate and gave reasonable values for rate constants of degradation as well as fitting the data quite closely without the need for optimisation.

These findings have significant ramifications for design. Clearly, for design purposes, the assumption that a CW is an ideal plug flow reactor is erroneous. The reactor must be seen as being much more complex than this. The way in which the effluent is fed into the treatment CW also requires detailed thought. Inlet lines should be well distributed and the outlet lines should at the very least not withdraw from the surface but from the bottom of the CW. The effluent may also not remediate fully if this is not done as the hull-shaped flow profile may exist. Care must be made to establish flow in the deepest layers in order to induce anaerobic conditions which are necessary for acetate reduction. This may not be required for all effluent streams, however, it is important for winery effluent and any other effluent stream which contains organic oxygenates (such as Fischer-Tropsch waste waters). It may be reasonable to force flow to the deeper levels by designing barriers within the CW which force the flow downwards. The complexity of flow and kinetic processes means that whilst ideal flow models are not appropriate; neither are more complex reactor models.

Thus for the design of a CW for winery effluent, it is recommended that a designer use the rate constants found in this study, and design a system with fully distributed feed and add a 10% excess capacity to accommodate any residual dead volume or short circuiting. In addition it is believed

that for accurate design for other effluents, additional research must be conducted into the composition of the lumped parameters that are often reported for these effluents and these must be piloted in a research rig specifically designed for that purpose. Or alternatively, impulse-response tracer studies can be conducted on existing CWs to accurately determine the hydraulic processes and using the convolution integral method, the rate constants of degradation can be found. These rates can then be utilised to design purposes. Unfortunately, the number of variables affecting the flow regime, which can be designed into the system up-front (such as depth, geometry of the CW, geometry of the inlet and outlet distributions etc) implies that the reactor equations are not likely to be applicable from one instance to another.

8.2. Concluding Remarks

It is considered that within this context, and the greater context of wastewater treatment in general, future research should endeavour to measure the specific components of various effluent streams together with the traditional lumped parameters. Potentially, the most important area for this unbundling is in municipal sewage. This is the domain in which most CWs are used and whilst the use of lumped parameters is recognised as a useful measure of effluent strength, they are less useful for accurate modelling of degradation processes. The characterisation of all effluent would be an expensive undertaking and may require the collaboration of universities and governments at local, regional and international level. A database, or index, of effluents could possibly be initiated since it is difficult to publish data on an individual effluent stream in the scientific literature. Such a resource would be of immense value to researchers or designers seeking information on a specific effluent.

Given the similarity between winery effluent and Fischer-Tropsch (FT) wastewater, it is believed that there is a real opportunity for the utilisation of the data found in this study to be explored for utilisation for modular FT plants which are being designed for use at small, modular dispersed locations which will require some form of wastewater treatment. There also exists a real opportunity to explore the use of CWs for a number of other threats to natural water resources which occur in South Africa. These include Acid Mine Drainage (AMD), petroleum impacted groundwater treatment (at depot and at service station leaks), landfill leachate and others. The missing data for the use of these is the rates of degradation and this study provides a method for determining the rates.

It is also strongly recommended that any natural wetlands which are observed to be impacted by the above-listed effluents/waste streams be investigated and assessed by trained botanists, and that the plants be studied. In particular, the plants should be tested against various effluents to determine their LD_{50} (the dose required to kill half the members of a tested population) to the effluents. For example, petrochemicals may possibly kill Zantedeschia in low concentration, yet Epilobium may be resistant to high concentrations of petrochemicals. The wealth of options available has not been utilised, and this aspect could be investigated in depth.

For the wine industry, it is important that the use of caustic soda (NaOH) as a cleaning agent be discontinued. It is recommended that either potassium hydroxide or calcium hydroxide is used for both cleaning and effluent pH adjustment since the cations of both compounds are biologically available to plants, do not contribute to the sodicity of soil and can be removed with ease relative to sodium (and potassium has been shown to be removed in this study). Providing that the use of NaOH is discontinued, CWs are recommended as a primary treatment option for the wine industry for COD values of less than 8 000 mg/L or 5mL/L of ethanol (0.5% V/V), or as a secondary/tertiary treatment system for effluent purification. The outflow from these systems can be irrigated onto vineyards (this is a legal practice in South Africa) and should reduce the amount of potassium required from fertilizers.

To conclude: it is considered that within the South African context, the approach initiated in this thesis be expanded from winery effluent treatment to include other effluents. South Africa is a country of contrasts, with components of both developed and developing worlds present throughout our society. It is considered that the use of CWs for the treatment of these effluents represents a good opportunity for isolated rural areas and impoverished urban areas where technical skills are scarce and or resources are lacking. The discharge from these treatment CWs could be released into rivers with the knowledge that, whilst this may not be ideal, it has a significantly lower environmental impact than the release of raw effluent, which can and does occur. Research into their use, under South African conditions, with South African flora should be initiated. Constructed wetlands can and do provide a useful, low maintenance method for treating waste water in an environmentally friendly manner.

9. References

Interventiewaarden Gevaarlike Stoffen. Available: http://www.refworks.com/refworks2/default.aspx?r=references|MainLayout::init#YOTbPk9wL9FjXtjuLe44|start [12/11, 2012].

US EPA Regional Screening Levels. Available: http://www.epa.gov/region9/superfund/prg/ [12/11, 2012].

ANDREOTTOLA, G., OLIVEIRA, E., FOLADORI, P. and ZIGLIO, R., 2007. Respirometric techniques for assessment of biological kinetics in constructed wetlands. *Water Science and Technology,* **56**(3), pp. 255-261.

ASUMAN KORKUSUZ, E., BEKLIOĞLU, M. and DEMIRER, G.N., 2007. Use of blast furnace granulated slag as a substrate in vertical flow reed beds: field application. *Bioresour Technol,* **98**(11), pp. 2089-2101.

AUSTEN, D.C., MACIOLEK, D.J. and LOHAN, E., 2002. *Integrated hydroponic and fixed-film wastewater treatment systems and associated methods.* 6,811,700 B2 edn. United States.

AUSTIN, D., WOLF, L. and STROUS, M., 2006. Mass transport and microbiological mechanisms of nitrification and denitrification in tidal flow constructed wetlands. *Proceedings of the 10th International Conference on Wetland Systems for Pollution Control.* 23-29 September 2006.

BATTY, L.C. and YOUNGER, P.L., 2004. Growth of Phragmites australis (Cav.) Trin ex. Steudel in mine water treatment wetlands: effects of metal and nutrient uptake. *Environmental Pollution,* **132**(1), pp. 85-93.

BEHRENDS, L., 1999. *Reciprocating subsurface flow constructed wetlands for improving wastewater treatment.* 5,863,433 edn. United States.

BELMONT, M.A. and METCALFE, C.D., 2003. Feasibility of using ornamental plants (Zantedeschia aethiopica) in subsurface flow treatment wetlands to remove nitrogen, chemical oxygen demand and nonylphenol ethoxylate surfactants—a laboratory-scale study. *Ecological Engineering,* **21**(4–5), pp. 233-247.

BENEFIELD, L.D. and RANDALL, C.W., 1980. *Biological Design for Wastewater Treatment.* engelwood Cliffs, NJ: Prentice Hall.

BORIN, M. and TOCCHETTO, D., 2006. Ornamental plants in sub-surface horizontal flow treatment system. *Proceedings of the 10th International Conference on Wetland Systems for Water Pollution Control*, 23-29 September 2006.

BRISSON, J., CHAZARENC, F. and BISAILLON, L.A., 2006. Maximising pollutant removal in constructed wetlands: should we pay more attention to macrophyte species selection? *Proceedings of the 10th international conference on wetland systems for water pollution control*, 23-29 September 2006.

BRIX, H., 1994. Use of constructed wetlands in water pollution control: historical development, present status and future perspectives. *Water Science and Technology,* **30**(8), pp. 209-233.

BUCHBERGER, S.G. and SHAW, G.B., 1995. An approach toward rational design of constructed wetlands for wastewater treatment. *Ecological Engineering,* **4**(4), pp. 249-275.

BUSTAMANTE, M.A., PAREDED, C., MORAL, R., MORENO-CASELLES, J., PEREZ-ESPINOSA, A. and PEREZ-MURCIA, M.D., 2005. Uses of winery and distillery effluents in agriculture: characterisation of nutrient and hazardous components. *Water Science and Technology,* **51**(1), pp. 145-151.

CARLETON, J.N. and MONTAS, H.J., 2010. An analysis of performance models for free water surface wetlands. *Water research,* **44**(12), pp. 3595-3606.

CHAPMAN, J., 1996. *Cleaner production for the wine industry handbook.* Adelaide, South Australia: South Australia Wine and Brandy Industry Association.

CHAZARENC, F., BRISSON, J. and COMEAU, Y., 2006. Slag columns for upgrading phosphorous removal in constructed wetlands. *Proceedings of the 10th International Conference on Wetland Systems for Pollution Control,* 23-29 September 2006.

CHAZARENC, F., MERLIN, G. and GONTHIER, Y., 2003. Hydrodynamics of horizontal subsurface flow constructed wetlands. *Ecological Engineering,* **21**(2-3), pp. 165-173.

CHEUNG, L.M., CHEUNG, P.C.K. and OOI, V.E.C., 2003. Antioxidant activity and total phenolics of edible mushroom extracts. *Food Chemistry,* **2**(81), pp. 249-255.

COLIN, T., BORIES, A., SIRE, Y. and PERRIN, R., 2005. Treatment and valorisation of winery wastewater by a new biophysical process (ECCF). *Water Science and Technology,* **21**(1), pp. 99-106.

COOPER, P.F., JOB, G.D., GREEN, M.B. and SHUTES, R.B.E., 1996. *Reedbeds and Constructed Wetlands for Wastewater Treatment.* 1 edn. UK: WRc Publications.

CRITES, R. and TCHOBANOGLOUS, G., 1998. *Small and Decentralised Wastewater Management Systems.* International edn. Singapore: WCB McGraw Hill.

CRONK, J.K., 1996. Constructed wetlands to treat wastewater from dairy and swine operations: a review. *Agriculture, Ecosystems & Environment,* **58**(2–3), pp. 97-114.

DUFAY, J.A., 2000. *Constructed wetland remediation system.* 6,159,371 edn. United States.

DUNNE, E.J., CULLETON, N., O'DONOVAN, G., HARRINGTON, R. and OLSEN, A.E., 2005. An integrated constructed wetland to treat contaminants and nutrients from dairy farmyard dirty water. *Ecological Engineering,* **24**(3), pp. 219-232.

EL-GENDY, E.J., 2006. Modeling of heavy metals removal from municipal landfill leachate using living biomass of water hyacinth. *Proceedings of the 10th International Conference on Wetland Systems for Water Pollution Control,* 23-29 September 2006.

FLOWERS, D.A., 2002. *Process and system for enhanced nitrogen removal in a wetland wastewater treatment facility.* 6,447,682 edn. United States.

FOGLER, H.S., 2005. *Elements of Chemical Reaction Engineering.* 4th edn. USA: Prentice Hall.

GERSBERG, R.M., ELKINS, B.V. and GOLDMAN, C.R., 1984. Use of Artificial Wetlands to Remove Nitrogen from Wastewater. *Journal (Water Pollution Control Federation),* **56**(2), pp. pp. 152-156.

GIRALDI, D., DE'MICHIELI VITTURI, M., ZARAMELLA, M., MARION, A. and IANNELLI, R., 2009. Hydrodynamics of vertical subsurface flow constructed wetlands: Tracer tests with rhodamine WT and numerical modelling. *Ecological Engineering,* **35**(2), pp. 265-273.

GOVERNMENT GAZETTE, 2009. No. 59 of 2008: National Environmental Management: Waste Act, 2008. *Government Gazette,* **525**(32000).

GOVERNMENT GAZETTE, 2001. *Section 39 of the National Water Act of South Africa, general Authorisations.* South Africa.

GOVERNMENT GAZETTE, 1998a. *National Environmental Management Act.* Cape Town: South Africa.

GOVERNMENT GAZETTE, 1998b. NATIONAL WATER ACT Act No 36 of 1998. *Government Gazette*.

GOVERNMENT GAZETTE, 1983. Conservation of agricultural resources act. *Government Gazette*.

GREENWAY, M., 2003. Suitability of macrophytes for nutrient removal from surface flow wetlands receiving secondary treated sewage effluent in Queensland, Australia. *Water Science and Technology,* **48**(2), pp. 121-128.

GRIFFIN, D.M., JR., BHATTARAI, R.R. and XIANG, H., 1999. The Effect of Temperature on Biochemical Oxygen Demand Removal in a Subsurface Flow Wetland. *Water Environment Research,* **71**(4), pp. pp. 475-482.

HAMMER, D.A., ed, 1989. *Performance of solid-matrix wetland systems viewed as fixed film bioreactors.* Chelsea, MI, US. Lewis Publishers.

HAUG, R.T., 1993. *The Practical Handbook of Compost Engineering.* Boca Raton: CRC Press.

HEADLEY, T.R., HERITY, E. and DAVISON, L., 2005. Treatment at different depths and vertical mixing within a 1-m deep horizontal subsurface-flow wetland. *Ecological Engineering,* **25**(5), pp. 567-582.

HESHKOWITZ, J., 1986. *Listowel artificial marsh project.* Ontario, Canada. Ontario Ministry of Environment, Water Resources Branch.

HUDDLESTON, G.M., GILLESPIE, W.B. and RODGERS, J.H., 2000. Using Constructed Wetlands to Treat Biochemical Oxygen Demand and Ammonia Associated with a Refinery Effluent. *Ecotoxicology and environmental safety,* **45**(2), pp. 188-193.

JETTEN, M.S.M., STROUS, M., VAN DE PAS-SCHOONEN, K.T., SCHALK, J., VAN DONGEN, U.G.J.M., VAN DE GRAAF, A.A., LOGEMANN, S., MUYZER, G., VAN LOOSDRECHT, M.C.M. and KUENEN, J.G., 1998. The anaerobic oxidation of ammonium. *FEMS microbiology reviews,* **22**(5), pp. 421-437.

JETTEN, M.S.M., WAGNER, M., FUERST, J., VAN LOOSDRECHT, M., KUENEN, G. and STROUS, M., 2001. Microbiology and application of the anaerobic ammonium oxidation ('anammox') process. *Current opinion in biotechnology,* **12**(3), pp. 283-288.

JI, G.D., SUN, T.H. and NI, J.R., 2007. Surface flow constructed wetland for heavy oil-produced water treatment. *Bioresource technology,* **98**(2), pp. 436-441.

KADLEC, R.H., 2009. Comparison of free water and horizontal subsurface treatment wetlands. *Ecological Engineering,* **35**, pp. 159-174.

KADLEC, R.H. and KNIGHT, R.L., 1996. *Treatment Wetlands.* Boca Raton, Fl: CRC Press.

KADLEC, R.H., KNIGHT, R.L., VYMAZAL, J., BRIX, H., COOPER, P. and HABERL, R., 2000. *Constructed Wetlands for Pollution Control. Processes, Performance, Design and Operation.* Cornwall, UK: IWA Publishing.

KADLEC, R.H., 2003. Effects of pollutant speciation in treatment wetlands design. *Ecological Engineering,* **20**(1), pp. 1-16.

KYAMBADDE, J., KANSIIME, F., GUMAELIUS, L. and DALHAMMAR, G., 2004. A comparative study of Cyperus papyrus and Miscanthidium violaceum-based constructed wetlands for wastewater treatment in a tropical climate. *Water research,* **38**(2), pp. 475-485.

LEVENSPIEL, O., 1972. *Chemical Reaction Engineering.* International edn. John Wiley and Sons.

LIEHR, S.K., KOZUB, D.D., RASH, J.K. and SLLOP, G.M., 2000. *Constructed wetlands treatment of high nitrogen landfill leachate. Project 94-IRM-U.* Virginia, United States. Water Environment Research Federation.

MALANDRA, L., WOLFAARDT, G., ZIETSMAN, A. and VILJOEN-BLOOM, M., 2003. Microbiology of a biological contactor for winery wastewater treatment. *Water Research,* **37**, pp. 4125-4134.

MAŁOSZEWSKI, P., WACHNIEW, P. and CZUPRYŃSKI, P., 2006. Study of hydraulic parameters in heterogeneous gravel beds: Constructed wetland in Nowa Słupia (Poland). *Journal of Hydrology,* **331**(3-4), pp. 630-642.

MARMIROLI, M., MARMIROLI, N., MAESTE, E., TAGLIAVINI, S., MANTOVI, P. and PICCININI, S., 2003. Wastewater from dairy parlours: Treatment with a constructed horizontal sub-surface wetlands. *Proceedings of the 1st International Seminar on the Use of Aquatic Macrophytes for Wastewater Treatment in Constructed Wetlands*, 8-10 May 2003.

MARSCHNER, H., 1983. General Introduction to the Mineral Nutrition of Plants. In: A. LAUCHLI and R.L. BIELESKI, eds, *Inorganic Plant Nutrition, Encyclopedia of Plant Physiology, New Series, Volume 15A.* .

MARSILI-LIBELLI, S. and CHECCHI, N., 2005. Identification of dynamic models for horizontal subsurface constructed wetlands. *Ecological Modelling,* **187**(2-3), pp. 201-218.

MARTINEZ, C.J. and WISE, W.R., 2003. Analysis of constructed treatment wetland hydraulics with the transient storage model OTIS. *Ecological Engineering,* **20**(3), pp. 211-222.

MASHAURI, D.A. and KAYOMBO, S., 2002. Application of the two coupled models for water quality management: facultative pond cum constructed wetland models. *Physics and Chemistry of the Earth,* **27**, pp. 773-781.

MASI, F., CONTI, G., MARTINUZZI, N. and PUCCI, B., Winery high strength organic wastewaters treated by constructed wetlands in Mediterranean climate. *Proceedings of the 8th International Conference on Wetland Systems for Water Pollution Control.*

MONOD, J., 1949. The growth of bacterial cultures. *Annual Reviews in Microbiology,* **3**, pp. 371-394.

MOORE, B.J., ROSS, S.D., GIBSON, D. and CALLOW, L., 2000. Constructed Wetlands for treatment of dissolved phase hydrocarbons in cold climates. J.L. MEANS and R.E. HINCHEE, eds. In: *Wetlands & Remediation: An International Conference; Salt Lake City, UT; USA*, 16 to 17 November 1999 2000, pp. 333.

NITISORAVUT, S. and KLOMJEK, P., 2005. Inhibition kinetics of salt-affected wetland for municipal wastewater treatment. *Water Research,* **39**, pp. 4413-4419.

OLESZKIEWICZ, J.A. and KOZIARSKI, S., 1986. Kinetics of piggery wastes treatment in anaerobic lagoons. *Agricultural Wastes,* **16**, pp. 13-25.

OLIVEIRA, E., MALVA, M., PEREIRA, R., CONCEIÇÃO, A. and CASTILHO, G., 2006. Constructed wetland system for wastewater using EPS (expandable polystyrene) support medium. *Proceedings of the 10th International Conference on Wetland Systems for Water Pollution Control*, 23-29 September 2006.

OMARI, K.O., REVITT, M., SHUTES, B. and GARELICK, H., 2003. Hydrocarbon removal in an experimental gravel bed constructed wetland. *Water Science and Technology,* **48**(5), pp. 275-281.

OUELLET-PLAMONDON, C., CHAZARENC, F., COMEAU, Y. and BRISSON, J., 2006. Artificial aeration to increase pollutant removal efficiency of constructed wetlands in cold climate. *Ecological Engineering,* **27**(3), pp. 258-264.

PARDUE, J.H., KASSENGA, G. and SHIN, W.S., 1999. Design approaches for chlorinated VOC treatment wetlands. R.E. HINCHEE and J.L. MEANS, eds. In: *Wetlands and Remediation: An international Conference* 1999.

PERRSON, J., SOMAS, N.L.G. and WONG, T.H.F., 1999. Hydraulic efficiency of constructed wetlands and ponds. *Water Science and Technology,* **40**, pp. 291-299.

PETRUCIOLLI, M., DUARTE, J., EUSEBIO, A. and FEDERICI, F., 2001. Aerobic treatment of winery wastewater using a jet loop activated sludge reactor. *Process Biochemistry,* **37**, pp. 821-829.

POPEK, E.P., 2002. *Sampling and Analysis of Environmental Chemical Pollutants - A complete guide.* Academic Press.

RADFORD, A., 2002. The Composition of Winery and Distillery Wastewater and Effects on Soil and Water. *Proceedings of the SASEV Cellar and Distillery Effluent Seminar* 2002.

REDDY, K.R., PATRICK, W.H. and BROADBENT, F.E., 1984. Nitrogen transformations and loss in flooded soils and sediments. *C R C Critical Reviews in Environmental Control,* **13**(4), pp. 273-309.

REED, S.C. and BROWN, D., 1995. Subsurface Flow Wetlands: A Performance Evaluation. *Water Environment Research,* **67**(2), pp. pp. 244-248.

RODGERS, J.H. and DUNN, A., 1995. Developing design guidelines for constructed wetlands to remove pesticides from agricultural runoff. *Ecological Engineering,* **1**, pp. 83-95.

ROUSSEAU, D.P.L., 2005. *Performance of constructed wetlands: model-based evaluation and impact of operation and maintenance.* Ghent University, Ghent, Belgium.

ROUSSEAU, D.P.L., VANROLLEGHEM, P.A. and DE PAUW, N., 2004. Model-based design of horizontal subsurface flow constructed treatment wetlands: a review. *Water Research,* **38**, pp. 1484-1493.

SAWIS, (2012-02-17), 2012-last update, South African Wine Industry Statistics (No.35). Available: South African Wine Industry Statistics [May/25, 2012].

SCHMID, B.H., HENGL, M.A. and STEPHAN, U., 2004. Salt tracer experiments in constructed wetland ponds with emergent vegetation: laboratory study on the formation of density layers and its influence on breakthrough curve analysis *Water Research,* **38**, pp. 2095-2102.

SCHMIDT, I., SLIEKERS, O., SCHMID, M., BOCK, E., FUERST, J., KUENEN, J.G., JETTEN, M.S.M. and STROUS, M., 2003. New concepts of microbial treatment processes for the nitrogen removal in wastewater. *FEMS microbiology reviews,* **27**(4), pp. 481-492.

SCHMIDT, I., SLIEKERS, O., SCHMID, M., CIRPUS, I., STROUS, M., BOCK, E., KUENEN, J.G. and JETTEN, M.S.M., 2002. Aerobic and anaerobic ammonia oxidizing bacteria – competitors or natural partners? *FEMS microbiology ecology,* **39**(3), pp. 175-181.

SCHNOOR, J.L., LIGHT, L.A., MCCUTCHEON, S.C., WOLFE, N.L. and CARREIA, L.H., 1995. Phytoremediation of organic and nutrient contaminants. *Environmental science & technology,* **29**(7), pp. 318A-323A.

SHEPHERD, H.L., TCHOBANOGLOUS, G. and GRISMER, M.E., 2001. Time-dependent retardation model for chemical oxygen demand removal in a sub-surface flow constructed wetland for winery wastewater treatment. *Water Environment Research,* **73**(5), pp. 597-606.

SHERIDAN, C.M., 2003. *A Critical Process Analysis of Wine Production to Improve Cost, Quality and Environmental Performance.* University of Stellenbosch.

SHERIDAN, C.M., BAUER, F.F., BURTON, S. and LORENZEN, L., 2005. A critical process analysis of wine production to improve cost, quality and environmental performance. *Water Science and Technology,* **51**(1), pp. 39-46.

SHERIDAN, C.M., GLASSER, D. and HILDEBRANDT, D., 2011a. A calculation of the hydraulic properties of a vegetated gravel bed filter using an impulse-response tracer experiment to quantify non-ideal behaviour, *Proceedings of the 12th Conference on Environmental Science and Technology*, 8 to 10 September 2011 2011a, pp. 1711-1716.

SHERIDAN, C.M., GLASSER, D., HILDEBRANDT, D., PETERSEN, J. and ROHWER, J., 2011b. An Annual and Seasonal Characterisation of Winery Effluent in South Africa. *South African Journal of Enology and Viticulture,* **32**(1), pp. 1-8.

SHERIDAN, C.M., KOLLER, E. and DE PRETTO, A., 2012. A comparison of charcoal- and slag-based constructed wetlands for acid mine drainage remediation, *Proceeding of the WISA 2012 Biennial Conference and Exhibition*, 6-10 May 2012, WRC.

SHERIDAN, C.M., PETERSON, J., ROHWER, J. and BURTON, S., 2006. Engineering design of subsurface flow constructed wetlands for the primary treatment of winery effluent. *Proceedings of the 10th international conference on wetland systems for water pollution control.*, 23-29 September 2006.

STEIN, O.R., TOWLER, B.W., HOOK, P.B. and BIEDERMAN, J.A., 2006. On fitting the k-C* first order model to batch loaded ssf wetlands. *Proceedings of the 10th international conference on wetland systems for water pollution control.*, 23-29 September, 2006.

STRONG, P.J., MCDONALD, B. and GAPES, D.J., 2011. Combined thermochemical and fermentative destruction of municipal biosolids: A comparison between thermal hydrolysis and wet oxidative pre-treatment. *Bioresource technology,* **102**(9), pp. 5520-5527.

STROUS, M., VAN GERVEN, E., ZHENG, P., KUENEN, J.G. and JETTEN, M.S.M., 1997. Ammonium removal from concentrated waste streams with the anaerobic ammonium oxidation (Anammox) process in different reactor configurations. *Water research,* **31**(8), pp. 1955-1962.

SULIMAN, F., FUTSAETHER, C., OXAAL, U., HAUGEN, L.E. and JENSSEN, P., 2006. Effect of the inlet–outlet positions on the hydraulic performance of horizontal subsurface-flow wetlands constructed with heterogeneous porous media. *Journal of contaminant hydrology,* **87**(1-2), pp. 22-36.

TANNER, C.C., 1996. Plants for constructed wetland treatment systems — A comparison of the growth and nutrient uptake of eight emergent species. *Ecological Engineering,* **7**(1), pp. 59-83.

TANNER, C.C., SUKIAS, J.P.S. and UPSDELL, M.P., 1998. Organic matter accumulation during maturation of gravel-bed constructed wetlands treating farm dairy wastewaters. *Water research,* **32**(10), pp. 3046-3054.

TCHOBANOGLOUS, G., BURTON, F.L. and STENSEL, H.D., eds, 2003. *Wastewater Engineering: treatment and reuse*
Metcalf and Eddy, Inc. Revised, International Edition. 4 edn. New York: McGraw Hill.

TEE, H., LIM, P., SENG, C. and NAWI, M.M., 2012. Newly developed baffled subsurface-flow constructed wetland for the enhancement of nitrogen removal. *Bioresource technology,* **104**(0), pp. 235-242.

TOMOKO, Y., PING, G., RYUHE, I., YOSHITAKA, E., YUHEI, V. and MASATOSHI, M., 2006. Comparative Analysis of Constructed Wetland Systems with Different Plants Species Focused on Performance of Wastewater Treatment and Characteristics of Greenhouse Effect Gases Emission, *Proceedings of the 10th international conference on wetland systems for water pollution control,* 23-29 September 2006.

TOWLER, B.W., CAHOON, J.E. and STEIN, O.R., 2004. Evapotranspiration Crop Coefficients for Cattail and Bulrush. *Journal of Hydrologic Engineering,* **9**(3), pp. 235-239.

US EPA, 2000. *Constructed Wetlands Treatment of Municipal Wastewaters.* EPA/625/R-99/010. US EPA.

VILLASEÑOR, J., MENA, J., FERNÁNDEZ, F.J., GÓMEZ, R. and DE LUCAS, A., 2011. Kinetics of domestic wastewater COD removal by subsurface flow constructed wetlands using different plant species in temperate period. *International journal of environmental analytical chemistry,* **91**(7-8), pp. 693-707.

VOHLA, C., KÕIV, M., BAVOR, H.J., CHAZARENC, F. and MANDER, Ü., 2011. Filter materials for phosphorus removal from wastewater in treatment wetlands—A review. *Ecological Engineering,* **37**(1), pp. 70-89.

VYAMAZAL, J., DUSEK, J. and KVET, J., 1999. Nutrient cycling and retention in natural and constructed wetlands. In: J. VYAMAZAL, ed, *Nutrient uptake and storage by plants in constructed wetlands with horizontal subsurface flow: A comparative study:* Lieden, The Netherlands: Backhuys.

VYMAZAL, J., 2006. Constructed wetlands with emergent macrophytes: from experiments to a high quality treatment technology. *Proceedings of the 10th international conference on wetland systems for water pollution control*, 23-29 September 2006.

VYMAZAL, J., 1998. *Czech constructed wetlands database. Ecology and use of wetlands.* Prague, Czech Republic.

VYMAZAL, J. and KRŐPFELOVÁ, L., 2005. Growth of Phragmites australis and Phalaris arundinacea in constructed wetlands for wastewater treatment in the Czech Republic. *Ecological Engineering,* **25**(5), pp. 606-621.

WALLACE, S.D., 2001a. *System for removing pollutants from water.* 6,200,469 edn. MN, USA.

WALLACE, S.D., 2001b. Treatment of cheese-processing waste using sub-surface flow wetlands. *Wetlands and Remediation: The second international conference.*, 5-6 September 2001 2001b, Battelle Institute.

WALLACE, S.D. and KADLEC, R.H., 2004. BTEX degradation in a cold-climated wetland system. *Proceedings of the 9th international conference on wetland systems for water pollution control*, 26-30 September 2004.

WALLACE, S.D. and KNIGHT, R.L., 2006. *Small-scale constructed wetland treatment systems.* Vancouver: IWA Publishing.

WALLACE, S.D. and NIVALA, J.A., 2005. Thermal response of a horizontal subsurface flow wetland in a cold temperate climate. *International Water Association's Specialist Group on the use of Macrophytes in Water Pollution Control,* **29**, pp. 25-30.

WANG, H. and JAWITZ, J.W., 2006. Hydraulic analysis of cell-network treatment wetlands. *Journal of Hydrology,* **330**(3-4), pp. 721-734.

WANG, W., GAO, J., GUO, X., LI, W., TIAN, X. and ZHANG, R., 2012. Long-term effects and performance of two-stage baffled surface flow constructed wetland treating polluted river. *Ecological Engineering,* **49**(0), pp. 93-103.

WEBER, D., DRIZO, A., TWOHIG, E., BIRD, S. and ROSS, D., 2006. Upgrading constructed wetlands phosphorous reduction from a dairy effluent using EAF steel slag filters. *Proceedings of the 10th international conference on wetland systems for water pollution control.*, 23-29 September 2006.

WEHNER, J.F. and WILHELM, R.H., 1956. Boundary conditions of flow reactor. *Chemical Engineering Science,* **6**(2), pp. 89-93.

WERNER, T.M. and KADLEC, R.H., 2000. Wetland residence time distribution modeling. *Ecological Engineering,* **15**(1-2), pp. 77-90.

WHITEHALL, T.J., 2003. *Wastewater treatment for small flow applications.* 6,351,062 edn. US.

WOOD, A., 1995. Constructed wetlands in water pollution control: Fundamentals to their understanding. *Water Science and Technology,* **32**(3), pp. 21-29.

WYNN, T.M. and LIEHR, S.K., 2001. Development of a constructed subsurface-flow wetland simulation model. *Ecological Engineering,* **16**(4), pp. 519-536.

10.Appendices

Appendix A. Yearly effluent composition at Cellar 1 170

Appendix B. Daily effluent composition at Cellar 2 for the duration of a harvest 171

Appendix C. Impulse-Response Tracer Experiment Data for the CW 172

Appendix D. Impulse-Response Tracer Experiment Data – Laterally Averaged Data 173

Appendix E. Impulse-Response Tracer Experiment Data – Mass Balance 174

Appendix F. RTD for Sample Port 1a/b 175

Appendix G. RTD graphs for Sample Port 1a/b 176

Appendix H. RTD for Sample Port 1 178

Appendix I. RTD graphs for Sample Port 1 179

Appendix J. RTD for Sample Port 2a/b 180

Appendix K. RTD graphs for Sample Port 2a/b 181

Appendix L. RTD for Sample Port 2 182

Appendix M. RTD graphs for Sample Port 2 183

Appendix N. RTD for Sample Port 3a/b 184

Appendix O. RTD graphs for Sample Port 3a/b 185

Appendix P. RTD for Sample Port 3 186

Appendix Q. RTD graphs for Sample Port 3 187

Appendix R. RTD for Sample Port 4a/b 188

Appendix S. RTD graphs for Sample Port 4a/b 189

Appendix T. RTD for Sample Port 4 190

Appendix U. RTD graphs for Sample Port 4 191

Appendix V. RTD for Sample Port 5a/b 192

Appendix W. RTD graphs for Sample Port 5a/b 193

Appendix X. RTD for Sample Port 5 194

Appendix Y. RTD graphs for Sample Port 5 195

Appendix Z. Experiment 1 – lab scale CW 196

Appendix AA. Experiment 2 – lab scale CW 197

Appendix BB. Experiment 3 – lab scale CW 198

Appendix CC. Experiment 4 – lab scale CW 199

Appendix DD. Experiment 5 – lab scale CW 200

Appendix EE. Experiment 6 – lab scale CW 201

Appendix FF. CW Characterisation February 5 2005 202

Appendix GG. CW Characterisation February 7 2005 203

Appendix HH. CW Characterisation February 8 2005 204

Appendix II. CW Characterisation February 9 2005 205

Appendix JJ. CW Characterisation February 10 2005 206

Appendix KK. CW Characterisation February 11 2005 207

Appendix LL. CW Characterisation February 14 2005 208

Appendix MM. CW Characterisation February 15 2005 209

Appendix NN. CW Characterisation February 16 2005 210

Appendix OO. CW Characterisation February 17 2005 211

Appendix PP. CW Characterisation February 18 2005 212

Appendix QQ. CW Characterisation February 19 2005 213

Appendix RR. CW Characterisation February 21 2005 214

Appendix SS. CW Characterisation February 22 2005 215

Appendix TT. CW Characterisation February 23 2005 216

Appendix UU. CW Characterisation February 24 2005 217

Appendix VV. CW Characterisation February 28 2005 218

Appendix WW. CW Characterisation March 1 2005 219

Appendix XX. CW Characterisation March 2 2005 220

Appendix YY. CW Characterisation March 3 2005 221

Appendix ZZ. CW Characterisation March 4 2005 222

Appendix AAA. CW Characterisation March 7 2005 223

Appendix BBB. CW Characterisation March 8 2005 224

Appendix CCC. CW Characterisation March 9 2005 225

Appendix DDD. CW Characterisation March 10 2005 226

Appendix EEE. CW Characterisation March 11 2005 227

Appendix FFF. CW Characterisation March 14 2005 228

Appendix GGG. CW Characterisation March 15 2005 229

Appendix HHH. CW Characterisation March 16 2005 230

Appendix III. CW Characterisation March 17 2005 231

Appendix JJJ. CW Characterisation March 18 2005 232

Appendix KKK. CW Characterisation March 22 2005 233

Appendix LLL. CW Characterisation March 24 2005 234

Appendix MMM. CW Characterisation March 29 2005 235

Appendix NNN. CW Characterisation March 30 2005 236

Appendix OOO. CW Characterisation March 31 2005 237

Appendix PPP. Average ethanol concentration with increasing length 238

Appendix QQQ. Average propanol concentration with increasing length 239

Appendix RRR. Average acetic acid concentration with increasing length 240

Appendix SSS. Average propanoic acid concentration with increasing length 241

Appendix TTT. Average butyric acid concentration with increasing length 242

Appendix UUU. Average sodium concentration with increasing length 243

Appendix VVV. Average potassium concentration with increasing length 244

Appendix WWW. Average COD with increasing length 245

Appendix XXX. Daily flow into the CW 246

Appendix YYY. Determination of ethanol rate constant from RTD 247

Appendix ZZZ. Finding conversion for average ethanol feed using RTD 248

Appendix AAAA. Scaling RTD of Port 5 to the 4m location within the reactor for ethanol degradation 249

Appendix BBBB. Scaling RTD of Port 5 to the 8m location within the reactor for ethanol degradation 250

Appendix CCCC. Scaling RTD of Port 5 to the 12m location within the reactor for ethanol degradation 251

Appendix DDDD. Scaling RTD of Port 5 to the 16m location within the reactor for ethanol degradation 252

Appendix EEEE. Reactor equation comparison for ethanol degradation 253

Appendix FFFF. Determination of potassium rate constant from RTD and scaling for various lengths 254

Appendix GGGG. Reactor equation comparison for ethanol degradation 255

Appendix HHHH. Proceedings of the 12th International Conference on Environmental Science and Technology, Rhodes, 8-10 September 2011 256

Appendix A. **Yearly effluent composition at Cellar 1**

Cellar 1 - Effluent Concentrations			Calc	Chemical							
Date	pH	COD	COD	Ethanol	Propanol	Acetic Acid	Propionic Acid	Butyric Acid	Sodium	Potassium	
07 July 2004	7.03	84									
18 August 2004	7.06	63							58.08	30.95	
08 October 2004	7.60	130	0	0.00	0.00	0.00	0.00	0.00	33.08	14.20	
28 November 2004	8.17	10	0	0.00	0.00	0.00	0.00	0.00	49.18	22.20	
27 January 2005	6.66	135	0	0.00	0.00	0.00	0.00	0.00	41.28	42.95	
15 February 2005	5.05	1755	1385	0.73	0.00	0.00	0.00	0.00	37.68	162.00	
28 February 2005	5.06	3760	3312	1.67	0.00	0.14	0.00	0.00	61.90	129.00	
17 March 2005	5.65	1360	1143	0.60	0.00	0.00	0.00	0.00	41.04	104.00	
04 May 2005	6.99	110	0	0.00	0.00	0.00	0.00	0.00	52.09	28.06	
01 June 2005	6.39	135	230	0.00	0.00	0.00	0.04	0.00	46.21	60.70	
27 July 2005	4.22	440	369	0.07	0.00	0.21	0.00	0.00	53.91	204.00	
Average	6.35	725.64	715.44	0.34	0.00	0.04	0.00	0.00	47.45	79.81	
Standard Deviation	1.21	1163.85	1105.46	0.57	0.00	0.08	0.01	0.00	9.25	66.33	
Maximum	8.17	3760.00	3312.00	1.67	0.00	0.21	0.04	0.00	61.90	204.00	
Minimum	4.22	10.00	0.00	0.00	0.00	0.00	0.00	0.00	33.08	14.20	

Appendix B. **Daily effluent composition at Cellar 2 for the duration of a harvest**

Cellar 2 - Effluent Concentrations			Calc	Chemical								
Date	pH	COD	COD	Ethanol	Propanol	Acetic Acid	Propionic Acid	Butyric Acid	Sodium	Potassium
31 January 2005	7.28	60.00	0.00	0.00	0.00	0.00	0.00	0.00	15.78	27.05
05 February 2005	4.36	1295.00	635.00	0.25	0.01	0.04	0.02	0.03	31.71	75.90
07 February 2005	4.39	570.00	810.00	0.32	0.00	0.12	0.14	0.00	17.03	38.70
08 February 2005	4.31	1230.00	779.00	0.41	0.00	0.00	0.00	0.00	10.03	46.59
09 February 2005	4.37	1680.00	1045.00	0.34	0.00	0.36	0.00	0.00	10.30	37.31
10 February 2005	4.30	2440.00	2280.00	0.92	0.07	0.36	0.00	0.00	20.98	64.89
11 February 2005	4.30	2400.00	2590.00	1.03	0.07	0.13	0.21	0.03	19.62	56.80
14 February 2005	4.53	2725.00	2345.00	1.15	0.09	0.00	0.00	0.00	27.00	67.00
15 February 2005	4.48	4620.00	4135.00	1.70	0.04	0.75	0.00	0.00	34.07	69.25
16 February 2005	5.42	3135.00	2390.00	0.89	0.10	0.46	0.00	0.00	83.00	100.00
17 February 2005	5.19	570.00	370.00	0.14	0.00	0.09	0.00	0.00	11.21	32.20
18 February 2005	5.48	3145.00	2005.00	1.06	0.00	0.00	0.00	0.00	47.98	154.00
19 February 2005	5.16	3350.00	2415.00	1.28	0.00	0.00	0.00	0.00	57.62	182.00
21 February 2005	5.11	2385.00	1505.00	0.77	0.02	0.00	0.00	0.00	36.43	148.00
22 February 2005	5.05	2690.00	2005.00	1.03	0.03	0.00	0.00	0.00	51.38	197.00
23 February 2005	4.90	1775.00	1315.00	0.66	0.03	0.00	0.00	0.00	33.16	120.00
24 February 2005	5.05	3090.00	2805.00	1.46	0.03	0.00	0.00	0.00	121.00	155.00
28 February 2005	4.72	4920.00	5020.00	2.66	0.00	0.00	0.00	0.00	48.20	142.00
01 March 2005	4.52	7000.00	7142.00	3.78	0.00	0.00	0.00	0.00	32.87	215.00
02 March 2005	4.62	3635.00	3474.00	1.84	0.00	0.00	0.00	0.00	28.23	145.00
03 March 2005	4.59	2125.00	1922.00	0.85	0.00	0.29	0.00	0.00	20.82	96.50
04 March 2005	4.65	1200.00	1590.00	0.84	0.02	0.00	0.00	0.00	25.30	138.00
07 March 2005	4.60	740.00	1440.00	0.80	0.00	0.00	0.00	0.00	19.87	120.00
08 March 2005	4.62	860.00	1230.00	1.25	0.00	0.00	0.00	0.00	28.10	155.00
09 March 2005	4.67	815.00	1155.00	0.45	0.00	0.00	0.00	0.00	22.50	118.00
10 March 2005	4.99	1855.00	1100.00	0.53	0.05	0.00	0.00	0.00	20.18	110.00
11 March 2005	4.85	1735.00	2138.00	0.96	0.03	0.00	0.00	0.00	28.50	143.00
14 March 2005	4.84	620.00	799.00	0.42	0.00	0.00	0.00	0.00	8.91	45.20
15 March 2005	5.04	765.00	1030.00	0.54	0.00	0.00	0.00	0.00	15.59	42.95
16 March 2005	4.83	515.00	661.00	0.26	0.00	0.05	0.04	0.04	16.91	66.95
17 March 2005	4.55	1030.00	1008.00	0.53	0.00	0.00	0.00	0.00	12.90	74.00
18 March 2005	4.55	2795.00	2609.00	1.31	0.00	0.12	0.00	0.00	30.26	35.22
22 March 2005	6.21	170.00	190.00	0.10	0.00	0.00	0.00	0.00	11.41	22.90
24 March 2005	5.51	785.00	535.00	0.28	0.00	0.00	0.00	0.00	20.81	77.50
29 March 2005	5.10	740.00	410.00	0.22	0.00	0.00	0.00	0.00	14.52	41.75
30 March 2005	6.28	555.00	360.00	0.19	0.00	0.00	0.00	0.00	29.03	53.91
31 March 2005	5.29	1760.00	1675.00	0.83	0.00	0.00	0.00	0.00	52.40	27.05
Average	4.94	1940.00	1754.51	0.87	0.02	0.07	0.01	0.00	30.15	93.02
Standard Deviation	0.61	1469.92	1409.75	0.73	0.03	0.16	0.04	0.01	21.69	52.72
Maximum	7.28	7000.00	7142.00	3.78	0.10	0.75	0.21	0.04	121.00	215.00
Minimum	4.30	60.00	0.00	0.00	0.00	0.00	0.00	0.00	8.91	22.90

Appendix C. **Impulse-Response Tracer Experiment Data for the CW**

Time / Hours	Meter Reading	Flow / m^3	**Port** Bromide Concentration /mg/L														
			1a	**1b**	**1**	**2a**	**2b**	**2**	**3a**	**3b**	**3**	**4a**	**4b**	**4**	**5a**	**5b**	**5**
0.00	125.37																
0.83	125.86	0.60	0.83	6.41	0.58	0.00	0.00	0.00	0.00	0.00	0.00	0.00	0.00	0.00	0.00	0.00	0.00
1.90	126.41	0.77	0.00	0.00	0.00	0.00	0.00	0.00	0.00	0.00	0.00	0.00	0.00	0.00	0.00	0.00	0.00
2.90	126.89	0.72	0.00	0.74	0.00	0.00	0.74	0.00	0.00	0.00	0.00	0.00	0.00	0.00	0.71	0.00	1.78
4.00	128.44	0.79	183.42	145.07	12.78	0.00	11.63	0.00	0.00	0.00	0.00	0.00	0.00	1.09	0.00	0.00	132.48
5.03	129.46	0.74	128.29	109.50	134.83	0.00	14.72	0.00	0.00	0.00	0.00	0.00	0.00	3.41	0.00	0.00	181.81
5.70	129.96	0.48	95.96	95.47	167.69	0.00	25.29	1.36	0.00	0.00	0.00	0.00	0.00	2.73	0.00	0.00	122.43
6.67	130.71	0.70	73.26	91.12	151.17	0.00	74.63	5.55	0.00	0.00	0.00	0.00	0.00	2.12	0.00	0.00	133.98
8.93	132.52	1.63	51.65	105.17	67.78	5.24	160.56	25.24	2.37	3.65	0.00	0.00	0.00	8.55	0.00	0.00	134.14
10.92	134.03	1.43	47.54	84.01	28.11	47.07	115.91	64.34	1.41	14.01	0.79	0.00	0.00	26.69	0.00	0.35	126.98
12.88	135.52	1.42	44.96	52.84	17.77	62.30	77.07	141.84	1.17	24.00	3.39	0.00	0.31	41.97	0.32	3.26	106.69
15.00	136.92	1.52	43.46	32.60	12.34	55.28	59.59	148.43	1.74	58.81	9.05	0.29	0.56	48.01	1.01	4.64	88.18
17.03	138.16	1.46	39.34	20.47	8.9	37.31	47.44	121.81	3.25	70.45	13.47	0.59	0.8	41.24	1.4	7.64	67.16
18.75	139.14	1.24	33.23	15.21	7.68	33.27	36.83	106.91	10.40	79.38	20.15	1.01	1.81	36.17	5.35	7.89	55.84
20.33	140.26	1.14	28.76	14.19	6.52	30.63	29.71	96.07	24.49	74.07	47.77	1.09	3.73	32.33	3.08	12.81	55.58
23.17	141.71	2.04	10.92	5.70	7.11	28.16	22.34	76.43	68.71	69.63	31.50	38.84	10.50	30.48	3.54	13.33	47.41
26.33	143.18	2.28	3.91	5.48	10.77	22.24	17.19	56.02	78.88	62.29	55.27	60.57	29.94	35.53	5.06	38.27	46.16
30.93	148.24	3.31	10.78	16.05	5.18	9.59	9.15	22.05	30.53	38.29	59.88	24.66	81.68	62.99	10.59	4.86	26.50
35.93	150.53	3.60	7.72	8.74	4.01	8.50	9.26	13.58	17.11	24.10	42.48	48.00	62.92	48.03	42.67	68.56	27.86
40.08	151.00	2.99	6.09	7.70	4.42	7.75	9.39	12.09	14.35	23.24	36.25	44.41	55.30	46.40	45.65	79.61	36.56
42.72	154.95	1.90	5.37	7.55	2.49	5.89	7.48	10.39	9.24	16.49	21.58	33.67	38.77	49.75	55.99	84.54	21.77
46.77	156.21	2.92	3.52	7.55	5.03	4.46	6.23	7.16	8.14	14.86	14.30	17.97	29.70	34.09	44.90	66.42	29.65
64.33	159.24	12.65	1.89	2.27	2.21	3.49	4.75	6.00	7.09	12.51	11.47	16.71	20.24	28.58	43.08	54.73	14.29
332.42	195.20	193.02	0.00	0.00	0.00	0.00	0.00	0.00	0.00	0.00	3.31	2.37	3.23	0.00	4.22	3.34	0.00
498.83	208.81	119.82	0.00	0.00	0.00	0.00	0.00	0.00	0.00	0.00	0.00	0.00	0.00	0.00	0.00	0.00	0.00
666.83	212.52	120.96	0.00	0.00	0.00	0.00	0.00	0.00	0.72	1.53	1.79	2.30	3.43	1.82	6.18	5.30	3.80
	Flow	33.67															
	Ave Flow	0.72	cubm/hr														

Appendix D. **Impulse-Response Tracer Experiment Data – Laterally Averaged Data**

Time / Hours	Meter Rea	Flow / m^	Port		Average a/b Concentration /mg/L									
			Port	1a/b	1	2a/b	2	3a/b	3	4a/b	4	5a/b	5	
0.00	125.37													
0.83	125.86	0.60		3.62	0.58	0.00	0.00	0.00	0.00	0.00	0.00	0.00	0.00	
1.90	126.41	0.77		0.00	0.00	0.00	0.00	0.00	0.00	0.00	0.00	0.00	0.00	
2.90	126.89	0.72		0.37	0.00	0.37	0.00	0.00	0.00	0.00	0.00	0.36	1.78	
4.00	128.44	0.79		164.25	12.78	5.82	0.00	0.00	0.00	0.00	1.09	0.00	132.48	
5.03	129.46	0.74		118.90	134.83	7.36	0.00	0.00	0.00	0.00	3.41	0.00	181.81	
5.70	129.96	0.48		95.72	167.69	12.65	1.36	0.00	0.00	0.00	2.73	0.00	122.43	
6.67	130.71	0.70		82.19	151.17	37.32	5.55	0.00	0.00	0.00	2.12	0.00	133.98	
8.93	132.52	1.63		78.41	67.78	82.90	25.24	3.01	0.00	0.00	8.55	0.00	134.14	
10.92	134.03	1.43		65.78	28.11	81.49	64.34	7.71	0.79	0.00	26.69	0.18	126.98	
12.88	135.52	1.42		48.90	17.77	69.69	141.84	12.59	3.39	0.16	41.97	1.79	106.69	
15.00	136.92	1.52		38.03	12.34	57.44	148.43	30.28	9.05	0.43	48.01	2.82	88.18	
17.03	138.16	1.46		29.91	8.9	42.38	121.81	36.85	13.47	0.70	41.24	4.52	67.16	
18.75	139.14	1.24		24.22	7.68	35.05	106.91	44.89	20.15	1.41	36.17	6.62	55.84	
20.33	140.26	1.14		21.48	6.52	30.17	96.07	49.28	47.77	2.41	32.33	7.95	55.58	
23.17	141.71	2.04		8.31	7.11	25.25	76.43	69.17	31.50	24.67	30.48	8.44	47.41	
26.33	143.18	2.28		4.70	10.77	19.72	56.02	70.59	55.27	45.26	35.53	21.67	46.16	
30.93	148.24	3.31		13.42	5.18	9.37	22.05	34.41	59.88	53.17	62.99	7.73	26.50	
35.93	150.53	3.60		8.23	4.01	8.88	13.58	20.61	42.48	55.46	48.03	55.62	27.86	
40.08	151.00	2.99		6.90	4.42	8.57	12.09	18.80	36.25	49.86	46.40	62.63	36.56	
42.72	154.95	1.90		6.46	2.49	6.69	10.39	12.87	21.58	36.22	49.75	70.27	21.77	
46.77	156.21	2.92		5.54	5.03	5.35	7.16	11.50	14.30	23.84	34.09	55.66	29.65	
64.33	159.24	12.65		2.08	2.21	4.12	6.00	9.80	11.47	18.48	28.58	48.91	14.29	
332.42	195.20	193.02		0.00	0.00	0.00	0.00	0.00	3.31	2.80	0.00	3.78	0.00	
498.83	208.81	119.82		0.00	0.00	0.00	0.00	0.00	0.00	0.00	0.00	0.00	0.00	
666.83	212.52	120.96		0.00	0.00	0.00	0.00	0.00	0.00	0.00	0.00	0.00	0.00	
	Flow	33.67		0.00	0.00	0.00	0.00	1.13	1.79	2.87	1.82	5.74	3.80	
	Ave Flow	0.72												

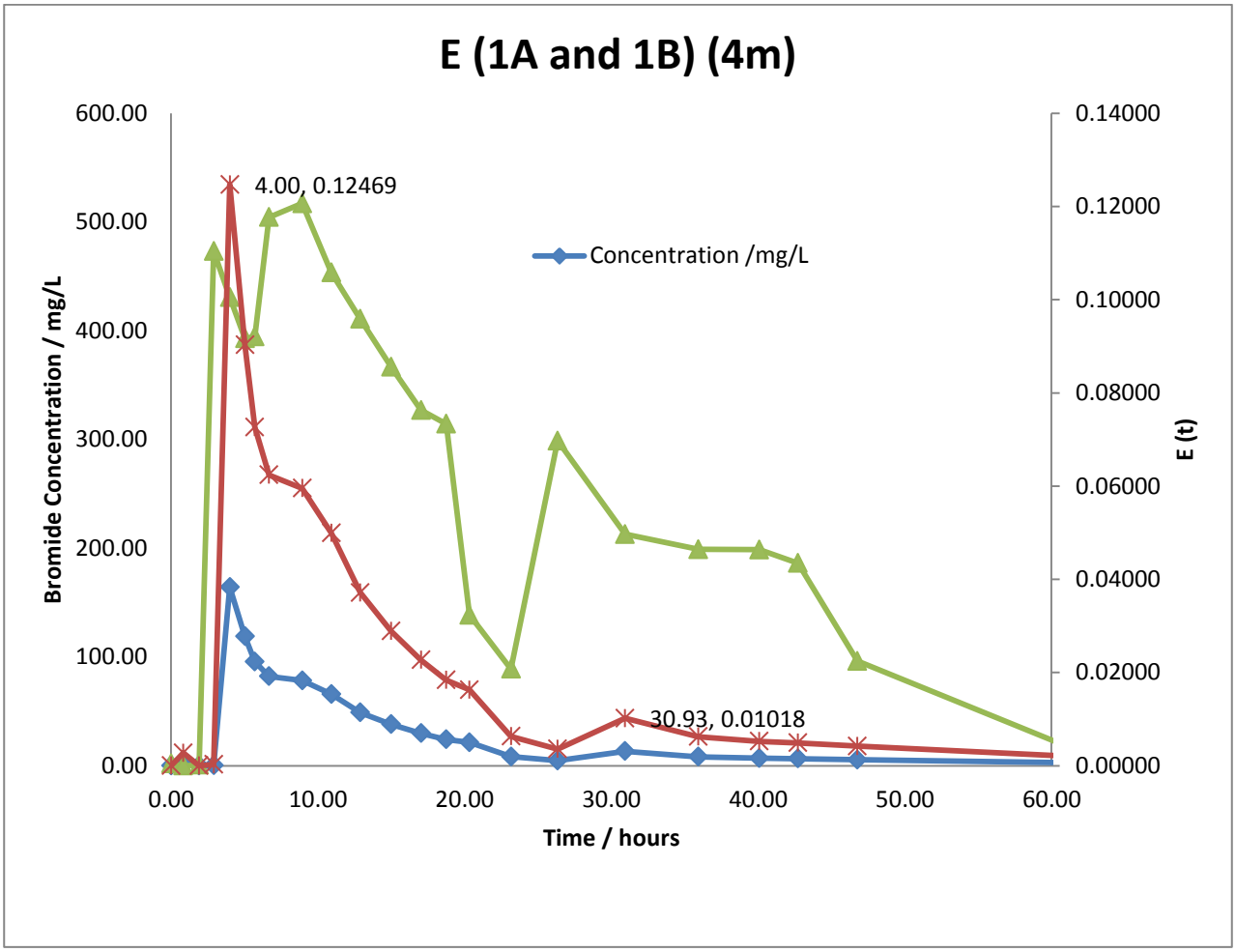
Appendix E. **Impulse-Response Tracer Experiment Data – Mass Balance**

	Mass Throughput	g Bromide														
Date and Time	Time / hours	1a	1b	1.00	2a	2b	2.00	3a	3b	3.00	4a	4b	4.00	5a	5b	5.00
2006/02/03 18:00	0.00	0.50	3.85	0.35	0.00	0.00	0.00	0.00	0.00	0.00	0.00	0.00	0.00	0.00	0.00	0.00
2006/02/03 19:04	0.83	0.00	0.00	0.00	0.00	0.00	0.00	0.00	0.00	0.00	0.00	0.00	0.00	0.00	0.00	0.00
2006/02/03 20:04	1.90	0.00	1.55	0.00	0.00	1.55	0.00	0.00	0.00	0.00	0.00	0.00	0.00	1.48	0.00	3.72
2006/02/03 21:10	2.90	528.25	417.80	36.81	0.00	33.49	0.00	0.00	0.00	0.00	0.00	0.00	3.14	0.00	0.00	381.54
2006/02/03 22:12	4.00	464.92	396.83	488.62	0.00	53.35	0.00	0.00	0.00	0.00	0.00	0.00	12.36	0.00	0.00	658.88
2006/02/03 22:52	5.03	393.82	391.81	688.20	0.00	103.79	5.58	0.00	0.00	0.00	0.00	0.00	11.20	0.00	0.00	502.45
2006/02/03 23:50	5.70	351.65	437.38	725.62	0.00	358.22	26.64	0.00	0.00	0.00	0.00	0.00	10.18	0.00	0.00	643.10
2006/02/04 02:06	6.67	332.21	676.45	435.96	33.70	1032.72	162.34	15.24	23.48	0.00	0.00	0.00	54.99	0.00	0.00	862.79
2006/02/04 04:05	8.93	373.66	660.32	220.94	369.97	911.05	505.71	11.09	110.12	6.21	0.00	0.00	209.78	0.00	2.75	998.06
2006/02/04 06:03	10.92	417.05	490.14	164.83	577.89	714.90	1315.71	10.85	222.62	31.45	0.00	2.88	389.31	2.97	30.24	989.66
2006/02/04 08:10	12.88	469.37	352.08	133.27	597.02	643.57	1603.04	18.79	635.15	97.74	3.13	6.05	518.51	10.89	50.11	952.34
2006/02/04 10:12	15.00	482.47	251.04	109.15	457.57	581.80	1493.88	39.86	864.00	165.20	7.24	9.81	505.77	17.17	93.70	823.65
2006/02/04 11:55	17.03	448.61	205.34	103.68	449.15	497.21	1443.29	140.40	1071.63	272.03	13.64	24.44	488.30	72.23	106.52	753.84
2006/02/04 13:30	18.75	421.05	207.74	95.45	448.42	434.95	1406.46	358.53	1084.38	699.35	15.96	54.61	473.31	45.09	187.54	813.69
2006/02/04 16:20	20.33	182.15	95.08	118.59	469.71	372.63	1274.85	1146.08	1161.43	525.42	647.85	175.14	508.41	59.05	222.34	790.80
2006/02/04 19:30	23.17	74.13	103.90	204.20	421.67	325.92	1062.14	1495.56	1181.02	1047.92	1148.41	567.66	673.65	95.94	725.60	875.19
2006/02/05 00:06	26.33	240.09	357.47	115.37	213.59	203.79	491.10	679.96	852.79	1333.65	549.23	1819.18	1402.91	235.86	108.24	590.21
2006/02/05 05:06	30.93	199.73	226.12	103.75	219.91	239.57	351.34	442.67	623.52	1099.04	1241.86	1627.87	1242.63	1103.96	1773.78	720.79
2006/02/05 09:15	35.93	175.76	222.22	127.56	223.66	271.00	348.92	414.14	670.71	1046.17	1281.67	1595.96	1339.10	1317.46	2297.54	1055.12
2006/02/05 11:53	40.08	165.16	232.21	76.58	181.15	230.05	319.55	284.19	507.17	663.71	1035.55	1192.41	1530.11	1722.03	2600.11	669.56
2006/02/05 15:56	42.72	118.53	254.22	169.37	150.18	209.78	241.09	274.09	500.37	481.51	605.09	1000.06	1147.88	1511.87	2236.49	998.37
2006/02/06 09:30	46.77	87.54	105.15	102.37	161.66	220.02	277.92	328.41	579.46	531.29	774.01	937.52	1323.83	1995.47	2535.09	661.91
2006/02/17 13:35	64.33	0.00	0.00	0.00	0.00	0.00	0.00	0.00	0.00	792.22	567.24	773.07	0.00	1010.01	799.40	0.00
2006/02/24 12:00	332.42	0.00	0.00	0.00	0.00	0.00	0.00	0.00	0.00	0.00	0.00	0.00	0.00	0.00	0.00	0.00
2006/03/03 12:00	498.83	0.00	0.00	0.00	0.00	0.00	0.00	345.69	734.58	859.41	1104.28	1646.81	873.82	2967.14	2544.64	1824.46
2006/03/10 00:06	666.83	0.00	0.00	0.00	0.00	0.00	0.00	0.00	0.00	0.00	0.00	0.00	0.00	0.00	0.00	0.00
		0.00	0.00	0.00	0.00	0.00	0.00	0.00	0.00	0.00	0.00	0.00	0.00	0.00	0.00	0.00
			5926.64	6088.69	4220.68	4975.26	7439.37	12329.57	6005.56	10822.42	9652.32	8995.13	11433.45	12719.19	12168.61	16314.10

Appendix F. **RTD for Sample Port 1a/b**

Date and Time	Time / hours	Meter Reading	Flow / m^3	Concentration /mg/L	Q (sigC.Dt)	E(C/Q)	Integral of E	ti.ei.dt	ti^2.Ei.dt		
2006/02/03 17:10	0.00	125.37		1a/b	1317.26	0.00000				Min	Mout
2006/02/03 18:00	0.83	125.86	0.49	3.62	3.02	0.00275	0.00	0.00	0.00	3357.00	1.77
2006/02/03 19:04	1.90	126.41	0.55	0.00	0.00	0.00000	0.00	0.00	0.00		0.00
2006/02/03 20:04	2.90	126.89	0.48	0.37	0.37	0.00028	0.00	0.00	0.00		0.18
2006/02/03 21:10	4.00	128.44	1.55	164.25	180.67	0.12469	0.14	0.55	2.19		254.58
2006/02/03 22:12	5.03	129.46	1.02	118.90	122.86	0.09026	0.09	0.47	2.36		121.27
2006/02/03 22:52	5.70	129.96	0.50	95.72	63.81	0.07266	0.05	0.28	1.57		47.86
2006/02/03 23:50	6.67	130.71	0.75	82.19	79.45	0.06239	0.06	0.40	2.68		61.64
2006/02/04 02:06	8.93	132.52	1.81	78.41	177.73	0.05952	0.13	1.21	10.77		141.92
2006/02/04 04:05	10.92	134.03	1.51	65.78	130.45	0.04993	0.10	1.08	11.80		99.32
2006/02/04 06:03	12.88	135.52	1.49	48.90	96.17	0.03712	0.07	0.94	12.12		72.86
2006/02/04 08:10	15.00	136.92	1.40	38.03	80.50	0.02887	0.06	0.92	13.75		53.24
2006/02/04 10:12	17.03	138.16	1.24	29.91	60.81	0.02270	0.05	0.79	13.39		37.08
2006/02/04 11:55	18.75	139.14	0.98	24.22	41.58	0.01839	0.03	0.59	11.10		23.74
2006/02/04 13:30	20.33	140.26	1.12	21.48	34.00	0.01630	0.03	0.52	10.67		24.05
2006/02/04 16:20	23.17	141.71	1.45	8.31	23.54	0.00631	0.02	0.41	9.59		12.05
2006/02/04 19:30	26.33	143.18	1.47	4.70	14.87	0.00356	0.01	0.30	7.83		6.90
2006/02/05 00:06	30.93	148.24	5.06	13.42	61.71	0.01018	0.05	1.45	44.83		67.88
2006/02/05 05:06	35.93	150.53	2.29	8.23	41.15	0.00625	0.03	1.12	40.34		18.85
2006/02/05 09:15	40.08	151.00	0.47	6.90	28.61	0.00523	0.02	0.87	34.90		3.24
2006/02/05 11:53	42.72	154.95	3.95	6.46	17.01	0.00490	0.01	0.55	23.56		25.52
2006/02/05 15:56	46.77	156.21	1.26	5.54	22.42	0.00420	0.02	0.80	37.22		6.97
2006/02/06 09:30	64.33	159.24	3.03	2.08	36.54	0.00158	0.03	1.78	114.80		6.30
2006/02/17 13:35	332.42	195.20	35.96	0.00	0.00	0.00000	0.00	0.00	0.00		0.00
2006/02/24 12:00	498.83	208.81	13.61	0.00	0.00	0.00000	0.00	0.00	0.00		0.00
2006/03/03 12:00	666.83	212.52	3.71	0.00	0.00	0.00000	0.00	0.00	0.00		0.00
			0.53			Sigma (Ei)	1.00				1087.23
							Tau	15.0313			
							Sigma^2	179.5451			
							N	1.2584			
							Sigma Theta^2	0.7947			
							Disp	134.9491			
							Sigma Theta^2	0.7947			
							N	1.2584			
							Pe	0.00741			

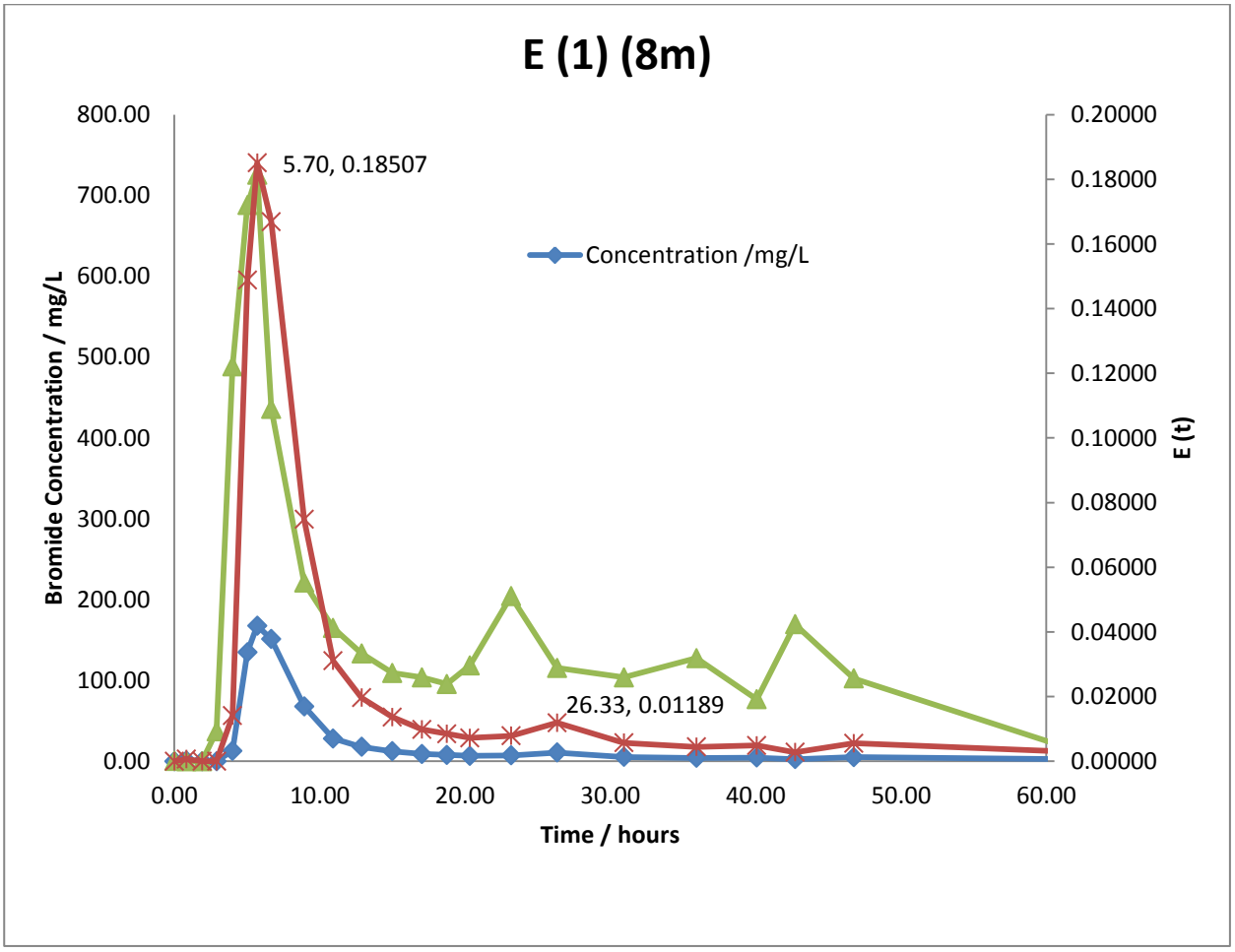
Appendix G. **RTD graphs for Sample Port 1a/b**



Appendix H. **RTD for Sample Port 1**

Date and Time	Time / hours	Meter Reading	Flow / m^3	Concentration /mg/L	Q.(sigC.Dt)	E(C/Q)	Integral of E	ti.ei.dt	ti^2.Ei.dt		
				Port 1	906.07	0.00000				Min	Mout
2006/02/03 17:10	0.00	125.37									
2006/02/03 18:00	0.83	125.86	0.49	0.58	0.48	0.00064	0.00	0.00	0.00	3357.00	0.28
2006/02/03 19:04	1.90	126.41	0.55	0.00	0.00	0.00000	0.00	0.00	0.00		0.00
2006/02/03 20:04	2.90	126.89	0.48	0.00	0.00	0.00000	0.00	0.00	0.00		0.00
2006/02/03 21:10	4.00	128.44	1.55	12.78	14.06	0.01410	0.02	0.06	0.25		19.81
2006/02/03 22:12	5.03	129.46	1.02	134.83	139.32	0.14881	0.15	0.77	3.90		137.53
2006/02/03 22:52	5.70	129.96	0.50	167.69	111.79	0.18507	0.12	0.70	4.01		83.85
2006/02/03 23:50	6.67	130.71	0.75	151.17	146.13	0.16684	0.16	1.08	7.17		113.38
2006/02/04 02:06	8.93	132.52	1.81	67.78	153.63	0.07481	0.17	1.51	13.53		122.68
2006/02/04 04:05	10.92	134.03	1.51	28.11	55.75	0.03102	0.06	0.67	7.33		42.45
2006/02/04 06:03	12.88	135.52	1.49	17.77	34.95	0.01961	0.04	0.50	6.40		26.48
2006/02/04 08:10	15.00	136.92	1.40	12.34	26.12	0.01362	0.03	0.43	6.49		17.28
2006/02/04 10:12	17.03	138.16	1.24	8.90	18.10	0.00982	0.02	0.34	5.79		11.04
2006/02/04 11:55	18.75	139.14	0.98	7.68	13.18	0.00848	0.01	0.27	5.12		7.53
2006/02/04 13:30	20.33	140.26	1.12	6.52	10.32	0.00720	0.01	0.23	4.71		7.30
2006/02/04 16:20	23.17	141.71	1.45	7.11	20.14	0.00785	0.02	0.52	11.93		10.31
2006/02/04 19:30	26.33	143.18	1.47	10.77	34.11	0.01189	0.04	0.99	26.10		15.83
2006/02/05 00:06	30.93	148.24	5.06	5.18	23.83	0.00572	0.03	0.81	25.16		26.21
2006/02/05 05:06	35.93	150.53	2.29	4.01	20.05	0.00443	0.02	0.80	28.57		9.18
2006/02/05 09:15	40.08	151.00	0.47	4.42	18.34	0.00488	0.02	0.81	32.53		2.08
2006/02/05 11:53	42.72	154.95	3.95	2.49	6.56	0.00275	0.01	0.31	13.21		9.84
2006/02/05 15:56	46.77	156.21	1.26	5.03	20.37	0.00555	0.02	1.05	49.17		6.34
2006/02/06 09:30	64.33	159.24	3.03	2.21	38.82	0.00244	0.04	2.76	177.33		6.70
2006/02/17 13:35	332.42	195.20	35.96	0.00	0.00	0.00000	0.00	0.00	0.00		0.00
2006/02/24 12:00	498.83	208.81	13.61	0.00	0.00	0.00000	0.00	0.00	0.00		0.00
2006/03/03 12:00	666.83	212.52	3.71	0.00	0.00	0.00000	0.00	0.00	0.00		0.00
						Sigma (Ei)	1.00				676.07
								Tau	14.6189		
								Sigma^2	214.9917		
								N	0.9941		
								Sigma Theta^2	1.0060		
								Disp	135.0021		
								Sigma Theta^2	1.0060		
								N	0.9941		
								Pe	0.00741		

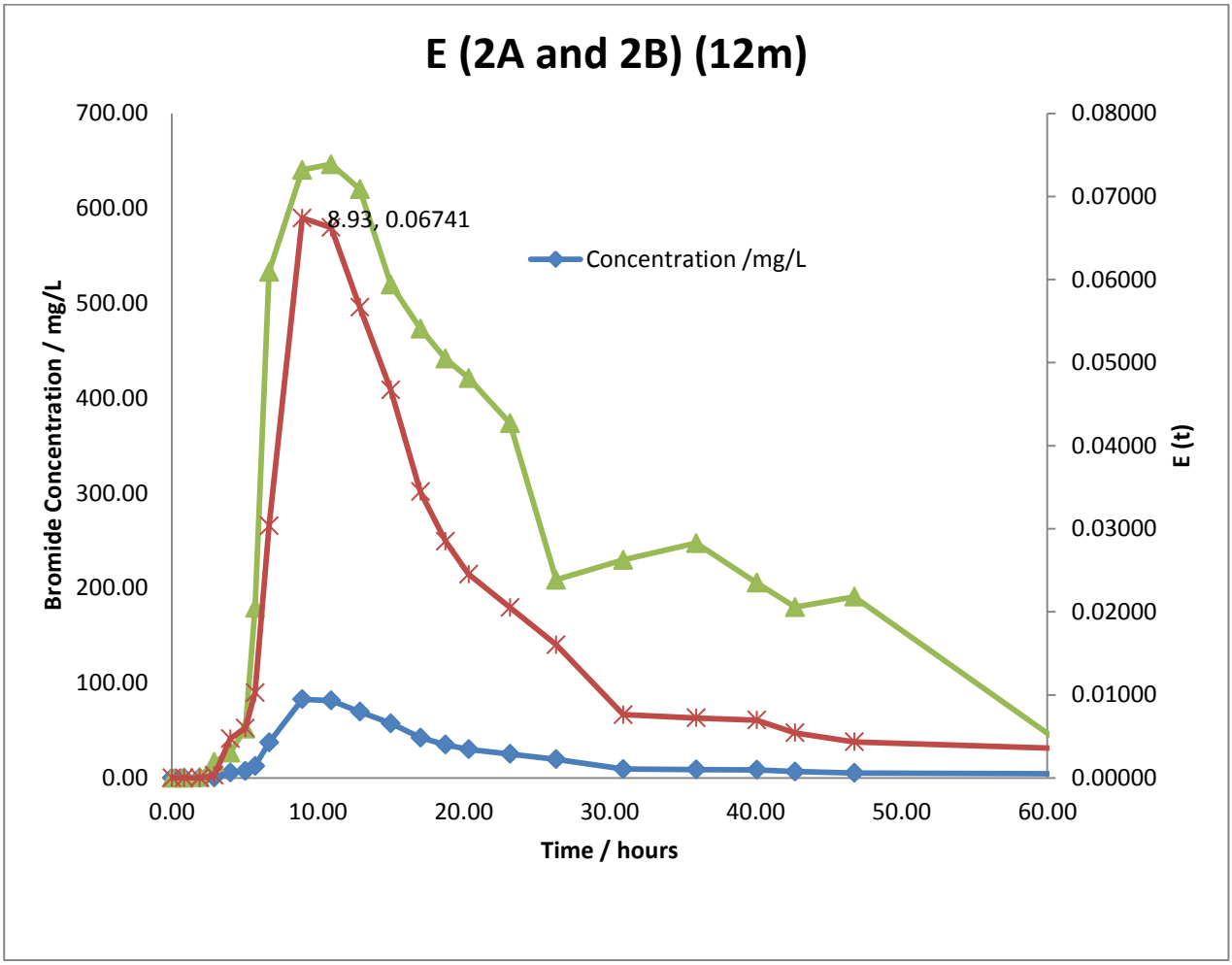
Appendix I. **RTD graphs for Sample Port 1**



Appendix J. **RTD for Sample Port 2a/b**

Time / hours	Meter Reading	Flow / m^3	Concentration /mg/L	Q (sigC.Dt)	E(C/Q)	Integral of E	ti.ei.dt	ti^2.Ei.dt		
0.00	125.37		2a/b	1229.79	0.00000				Min	Mout
0.83	125.86	0.49	0.00	0.00	0.00000	0.00	0.00	0.00	3357.00	0.00
1.90	126.41	0.55	0.00	0.00	0.00000	0.00	0.00	0.00		0.00
2.90	126.89	0.48	0.37	0.37	0.00030	0.00	0.00	0.00		0.18
4.00	128.44	1.55	5.82	6.40	0.00473	0.01	0.02	0.08		9.01
5.03	129.46	1.02	7.36	7.61	0.00598	0.01	0.03	0.16		7.51
5.70	129.96	0.50	12.65	8.43	0.01028	0.01	0.04	0.22		6.32
6.67	130.71	0.75	37.32	36.07	0.03034	0.03	0.20	1.30		27.99
8.93	132.52	1.81	82.90	187.91	0.06741	0.15	1.36	12.19		150.05
10.92	134.03	1.51	81.49	161.62	0.06626	0.13	1.43	15.66		123.05
12.88	135.52	1.49	69.69	137.05	0.05666	0.11	1.44	18.50		103.83
15.00	136.92	1.40	57.44	121.57	0.04670	0.10	1.48	22.24		80.41
17.03	138.16	1.24	42.38	86.16	0.03446	0.07	1.19	20.33		52.55
18.75	139.14	0.98	35.05	60.17	0.02850	0.05	0.92	17.20		34.35
20.33	140.26	1.12	30.17	47.77	0.02453	0.04	0.79	16.06		33.79
23.17	141.71	1.45	25.25	71.54	0.02053	0.06	1.35	31.22		36.61
26.33	143.18	1.47	19.72	62.43	0.01603	0.05	1.34	35.20		28.98
30.93	148.24	5.06	9.37	43.10	0.00762	0.04	1.08	33.54		47.41
35.93	150.53	2.29	8.88	44.40	0.00722	0.04	1.30	46.62		20.34
40.08	151.00	0.47	8.57	35.57	0.00697	0.03	1.16	46.47		4.03
42.72	154.95	3.95	6.69	17.60	0.00544	0.01	0.61	26.12		26.41
46.77	156.21	1.26	5.35	21.65	0.00435	0.02	0.82	38.50		6.73
64.33	159.24	3.03	4.12	72.37	0.00335	0.06	3.79	243.57		12.48
332.42	195.20	35.96	0.00	0.00	0.00000	0.00	0.00	0.00		0.00
498.83	208.81	13.61	0.00	0.00	0.00000	0.00	0.00	0.00		0.00
666.83	212.52	3.71	0.00	0.00	0.00000	0.00	0.00	0.00		0.00
					Sigma (Ei)	1.00				812.02
						Tau	20.3523			
						Sigma^2	210.9733			
						N	1.9634			
						Sigma Theta^2	0.5093			
						Disp	0.4044			
						Sigma Theta^2	0.5093			
						N	1.9634			
						Pe	2.47			

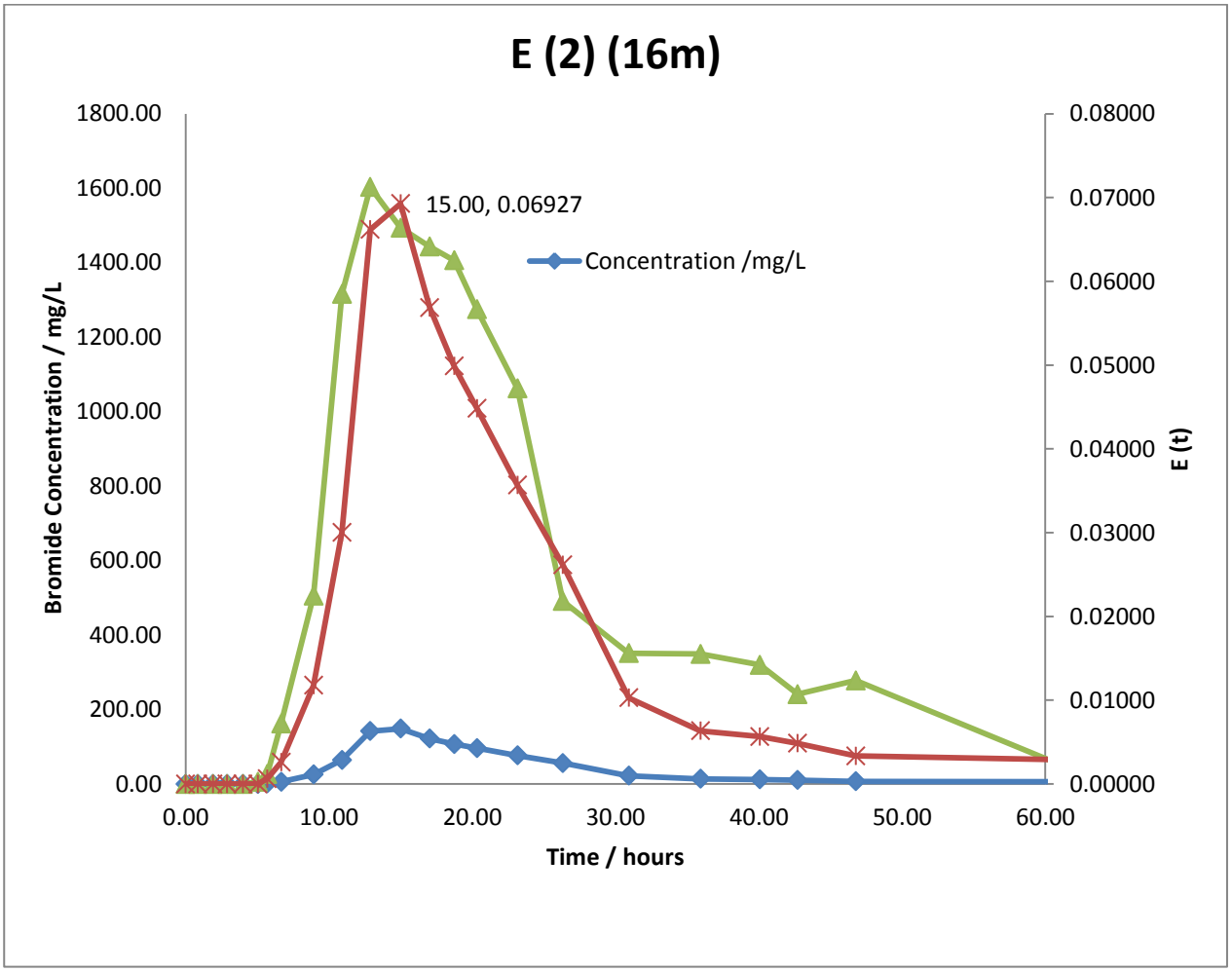
Appendix K. **RTD graphs for Sample Port 2a/b**



Appendix L. **RTD for Sample Port 2**

Date and Time	Time / hours	Meter Reading	Flow / m^3	Concentration /mg/L	Q (sigC.Dt)	E(C/Q)	Integral of E	ti.ei.dt	ti^2.Ei.dt		
				Port 2	2142.75	0.00000				Min	Mout
2006/02/03 17:10	0.00	125.37		0.00	0.00	0.00000	0.00	0.00	0.00	3357.00	0.00
2006/02/03 18:00	0.83	125.86	0.49	0.00	0.00	0.00000	0.00	0.00	0.00		0.00
2006/02/03 19:04	1.90	126.41	0.55	0.00	0.00	0.00000	0.00	0.00	0.00		0.00
2006/02/03 20:04	2.90	126.89	0.48	0.00	0.00	0.00000	0.00	0.00	0.00		0.00
2006/02/03 21:10	4.00	128.44	1.55	0.00	0.00	0.00000	0.00	0.00	0.00		0.00
2006/02/03 22:12	5.03	129.46	1.02	0.00	0.00	0.00000	0.00	0.00	0.00		0.00
2006/02/03 22:52	5.70	129.96	0.50	1.36	0.91	0.00063	0.00	0.00	0.01		0.68
2006/02/03 23:50	6.67	130.71	0.75	5.55	5.37	0.00259	0.00	0.02	0.11		4.16
2006/02/04 02:06	8.93	132.52	1.81	25.24	57.21	0.01178	0.03	0.24	2.13		45.68
2006/02/04 04:05	10.92	134.03	1.51	64.34	127.61	0.03003	0.06	0.65	7.10		97.15
2006/02/04 06:03	12.88	135.52	1.49	141.84	278.95	0.06620	0.13	1.68	21.61		211.34
2006/02/04 08:10	15.00	136.92	1.40	148.43	314.18	0.06927	0.15	2.20	32.99		207.80
2006/02/04 10:12	17.03	138.16	1.24	121.81	247.68	0.05685	0.12	1.97	33.54		151.04
2006/02/04 11:55	18.75	139.14	0.98	106.91	183.53	0.04989	0.09	1.61	30.11		104.77
2006/02/04 13:30	20.33	140.26	1.12	96.07	152.11	0.04483	0.07	1.44	29.35		107.60
2006/02/04 16:20	23.17	141.71	1.45	76.43	216.55	0.03567	0.10	2.34	54.24		110.82
2006/02/04 19:30	26.33	143.18	1.47	56.02	177.40	0.02614	0.08	2.18	57.41		82.35
2006/02/05 00:06	30.93	148.24	5.06	22.05	101.43	0.01029	0.05	1.46	45.29		111.57
2006/02/05 05:06	35.93	150.53	2.29	13.58	67.90	0.00634	0.03	1.14	40.92		31.10
2006/02/05 09:15	40.08	151.00	0.47	12.09	50.17	0.00564	0.02	0.94	37.62		5.68
2006/02/05 11:53	42.72	154.95	3.95	10.39	27.36	0.00485	0.01	0.55	23.30		41.04
2006/02/05 15:56	46.77	156.21	1.26	7.16	29.00	0.00334	0.01	0.63	29.60		9.02
2006/02/06 09:30	64.33	159.24	3.03	6.00	105.40	0.00280	0.05	3.16	203.58		18.18
2006/02/17 13:35	332.42	195.20	35.96	0.00	0.00	0.00000	0.00	0.00	0.00		0.00
2006/02/24 12:00	498.83	208.81	13.61	0.00	0.00	0.00000	0.00	0.00	0.00		0.00
2006/03/03 12:00	666.83	212.52	3.71	0.00	0.00	0.00000	0.00	0.00	0.00		0.00
						Sigma (Ei)	1.00				1340.01
								Tau	22.2083		
								Sigma^2	155.7020		
								N	3.1677		
								Sigma Theta^2	0.3157		
								Disp	0.1961		
								Sigma Theta^2	0.3157		
								N	3.1677		
								Pe	5.10		

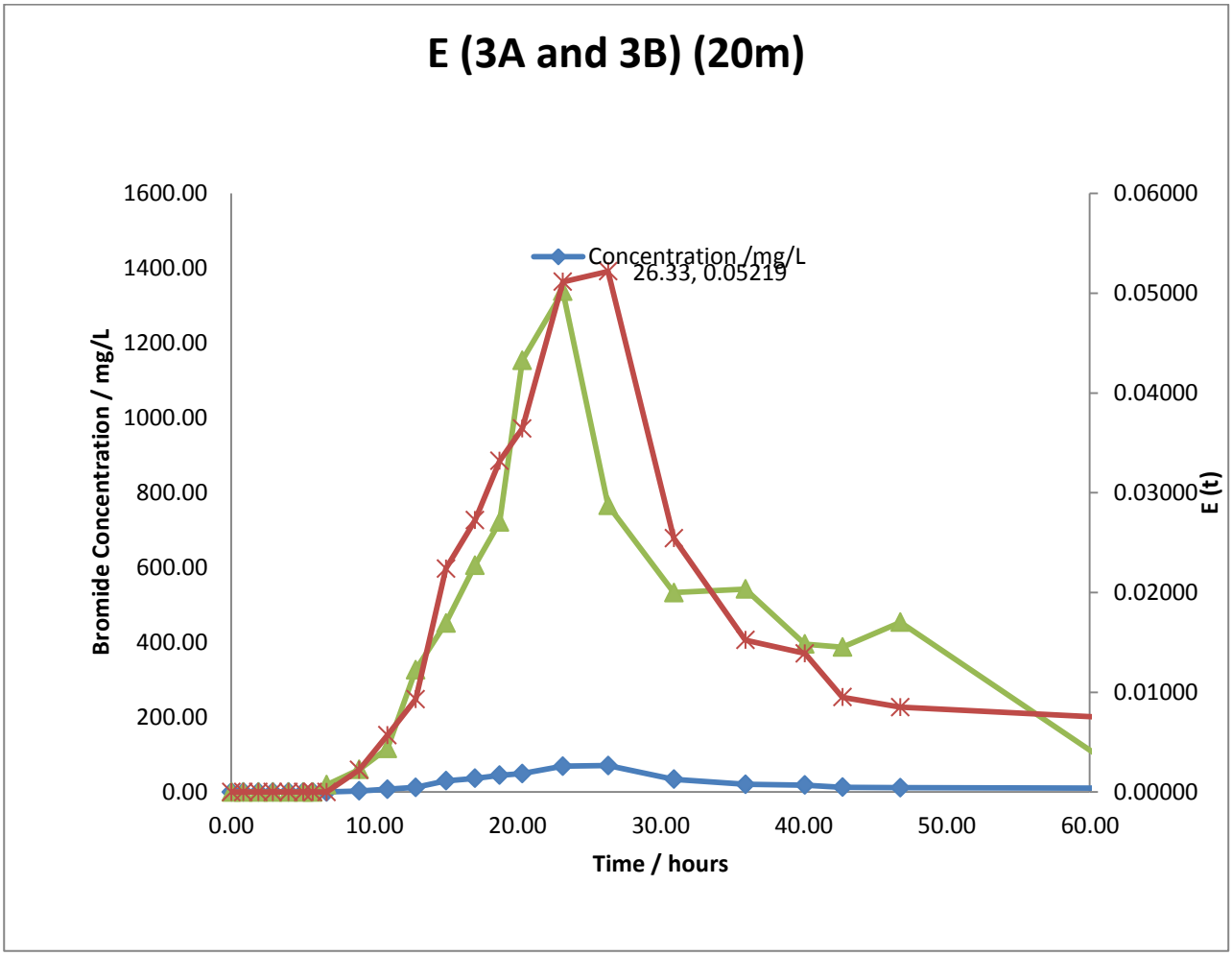
Appendix M. **RTD graphs for Sample Port 2**



Appendix N. **RTD for Sample Port 3a/b**

Date and Time	Time / hours	Meter Reading	Flow / m^3	Concentration /mg/L	Q (sigC.Dt)	E(C/Q)	Integral of E	ti.ei.dt	ti^2.Ei.dt		
				3a/b	1352.38	0.00000				Min	Mout
2006/02/03 17:10	0.00	125.37									
2006/02/03 18:00	0.83	125.86	0.49	0.00	0.00	0.00000	0.00	0.00	0.00	3357.00	0.00
2006/02/03 19:04	1.90	126.41	0.55	0.00	0.00	0.00000	0.00	0.00	0.00		0.00
2006/02/03 20:04	2.90	126.89	0.48	0.00	0.00	0.00000	0.00	0.00	0.00		0.00
2006/02/03 21:10	4.00	128.44	1.55	0.00	0.00	0.00000	0.00	0.00	0.00		0.00
2006/02/03 22:12	5.03	129.46	1.02	0.00	0.00	0.00000	0.00	0.00	0.00		0.00
2006/02/03 22:52	5.70	129.96	0.50	0.00	0.00	0.00000	0.00	0.00	0.00		0.00
2006/02/03 23:50	6.67	130.71	0.75	0.00	0.00	0.00000	0.00	0.00	0.00		0.00
2006/02/04 02:06	8.93	132.52	1.81	3.01	6.82	0.00223	0.01	0.05	0.40		5.45
2006/02/04 04:05	10.92	134.03	1.51	7.71	15.29	0.00570	0.01	0.12	1.35		11.64
2006/02/04 06:03	12.88	135.52	1.49	12.59	24.75	0.00931	0.02	0.24	3.04		18.75
2006/02/04 08:10	15.00	136.92	1.40	30.28	64.08	0.02239	0.05	0.71	10.66		42.38
2006/02/04 10:12	17.03	138.16	1.24	36.85	74.93	0.02725	0.06	0.94	16.07		45.69
2006/02/04 11:55	18.75	139.14	0.98	44.89	77.06	0.03319	0.06	1.07	20.03		43.99
2006/02/04 13:30	20.33	140.26	1.12	49.28	78.03	0.03644	0.06	1.17	23.85		55.19
2006/02/04 16:20	23.17	141.71	1.45	69.17	195.98	0.05115	0.14	3.36	77.78		100.30
2006/02/04 19:30	26.33	143.18	1.47	70.59	223.52	0.05219	0.17	4.35	114.61		103.76
2006/02/05 00:06	30.93	148.24	5.06	34.41	158.29	0.02544	0.12	3.62	111.99		174.11
2006/02/05 05:06	35.93	150.53	2.29	20.61	103.03	0.01524	0.08	2.74	98.36		47.19
2006/02/05 09:15	40.08	151.00	0.47	18.80	78.00	0.01390	0.06	2.31	92.67		8.83
2006/02/05 11:53	42.72	154.95	3.95	12.87	33.88	0.00951	0.03	1.07	45.71		50.82
2006/02/05 15:56	46.77	156.21	1.26	11.50	46.58	0.00850	0.03	1.61	75.32		14.49
2006/02/06 09:30	64.33	159.24	3.03	9.80	172.15	0.00725	0.13	8.19	526.85		29.69
2006/02/17 13:35	332.42	195.20	35.96	0.00	0.00	0.00000	0.00	0.00	0.00		0.00
2006/02/24 12:00	498.83	208.81	13.61	0.00	0.00	0.00000	0.00	0.00	0.00		0.00
2006/03/03 12:00	666.83	212.52	3.71	0.00	0.00	0.00000	0.00	0.00	0.00		0.00
						Sigma (Ei)	1.00				752.30
								Tau	31.5497		
								Sigma^2	223.3209		
								N	4.4572		
								Sigma Theta^2	0.2244		
								Disp	0.1288		
								Sigma Theta^2	0.2244		
								N	4.4572		
								Pe	7.76		

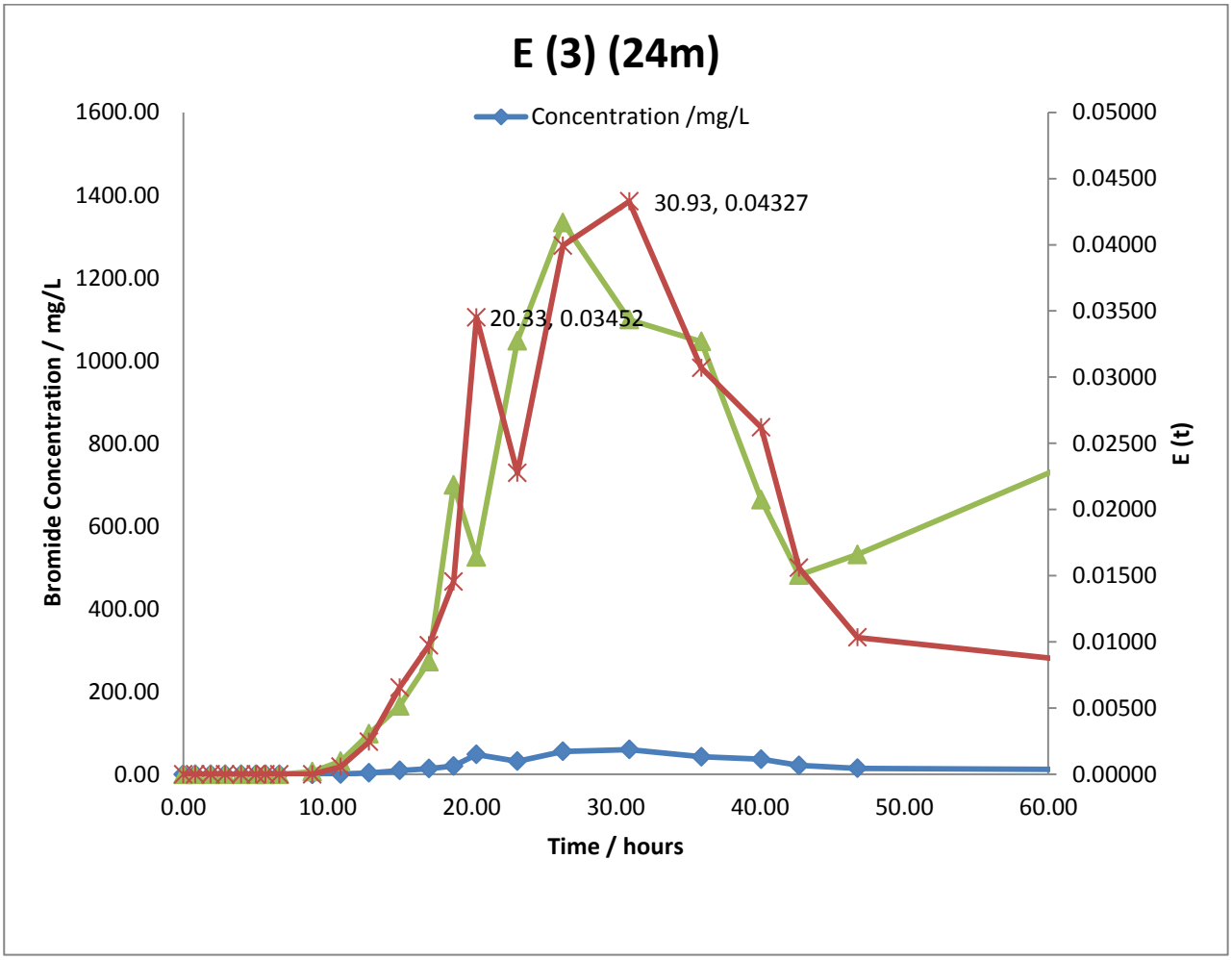
Appendix O. **RTD graphs for Sample Port 3a/b**



Appendix P. **RTD for Sample Port 3**

Date and Time	Time / hours	Meter Reading	Flow / m^3/mg/L		Q (sigC.Dt)	E(C/Q)	Integral of E	ti.ei.dt	ti^2.Ei.dt		
			Port 3		1383.79	0.00000				Min	Mout
2006/02/03 17:10	0.00	125.37									
2006/02/03 18:00	0.83	125.86	0.49	0.00	0.00	0.00000	0.00	0.00	0.00	3357.00	0.00
2006/02/03 19:04	1.90	126.41	0.55	0.00	0.00	0.00000	0.00	0.00	0.00		0.00
2006/02/03 20:04	2.90	126.89	0.48	0.00	0.00	0.00000	0.00	0.00	0.00		0.00
2006/02/03 21:10	4.00	128.44	1.55	0.00	0.00	0.00000	0.00	0.00	0.00		0.00
2006/02/03 22:12	5.03	129.46	1.02	0.00	0.00	0.00000	0.00	0.00	0.00		0.00
2006/02/03 22:52	5.70	129.96	0.50	0.00	0.00	0.00000	0.00	0.00	0.00		0.00
2006/02/03 23:50	6.67	130.71	0.75	0.00	0.00	0.00000	0.00	0.00	0.00		0.00
2006/02/04 02:06	8.93	132.52	1.81	0.00	0.00	0.00000	0.00	0.00	0.00		0.00
2006/02/04 04:05	10.92	134.03	1.51	0.79	1.57	0.00057	0.00	0.01	0.13		1.19
2006/02/04 06:03	12.88	135.52	1.49	3.39	6.67	0.00245	0.00	0.06	0.80		5.05
2006/02/04 08:10	15.00	136.92	1.40	9.05	19.16	0.00654	0.01	0.21	3.11		12.67
2006/02/04 10:12	17.03	138.16	1.24	13.47	27.39	0.00973	0.02	0.34	5.74		16.70
2006/02/04 11:55	18.75	139.14	0.98	20.15	34.59	0.01456	0.02	0.47	8.79		19.75
2006/02/04 13:30	20.33	140.26	1.12	47.77	75.64	0.03452	0.05	1.11	22.60		53.50
2006/02/04 16:20	23.17	141.71	1.45	31.50	89.25	0.02276	0.06	1.49	34.61		45.68
2006/02/04 19:30	26.33	143.18	1.47	55.27	175.02	0.03994	0.13	3.33	87.71		81.25
2006/02/05 00:06	30.93	148.24	5.06	59.88	275.45	0.04327	0.20	6.16	190.47		302.99
2006/02/05 05:06	35.93	150.53	2.29	42.48	212.40	0.03070	0.15	5.52	198.19		97.28
2006/02/05 09:15	40.08	151.00	0.47	36.25	150.44	0.02620	0.11	4.36	174.67		17.04
2006/02/05 11:53	42.72	154.95	3.95	21.58	56.83	0.01559	0.04	1.75	74.93		85.24
2006/02/05 15:56	46.77	156.21	1.26	14.30	57.92	0.01033	0.04	1.96	91.54		18.02
2006/02/06 09:30	64.33	159.24	3.03	11.47	201.49	0.00829	0.15	9.37	602.63		34.75
2006/02/17 13:35	332.42	195.20	35.96	0.00	0.00	0.00000	0.00	0.00	0.00		0.00
2006/02/24 12:00	498.83	208.81	13.61	0.00	0.00	0.00000	0.00	0.00	0.00		0.00
2006/03/03 12:00	666.83	212.52	3.71	0.00	0.00	0.00000	0.00	0.00	0.00		0.00
						Sigma (Ei)	1.00				791.11
								Tau	36.1334		
								Sigma^2	190.3061		
								N	6.8606		
								Sigma Theta^2	0.1458		
								Disp	0.0792		
								Sigma Theta^2	0.1459		
								N	6.8606		
								Pe	12.62		

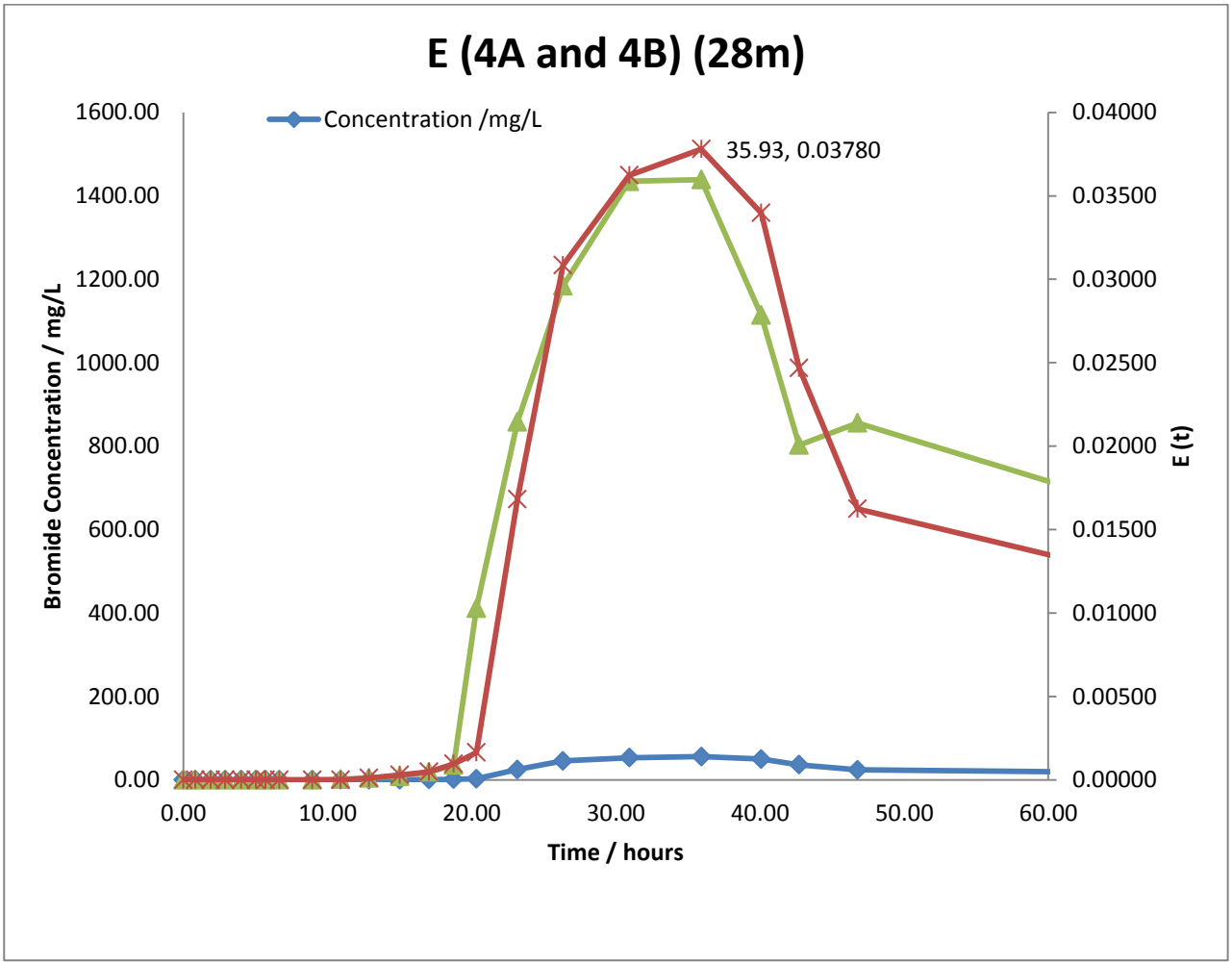
Appendix Q. **RTD graphs for Sample Port 3**



Appendix R. **RTD for Sample Port 4a/b**

Date and Time	Time / hours	Meter Reading	Flow / m^3	concentration /mg/L		Q (sigC.Dt)	E(C/Q)	Integral of E	ti.ei.dt	ti^2.Ei.dt		
				4a/b							Min	Mout
2006/02/03 17:10	0.00	125.37				1467.30	0.00000					0.00
2006/02/03 18:00	0.83	125.86	0.49	0.00		0.00	0.00000	0.00	0.00	0.00	3357.00	0.00
2006/02/03 19:04	1.90	126.41	0.55	0.00		0.00	0.00000	0.00	0.00	0.00		0.00
2006/02/03 20:04	2.90	126.89	0.48	0.00		0.00	0.00000	0.00	0.00	0.00		0.00
2006/02/03 21:10	4.00	128.44	1.55	0.00		0.00	0.00000	0.00	0.00	0.00		0.00
2006/02/03 22:12	5.03	129.46	1.02	0.00		0.00	0.00000	0.00	0.00	0.00		0.00
2006/02/03 22:52	5.70	129.96	0.50	0.00		0.00	0.00000	0.00	0.00	0.00		0.00
2006/02/03 23:50	6.67	130.71	0.75	0.00		0.00	0.00000	0.00	0.00	0.00		0.00
2006/02/04 02:06	8.93	132.52	1.81	0.00		0.00	0.00000	0.00	0.00	0.00		0.00
2006/02/04 04:05	10.92	134.03	1.51	0.00		0.00	0.00000	0.00	0.00	0.00		0.00
2006/02/04 06:03	12.88	135.52	1.49	0.16		0.30	0.00011	0.00	0.00	0.03		0.23
2006/02/04 08:10	15.00	136.92	1.40	0.43		0.90	0.00029	0.00	0.01	0.14		0.59
2006/02/04 10:12	17.03	138.16	1.24	0.70		1.41	0.00047	0.00	0.02	0.28		0.86
2006/02/04 11:55	18.75	139.14	0.98	1.41		2.42	0.00096	0.00	0.03	0.58		1.38
2006/02/04 13:30	20.33	140.26	1.12	2.41		3.82	0.00164	0.00	0.05	1.08		2.70
2006/02/04 16:20	23.17	141.71	1.45	24.67		69.90	0.01681	0.05	1.10	25.57		35.77
2006/02/04 19:30	26.33	143.18	1.47	45.26		143.31	0.03084	0.10	2.57	67.73		66.52
2006/02/05 00:06	30.93	148.24	5.06	53.17		244.58	0.03624	0.17	5.16	159.50		269.04
2006/02/05 05:06	35.93	150.53	2.29	55.46		277.30	0.03780	0.19	6.79	244.02		127.00
2006/02/05 09:15	40.08	151.00	0.47	49.86		206.90	0.03398	0.14	5.65	226.55		23.43
2006/02/05 11:53	42.72	154.95	3.95	36.22		95.38	0.02468	0.07	2.78	118.61		143.07
2006/02/05 15:56	46.77	156.21	1.26	23.84		96.53	0.01624	0.07	3.08	143.89		30.03
2006/02/06 09:30	64.33	159.24	3.03	18.48		324.54	0.01259	0.22	14.23	915.44		55.98
2006/02/17 13:35	332.42	195.20	35.96	0.00		0.00	0.00000	0.00	0.00	0.00		0.00
2006/02/24 12:00	498.83	208.81	13.61	0.00		0.00	0.00000	0.00	0.00	0.00		0.00
2006/03/03 12:00	666.83	212.52	3.71	0.00		0.00	0.00000	0.00	0.00	0.00		0.00
							Sigma (Ei)	1.00				756.62
									Tau	41.4699		
									Sigma^2	183.6624		
									N	9.3636		
									Sigma Theta^2	0.1068		
									Disp	0.0566		
									Sigma Theta^2	0.1069		
									N	9.3636		
									Pe	17.66		

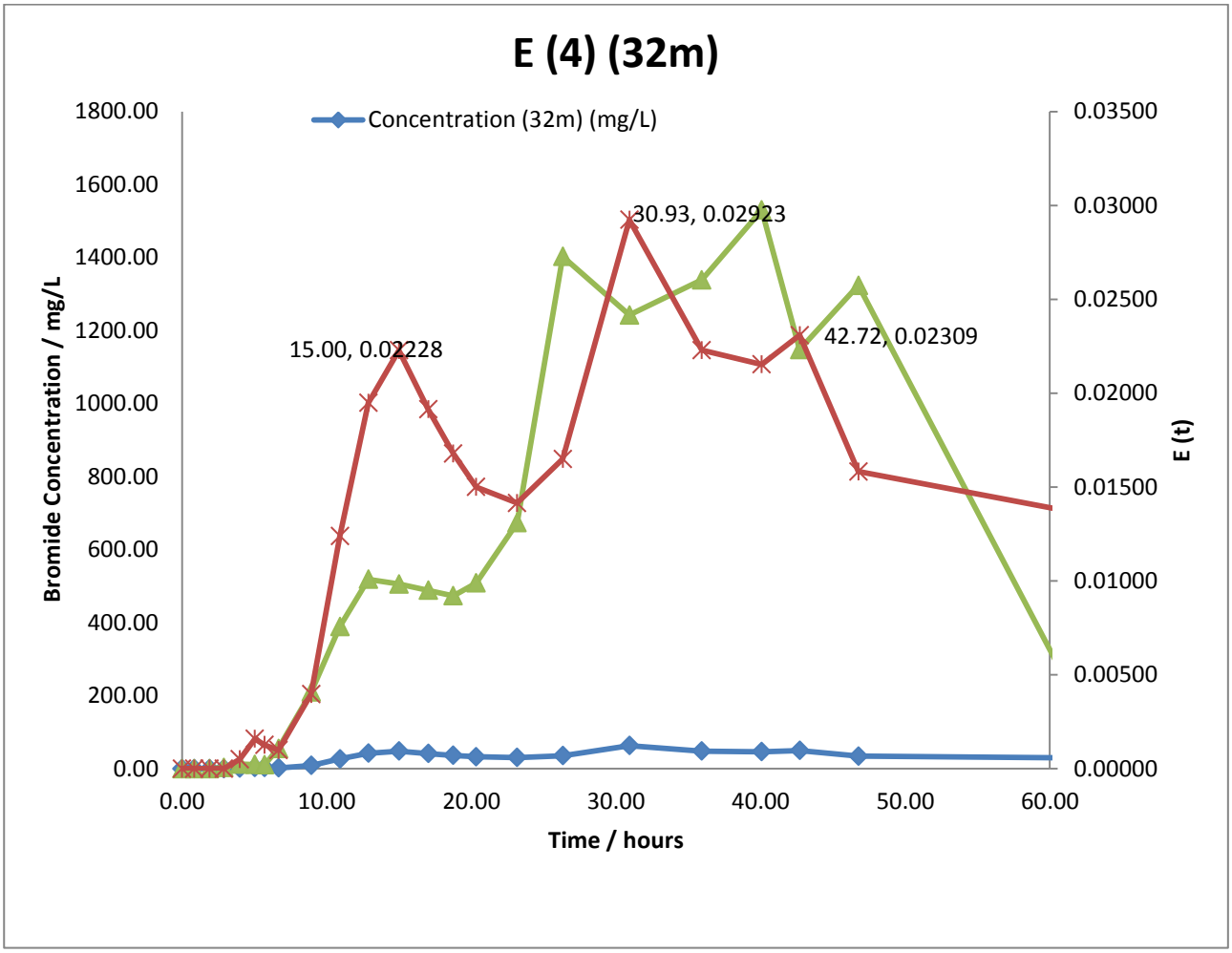
Appendix S. **RTD graphs for Sample Port 4a/b**



Appendix T. **RTD for Sample Port 4**

Date and Time	Time / hours	Meter Reading	Flow / m^3/ration (32m) (mg/L)	Q (sigC.Dt)	E(t) 32m	Integral of E	ti.ei.dt	ti^2.Ei.dt		
									Min	Mout
2006/02/03 17:10	0.00	125.37	0.00	2154.67	0.00000					
2006/02/03 18:00	0.83	125.86	0.49	0.00	0.00000	0.00	0.00	0.00	3357.00	0.00
2006/02/03 19:04	1.90	126.41	0.55	0.00	0.00000	0.00	0.00	0.00		0.00
2006/02/03 20:04	2.90	126.89	0.48	0.00	0.00000	0.00	0.00	0.00		0.00
2006/02/03 21:10	4.00	128.44	1.55	1.09	0.00051	0.00	0.00	0.01		1.69
2006/02/03 22:12	5.03	129.46	1.02	3.41	0.00158	0.00	0.01	0.04		3.48
2006/02/03 22:52	5.70	129.96	0.50	2.73	0.00127	0.00	0.00	0.03		1.37
2006/02/03 23:50	6.67	130.71	0.75	2.12	0.00098	0.00	0.01	0.04		1.59
2006/02/04 02:06	8.93	132.52	1.81	8.55	0.00397	0.01	0.08	0.72		15.48
2006/02/04 04:05	10.92	134.03	1.51	26.69	0.01239	0.02	0.27	2.93		40.30
2006/02/04 06:03	12.88	135.52	1.49	41.97	0.01948	0.04	0.49	6.36		62.54
2006/02/04 08:10	15.00	136.92	1.40	48.01	0.02228	0.05	0.71	10.61		67.21
2006/02/04 10:12	17.03	138.16	1.24	41.24	0.01914	0.04	0.66	11.29		51.14
2006/02/04 11:55	18.75	139.14	0.98	36.17	0.01679	0.03	0.54	10.13		35.45
2006/02/04 13:30	20.33	140.26	1.12	32.33	0.01500	0.02	0.48	9.82		36.21
2006/02/04 16:20	23.17	141.71	1.45	30.48	0.01415	0.04	0.93	21.51		44.20
2006/02/04 19:30	26.33	143.18	1.47	35.53	0.01649	0.05	1.38	36.21		52.23
2006/02/05 00:06	30.93	148.24	5.06	62.99	0.02923	0.13	4.16	128.68		318.73
2006/02/05 05:06	35.93	150.53	2.29	48.03	0.02229	0.11	4.00	143.91		109.99
2006/02/05 09:15	40.08	151.00	0.47	46.40	0.02153	0.09	3.58	143.59		21.81
2006/02/05 11:53	42.72	154.95	3.95	49.75	0.02309	0.06	2.60	110.95		196.51
2006/02/05 15:56	46.77	156.21	1.26	34.09	0.01582	0.06	3.00	140.14		42.95
2006/02/06 09:30	64.33	159.24	3.03	28.58	0.01326	0.23	14.99	964.37		86.60
2006/02/17 13:35	332.42	195.20	35.96	0.00	0.00000	0.00	0.00	0.00		0.00
2006/02/24 12:00	498.83	208.81	13.61	0.00	0.00000	0.00	0.00	0.00		0.00
2006/03/03 12:00	666.83	212.52	3.71	0.00	0.00000	0.00	0.00	0.00		0.00
					Sigma (Ei)	1.00				1189.46
						Tau	37.8921			
						Sigma^2	305.5223			
						N	4.6995			
						Sigma Theta^2	0.2128			
						Disp	0.1211			
						Sigma Theta^2	0.2128			
						N	4.6995			
						Pe	8.26			

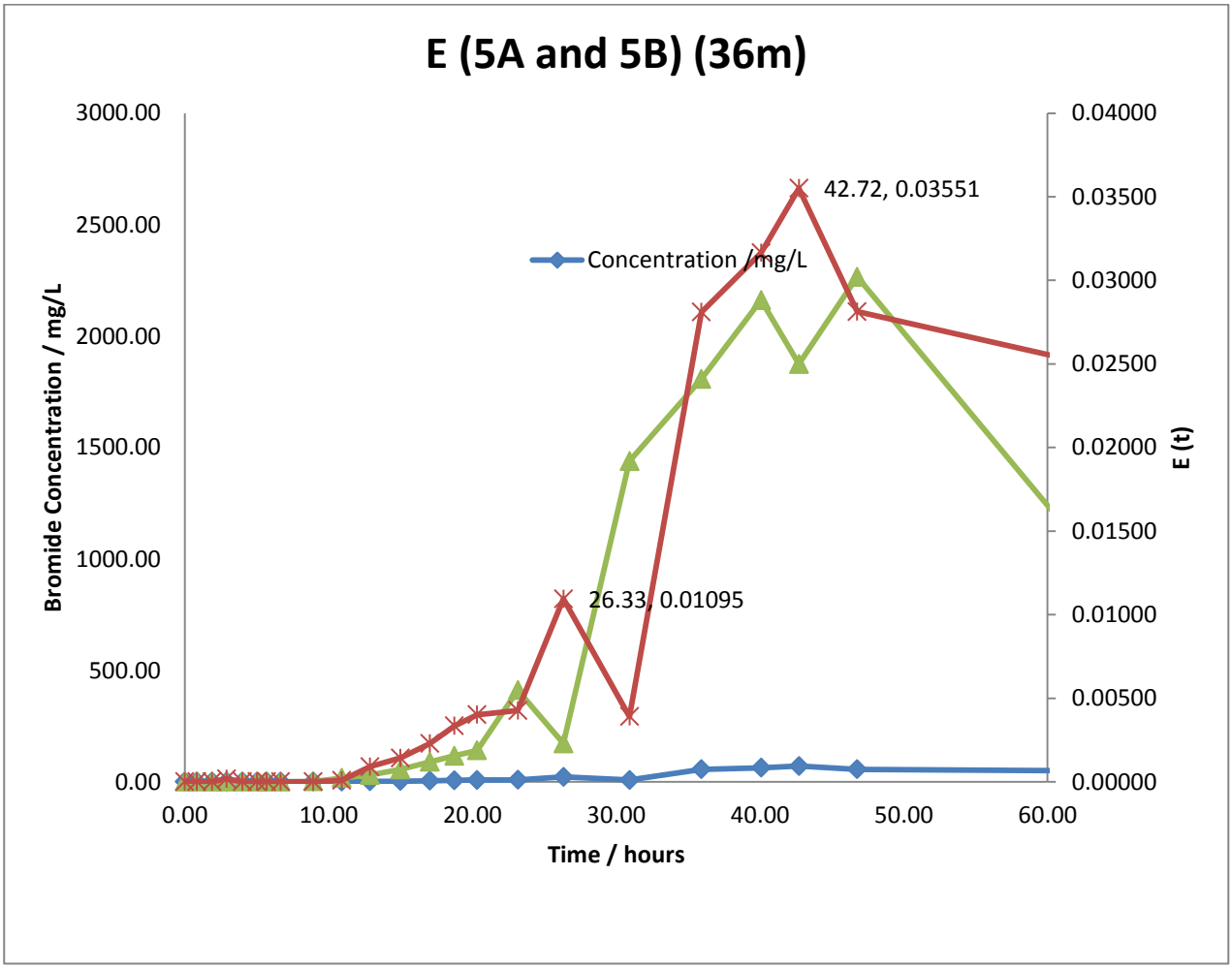
Appendix U. **RTD graphs for Sample Port 4**



Appendix V. **RTD for Sample Port 5a/b**

Date and Time	Time / hours	Meter Reading	Flow / m^3	Concentration /mg/L	Q (sigC.Dt)	E(C/Q)	Integral of E	ti.ei.dt	ti^2.Ei.dt		
									Min	Mout	
2006/02/03 17:10	0.00	125.37		0.00	1978.92	0.00000			0.00	3357.00	0.00
2006/02/03 18:00	0.83	125.86	0.49	0.00	0.00	0.00000	0.00	0.00	0.00		0.00
2006/02/03 19:04	1.90	126.41	0.55	0.00	0.00	0.00000	0.00	0.00	0.00		0.00
2006/02/03 20:04	2.90	126.89	0.48	0.36	0.35	0.00018	0.00	0.00	0.00		0.17
2006/02/03 21:10	4.00	128.44	1.55	0.00	0.00	0.00000	0.00	0.00	0.00		0.00
2006/02/03 22:12	5.03	129.46	1.02	0.00	0.00	0.00000	0.00	0.00	0.00		0.00
2006/02/03 22:52	5.70	129.96	0.50	0.00	0.00	0.00000	0.00	0.00	0.00		0.00
2006/02/03 23:50	6.67	130.71	0.75	0.00	0.00	0.00000	0.00	0.00	0.00		0.00
2006/02/04 02:06	8.93	132.52	1.81	0.00	0.00	0.00000	0.00	0.00	0.00		0.00
2006/02/04 04:05	10.92	134.03	1.51	0.18	0.35	0.00009	0.00	0.00	0.02		0.26
2006/02/04 06:03	12.88	135.52	1.49	1.79	3.52	0.00090	0.00	0.02	0.30		2.67
2006/02/04 08:10	15.00	136.92	1.40	2.82	5.98	0.00143	0.00	0.05	0.68		3.95
2006/02/04 10:12	17.03	138.16	1.24	4.52	9.19	0.00228	0.00	0.08	1.35		5.60
2006/02/04 11:55	18.75	139.14	0.98	6.62	11.36	0.00335	0.01	0.11	2.02		6.49
2006/02/04 13:30	20.33	140.26	1.12	7.95	12.58	0.00401	0.01	0.13	2.63		8.90
2006/02/04 16:20	23.17	141.71	1.45	8.44	23.90	0.00426	0.01	0.28	6.48		12.23
2006/02/04 19:30	26.33	143.18	1.47	21.67	68.61	0.01095	0.03	0.91	24.04		31.85
2006/02/05 00:06	30.93	148.24	5.06	7.73	35.53	0.00390	0.02	0.56	17.18		39.09
2006/02/05 05:06	35.93	150.53	2.29	55.62	278.08	0.02810	0.14	5.05	181.44		127.36
2006/02/05 09:15	40.08	151.00	0.47	62.63	259.91	0.03165	0.13	5.26	211.02		29.44
2006/02/05 11:53	42.72	154.95	3.95	70.27	185.03	0.03551	0.09	3.99	170.61		277.55
2006/02/05 15:56	46.77	156.21	1.26	55.66	225.42	0.02813	0.11	5.33	249.14		70.13
2006/02/06 09:30	64.33	159.24	3.03	48.91	859.10	0.02471	0.43	27.93	1796.75		148.18
2006/02/17 13:35	332.42	195.20	35.96	0.00	0.00	0.00000	0.00	0.00	0.00		0.00
2006/02/24 12:00	498.83	208.81	13.61	0.00	0.00	0.00000	0.00	0.00	0.00		0.00
2006/03/03 12:00	666.83	212.52	3.71	0.00	0.00	0.00000	0.00	0.00	0.00		0.00
						Sigma (Ei)	1.00				763.87
								Tau	49.6989		
								Sigma^2	193.6785		
								N	12.7530		
								Sigma Theta^2	0.0784		
								Disp	0.0407		
								Sigma Theta^2	0.0781		
								N	12.7530		
								Pe	24.56		

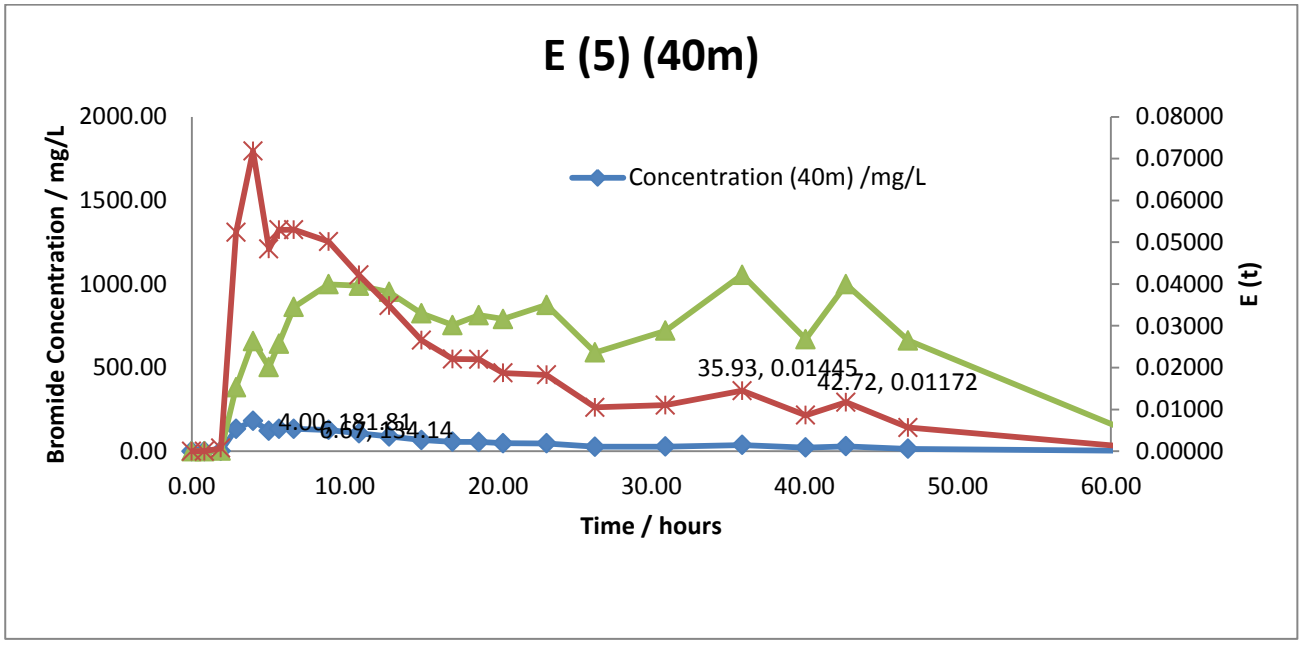
Appendix W. **RTD graphs for Sample Port 5a/b**



Appendix X. **RTD for Sample Port 5**

Date and Time	Time / hours		Meter Reading	Flow / m^3	Concentration (40m) /mg/L		Q (sigC.Dt)	E(t) (40m)	Integral of E	ti.ei.dt	ti^2.Ei.dt		
												Min	Mout
2006/02/03 17:10	0.00		125.37		0.00		2530.85	0.00000					
2006/02/03 18:00	0.83		125.86	0.60	0.00		0.000000	0.00000	0.00	0.00	0.00	3357.00	0.00
2006/02/03 19:04	1.90		126.41	0.77	1.78		1.898667	0.00070	0.00	0.00	0.00		0.00
2006/02/03 20:04	2.90		126.89	0.72	132.48		132.480000	0.05235	0.05	0.15	0.44		1.28
2006/02/03 21:10	4.00		128.44	0.79	181.81		199.991000	0.07184	0.08	0.32	1.26		104.92
2006/02/03 22:12	5.03		129.46	0.74	122.43		126.511000	0.04838	0.05	0.25	1.27		135.27
2006/02/03 22:52	5.70		129.96	0.48	133.98		89.320000	0.05294	0.04	0.20	1.15		58.77
2006/02/03 23:50	6.67		130.71	0.70	134.14		129.668667	0.05300	0.05	0.34	2.28		93.25
2006/02/04 02:06	8.93		132.52	1.63	126.98		287.821333	0.05017	0.11	1.02	9.08		218.92
2006/02/04 04:05	10.92		134.03	1.43	106.69		211.601833	0.04216	0.08	0.91	9.96		181.33
2006/02/04 06:03	12.88		135.52	1.42	88.18		173.420667	0.03484	0.07	0.88	11.37		151.07
2006/02/04 08:10	15.00		136.92	1.52	67.16		142.155333	0.02654	0.06	0.84	12.64		134.39
2006/02/04 10:12	17.03		138.16	1.46	55.84		113.541333	0.02206	0.04	0.76	13.02		98.32
2006/02/04 11:55	18.75		139.14	1.24	55.58		95.412333	0.02196	0.04	0.71	13.25		69.02
2006/02/04 13:30	20.33		140.26	1.14	47.41		75.065833	0.01873	0.03	0.60	12.26		63.36
2006/02/04 16:20	23.17		141.71	2.04	46.16		130.786667	0.01824	0.05	1.20	27.73		96.72
2006/02/04 19:30	26.33		143.18	2.28	26.50		83.916667	0.01047	0.03	0.87	22.99		105.24
2006/02/05 00:06	30.93		148.24	3.31	27.86		128.156000	0.01101	0.05	1.57	48.45		87.77
2006/02/05 05:06	35.93		150.53	3.60	36.56		182.800000	0.01445	0.07	2.60	93.26		100.30
2006/02/05 09:15	40.08		151.00	2.99	21.77		90.345500	0.00860	0.04	1.43	57.35		109.24
2006/02/05 11:53	42.72		154.95	1.90	29.65		78.078333	0.01172	0.03	1.32	56.29		41.28
2006/02/05 15:56	46.77		156.21	2.92	14.29		57.874500	0.00565	0.02	1.07	50.01		86.46
2006/02/06 09:30	64.33		159.24	12.65	0.00		0.000000	0.00000	0.00	0.00	0.00		180.74
2006/02/17 13:35	332.42		195.20	193.02	0.00		0.000000	0.00000	0.00	0.00	0.00		0.00
2006/02/24 12:00	498.83		208.81	119.82	0.00		0.000000	0.00000	0.00	0.00	0.00		0.00
2006/03/03 12:00	666.83		212.52	120.96			0.000000	0.00000	0.00	0.00	0.00		0.00
		Flow		33.67									
		Ave Flow						Sigma (Ei)	1.00				2117.64
										Tau	17.0421		
									Sigma^2		153.6541		
										N	1.8902		
										Sigma Theta^2	0.5291		
										Disp	0.4343		
										Sigma Theta^2	0.5291		
										N	1.8902		
										Pe	2.30		

Appendix Y. **RTD graphs for Sample Port 5**



Date:	26-May-11		Inlet:	Centre Centre			
			Outlet:	Centre Centre			

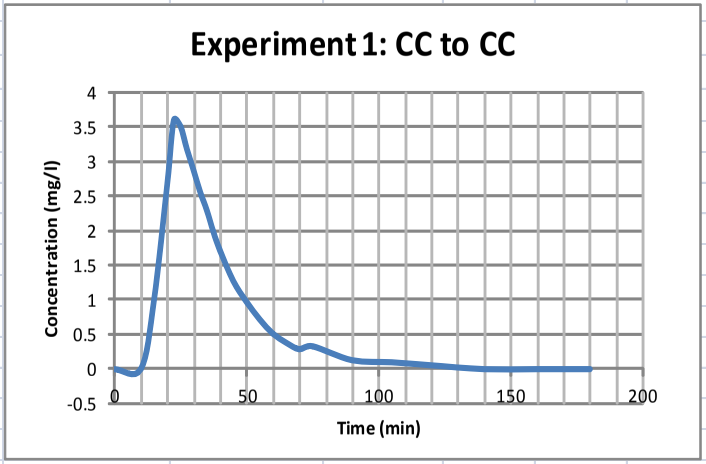
Container	Time (min)	ABS	Concentration (mg/l)	Qi	Ei	ti.Ei.Δt	ti².Ei.Δt
0	0	0	0	0	0	0	0
1	10	0.0477	0	0.000	0.000	0.000	0.000
2	15	0.0784	0.9965	0.083	0.604	0.013	0.003
3	20	0.1259	2.6676	0.222	1.616	0.045	0.015
3.5	22.5	0.1521	3.5911	0.150	2.175	0.034	0.013
4	25	0.1497	3.5052	0.146	2.123	0.037	0.015
4.5	27.5	0.14	3.1659	0.132	1.918	0.037	0.017
5	30	0.1315	2.8652	0.119	1.735	0.036	0.018
5.5	32.5	0.1226	2.5516	0.106	1.545	0.035	0.019
6	35	0.1151	2.2895	0.095	1.387	0.034	0.020
6.5	37.5	0.1062	1.9759	0.082	1.197	0.031	0.019
7	40	0.0986	1.7096	0.071	1.035	0.029	0.019
8	45	0.0862	1.2715	0.106	0.770	0.048	0.036
9	50	0.0776	0.9708	0.081	0.588	0.041	0.034
10	55	0.0704	0.7173	0.060	0.434	0.033	0.030
11	60	0.0646	0.5111	0.043	0.310	0.026	0.026
12	65	0.0609	0.3822	0.032	0.231	0.021	0.023
13	70	0.0582	0.2877	0.024	0.174	0.017	0.020
14	75	0.0594	0.3307	0.028	0.200	0.021	0.026
15	90	0.0537	0.1288	0.032	0.078	0.029	0.044
16	105	0.0529	0.0987	0.025	0.060	0.026	0.046
17	120	0.0516	0.0558	0.014	0.034	0.017	0.034
18	140	0.0477	0	0.000	0.000	0.000	0.000
19	160	0.0466	0	0.000	0.000	0.000	0.000
20	180	0.0466	0	0.000	0.000	0.000	0.000

ΣQi	1.651
τm (hr)	0.609
τ(ideal)	1.200
Veff	0.507
σ^2	0.106
$\sigma\theta^2$	0.287
$\sigma\theta^2=2D-2D^2*(1-e^{(-1/D)})$	
D	0.174
λ	0.362
N	3.486
N(check)	3.486

solving iteratively

Gulp Concentration (mg/l)	Gulp Volume (l)	Tank Volume (l)
1000	0.02	25

Tracer Concentration in Tank (mg/l)
0.8



Date:	26-May-11		**Inlet:**	Centre Bottom			
			Outlet:	Centre Top			

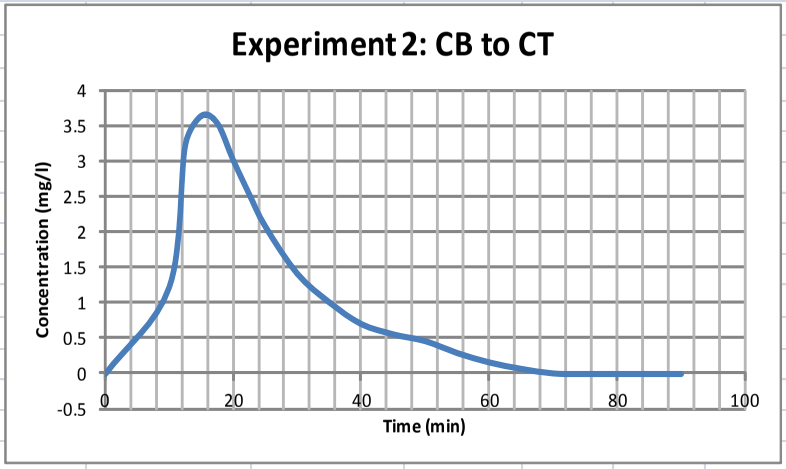
Container	Time (min)	ABS	Concentration (mg/l)	Qi	Ei	ti.Ei.Δt	$ti^2.Ei.\Delta t$
0	0	0	0	0	0	0	0
1	10	0.0848	1.2242	0.204	0.910	0.025	0.004
1.5	12.5	0.1416	3.2217	0.134	2.395	0.021	0.004
2	15	0.1533	3.6341	0.151	2.702	0.028	0.007
2.5	17.5	0.1504	3.531	0.147	2.625	0.032	0.009
3	20	0.1355	3.0069	0.125	2.236	0.031	0.010
3.5	22.5	0.1219	2.5301	0.105	1.881	0.029	0.011
4	25	0.1091	2.079	0.087	1.546	0.027	0.011
5	30	0.0902	1.4132	0.118	1.051	0.044	0.022
6	35	0.0787	1.0094	0.084	0.750	0.036	0.021
7	40	0.0701	0.7044	0.059	0.524	0.029	0.019
8	45	0.0659	0.5584	0.047	0.415	0.026	0.019
9	50	0.0632	0.4639	0.039	0.345	0.024	0.020
10	55	0.0585	0.2963	0.025	0.220	0.017	0.015
11	60	0.0547	0.1632	0.014	0.121	0.010	0.010
12	65	0.0521	0.073	0.006	0.054	0.005	0.005
13	70	0.0503	0.0085	0.001	0.006	0.001	0.001
14	75	0.05	0	0.000	0.000	0.000	0.000
15	90	0.0488	0	0.000	0.000	0.000	0.000

ΣQi	1.345
τm (hr)	0.385
τ(ideal)	1.200
Veff	0.321
σ^2	0.043
$\sigma\theta^2$	0.288
$\sigma\theta^2=2D-2D^2*(1-e^{(-1/D)})$	
D	0.174
λ	0.229
N	3.475
N(check)	3.475

solving iteratively

Gulp Concentration (mg/l)	Gulp Volume (l)	Tank Volume (l)
1000	0.02	25

Tracer Concentration in Tank (mg/l)
0.8



Date:	11-Jul-11		**Inlet:**	Centre Top					
			Outlet:	Centre Top					

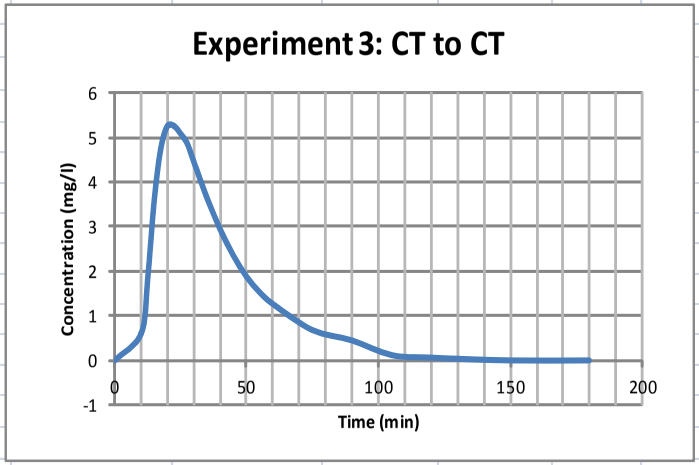
Container	Time (min)	ABS	Concentration (mg/l)	Qi	Ei	ti.Ei.Δt	ti².Ei.Δt
0	0	0	0	0	0	0	0
1	10	0.0669	0.5927	0.099	0.196	0.005	0.001
2	12.5	0.1013	1.8041	0.075	0.596	0.005	0.001
3	15	0.1522	3.5954	0.150	1.188	0.012	0.003
4	17.5	0.1852	4.7553	0.198	1.571	0.019	0.006
5	20	0.1996	5.2622	0.219	1.739	0.024	0.008
6	22.5	0.1997	5.2665	0.219	1.740	0.027	0.010
7	25	0.1947	5.0903	0.212	1.682	0.029	0.012
8	27.5	0.1885	4.8713	0.203	1.610	0.031	0.014
9	30	0.1769	4.4632	0.186	1.475	0.031	0.015
10	35	0.1538	3.6513	0.304	1.206	0.059	0.034
11	40	0.1338	2.9468	0.246	0.974	0.054	0.036
12	45	0.1171	2.3583	0.197	0.779	0.049	0.037
13	50	0.1035	1.8814	0.157	0.622	0.043	0.036
14	55	0.0935	1.5292	0.127	0.505	0.039	0.035
15	60	0.0861	1.2672	0.106	0.419	0.035	0.035
16	75	0.0695	0.6829	0.171	0.226	0.071	0.088
17	90	0.0629	0.451	0.113	0.149	0.056	0.084
18	105	0.0535	0.1202	0.030	0.040	0.017	0.030
19	120	0.0518	0.0601	0.015	0.020	0.010	0.020
20	150	0.0482	0	0.000	0.000	0.000	0.000
21	180	0.0463	0	0.000	0.000	0.000	0.000

ΣQi	3.026
τm (hr)	0.616
τ(ideal)	1.233
Veff	0.500
σ²	0.126
σθ²	0.333
σθ²=2D-2D²*(1-e^(-1/D))	
D	0.2104
λ	0.333
N	3.000
N(check)	3.000

solving iteratively

Gulp Concentration (mg/l)	Gulp Volume (l)	Tank Volume (l)	Flow Rate (m³/hr
1000	0.02	18.75	0.0073

Tracer Concentration in Tank (mg/l)
1.066666667



Date:	12-Jul-11	**Inlet:**	Centre Bottom		
		Outlet:	All Top		

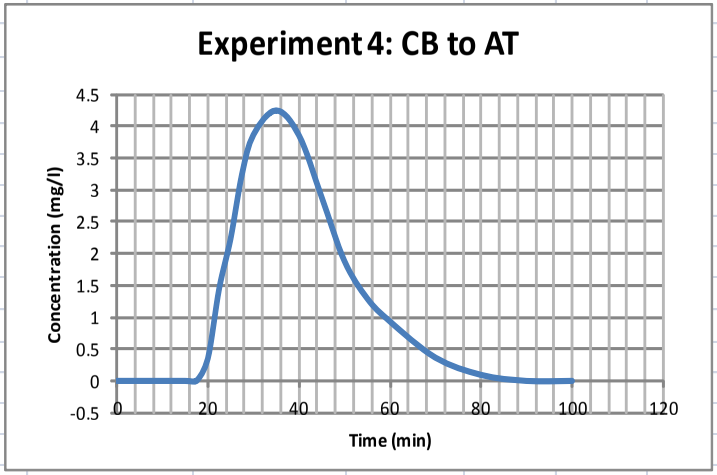
Container	Time (min)	ABS	Concentration (mg/l)	Qi	Ei	ti.Ei.Δt	$ti^2.Ei.\Delta t$
0	0	0	0	0	0	0	0
1	15	0.047	0	0.000	0.000	0.000	0.000
2	17.5	0.0471	0	0.000	0.000	0.000	0.000
3	20	0.0599	0.3479	0.014	0.194	0.003	0.001
4	22.5	0.0913	1.4519	0.060	0.808	0.013	0.005
5	25	0.1133	2.2252	0.093	1.238	0.022	0.009
6	27.5	0.1421	3.2389	0.135	1.803	0.034	0.016
7	30	0.1597	3.8575	0.161	2.147	0.045	0.022
8	35	0.1705	4.2398	0.353	2.360	0.115	0.067
9	40	0.1595	3.8532	0.321	2.144	0.119	0.079
10	45	0.132	2.8823	0.240	1.604	0.100	0.075
11	50	0.1035	1.8814	0.157	1.047	0.073	0.061
12	55	0.0868	1.2929	0.108	0.720	0.055	0.050
13	60	0.0765	0.9321	0.078	0.519	0.043	0.043
14	70	0.0604	0.3651	0.061	0.203	0.040	0.046
15	80	0.0527	0.0944	0.016	0.053	0.012	0.016
16	90	0.0463	0	0.000	0.000	0.000	0.000
17	100	0.0468	0	0.000	0.000	0.000	0.000

ΣQi	1.797
τm (hr)	0.672
τ(ideal)	1.200
Veff	0.560
σ^2	0.038
$\sigma\theta^2$	0.085
$\sigma\theta^2=2D-2D^2*(1-e^{(-1/D)})$	
D	0.045
λ	0.513
N	11.788
N(check)	11.788

solving iteratively

Gulp Concentration (mg/l)	Gulp Volume (l)	Tank Volume (l)
1000	0.02	25

Tracer Concentration in Tank (mg/l)
0.8



Date:	13-Jul-11	**Inlet:**	Left Bottom	
		Outlet:	Right Top	

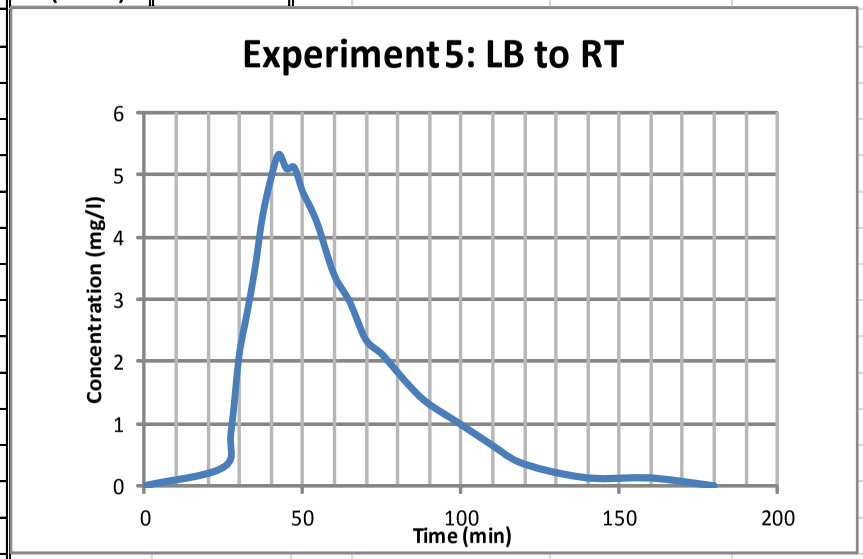
Container	Time (min)	ABS	Concentration (mg/l)	Qi	Ei	ti.Ei.Δt	ti².Ei.Δt
0	0	0	0	0	0	0	0
1	25	0.0585	0.2963	0.123	0.078	0.013	0.006
2	27.5	0.0748	0.872	0.036	0.228	0.004	0.002
3	30	0.1094	2.0876	0.087	0.546	0.011	0.006
4	32.5	0.1288	2.7707	0.115	0.725	0.016	0.009
5	35	0.1493	3.4923	0.146	0.914	0.022	0.013
6	37.5	0.1741	4.3644	0.182	1.142	0.030	0.019
7	40	0.1904	4.94	0.206	1.293	0.036	0.024
8	42.5	0.2019	5.3438	0.223	1.399	0.041	0.029
9	45	0.1954	5.1161	0.213	1.339	0.042	0.031
10	47.5	0.1958	5.129	0.214	1.343	0.044	0.035
11	50	0.1852	4.7553	0.198	1.245	0.043	0.036
12	52.5	0.1777	4.4932	0.187	1.176	0.043	0.038
13	55	0.1692	4.1925	0.175	1.097	0.042	0.038
14	60	0.1469	3.4064	0.284	0.892	0.074	0.074
15	65	0.1343	2.964	0.247	0.776	0.070	0.076
16	70	0.1171	2.3583	0.197	0.617	0.060	0.070
17	75	0.1106	2.1306	0.178	0.558	0.058	0.073
18	80	0.1022	1.8342	0.153	0.480	0.053	0.071
19	85	0.094	1.5464	0.129	0.405	0.048	0.068
20	90	0.0875	1.3187	0.110	0.345	0.043	0.065
21	100	0.0782	0.9922	0.165	0.260	0.072	0.120
22	110	0.0686	0.6529	0.109	0.171	0.052	0.096
23	120	0.0601	0.3522	0.059	0.092	0.031	0.061
24	140	0.0537	0.1288	0.043	0.034	0.026	0.061
25	160	0.0537	0.1288	0.043	0.034	0.030	0.080
26	180	0.0494	0	0.000	0.000	0.000	0.000

ΣQi	3.820
τm (hr)	1.007
τ(ideal)	1.600
Veff	0.629
σ^2	0.186
$\sigma\theta^2$	0.184
$\sigma\theta^2=2D-2D^2*(1-e^{(-1/D)})$	
D	0.103
λ	0.514
N	5.442
N(check)	5.442

solving iteratively

Gulp Concentration (mg/l)	Gulp Volume (l)	Tank Volume (l)
1000	0.02	25

Tracer Concentration in Tank (mg/l)
0.8



Date:	15-Jul-11		**Inlet:**	Centre Bottom	
			Outlet:	All Top + Wedge	

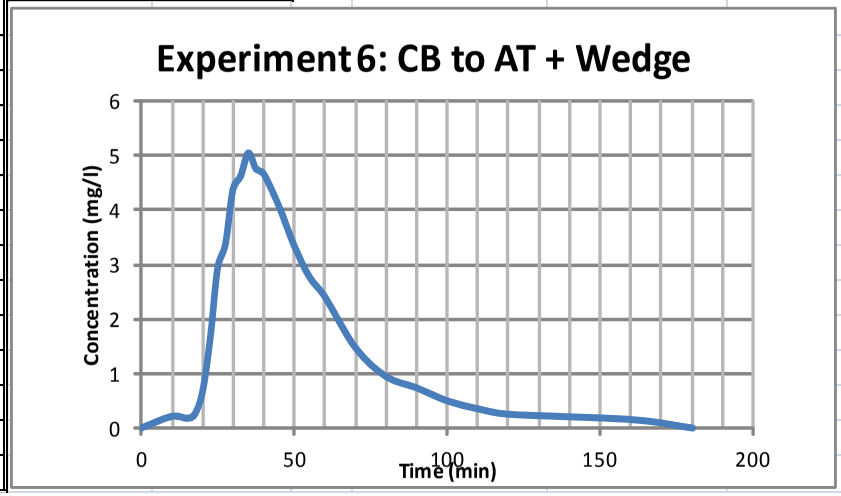
Container	Time (min)	ABS	Concentration (mg/l)	Qi	Ei	ti.Ei.Δt	ti².Ei.Δt
0	0	0	0	0	0	0	0
1	10	0.0562	0.2147	0.036	0.066	0.002	0.000
2	15	0.0552	0.1803	0.015	0.055	0.001	0.000
3	17.5	0.0571	0.2491	0.010	0.076	0.001	0.000
4	20	0.0686	0.6529	0.027	0.200	0.003	0.001
5	22.5	0.0956	1.6022	0.067	0.492	0.008	0.003
6	25	0.1335	2.9382	0.122	0.901	0.016	0.007
7	27.5	0.1456	3.3635	0.140	1.032	0.020	0.009
8	30	0.1747	4.3858	0.183	1.345	0.028	0.014
9	32.5	0.1814	4.6221	0.193	1.418	0.032	0.017
10	35	0.1936	5.0517	0.210	1.550	0.038	0.022
11	37.5	0.1852	4.7553	0.198	1.459	0.038	0.024
12	40	0.1827	4.6694	0.195	1.432	0.040	0.027
13	45	0.1659	4.0765	0.340	1.251	0.078	0.059
14	50	0.1451	3.3463	0.279	1.027	0.071	0.059
15	55	0.1288	2.7707	0.231	0.850	0.065	0.060
16	60	0.1185	2.4098	0.201	0.739	0.062	0.062
17	70	0.0919	1.4733	0.246	0.452	0.088	0.103
18	80	0.0769	0.945	0.158	0.290	0.064	0.086
19	90	0.071	0.7388	0.123	0.227	0.057	0.085
20	100	0.0642	0.4982	0.083	0.153	0.042	0.071
21	110	0.0601	0.3522	0.059	0.108	0.033	0.061
22	120	0.0573	0.2534	0.042	0.078	0.026	0.052
23	160	0.0544	0.1546	0.103	0.047	0.084	0.225
24	180	0.0466	0	0.000	0.000	0.000	0.000

ΣQi	3.260
τm (hr)	0.896
τ(ideal)	1.123
Veff	0.798
σ^2	0.242
$\sigma\theta^2$	0.301
$\sigma\theta^2=2D-2D^2*(1-e^{(-1/D)})$	
D	0.184
λ	0.557
N	3.319
N(check)	3.319

solving iteratively

Gulp Concentration (mg/l)	Gulp Volume (l)	Tank Volume (l)
1000	0.02	23.4

Tracer Concentration in Tank (mg/l)
0.854700855



Appendix FF. **CW Characterisation February 5 2005**

Sample	Concentrations	ml/l					Calc TOC	Sample	AA Work / mg/L			COD	TOC	COD Calc
	Ethanol	Propanol	Dioxane	Acetic Acid	Propanoic Acid	Butyric Acid	g/L		pH	Na	K	mg/L	mg/L	mg/L
0	0.25	0.01	1.98	0.04	0.02	0.03	0.17	0	4.36	31.71	75.9	1295.00		635.8266551
1a	0.00	0.00	1.98	0.00	0.00	0.00	0.00	1a	6.78	50.10	47.69			0
1b	0.00	0.00	1.98	0.00	0.00	0.00	0.00	1b	6.85	47.71	47.45			0
1	0.00	0.00	1.98	0.00	0.00	0.00	0.00	1	6.78	45.58	49.99	125.00		0
2a	0.00	0.00	1.98	0.00	0.00	0.00	0.00	2a	7.00	39.27	32.85			0
2b	0.00	0.00	1.98	0.00	0.00	0.00	0.00	2b	6.94	40.29	40.45			0
2	0.00	0.00	1.98	0.00	0.00	0.00	0.00	2	7.04	38.30	31.76	15.00		0
3a	0.00	0.00	1.98	0.00	0.00	0.00	0.00	3a	7.13	34.17	34.56			0
3b	0.00	0.00	1.98	0.00	0.00	0.00	0.00	3b	6.89	34.97	35.10			0
3	0.00	0.00	1.98	0.00	0.00	0.00	0.00	3	6.92	32.72	36.53	40.00		0
4a	0.00	0.00	1.98	0.00	0.00	0.00	0.00	4a	7.08	34.96	43.88			0
4b	0.00	0.00	1.98	0.00	0.00	0.00	0.00	4b	7.24	34.64	43.41			0
4	0.00	0.00	1.98	0.00	0.00	0.00	0.00	4	7.12	40.94	45.84	35.00		0
5a	0.00	0.00	1.98	0.00	0.00	0.00	0.00	5a	7.80	53.74	36.29			0
5b	0.00	0.00	1.98	0.00	0.00	0.00	0.00	5b	7.56	50.32	40.18			0
5	0.00	0.00	1.98	0.00	0.00	0.00	0.00	5	7.42	51.14	37.30	35.00		0

Appendix GG. **CW Characterisation February 7 2005**

Sample	Concentrations	ml/l					Calc TOC	Sample		AA Work / mg/L		COD	TOC	COD Calc
	Ethanol	Propanol	Dioxane	Acetic Acid	Propanoic Acid	Butyric Acid	g/L		pH	Na	K	mg/L	mg/L	mg/L
0	0.32	0.00	1.98	0.12	0.04	0.00	0.22	0	4.39	17.03	38.70	570.00		810.8088
1a	0.02	0.00	1.98	0.06	0.04	0.00	0.06	1a	6.65	31.71	45.90			172.8127
1b	0.10	0.00	1.98	0.00	0.00	0.00	0.05	1b	6.66	33.92	47.90			192.6484
1	0.10	0.00	1.98	0.00	0.00	0.00	0.05	1	6.52	24.68	58.10	500.00		184.2042
2a	0.00	0.00	1.98	0.00	0.00	0.00	0.00	2a	6.96	25.13	22.40			0
2b	0.00	0.00	1.98	0.00	0.00	0.00	0.00	2b	6.59	24.14	36.90			0
2	0.00	0.00	1.98	0.00	0.00	0.00	0.00	2	7.13	47.19	35.70	25.00		0
3a	0.00	0.00	1.98	0.00	0.00	0.00	0.00	3a	7.14	38.77	32.90			0
3b	0.00	0.00	1.98	0.00	0.00	0.00	0.00	3b	7.14	29.16	23.50			0
3	0.00	0.00	1.98	0.00	0.00	0.00	0.00	3	7.04	41.56	34.60	0.00		0
4a	0.00	0.00	1.98	0.00	0.00	0.00	0.00	4a	7.05	25.47	27.00			0
4b	0.00	0.00	1.98	0.00	0.00	0.00	0.00	4b	7.10	28.63	29.20			0
4	0.00	0.00	1.98	0.00	0.00	0.00	0.00	4	7.29	32.33	34.80	70.00		0
5a	0.00	0.00	1.98	0.00	0.00	0.00	0.00	5a	7.48	36.31	31.50			0
5b	0.00	0.00	1.98	0.00	0.00	0.00	0.00	5b	7.81	31.90	30.50			0
5	0.00	0.00	1.98	0.00	0.00	0.00	0.00	5	5.54	41.86	34.10	35.00		0

Appendix HH. **CW Characterisation February 8 2005**

Sample	Concentrations	ml/l						Calc TOC	Sample	AA Work / mg/L			COD	TOC	COD Calc
	Ethanol	Propanol	Dioxane	Acetic Acid	Propanoic Acid	Butyric Acid	g/L		pH	Na	K		mg/L	mg/L	mg/L
0	0.41	0.00	1.98	0.00	0.00	0.00	0.20	0	4.31	10.03	46.59	1230.00		779.3959054
1a	0.02	0.02	1.98	0.00	0.00	0.00	0.02	1a	6.60	19.03	58.51			78.63847185
1b	0.12	0.02	1.98	0.00	0.00	0.00	0.07	1b	6.53	11.72	35.45			267.6518546
1	0.00	0.00	1.98	0.00	0.00	0.00	0.00	1	6.38	12.22	34.43	645.00			0
2a	0.00	0.00	1.98	0.00	0.00	0.00	0.00	2a	6.86	26.70	49.80				0
2b	0.00	0.00	1.98	0.00	0.00	0.00	0.00	2b	6.70	15.70	34.93				0
2	0.00	0.00	1.98	0.00	0.00	0.00	0.00	2	7.09	35.81	35.48	175.00			0
3a	0.00	0.00	1.98	0.00	0.00	0.00	0.00	3a	7.16	22.83	25.95				0
3b	0.00	0.00	1.98	0.00	0.00	0.00	0.00	3b	7.10	37.40	33.25				0
3	0.00	0.00	1.98	0.00	0.00	0.00	0.00	3	7.20	36.33	32.49	195.00			0
4a	0.00	0.00	1.98	0.00	0.00	0.00	0.00	4a	7.14	21.63	21.63				0
4b	0.00	0.00	1.98	0.00	0.00	0.00	0.00	4b	7.40	27.35	28.40				0
4	0.00	0.00	1.98	0.00	0.00	0.00	0.00	4	7.79	26.48	30.71	0.00			0
5a	0.00	0.00	1.98	0.00	0.00	0.00	0.00	5a	7.88	37.20	35.05				0
5b	0.00	0.00	1.98	0.00	0.00	0.00	0.00	5b	7.88	32.60	32.68				0
5	0.00	0.00	1.98	0.00	0.00	0.00	0.00	5	7.68	33.92	33.45	0.00			0

Appendix II. **CW Characterisation February 9 2005**

Sample	Concentrations	ml/l						Calc TOC	Sample		AA Work / mg/L			COD	TOC	COD Calc
	Ethanol	Propanol	Dioxane	Acetic Acid	Propanoic Acid	Butyric Acid		g/L		pH	Na	K		mg/L	mg/L	mg/L
0	0.34	0.00	1.98	0.36	0.00	0.00		0.31	0	4.37	10.30	37.31		1680.00		1044.701214
1a	0.00	0.00	1.98	0.00	0.00	0.00		0.00	1a	6.47	14.06	38.96				0
1b	0.00	0.00	1.98	0.00	0.00	0.00		0.00	1b	6.66	14.61	39.03				0
1	0.00	0.00	1.98	0.00	0.00	0.00		0.00	1	6.53	19.77	52.55		920.00		0
2a	0.00	0.00	1.98	0.00	0.00	0.00		0.00	2a	6.82	48.19	66.86				0
2b	0.00	0.00	1.98	0.00	0.00	0.00		0.00	2b	6.73	14.74	37.68				0
2	0.00	0.00	1.98	0.00	0.00	0.00		0.00	2	6.78	49.12	51.54		430.00		0
3a	0.00	0.00	1.98	0.00	0.00	0.00		0.00	3a	6.92	36.39	33.93				0
3b	0.00	0.00	1.98	0.00	0.00	0.00		0.00	3b	7.03	35.09	34.75				0
3	0.00	0.00	1.98	0.00	0.00	0.00		0.00	3	7.18	34.98	29.00		55.00		0
4a	0.00	0.00	1.98	0.00	0.00	0.00		0.00	4a	7.06	40.31	34.53				0
4b	0.00	0.00	1.98	0.00	0.00	0.00		0.00	4b	7.26	38.89	35.25				0
4	0.00	0.00	1.98	0.00	0.00	0.00		0.00	4	7.16	32.49	29.40		20.00		0
5a	0.00	0.00	1.98	0.00	0.00	0.00		0.00	5a	7.84	42.17	39.50				0
5b	0.00	0.00	1.98	0.00	0.00	0.00		0.00	5b	7.24	30.67	31.33				0
5	0.00	0.00	1.98	0.00	0.00	0.00		0.00	5	7.79	44.70	29.13		50.00		0

Appendix JJ. **CW Characterisation February 10 2005**

Sample	Concentrations	ml/l					Calc TOC	Sample	AA Work / mg/L			COD	TOC	COD Calc
	Ethanol	Propanol	Dioxane	Acetic Acid	Propanoic Acid	Butyric Acid	g/L		pH	Na	K	mg/L	mg/L	mg/L
0	0.92	0.07	1.98	0.36	0.00	0.00	0.62	0	4.30	20.98	64.89	2440.00		2280.66714
1a	0.29	0.07	1.98	0.26	0.00	0.00	0.28	1a	6.49	16.06	42.29			967.6137704
1b	0.41	0.09	1.98	0.38	0.00	0.00	0.39	1b	6.64	12.70	36.06			1356.480624
1	0.29	0.13	1.98	0.14	0.00	0.00	0.26	1	6.24	18.81	55.81	1870.00		951.8446448
2a	0.00	0.00	1.98	0.00	0.00	0.00	0.00	2a	6.72	24.78	47.23			0
2b	0.03	0.00	1.98	0.00	0.00	0.00	0.01	2b	6.67	15.89	47.84			54.14513387
2	0.00	0.00	1.98	0.00	0.00	0.00	0.00	2	6.65	48.39	59.91	705.00		0
3a	0.00	0.00	1.98	0.00	0.00	0.00	0.00	3a	6.68	34.24	41.68			0
3b	0.00	0.00	1.98	0.00	0.00	0.00	0.00	3b	6.55	35.91	51.85			0
3	0.00	0.00	1.98	0.00	0.00	0.00	0.00	3	6.75	47.84	50.34	170.00		0
4a	0.00	0.00	1.98	0.00	0.00	0.00	0.00	4a	7.02	32.38	28.06			0
4b	0.00	0.00	1.98	0.00	0.00	0.00	0.00	4b	6.93	32.36	28.25			0
4	0.00	0.00	1.98	0.00	0.00	0.00	0.00	4	6.95	32.53	27.76	125.00		0
5a	0.00	0.00	1.98	0.00	0.00	0.00	0.00	5a	7.66	45.93	54.16			0
5b	0.00	0.00	1.98	0.00	0.00	0.00	0.00	5b	7.28	30.58	33.44			0
5	0.00	0.00	1.98	0.00	0.00	0.00	0.00	5	7.28	33.30	33.24	0.00		0

Appendix KK. **CW Characterisation February 11 2005**

Sample	Concentrations	ml/l					Calc TOC	Sample		AA Work / mg/L			COD	TOC	COD Calc
	Ethanol	Propanol	Dioxane	Acetic Acid	Propanoic Acid	Butyric Acid	g/L		pH	Na	K		mg/L	mg/L	mg/L
0	1.03	0.07	1.98	0.13	0.21	0.03	0.69	0	4.31	19.62	56.80	2400.00			2593.30403
1a	0.24	0.04	1.98	0.00	0.07	0.00	0.17	1a	6.69	13.17	34.15				641.3151859
1b	0.27	0.13	1.98	0.00	0.00	0.00	0.19	1b	6.65	12.31	32.68				767.6487194
1	0.32	0.23	1.98	0.00	0.00	0.00	0.26	1	6.29	17.16	50.15	1630.00			1044.546287
2a	0.04	0.03	1.98	0.00	0.00	0.00	0.04	2a	6.93	22.88	60.94				144.2864557
2b	0.10	0.07	1.98	0.00	0.00	0.00	0.08	2b	6.67	16.49	46.63				325.6418028
2	0.00	0.00	1.98	0.00	0.00	0.00	0.00	2	6.85	27.73	63.06	1200.00			0
3a	0.00	0.00	1.98	0.00	0.00	0.00	0.00	3a	7.01	18.70	33.71				0
3b	0.00	0.00	1.98	0.00	0.00	0.00	0.00	3b	6.87	18.41	43.34				0
3	0.00	0.00	1.98	0.00	0.00	0.00	0.00	3	6.94	46.36	65.96	530.00			0
4a	0.00	0.00	1.98	0.00	0.00	0.00	0.00	4a	7.13	43.32	39.53				0
4b	0.00	0.00	1.98	0.00	0.00	0.00	0.00	4b	6.76	32.31	32.25				0
4	0.00	0.00	1.98	0.00	0.00	0.00	0.00	4	7.12	29.30	29.63	0.00			0
5a	0.00	0.00	1.98	0.00	0.00	0.00	0.00	5a	7.71	34.33	32.76				0
5b	0.00	0.00	1.98	0.00	0.00	0.00	0.00	5b	7.31	39.99	38.16				0
5	0.00	0.00	1.98	0.00	0.00	0.00	0.00	5	7.52	13.17	30.85	0.00			0

Appendix LL. **CW Characterisation February 14 2005**

Sample	Concentrations	ml/l						Calc TOC	Sample		AA Work / mg/L			COD	TOC	COD Calc
	Ethanol	Propanol	Dioxane	Acetic Acid	Propanoic Acid	Butyric Acid		g/L		pH	Na	K		mg/L	mg/L	mg/L
0	1.03	0.07	1.98	0.13	0.21	0.03		0.69	0	4.31	19.62	56.80		2400.00		2593.30403
1a	0.24	0.04	1.98	0.00	0.07	0.00		0.17	1a	6.69	13.17	34.15				641.3151859
1b	0.27	0.13	1.98	0.00	0.00	0.00		0.19	1b	6.65	12.31	32.68				767.6487194
1	0.32	0.23	1.98	0.00	0.00	0.00		0.26	1	6.29	17.16	50.15		1630.00		1044.546287
2a	0.04	0.03	1.98	0.00	0.00	0.00		0.04	2a	6.93	22.88	60.94				144.2864557
2b	0.10	0.07	1.98	0.00	0.00	0.00		0.08	2b	6.67	16.49	46.63				325.6418028
2	0.00	0.00	1.98	0.00	0.00	0.00		0.00	2	6.85	27.73	63.06		1200.00		0
3a	0.00	0.00	1.98	0.00	0.00	0.00		0.00	3a	7.01	18.70	33.71				0
3b	0.00	0.00	1.98	0.00	0.00	0.00		0.00	3b	6.87	18.41	43.34				0
3	0.00	0.00	1.98	0.00	0.00	0.00		0.00	3	6.94	46.36	65.96		530.00		0
4a	0.00	0.00	1.98	0.00	0.00	0.00		0.00	4a	7.13	43.32	39.53				0
4b	0.00	0.00	1.98	0.00	0.00	0.00		0.00	4b	6.76	32.31	32.25				0
4	0.00	0.00	1.98	0.00	0.00	0.00		0.00	4	7.12	29.30	29.63		0.00		0
5a	0.00	0.00	1.98	0.00	0.00	0.00		0.00	5a	7.71	34.33	32.76				0
5b	0.00	0.00	1.98	0.00	0.00	0.00		0.00	5b	7.31	39.99	38.16				0
5	0.00	0.00	1.98	0.00	0.00	0.00		0.00	5	7.52	13.17	30.85		0.00		0

Appendix MM.**CW Characterisation February 15 2005**

Sample	Concentrations	ml/l					Calc TOC	Sample	AA Work / mg/L			COD	TOC	COD Calc
	Ethanol	Propanol	Dioxane	Acetic Acid	Propanoic Acid	Butyric Acid	g/L		pH	Na	K	mg/L	mg/L	mg/L
0	1.70	0.04	1.98	0.75	0.00	0.00	1.14	0	4.48	34.07	69.25	4620.00		4133.736696
1a	0.00	0.00	1.98	0.00	0.00	0.00	0.00	1a						0
1b	0.00	0.00	1.98	0.00	0.00	0.00	0.00	1b						0
1	0.00	0.00	1.98	0.00	0.00	0.00	0.00	1						0
2a	0.00	0.00	1.98	0.00	0.00	0.00	0.00	2a						0
2b	0.00	0.00	1.98	0.00	0.00	0.00	0.00	2b						0
2	0.00	0.00	1.98	0.00	0.00	0.00	0.00	2						0
3a	0.00	0.00	1.98	0.00	0.00	0.00	0.00	3a						0
3b	0.00	0.00	1.98	0.00	0.00	0.00	0.00	3b						0
3	0.00	0.00	1.98	0.00	0.00	0.00	0.00	3						0
4a	0.00	0.00	1.98	0.00	0.00	0.00	0.00	4a						0
4b	0.00	0.00	1.98	0.00	0.00	0.00	0.00	4b						0
4	0.00	0.00	1.98	0.00	0.00	0.00	0.00	4						0
5a	0.00	0.00	1.98	0.00	0.00	0.00	0.00	5a						0
5b	0.00	0.00	1.98	0.00	0.00	0.00	0.00	5b						0
5	0.00	0.00	1.98	0.00	0.00	0.00	0.00	5						0

Appendix NN. **CW Characterisation February 16 2005**

Sample	Concentrations	ml/l					Calc TOC	Sample	AA Work / mg/L			COD	TOC	COD Calc
	Ethanol	Propanol	Dioxane	Acetic Acid	Propanoic Acid	Butyric Acid	g/L		pH	Na	K	mg/L	mg/L	mg/L
0	0.89	0.10	1.98	0.46	0.00	0.00	0.66	0	5.42	83.00	100.00	3135.00		2392.923198
1a	0.00	0.00	1.98	0.00	0.00	0.00	0.00	1a						0
1b	0.00	0.00	1.98	0.00	0.00	0.00	0.00	1b						0
1	0.00	0.00	1.98	0.00	0.00	0.00	0.00	1						0
2a	0.00	0.00	1.98	0.00	0.00	0.00	0.00	2a						0
2b	0.00	0.00	1.98	0.00	0.00	0.00	0.00	2b						0
2	0.00	0.00	1.98	0.00	0.00	0.00	0.00	2						0
3a	0.00	0.00	1.98	0.00	0.00	0.00	0.00	3a						0
3b	0.00	0.00	1.98	0.00	0.00	0.00	0.00	3b						0
3	0.00	0.00	1.98	0.00	0.00	0.00	0.00	3						0
4a	0.00	0.00	1.98	0.00	0.00	0.00	0.00	4a						0
4b	0.00	0.00	1.98	0.00	0.00	0.00	0.00	4b						0
4	0.00	0.00	1.98	0.00	0.00	0.00	0.00	4						0
5a	0.00	0.00	1.98	0.00	0.00	0.00	0.00	5a						0
5b	0.00	0.00	1.98	0.00	0.00	0.00	0.00	5b						0
5	0.00	0.00	1.98	0.00	0.00	0.00	0.00	5						0

Appendix OO. **CW Characterisation February 17 2005**

Sample	Concentrations	ml/l					Calc TOC	Sample	AA Work / mg/L			COD	TOC	COD Calc
	Ethanol	Propanol	Dioxane	Acetic Acid	Propanoic Acid	Butyric Acid	g/L		pH	Na	K	mg/L	mg/L	mg/L
0	0.14	0.00	1.98	0.09	0.00	0.00	0.11	0	5.19	11.21	32.20	570.00		370.1881582
1a	0.00	0.00	1.98	0.00	0.00	0.00	0.00	1a						0
1b	0.00	0.00	1.98	0.00	0.00	0.00	0.00	1b						0
1	0.00	0.00	1.98	0.00	0.00	0.00	0.00	1						0
2a	0.00	0.00	1.98	0.00	0.00	0.00	0.00	2a						0
2b	0.00	0.00	1.98	0.00	0.00	0.00	0.00	2b						0
2	0.00	0.00	1.98	0.00	0.00	0.00	0.00	2						0
3a	0.00	0.00	1.98	0.00	0.00	0.00	0.00	3a						0
3b	0.00	0.00	1.98	0.00	0.00	0.00	0.00	3b						0
3	0.00	0.00	1.98	0.00	0.00	0.00	0.00	3						0
4a	0.00	0.00	1.98	0.00	0.00	0.00	0.00	4a						0
4b	0.00	0.00	1.98	0.00	0.00	0.00	0.00	4b						0
4	0.00	0.00	1.98	0.00	0.00	0.00	0.00	4						0
5a	0.00	0.00	1.98	0.00	0.00	0.00	0.00	5a						0
5b	0.00	0.00	1.98	0.00	0.00	0.00	0.00	5b						0
5	0.00	0.00	1.98	0.00	0.00	0.00	0.00	5						0

Appendix PP. **CW Characterisation February 18 2005**

Sample	Concentrations	ml/l					Calc TOC	Sample	AA Work / mg/L			COD	TOC	COD Calc
	Ethanol	Propanol	Dioxane	Acetic Acid	Propanoic Acid	Butyric Acid	g/L		pH	Na	K	mg/L	mg/L	mg/L
0	1.06	0.00	1.98	0.00	0.00	0.00	0.50	0	5.48	47.98	154.00	3145.00		2004.397833
1a	0.00	0.00	1.98	0.00	0.00	0.00	0.00	1a						0
1b	0.00	0.00	1.98	0.00	0.00	0.00	0.00	1b						0
1	0.00	0.00	1.98	0.00	0.00	0.00	0.00	1						0
2a	0.00	0.00	1.98	0.00	0.00	0.00	0.00	2a						0
2b	0.00	0.00	1.98	0.00	0.00	0.00	0.00	2b						0
2	0.00	0.00	1.98	0.00	0.00	0.00	0.00	2						0
3a	0.00	0.00	1.98	0.00	0.00	0.00	0.00	3a						0
3b	0.00	0.00	1.98	0.00	0.00	0.00	0.00	3b						0
3	0.00	0.00	1.98	0.00	0.00	0.00	0.00	3						0
4a	0.00	0.00	1.98	0.00	0.00	0.00	0.00	4a						0
4b	0.00	0.00	1.98	0.00	0.00	0.00	0.00	4b						0
4	0.00	0.00	1.98	0.00	0.00	0.00	0.00	4						0
5a	0.00	0.00	1.98	0.00	0.00	0.00	0.00	5a						0
5b	0.00	0.00	1.98	0.00	0.00	0.00	0.00	5b						0
5	0.00	0.00	1.98	0.00	0.00	0.00	0.00	5						0

Appendix QQ. **CW Characterisation February 19 2005**

Sample	Concentrations	ml/l					Calc TOC	Sample	AA Work / mg/L			COD	TOC	COD Calc
	Ethanol	Propanol	Dioxane	Acetic Acid	Propanoic Acid	Butyric Acid	g/L		pH	Na	K	mg/L	mg/L	mg/L
0	1.28	0.00	1.98	0.00	0.00	0.00	0.60	0	5.16	57.62	182.00	3350.00		2412.70191
1a	0.00	0.00	1.98	0.00	0.00	0.00	0.00	1a						0
1b	0.00	0.00	1.98	0.00	0.00	0.00	0.00	1b						0
1	0.00	0.00	1.98	0.00	0.00	0.00	0.00	1						0
2a	0.00	0.00	1.98	0.00	0.00	0.00	0.00	2a						0
2b	0.00	0.00	1.98	0.00	0.00	0.00	0.00	2b						0
2	0.00	0.00	1.98	0.00	0.00	0.00	0.00	2						0
3a	0.00	0.00	1.98	0.00	0.00	0.00	0.00	3a						0
3b	0.00	0.00	1.98	0.00	0.00	0.00	0.00	3b						0
3	0.00	0.00	1.98	0.00	0.00	0.00	0.00	3						0
4a	0.00	0.00	1.98	0.00	0.00	0.00	0.00	4a						0
4b	0.00	0.00	1.98	0.00	0.00	0.00	0.00	4b						0
4	0.00	0.00	1.98	0.00	0.00	0.00	0.00	4						0
5a	0.00	0.00	1.98	0.00	0.00	0.00	0.00	5a						0
5b	0.00	0.00	1.98	0.00	0.00	0.00	0.00	5b						0
5	0.00	0.00	1.98	0.00	0.00	0.00	0.00	5						0

Appendix RR. **CW Characterisation February 21 2005**

Sample	Concentrations	ml/l					Calc TOC	Sample	AA Work / mg/L			COD	TOC	COD Calc
	Ethanol	Propanol	Dioxane	Acetic Acid	Propanoic Acid	Butyric Acid	g/L		pH	Na	K	mg/L	mg/L	mg/L
0	0.77	0.02	1.98	0.00	0.00	0.00	0.38	0	5.11	36.43	148.00	2385.00		1505.422851
1a	0.00	0.00	1.98	0.00	0.00	0.00	0.00	1a						0
1b	0.00	0.00	1.98	0.00	0.00	0.00	0.00	1b						0
1	0.00	0.00	1.98	0.00	0.00	0.00	0.00	1						0
2a	0.00	0.00	1.98	0.00	0.00	0.00	0.00	2a						0
2b	0.00	0.00	1.98	0.00	0.00	0.00	0.00	2b						0
2	0.00	0.00	1.98	0.00	0.00	0.00	0.00	2						0
3a	0.00	0.00	1.98	0.00	0.00	0.00	0.00	3a						0
3b	0.00	0.00	1.98	0.00	0.00	0.00	0.00	3b						0
3	0.00	0.00	1.98	0.00	0.00	0.00	0.00	3						0
4a	0.00	0.00	1.98	0.00	0.00	0.00	0.00	4a						0
4b	0.00	0.00	1.98	0.00	0.00	0.00	0.00	4b						0
4	0.00	0.00	1.98	0.00	0.00	0.00	0.00	4						0
5a	0.00	0.00	1.98	0.00	0.00	0.00	0.00	5a						0
5b	0.00	0.00	1.98	0.00	0.00	0.00	0.00	5b						0
5	0.00	0.00	1.98	0.00	0.00	0.00	0.00	5						0

Appendix SS. **CW Characterisation February 22 2005**

Sample	Concentrations	ml/l					Calc TOC	Sample		AA Work / mg/L		COD	TOC	COD Calc
	Ethanol	Propanol	Dioxane	Acetic Acid	Propanoic Acid	Butyric Acid	g/L		pH	Na	K	mg/L	mg/L	mg/L
0	1.03	0.03	1.98	0.00	0.00	0.00	0.50	0	5.05	51.38	197.00	2690.00		2003.194923
1a	0.00	0.00	1.98	0.00	0.00	0.00	0.00	1a						0
1b	0.00	0.00	1.98	0.00	0.00	0.00	0.00	1b						0
1	0.00	0.00	1.98	0.00	0.00	0.00	0.00	1						0
2a	0.00	0.00	1.98	0.00	0.00	0.00	0.00	2a						0
2b	0.00	0.00	1.98	0.00	0.00	0.00	0.00	2b						0
2	0.00	0.00	1.98	0.00	0.00	0.00	0.00	2						0
3a	0.00	0.00	1.98	0.00	0.00	0.00	0.00	3a						0
3b	0.00	0.00	1.98	0.00	0.00	0.00	0.00	3b						0
3	0.00	0.00	1.98	0.00	0.00	0.00	0.00	3						0
4a	0.00	0.00	1.98	0.00	0.00	0.00	0.00	4a						0
4b	0.00	0.00	1.98	0.00	0.00	0.00	0.00	4b						0
4	0.00	0.00	1.98	0.00	0.00	0.00	0.00	4						0
5a	0.00	0.00	1.98	0.00	0.00	0.00	0.00	5a						0
5b	0.00	0.00	1.98	0.00	0.00	0.00	0.00	5b						0
5	0.00	0.00	1.98	0.00	0.00	0.00	0.00	5						0

Appendix TT. **CW Characterisation February 23 2005**

Sample	Concentrations	ml/l					Calc TOC	Sample	AA Work / mg/L			COD	TOC	COD Calc
	Ethanol	Propanol	Dioxane	Acetic Acid	Propanoic Acid	Butyric Acid	g/L		pH	Na	K	mg/L	mg/L	mg/L
0	0.66	0.03	1.98	0.00	0.00	0.00	0.33	0	4.90	33.16	120.00	1775.00		1316.499338
1a	0.00	0.00	1.98	0.00	0.00	0.00	0.00	1a						0
1b	0.00	0.00	1.98	0.00	0.00	0.00	0.00	1b						0
1	0.00	0.00	1.98	0.00	0.00	0.00	0.00	1						0
2a	0.00	0.00	1.98	0.00	0.00	0.00	0.00	2a						0
2b	0.00	0.00	1.98	0.00	0.00	0.00	0.00	2b						0
2	0.00	0.00	1.98	0.00	0.00	0.00	0.00	2						0
3a	0.00	0.00	1.98	0.00	0.00	0.00	0.00	3a						0
3b	0.00	0.00	1.98	0.00	0.00	0.00	0.00	3b						0
3	0.00	0.00	1.98	0.00	0.00	0.00	0.00	3						0
4a	0.00	0.00	1.98	0.00	0.00	0.00	0.00	4a						0
4b	0.00	0.00	1.98	0.00	0.00	0.00	0.00	4b						0
4	0.00	0.00	1.98	0.00	0.00	0.00	0.00	4						0
5a	0.00	0.00	1.98	0.00	0.00	0.00	0.00	5a						0
5b	0.00	0.00	1.98	0.00	0.00	0.00	0.00	5b						0
5	0.00	0.00	1.98	0.00	0.00	0.00	0.00	5						0

Appendix UU. **CW Characterisation February 24 2005**

Sample	Concentrations	ml/l						Calc TOC	Sample	AA Work / mg/L			COD	TOC	COD Calc
	Ethanol	Propanol	Dioxane	Acetic Acid	Propanoic Acid	Butyric Acid	g/L		pH	Na	K		mg/L	mg/L	mg/L
0	1.46	0.03	1.98	0.00	0.00	0.00	0.70	0	5.05	121.00	155.00	3090.00			2804.515951
1a	0.00	0.00	1.98	0.00	0.00	0.00	0.00	1a							0
1b	0.00	0.00	1.98	0.00	0.00	0.00	0.00	1b							0
1	0.00	0.00	1.98	0.00	0.00	0.00	0.00	1							0
2a	0.00	0.00	1.98	0.00	0.00	0.00	0.00	2a							0
2b	0.00	0.00	1.98	0.00	0.00	0.00	0.00	2b							0
2	0.00	0.00	1.98	0.00	0.00	0.00	0.00	2							0
3a	0.00	0.00	1.98	0.00	0.00	0.00	0.00	3a							0
3b	0.00	0.00	1.98	0.00	0.00	0.00	0.00	3b							0
3	0.00	0.00	1.98	0.00	0.00	0.00	0.00	3							0
4a	0.00	0.00	1.98	0.00	0.00	0.00	0.00	4a							0
4b	0.00	0.00	1.98	0.00	0.00	0.00	0.00	4b							0
4	0.00	0.00	1.98	0.00	0.00	0.00	0.00	4							0
5a	0.00	0.00	1.98	0.00	0.00	0.00	0.00	5a							0
5b	0.00	0.00	1.98	0.00	0.00	0.00	0.00	5b							0
5	0.00	0.00	1.98	0.00	0.00	0.00	0.00	5							0

Appendix VV. **CW Characterisation February 28 2005**

Sample	Concentrations	ml/l					Calc TOC	Sample	AA Work / mg/L			COD	TOC	COD Calc
	Ethanol	Propanol	Dioxane	Acetic Acid	Propanoic Acid	Butyric Acid	g/L		pH	Na	K	mg/L	mg/L	mg/L
0	2.66	0.00	1.98	0.00	0.00	0.00	1.26	0	4.72	48.20	142.00	4920.00		5019.850569
1a	0.00	0.00	1.98	0.00	0.00	0.00	0.00	1a						0
1b	0.00	0.00	1.98	0.00	0.00	0.00	0.00	1b						0
1	0.00	0.00	1.98	0.00	0.00	0.00	0.00	1						0
2a	0.00	0.00	1.98	0.00	0.00	0.00	0.00	2a						0
2b	0.00	0.00	1.98	0.00	0.00	0.00	0.00	2b						0
2	0.00	0.00	1.98	0.00	0.00	0.00	0.00	2						0
3a	0.00	0.00	1.98	0.00	0.00	0.00	0.00	3a						0
3b	0.00	0.00	1.98	0.00	0.00	0.00	0.00	3b						0
3	0.00	0.00	1.98	0.00	0.00	0.00	0.00	3						0
4a	0.00	0.00	1.98	0.00	0.00	0.00	0.00	4a						0
4b	0.00	0.00	1.98	0.00	0.00	0.00	0.00	4b						0
4	0.00	0.00	1.98	0.00	0.00	0.00	0.00	4						0
5a	0.00	0.00	1.98	0.00	0.00	0.00	0.00	5a						0
5b	0.00	0.00	1.98	0.00	0.00	0.00	0.00	5b						0
5	0.00	0.00	1.98	0.00	0.00	0.00	0.00	5						0

Appendix WW. **CW Characterisation March 1 2005**

Sample	Concentrations	ml/l					Calc TOC	Sample		AA Work / mg/L			COD	TOC	COD Calc
	Ethanol	Propanol	Dioxane	Acetic Acid	Propanoic Acid	Butyric Acid	g/L		pH	Na	K		mg/L	mg/L	mg/L
0	3.78	0.00	1.98	0.00	0.00	0.00	1.79	0	4.52		32.87	215.00	7000		7141.575789
1a	1.43	0.00	1.98	0.23	0.10	0.00	0.82	1a	7.12		53.49	171.00			
1b	1.26	0.04	1.98	0.00	0.00	0.00	0.62	1b	6.66		40.31	171.00			
1	1.41	0.09	1.98	0.00	0.00	0.00	0.71	1	6.05		47.68	168.00	4315		2837.970128
2a	0.00	0.00	1.98	0.24	0.06	0.00	0.13	2a	7.27		82.87	111.00			
2b	0.29	0.00	1.98	0.47	0.20	0.00	0.43	2b	7.06		69.37	142.00			
2	0.00	0.00	1.98	0.41	0.10	0.00	0.22	2	7.49		81.33	116.00	620		598.1275297
3a	0.00	0.00	1.98	0.32	0.00	0.00	0.13	3a	7.28		58.19	131.00			
3b	0.00	0.00	1.98	0.40	0.00	0.00	0.17	3b	7.12		59.43	110.00			
3	0.00	0.00	1.98	0.38	0.00	0.00	0.16	3	7.14		53.80	120.00	530		419.4079319
4a	0.00	0.00	1.98	0.91	0.11	0.00	0.44	4a	7.55		30.78	70.20			
4b	0.00	0.00	1.98	0.45	0.00	0.00	0.19	4b	7.72		40.63	99.85			
4	0.00	0.00	1.98	0.44	0.00	0.00	0.19	4	8.73		32.10	71.65	25		493.5641419
5a	0.00	0.00	1.98	0.37	0.00	0.00	0.16	5a	8.02		29.07	55.90			
5b	0.00	0.00	1.98	0.31	0.00	0.00	0.13	5b	7.54		32.57	61.00			
5	0.00	0.00	1.98	0.00	0.00	0.00	0.00	5	7.61		26.38	52.05	25		0

Appendix XX. **CW Characterisation March 2 2005**

Sample	Concentrations	ml/l					Calc TOC	Sample		AA Work / mg/L		COD	COD Calc		TOC	TOC Calc
	Ethanol	Propanol	Dioxane	Acetic Acid	Propanoic Acid	Butyric Acid	g/L		pH	Na	K	mg/L	mg/L	mg/L	mg/L	
0	1.84	0.00	1.98	0.00	0.00	0.00	0.87	0	4.62	28.32	145.00	3635		3474.265		
1a	0.32	0.00	1.98	0.59	0.00	0.00	0.40	1a	6.38	23.07	82.00					
1b	0.24	0.08	1.98	0.00	0.00	0.00	0.15	1b	6.27	59.69	220.00					
1	0.17	0.00	1.98	0.00	0.00	0.00	0.08	1	6.30	53.13	207.00	2880		325.4117		
2a	0.24	0.00	1.98	0.00	0.00	0.00	0.11	2a	7.43	72.03	127.00					
2b	0.00	0.00	1.98	0.24	0.00	0.00	0.10	2b	6.94	69.43	125.00					
2	0.00	0.00	1.98	0.00	0.00	0.00	0.00	2	7.81	35.41	62.80	270		0		
3a	0.00	0.00	1.98	0.00	0.00	0.00	0.00	3a	7.24	46.74	94.75					
3b	0.00	0.00	1.98	0.00	0.00	0.00	0.00	3b	7.13	60.06	113.00					
3	0.00	0.00	1.98	0.00	0.00	0.00	0.00	3	7.40	53.43	130.00	290		0		
4a	0.00	0.00	1.98	0.00	0.00	0.00	0.00	4a	7.86	31.09	62.90					
4b	0.00	0.00	1.98	0.00	0.00	0.00	0.00	4b	7.65	30.11	58.80					
4	0.00	0.00	1.98	0.00	0.00	0.00	0.00	4	7.84	27.08	60.30	20		0		
5a	0.00	0.00	1.98	0.00	0.00	0.00	0.00	5a	7.82	22.12	41.45					
5b	0.00	0.00	1.98	0.00	0.00	0.00	0.00	5b	7.29	10.12	21.10					
5	0.00	0.00	1.98	0.00	0.00	0.00	0.00	5	9.23	27.53	62.10	55		0		

Appendix YY. **CW Characterisation March 3 2005**

Sample	Concentrations	ml/l					Calc TOC	Sample		AA Work / mg/L			COD	TOC	COD Calc
	Ethanol	Propanol	Dioxane	Acetic Acid	Propanoic Acid	Butyric Acid	g/L		pH	Na	K		mg/L	mg/L	mg/L
0	0.85	0.00	1.98	0.29	0.00	0.00	0.52	0	4.59	20.82	96.50	2125			1922.255
1a	0.00	0.00	1.98	0.36	0.00	0.00	0.15	1a	6.26	14.66	43.70				404.9018
1b	0.05	0.00	1.98	0.40	0.00	0.00	0.19	1b	6.31	16.81	66.80				545.2191
1	0.18	0.00	1.98	0.43	0.00	0.00	0.26	1	6.29	16.60	66.30	1360			816.1806
2a	0.00	0.00	1.98	0.46	0.00	0.00	0.19	2a	7.48	24.11	36.20				518.6399
2b	0.00	0.00	1.98	0.45	0.00	0.00	0.19	2b	7.63	25.58	50.55				499.1036
2	0.00	0.00	1.98	0.34	0.00	0.00	0.14	2	7.51	57.07	92.05	555			377.8617
3a	0.00	0.00	1.98	0.60	0.00	0.00	0.25	3a	7.64	25.48	50.60				668.1501
3b	0.00	0.00	1.98	0.20	0.00	0.00	0.09	3b	7.35	44.11	80.70				226.7807
3	0.00	0.00	1.98	0.08	0.00	0.00	0.03	3	8.22	36.68	84.10	90			86.27741
4a	0.00	0.00	1.98	0.10	0.00	0.00	0.04	4a	8.70	11.92	23.25				114.0042
4b	0.00	0.00	1.98	0.00	0.00	0.00	0.00	4b	7.78	25.69	51.90				0
4	0.00	0.00	1.98	0.00	0.00	0.00	0.00	4	8.46	12.86	26.65	70			0
5a	0.00	0.00	1.98	0.00	0.00	0.00	0.00	5a	9.26	21.38	39.00				0
5b	0.00	0.00	1.98	0.00	0.00	0.00	0.00	5b	8.10		18.55				0
5	0.00	0.00	1.98	0.54	0.00	0.00	0.23	5	8.12	12.81	22.30	20			604.7823

Appendix ZZ. **CW Characterisation March 4 2005**

Sample	Concentrations	ml/l	GC Work				Calc TOC	Sample		AA Work / mg/L				COD	TOC	COD Calc
	Ethanol	Propanol	Dioxane	Acetic Acid	Propanoic Acid	Butyric Acid	g/L		pH	Na	K	Ca	Mg	mg/L	mg/L	mg/L
0	0.84	0.02	10.00	0.18	0.11	0.05	0.56	0	4.65	25.30	138.00	19.88	3.85	1200	1700	2200.46
1a	0.00	0.00	10.00	0.15	0.08	0.06	0.13	1a	7.36	22.85	66.31	135.00	48.30			
1b	0.00	0.00	10.00	0.20	0.10	0.06	0.16	1b	6.49	15.00	65.58	138.00	47.60			
1	0.00	0.00	10.00	0.17	0.08	0.05	0.14	1	6.74	15.10	58.98	101.00	33.80			419.9811
2a	0.00	0.00	10.00	0.16	0.07	0.02	0.11	2a	7.22	36.70	46.73	23.91	26.70			
2b	0.00	0.00	10.00	0.08	0.03	0.01	0.05	2b	7.77	42.30	73.11	27.71	40.40			
2	0.00	0.00	10.00	0.17	0.10	0.04	0.14	2	7.46	48.20	71.34	17.69	34.10			433.53
3a	0.00	0.00	10.00	0.15	0.08	0.03	0.12	3a	7.18	35.87	61.66	28.72	31.60			
3b	0.00	0.00	10.00	0.17	0.07	0.01	0.11	3b	7.48	39.16	66.51	15.58	29.60			
3	0.00	0.00	10.00	0.10	0.04	0.00	0.06	3	7.70	42.39	93.34	11.93	43.40			181.8487
4a	0.00	0.00	10.00	0.06	0.04	0.00	0.05	4a	7.51	20.18	38.13	13.99	22.70			
4b	0.00	0.00	10.00	0.07	0.03	0.01	0.05	4b	8.02	33.18	62.79	11.12	36.50			
4	0.00	0.00	10.00	0.15	0.07	0.00	0.10	4	7.68	12.03	17.31	9.11	13.50			299.8003
5a	0.00	0.00	10.00	0.09	0.04	0.00	0.06	5a	8.64	25.78	39.10	8.69	32.10			
5b	0.00	0.00	10.00	0.09	0.04	0.00	0.06	5b	8.59	13.87	15.44	7.64	12.90			
5	0.00	0.00	10.00	0.08	0.03	0.00	0.05	5	7.63	21.38	28.55	19.87	23.90	60	104	141.5516

Appendix AAA.**CW Characterisation March 7 2005**

Sample	Concentrations	ml/l					Calc TOC	Sample		AA Work / mg/L					COD	TOC	COD Calc
	Ethanol	Propanol	Dioxane	Acetic Acid	Propanoic Acid	Butyric Acid	g/L		pH	Na	K	Ca	Mg		mg/L	mg/L	mg/L
0	0.76	0.00	10.00	0.00	0.00	0.00	0.36	0	4.6	19.87	120	21.4	3.65		740		1441.981
1a	0.00	0.00	10.00	0.14	0.09	0.05	0.13	1a	7.3	29.82	112	65.9	83.2				
1b	0.00	0.00	10.00	0.13	0.08	0.04	0.12	1b	7.5	19.57	90.95	66.05	64.7				
1	0.00	0.00	10.00	0.10	0.07	0.03	0.09	1	8.1	27.74	107	31.97	75.9		125		272.1974
2a	0.00	0.00	10.00	0.07	0.05	0.00	0.05	2a	7.8	53.39	76.7	22.34	40.5				
2b	0.00	0.00	10.00	0.10	0.07	0.03	0.09	2b	7.9	38.32	60.8	23.01	33.5				
2	0.00	0.00	10.00	0.07	0.05	0.02	0.06	2	7.8	39.98	59.4	16.74	29.3		45		187.0031
3a	0.00	0.00	10.00	0.06	0.05	0.03	0.06	3a	7.8	44.04	86.7	12.26	40.2				
3b	0.00	0.00	10.00	0.06	0.04	0.00	0.04	3b	7.5	38.96	70.5	18.14	33				
3	0.00	0.00	10.00	0.07	0.05	0.00	0.05	3	8	31.19	71.4	14.34	32.7		0		151.2787
4a	0.00	0.00	10.00	0.08	0.05	0.02	0.07	4a	7.8	27.46	62.2	12.18	30.9				
4b	0.00	0.00	10.00	0.00	0.00	0.00	0.00	4b	8.5	36.51	80	7.64	37.9				
4	0.00	0.00	10.00	0.06	0.04	0.00	0.04	4	7.9	21.72	53.4	15.23	30.7		0		127.3243
5a	0.00	0.00	10.00	0.04	0.03	0.00	0.03	5a	8	21.58	34.4	12.13	26.8				
5b	0.00	0.00	10.00	0.03	0.02	0.00	0.02	5b	7.6	18.3	33.8	23.36	24.1				
5	0.00	0.00	10.00	0.10	0.06	0.04	0.09	5	7.8	25.73	49.2	15.29	30.7		50		266.1546

Appendix BBB. **CW Characterisation March 8 2005**

Sample	Concentrations	ml/l					Calc TOC	Sample		AA Work / mg/L			COD	TOC	COD Calc
	Ethanol	Propanol	Dioxane	Acetic Acid	Propanoic Acid	Butyric Acid	g/L		pH	Na	K		mg/L	mg/L	mg/L
0	0.65	0.00	10.00	0.00	0.00	0.00	0.31	0	4.62	28.10	155.00	860	1150	1227.928	
1a	0.00	0.00	10.00	0.12	0.08	0.02	0.10	1a	7.14	19.40	88.80				
1b	0.00	0.00	10.00	0.24	0.16	0.09	0.22	1b	7.28	22.00	94.40				
1	0.11	0.01	10.00	0.17	0.12	0.05	0.21	1	7.32	23.50	116.00	485	725	677.9438	
2a	0.00	0.00	10.00	0.14	0.09	0.05	0.13	2a	7.72	51.30	95.10				
2b	0.00	0.00	10.00	0.17	0.14	0.02	0.15	2b	7.88	43.30	167.00				
2	0.00	0.00	10.00	0.10	0.09	0.02	0.09	2	8.21	51.30	88.70	0	46.3	267.5259	
3a	0.00	0.00	10.00	0.11	0.10	0.00	0.09	3a	8.00	41.50	63.40				
3b	0.00	0.00	10.00	0.10	0.08	0.00	0.08	3b	7.76	41.90	60.80				
3	0.00	0.00	10.00	0.09	0.07	0.00	0.07	3	8.55	71.60	143.00	0	43	212.4725	
4a	0.00	0.00	10.00	0.07	0.07	0.00	0.06	4a	8.43	24.70	49.60				
4b	0.00	0.00	10.00	0.07	0.06	0.00	0.06	4b	8.04	31.30	68.30				
4	0.00	0.00	10.00	0.07	0.05	0.00	0.05	4	8.33	26.20	53.30	0	42.6	156.1561	
5a	0.00	0.00	10.00	0.08	0.05	0.00	0.06	5a	7.62	18.70	31.30				
5b	0.00	0.00	10.00	0.06	0.04	0.00	0.05	5b	7.73	16.70	35.60				
5	0.00	0.00	10.00	0.07	0.03	0.00	0.04	5	7.98	25.90	48.40	0	50.6	116.963	

Appendix CCC. **CW Characterisation March 9 2005**

Sample	Concentrations	ml/l					Calc TOC	Sample	AA Work / mg/L			COD	TOC	COD Calc
	Ethanol	Propanol	Dioxane	Acetic Acid	Propanoic Acid	Butyric Acid	g/L		pH	Na	K	mg/L	mg/L	mg/L
0	0.61	0.00	1.00	0.00	0.00	0.00	0.29	0	4.67	22.50	118.00	815	1556	1156.869
1a	0.00	0.00	1.00	0.13	0.08	0.02	0.10	1a	7.10	13.90	59.40			
1b	0.00	0.00	1.00	0.05	0.04	0.02	0.05	1b	7.85	14.50	69.20			
1	0.00	0.00	1.00	0.08	0.05	0.02	0.07	1	8.55	16.20	77.10	220	280	199.8569
2a	0.00	0.00	1.00	0.07	0.06	0.04	0.08	2a	8.27	55.00	105.00			
2b	0.00	0.00	1.00	0.06	0.05	0.00	0.05	2b	8.57	15.00	57.80			
2	0.00	0.00	1.00	0.08	0.06	0.00	0.06	2	7.94	41.30	61.60	20	157	171.0889
3a	0.00	0.00	1.00	0.03	0.03	0.00	0.02	3a	8.10	27.30	51.65			
3b	0.00	0.00	1.00	0.03	0.02	0.00	0.03	3b	8.07	36.00	58.00			
3	0.00	0.00	1.00	0.06	0.03	0.00	0.04	3	8.06	43.80	84.50	10	94	106.6138
4a	0.00	0.00	1.00	0.04	0.02	0.00	0.03	4a	8.07	22.30	46.90			
4b	0.00	0.00	1.00	0.01	0.02	0.00	0.02	4b	8.32	26.80	49.30			
4	0.00	0.00	1.00	0.00	0.01	0.00	0.01	4	7.94	21.50	40.60	30	34.5	18.57272
5a	0.00	0.00	1.00	0.00	0.02	0.00	0.01	5a	8.09	19.34	36.50			
5b	0.00	0.00	1.00	0.03	0.02	0.00	0.02	5b	8.17	20.70	40.00			
5	0.00	0.00	1.00	0.00	0.00	0.00	0.00	5	8.21	22.70	42.50	10	34	0

Appendix DDD. **CW Characterisation March 10 2005**

Sample	Concentrations	ml/l					Calc TOC	Sample		AA Work / mg/L		COD	TOC	COD Calc
	Ethanol	Propanol	Dioxane	Acetic Acid	Propanoic Acid	Butyric Acid	g/L		pH	Na	K	mg/L	mg/L	mg/L
0	0.58	0.00	1.98	0.00	0.00	0.00	0.27	0	4.99	20.18	110.00	1855	4150	1096.528
1a	0.00	0.00	1.98	0.12	0.17	0.49	0.39	1a	7.72	32.71	49.95			
1b	0.37	0.06	1.98	0.10	0.14	0.33	0.48	1b	6.80	24.06	87.05			
1	0.14	0.03	1.98	0.13	0.16	0.36	0.40	1	6.14	18.22	86.65	1315	1675	1327.984
2a	0.38	0.04	1.98	0.13	0.14	0.31	0.49	2a	7.45	35.27	110.00			
2b	0.00	0.00	1.98	0.13	0.16	0.33	0.31	2b	7.14	30.58	133.00			
2	0.00	0.00	1.98	0.14	0.14	0.28	0.27	2	8.47	37.82	78.00	265	683	858.2604
3a	0.00	0.00	1.98	0.10	0.13	0.27	0.25	3a	8.60	60.57	86.60			
3b	0.00	0.00	1.98	0.04	0.07	0.09	0.10	3b	9.08	53.70	72.15			
3	0.00	0.00	1.98	0.00	0.00	0.00	0.00	3	8.69	45.74	64.50	110	280	0
4a	0.00	0.00	1.98	0.06	0.08	0.11	0.13	4a	8.14	18.18	65.05			
4b	0.00	0.00	1.98	0.07	0.06	0.08	0.10	4b	8.87	30.90	54.15			
4	0.00	0.00	1.98	0.07	0.07	0.06	0.10	4	7.47	28.17	60.40	100	154	292.1862
5a	0.00	0.00	1.98	0.04	0.04	0.03	0.05	5a	8.87	29.04	40.90			
5b	0.00	0.00	1.98	0.04	0.04	0.03	0.06	5b	8.14	18.54	48.05			
5	0.00	0.00	1.98	0.00	0.03	0.02	0.03	5	7.42	21.77	43.15	115	46	83.7864

Appendix EEE. **CW Characterisation March 11 2005**

Sample	Concentrations	ml/l					Calc TOC	Sample		AA Work / mg/L		COD	TOC	COD Calc
	Ethanol	Propanol	Dioxane	Acetic Acid	Propanoic Acid	Butyric Acid	g/L		pH	Na	K	mg/L	mg/L	mg/L
0	1.13	0.00	1.98	0.00	0.00	0.00	0.54	0	4.85	28.50	143.00	1735		2138.797
1a	0.04	0.00	1.98	0.35	0.08	0.09	0.26	1a	6.34	13.00	60.40			
1b	0.00	0.00	1.98	0.31	0.07	0.02	0.18	1b	7.07	13.53	79.05			
1	0.19	0.00	1.98	0.13	0.04	0.02	0.18	1	6.62	27.78	140.00	1365		618.6625
2a	0.00	0.00	1.98	0.29	0.08	0.08	0.21	2a	7.36	26.21	124.00			
2b	0.00	0.00	1.98	0.40	0.15	0.12	0.30	2b	7.31	17.11	116.00			
2	0.00	0.00	1.98	0.22	0.08	0.05	0.16	2	7.84	12.40	68.50	405		446.4162
3a	0.00	0.00	1.98	0.29	0.11	0.08	0.22	3a	8.99	28.06	90.25			
3b	0.00	0.00	1.98	0.17	0.07	0.00	0.11	3b	9.13	35.82	130.00			
3	0.00	0.00	1.98	0.13	0.04	0.00	0.07	3	7.96	18.94	42.80	15		199.2766
4a	0.00	0.00	1.98	0.18	0.06	0.00	0.10	4a	8.53	15.16	30.15			
4b	0.00	0.00	1.98	0.11	0.00	0.00	0.05	4b	7.60	31.72	51.53			
4	0.00	0.00	1.98	0.07	0.04	0.00	0.05	4	8.77	43.93	73.75	0		142.6352
5a	0.00	0.00	1.98	0.14	0.05	0.00	0.08	5a	7.50	11.90	27.50			
5b	0.00	0.00	1.98	0.17	0.06	0.00	0.10	5b	7.51	15.38	38.25			
5	0.00	0.00	1.98	0.03	0.05	0.00	0.04	5	8.31	29.26	69.20	0		105.5073

Appendix FFF. **CW Characterisation March 14 2005**

Sample	Concentrations	ml/l					Calc TOC	Sample	AA Work / mg/L			COD	TOC	COD Calc
	Ethanol	Propanol	Dioxane	Acetic Acid	Propanoic Acid	Butyric Acid	g/L		pH	Na	K	mg/L	mg/L	mg/L
0	0.42	0.00	1.98	0.00	0.00	0.00	0.20	0	4.84	8.91	45.20			799.501
1a	0.06	0.00	1.98	0.00	0.03	0.00	0.04	1a	7.26	12.28	65.95			
1b	0.00	0.00	1.98	0.09	0.05	0.00	0.06	1b	6.86	4.07	32.50			
1	0.06	0.00	1.98	0.09	0.05	0.05	0.12	1	7.27	6.71	81.60			377.2818
2a	0.00	0.00	1.98	0.09	0.05	0.04	0.08	2a	7.63	6.20	45.05			
2b	0.00	0.00	1.98	0.11	0.06	0.06	0.10	2b	8.06	9.99	103.00			
2	0.00	0.00	1.98	0.10	0.05	0.00	0.07	2	9.06	15.01	152.00			188.6518
3a	0.00	0.00	1.98	0.14	0.08	0.00	0.10	3a	8.24	11.67	70.10			
3b	0.00	0.00	1.98	0.22	0.10	0.00	0.14	3b	8.84	8.50	76.05			
3	0.00	0.00	1.98	0.17	0.07	0.00	0.11	3	8.83	13.92	61.10			297.1967
4a	0.00	0.00	1.98	0.08	0.05	0.00	0.06	4a	8.41	29.75	53.40			
4b	0.00	0.00	1.98	0.00	0.00	0.00	0.00	4b	8.03	9.38	33.65			
4	0.00	0.00	1.98	0.00	0.00	0.00	0.00	4	7.71	11.64	41.70			0
5a	0.00	0.00	1.98	0.07	0.03	0.00	0.04	5a	8.83	15.44	43.15			
5b	0.00	0.00	1.98	0.14	0.07	0.00	0.09	5b	8.42	22.54	67.30			
5	0.00	0.00	1.98	0.09	0.07	0.04	0.09	5	7.39	9.75	36.10			264.0294

Appendix GGG. **CW Characterisation March 15 2005**

Sample	Concentrations	ml/l					Calc TOC	Sample		AA Work / mg/L		COD	TOC	COD Calc
	Ethanol	Propanol	Dioxane	Acetic Acid	Propanoic Acid	Butyric Acid	g/L		pH	Na	K	mg/L	mg/L	mg/L
0	0.54	0.00	1.98	0.00	0.00	0.00	0.26	0	5.04	15.59	42.95	765		1029.159
1a	0.19	0.00	1.98	0.00	0.00	0.00	0.09	1a	7.54	21.16	72.25			
1b	0.26	0.00	1.98	0.00	0.00	0.00	0.12	1b	7.69	21.81	75.85			
1	0.00	0.00	1.98	0.12	0.07	0.00	0.08	1	7.19	6.99	29.15	490		240.9275
2a	0.00	0.00	1.98	0.00	0.00	0.00	0.00	2a	7.72	7.67	28.95			
2b	0.00	0.00	1.98	0.09	0.04	0.02	0.07	2b	7.85	9.36	40.85			
2	0.00	0.00	1.98	0.18	0.11	0.05	0.15	2	7.77	19.70	102.00	205		439.1382
3a	0.00	0.00	1.98	0.18	0.09	0.01	0.13	3a	7.83	17.90	91.60			
3b	0.00	0.00	1.98	0.11	0.04	0.01	0.07	3b	7.92	16.37	75.95			
3	0.00	0.00	1.98	0.08	0.04	0.00	0.05	3	8.22	29.69	132.00	30		143.4212
4a	0.00	0.00	1.98	0.14	0.07	0.00	0.09	4a	8.55	27.19	94.70			
4b	0.00	0.00	1.98	0.10	0.06	0.00	0.07	4b	9.13	40.20	112.00			
4	0.00	0.00	1.98	0.08	0.00	0.00	0.04	4	8.82	42.37	102.00	125		93.7361
5a	0.00	0.00	1.98	0.10	0.00	0.00	0.04	5a	8.88	41.66	77.40			
5b	0.00	0.00	1.98	0.00	0.00	0.00	0.00	5b	9.07	58.79	99.40			
5	0.00	0.00	1.98	0.00	0.00	0.00	0.00	5	8.91	40.28	125.00	0		0

Appendix HHH. **CW Characterisation March 16 2005**

Sample	Concentrations	ml/l					Calc TOC	Sample		AA Work / mg/L			COD	TOC	COD Calc
	Ethanol	Propanol	Dioxane	Acetic Acid	Propanoic Acid	Butyric Acid	g/L		pH	Na	K		mg/L	mg/L	mg/L
0	0.26	0.00	1.98	0.05	0.04	0.04	0.18	0	4.83	16.91	66.95		515		661.27
1a	0.06	0.00	1.98	0.30	0.07	0.06	0.22	1a	7.06	10.30	36.00				651.0458
1b	0.06	0.00	1.98	0.35	0.05	0.04	0.22	1b	7.35	19.63	61.25				642.8279
1	0.00	0.00	1.98	0.41	0.08	0.05	0.24	1	7.37	15.33	43.06		90		672.896
2a	0.00	0.00	1.98	0.17	0.00	0.00	0.07	2a	7.55	8.97	31.05				190.4709
2b	0.00	0.00	1.98	0.08	0.00	0.00	0.03	2b	7.25	18.37	38.70				85.61841
2	0.00	0.00	1.98	0.00	0.00	0.02	0.01	2	7.66	22.30	76.75		70		32.96019
3a	0.00	0.00	1.98	0.00	0.00	0.02	0.01	3a	7.78	14.52	72.85				43.34883
3b	0.00	0.00	1.98	0.00	0.00	0.00	0.00	3b	7.49	11.38	55.95				0
3	0.00	0.00	1.98	0.00	0.00	0.00	0.00	3	7.55	50.64	93.15		110		0
4a	0.00	0.00	1.98	0.07	0.00	0.00	0.03	4a	8.08	27.18	150.00				72.97932
4b	0.00	0.00	1.98	0.00	0.00	0.00	0.00	4b	7.74	10.72	56.55				0
4	0.00	0.00	1.98	0.00	0.00	0.00	0.00	4	7.62	31.32	73.95		35		0
5a	0.00	0.00	1.98	0.00	0.00	0.00	0.00	5a	8.02	19.68	39.10				0
5b	0.00	0.00	1.98	0.00	0.00	0.00	0.00	5b	8.05	27.01	62.95				0
5	0.00	0.00	1.98	0.00	0.00	0.00	0.00	5	7.90	34.37	82.55		55		0

Appendix III. **CW Characterisation March 17 2005**

Sample	Concentrations	ml/l					Calc TOC	Sample		AA Work / mg/L		COD	TOC	COD Calc
	Ethanol	Propanol	Dioxane	Acetic Acid	Propanoic Acid	Butyric Acid	g/L		pH	Na	K	mg/L	mg/L	mg/L
0	0.53	0.00	1.98	0.00	0.00	0.00	0.25	0	4.55	12.90	74.00	1030		1008.514
1a	0.05	0.00	1.98	0.00	0.00	0.00	0.03	1a	7.62	32.33	135.00			102.1183
1b	0.44	0.00	1.98	0.00	0.00	0.00	0.21	1b	7.02	21.87	95.80			831.2478
1	0.02	0.00	1.98	0.00	0.00	0.00	0.01	1	7.13	17.27	83.10	655		45.06476
2a	0.00	0.00	1.98	0.00	0.00	0.00	0.00	2a	8.78	25.29	87.50			0
2b	0.00	0.00	1.98	0.00	0.00	0.00	0.00	2b	8.30	22.30	95.15			0
2	0.00	0.00	1.98	0.00	0.00	0.00	0.00	2	8.66	26.12	94.65	445		0
3a	0.00	0.00	1.98	0.00	0.00	0.00	0.00	3a	9.07	25.61	96.40			0
3b	0.00	0.00	1.98	0.00	0.00	0.00	0.00	3b	8.97	22.80	98.85			0
3	0.00	0.00	1.98	1.20	0.11	0.04	0.58	3	8.39	22.43	91.75	355		1571.323
4a	0.00	0.00	1.98	0.14	0.03	0.03	0.09	4a	7.50	25.53	123.00			253.9365
4b	0.00	0.00	1.98	0.52	0.05	0.00	0.24	4b	9.05	25.23	135.00			661.7482
4	0.07	0.00	1.98	1.08	0.09	0.02	0.54	4	9.01	31.19	154.00	105		1515.456
5a	0.00	0.00	1.98	0.52	0.02	0.01	0.23	5a	8.06	42.69	167.00			617.2726
5b	0.00	0.00	1.98	0.21	0.00	0.00	0.09	5b	8.99	37.12	187.00			233.4385
5	0.00	0.00	1.98	0.21	0.00	0.00	0.09	5	8.49	41.80	164.00	120		231.1355

Appendix JJJ. **CW Characterisation March 18 2005**

Sample	Concentrations	ml/l					Calc TOC	Sample		AA Work / mg/L		COD	TOC	COD Calc
	Ethanol	Propanol	Dioxane	Acetic Acid	Propanoic Acid	Butyric Acid	g/L		pH	Na	K	mg/L	mg/L	mg/L
0	1.31	0.00	1.98	0.12	0.00	0.00	0.67	0	4.55	30.26	35.22	2795		2609.955
1a	0.08	0.08	1.98	0.14	0.00	0.00	0.14	1a	6.73	24.48	29.60			475.0084
1b	0.00	0.00	1.98	0.00	0.00	0.00	0.00	1b	6.56	18.59	23.81			0
1	0.40	0.03	1.98	0.00	0.00	0.00	0.20	1	6.24	19.12	23.63	2755		818.1744
2a	0.00	0.00	1.98	0.00	0.00	0.00	0.00	2a	6.91	21.38	22.17			0
2b	0.12	0.00	1.98	0.28	0.00	0.00	0.17	2b	6.57	17.99	26.68			529.6497
2	0.03	0.00	1.98	1.53	0.15	0.00	0.73	2	6.85	23.42	24.81	1985		1991.27
3a	0.00	0.00	1.98	0.57	0.05	0.00	0.26	3a	6.96	17.62	14.41			715.2677
3b	0.00	0.00	1.98	0.28	0.04	0.00	0.14	3b	6.86	19.96	21.79			383.2075
3	0.00	0.00	1.98	0.41	0.00	0.00	0.17	3	6.91	26.53	21.34	1175		462.5581
4a	0.00	0.00	1.98	0.32	0.00	0.00	0.13	4a	6.99	31.14	25.51			356.0349
4b	0.00	0.00	1.98	0.22	0.00	0.00	0.09	4b	7.31	23.90	20.41			246.2923
4	0.00	0.00	1.98	0.00	0.00	0.00	0.00	4	7.06	26.83	20.16	470		0
5a	0.04	0.00	1.98	1.34	0.04	0.00	0.61	5a	7.53	28.76	21.38			1650.485
5b	0.08	0.00	1.98	1.15	0.17	0.00	0.60	5b	7.48	30.54	23.29			1695.788
5	0.00	0.00	1.98	1.56	0.00	0.00	0.66	5	6.86	27.09	22.52	780		1746.77

Appendix KKK. **CW Characterisation March 22 2005**

Sample	Concentrations	ml/l					Calc TOC	Sample		AA Work / mg/L		COD	TOC	COD Calc
	Ethanol	Propanol	Dioxane	Acetic Acid	Propanoic Acid	Butyric Acid	g/L		pH	Na	K	mg/L	mg/L	mg/L
0	0.10	0.00	1.98	1.59	0.20	0.00	0.81	0	6.21	11.41	22.90	170.00		2277.07
1a	0.00	0.00	1.98	0.49	0.06	0.02	0.24	1a	8.38	13.21	37.30			668.7371
1b	0.00	0.00	1.98	1.47	0.06	0.11	0.71	1b	8.55	17.40	48.30			1935.872
1	0.00	0.00	1.98	0.56	0.04	0.00	0.26	1	8.76	17.70	47.70	205.00		692.5539
2a	0.00	0.00	1.98	0.45	0.00	0.00	0.19	2a	8.88	26.63	84.05			499.7525
2b	0.00	0.00	1.98	0.17	0.00	0.00	0.07	2b	8.83	27.00	80.10			193.857
2	0.00	0.00	1.98	0.00	0.00	0.00	0.00	2	8.95	63.80	191.00	320.00		0
3a	0.00	0.00	1.98	0.00	0.00	0.00	0.00	3a	7.96	58.19	196.00			0
3b	0.00	0.00	1.98	0.00	0.00	0.00	0.00	3b	8.83	52.97	175.00			0
3	0.00	0.00	1.98	0.27	0.00	0.00	0.12	3	8.62	35.24	134.00	685.00		307.2794
4a	0.00	0.00	1.98	0.29	0.00	0.00	0.12	4a	7.78	19.68	112.00			325.5987
4b	0.14	0.00	1.98	0.76	0.00	0.00	0.39	4b	7.99	18.30	94.95			1117.402
4	0.00	0.00	1.98	0.71	0.00	0.00	0.30	4	8.17	18.76	89.40	680.00		797.9817
5a	0.00	0.00	1.98	0.64	0.00	0.00	0.27	5a	7.81	14.06	64.55			711.0672
5b	0.00	0.00	1.98	0.61	0.00	0.00	0.25	5b	7.73	20.83	106.00			678.075
5	0.00	0.00	1.98	0.59	0.00	0.00	0.25	5	7.88	33.09	140.00	730.00		655.1776

Appendix LLL. **CW Characterisation March 24 2005**

Sample	Concentrations	ml/l					Calc TOC	Sample		AA Work / mg/L			COD	TOC	COD Calc
	Ethanol	Propanol	Dioxane	Acetic Acid	Propanoic Acid	Butyric Acid	g/L		pH	Na	K		mg/L	mg/L	mg/L
0	0.28	0.00	1.98	0.00	0.00	0.00	0.13	0	5.51	20.81	77.50	785.00		533.7942
1a	0.00	0.00	1.98	0.00	0.00	0.00	0.00	1a		25.78	94.45				0
1b	0.00	0.00	1.98	0.00	0.00	0.00	0.00	1b		37.27	122.00				0
1	0.00	0.00	1.98	0.00	0.00	0.00	0.00	1		25.25	108.00				0
2a	0.00	0.00	1.98	0.00	0.00	0.00	0.00	2a		23.16	92.00				0
2b	0.00	0.00	1.98	0.00	0.00	0.00	0.00	2b		31.89	118.00				0
2	0.00	0.00	1.98	0.00	0.00	0.00	0.00	2		25.89	95.00				0
3a	0.00	0.00	1.98	0.00	0.00	0.00	0.00	3a		25.87	97.55				0
3b	0.00	0.00	1.98	0.00	0.00	0.00	0.00	3b		30.97	90.50				0
3	0.00	0.00	1.98	0.00	0.00	0.00	0.00	3		23.22	79.50				0
4a	0.00	0.00	1.98	0.00	0.00	0.00	0.00	4a		26.21	89.15				0
4b	0.00	0.00	1.98	0.00	0.00	0.00	0.00	4b		32.92	105.00				0
4	0.00	0.00	1.98	0.00	0.00	0.00	0.00	4		37.26	139.00				0
5a	0.00	0.00	1.98	0.00	0.00	0.00	0.00	5a		31.49	119.00				0
5b	0.00	0.00	1.98	0.00	0.00	0.00	0.00	5b		38.40	127.00				0
5	0.00	0.00	1.98	0.00	0.00	0.00	0.00	5		39.87	162.00				0

Appendix MMM. **CW Characterisation March 29 2005**

Sample	Concentrations	ml/l					Calc TOC	Sample		AA Work / mg/L		COD	TOC	COD Calc
	Ethanol	Propanol	Dioxane	Acetic Acid	Propanoic Acid	Butyric Acid	g/L		pH	Na	K	mg/L	mg/L	mg/L
0	0.22	0.00	1.98	0.00	0.00	0.00	0.10	0	5.10	14.52	41.75	740.00		411.6734
1a	0.00	0.00	1.98	0.00	0.00	0.00	0.00	1a						0
1b	0.00	0.00	1.98	0.00	0.00	0.00	0.00	1b						0
1	0.00	0.00	1.98	0.00	0.00	0.00	0.00	1						0
2a	0.00	0.00	1.98	0.00	0.00	0.00	0.00	2a						0
2b	0.00	0.00	1.98	0.00	0.00	0.00	0.00	2b						0
2	0.00	0.00	1.98	0.00	0.00	0.00	0.00	2						0
3a	0.00	0.00	1.98	0.00	0.00	0.00	0.00	3a						0
3b	0.00	0.00	1.98	0.00	0.00	0.00	0.00	3b						0
3	0.00	0.00	1.98	0.00	0.00	0.00	0.00	3						0
4a	0.00	0.00	1.98	0.00	0.00	0.00	0.00	4a						0
4b	0.00	0.00	1.98	0.00	0.00	0.00	0.00	4b						0
4	0.00	0.00	1.98	0.00	0.00	0.00	0.00	4						0
5a	0.00	0.00	1.98	0.00	0.00	0.00	0.00	5a						0
5b	0.00	0.00	1.98	0.00	0.00	0.00	0.00	5b						0
5	0.00	0.00	1.98	0.00	0.00	0.00	0.00	5						0

Appendix NNN. **CW Characterisation March 30 2005**

Sample	Concentrations	ml/l					Calc TOC	Sample		AA Work / mg/L		COD	TOC	COD Calc
	Ethanol	Propanol	Dioxane	Acetic Acid	Propanoic Acid	Butyric Acid	g/L		pH	Na	K	mg/L	mg/L	mg/L
0	0.19	0.00	1.98	0.00	0.00	0.00	0.09	0	6.28	29.03	53.91	555.00		358.8095
1a	0.00	0.00	1.98	0.00	0.00	0.00	0.00	1a						0
1b	0.00	0.00	1.98	0.00	0.00	0.00	0.00	1b						0
1	0.00	0.00	1.98	0.00	0.00	0.00	0.00	1						0
2a	0.00	0.00	1.98	0.00	0.00	0.00	0.00	2a						0
2b	0.00	0.00	1.98	0.00	0.00	0.00	0.00	2b						0
2	0.00	0.00	1.98	0.00	0.00	0.00	0.00	2						0
3a	0.00	0.00	1.98	0.00	0.00	0.00	0.00	3a						0
3b	0.00	0.00	1.98	0.00	0.00	0.00	0.00	3b						0
3	0.00	0.00	1.98	0.00	0.00	0.00	0.00	3						0
4a	0.00	0.00	1.98	0.00	0.00	0.00	0.00	4a						0
4b	0.00	0.00	1.98	0.00	0.00	0.00	0.00	4b						0
4	0.00	0.00	1.98	0.00	0.00	0.00	0.00	4						0
5a	0.00	0.00	1.98	0.00	0.00	0.00	0.00	5a						0
5b	0.00	0.00	1.98	0.00	0.00	0.00	0.00	5b						0
5	0.00	0.00	1.98	0.00	0.00	0.00	0.00	5						0

Appendix OOO. **CW Characterisation March 31 2005**

Sample	Concentrations	ml/l						Calc TOC	Sample	AA Work / mg/L			COD	TOC	COD Calc
	Ethanol	Propanol	Dioxane	Acetic Acid	Propanoic Acid	Butyric Acid	g/L		pH	Na	K		mg/L	mg/L	mg/L
0	0.83	0.00	1.98	0.09	0.00	0.00	0.43	0	5.29	52.4	27.05		1760.00		1674.771624
1a	0.00	0.00	1.98	0.00	0.00	0.00	0.00	1a							0
1b	0.00	0.00	1.98	0.00	0.00	0.00	0.00	1b							0
1	0.00	0.00	1.98	0.00	0.00	0.00	0.00	1							0
2a	0.00	0.00	1.98	0.00	0.00	0.00	0.00	2a							0
2b	0.00	0.00	1.98	0.00	0.00	0.00	0.00	2b							0
2	0.00	0.00	1.98	0.00	0.00	0.00	0.00	2							0
3a	0.00	0.00	1.98	0.00	0.00	0.00	0.00	3a							0
3b	0.00	0.00	1.98	0.00	0.00	0.00	0.00	3b							0
3	0.00	0.00	1.98	0.00	0.00	0.00	0.00	3							0
4a	0.00	0.00	1.98	0.00	0.00	0.00	0.00	4a							0
4b	0.00	0.00	1.98	0.00	0.00	0.00	0.00	4b							0
4	0.00	0.00	1.98	0.00	0.00	0.00	0.00	4							0
5a	0.00	0.00	1.98	0.00	0.00	0.00	0.00	5a							0
5b	0.00	0.00	1.98	0.00	0.00	0.00	0.00	5b							0
5	0.00	0.00	1.98	0.00	0.00	0.00	0.00	5							0

Appendix PPP. **Average ethanol concentration with increasing length**

	0	1a/b	1	2a/b	2	3a/b	3	4a/b	4	5a/b	5
Date	0	4	8	12	16	20	24	28	32	36	40
07-Feb	0.04	0.02	0.00	0.00	0.00	0.00	0.00	0.00	0.00	0.00	0.00
08-Feb	0.00	0.00	0.00	0.00	0.00	0.00	0.00	0.00	0.00	0.00	0.00
09-Feb	0.00	0.00	0.00	0.00	0.00	0.00	0.00	0.00	0.00	0.00	0.00
10-Feb	0.00	0.00	0.00	0.00	0.00	0.00	0.00	0.00	0.00	0.00	0.00
11-Feb	0.21	0.04	0.00	0.00	0.00	0.00	0.00	0.00	0.00	0.00	0.00
01-Mar	0	0.048313	0	0.130265	0.096458	0	0	0.055375	0	0	0
02-Mar	0	0	0	0	0	0	0	0	0	0	0
03-Mar	0	0	0	0	0	0	0	0	0	0	0
04-Mar	0.112367	0.09119	0.076446	0.050855	0.104424	0.076895	0.042688	0.033906	0.073602	0.040621	0.031724
07-Mar	0	0.085299	0.068519	0.057676	0.049665	0.045449	0.047938	0.024843	0.040039	0.023809	0.063903
08-Mar	0	0.118126	0.118312	0.114182	0.085702	0.087713	0.073348	0.060012	0.048229	0.046162	0.029245
09-Mar	0	0.058751	0.054535	0.056127	0.055196	0.025217	0.029286	0.020506	0.012372	0.018594	0
10-Mar	0	0.154579	0.156363	0.15357	0.143069	0.100364	0	0.074475	0.065936	0.042645	0.031825
11-Mar	0	0.075769	0.041392	0.115262	0.079759	0.090511	0.038881	0.028175	0.044523	0.055348	0.049823
14-Mar	0	0.039125	0.049338	0.055787	0.048283	0.090299	0.074124	0.026023	0	0.049617	0.068439
15-Mar	0	0	0.070634	0.019149	0.106805	0.064076	0.035677	0.067007	0	0	0
16-Mar	0.03699	0.062703	0.081849	0.00	0.00	0.00	0.00	0.00	0.00	0.00	0.00
17-Mar	0	0	0	0	0	0	0.111522	0.041338	0.092523	0.008372	0
18-Mar	0	0	0	0	0.151594	0.048583	0	0	0	0.108928	0
Average	0.02	0.04	0.04	0.04	0.05	0.03	0.02	0.02	0.02	0.02	0.01
tm	0	21.468	42.936	64.404	85.872	107.34	128.808	150.276	171.744	193.212	214.68

Appendix QQQ. **Average propanol concentration with increasing length**

	0	1a/b	1	2a/b	2	3a/b	3	4a/b	4	5a/b	5
Date	0	4	8	12	16	20	24	28	32	36	40
07-Feb	0.00	0.00	0.00	0.00	0.00	0.00	0.00	0.00	0.00	0.00	0.00
08-Feb	0.00	0.02	0.00	0.00	0.00	0.00	0.00	0.00	0.00	0.00	0.00
09-Feb	0.00	0.00	0.00	0.00	0.00	0.00	0.00	0.00	0.00	0.00	0.00
10-Feb	0.07	0.08	0.13	0.00	0.00	0.00	0.00	0.00	0.00	0.00	0.00
11-Feb	0.07	0.09	0.23	0.05	0.00	0.00	0.00	0.00	0.00	0.00	0.00
01-Mar	0	0.021786	0.087031	0	0	0	0	0	0	0	0
02-Mar	0.00	0.04	0.00	0.00	0.00	0.00	0.00	0.00	0.00	0.00	0.00
03-Mar	0.00	0.00	0.00	0.00	0.00	0.00	0.00	0.00	0.00	0.00	0.00
04-Mar	0.02	0.00	0.00	0.00	0.00	0.00	0.00	0.00	0.00	0.00	0.00
07-Mar	0.00	0.00	0.00	0.00	0.00	0.00	0.00	0.00	0.00	0.00	0.00
08-Mar	0.00	0.00	0.01	0.00	0.00	0.00	0.00	0.00	0.00	0.00	0.00
09-Mar	0.00	0.00	0.00	0.00	0.00	0.00	0.00	0.00	0.00	0.00	0.00
10-Mar	0	0.031733	0.027047	0.02001	0.00	0.00	0.00	0.00	0.00	0.00	0.00
11-Mar	0.00	0.00	0.00	0.00	0.00	0.00	0.00	0.00	0.00	0.00	0.00
14-Mar	0.00	0.00	0.00	0.00	0.00	0.00	0.00	0.00	0.00	0.00	0.00
15-Mar	0.00	0.00	0.00	0.00	0.00	0.00	0.00	0.00	0.00	0.00	0.00
16-Mar	0.00	0.00	0.00	0.00	0.00	0.00	0.00	0.00	0.00	0.00	0.00
17-Mar	0.00	0.00	0.00	0.00	0.00	0.00	0.00	0.00	0.00	0.00	0.00
18-Mar	0	0.040124	0.03304	0.00	0.00	0.00	0.00	0.00	0.00	0.00	0.00
Average	0.01	0.02	0.03	0.00	0.00	0.00	0.00	0.00	0.00	0.00	0.00
tm	0	21.468	42.936	64.404	85.872	107.34	128.808	150.276	171.744	193.212	214.68

Appendix RRR. **Average acetic acid concentration with increasing length**

	0	1a/b	1	2a/b	2	3a/b	3	4a/b	4	5a/b	5
Date	0.00	4.00	8.00	12.00	16.00	20.00	24.00	28.00	32.00	36.00	40.00
07-Feb	0.12	0.03	0.00	0.00	0.00	0.00	0.00	0.00	0.00	0.00	0.00
08-Feb	0.00	0.00	0.00	0.00	0.00	0.00	0.00	0.00	0.00	0.00	0.00
09-Feb	0.36	0.00	0.00	0.00	0.00	0.00	0.00	0.00	0.00	0.00	0.00
10-Feb	0.36	0.32	0.14	0.00	0.00	0.00	0.00	0.00	0.00	0.00	0.00
11-Feb	0.13	0.00	0.00	0.00	0.00	0.00	0.00	0.00	0.00	0.00	0.00
01-Mar	0.00	0.12	0.00	0.35	0.41	0.36	0.38	0.68	0.44	0.34	0.00
02-Mar	0.00	0.29	0.00	0.12	0.00	0.00	0.00	0.00	0.00	0.00	0.00
03-Mar	0.29	0.38	0.43	0.46	0.34	0.40	0.08	0.05	0.00	0.00	0.54
04-Mar	0.18	0.18	0.17	0.12	0.17	0.16	0.10	0.06	0.15	0.09	0.08
07-Mar	0.00	0.13	0.10	0.09	0.07	0.06	0.07	0.04	0.06	0.04	0.10
08-Mar	0.00	0.18	0.17	0.15	0.10	0.11	0.09	0.07	0.07	0.07	0.07
09-Mar	0.00	0.09	0.08	0.07	0.08	0.03	0.06	0.03	0.00	0.02	0.00
10-Mar	0.00	0.11	0.13	0.13	0.14	0.07	0.00	0.07	0.07	0.04	0.00
11-Mar	0.00	0.12	0.13	0.14	0.22	0.04	0.13	0.07	0.07	0.02	0.03
14-Mar	0.00	0.05	0.09	0.10	0.10	0.18	0.17	0.04	0.00	0.10	0.09
15-Mar	0.00	0.00	0.12	0.04	0.18	0.14	0.08	0.12	0.08	0.05	0.00
16-Mar	0.05	0.32	0.41	0.12	0.00	0.00	0.00	0.03	0.00	0.00	0.00
17-Mar	0.00	0.00	0.00	0.00	0.00	0.00	1.20	0.33	1.08	0.36	0.21
18-Mar	0.12	0.14	0.00	0.00	1.53	0.57	0.41	0.32	0.00	1.34	1.56
Average	0.08	0.13	0.10	0.10	0.18	0.11	0.14	0.10	0.11	0.13	0.14
tm	0	21.468	42.936	64.404	85.872	107.34	128.808	150.276	171.744	193.212	214.68

Appendix SSS. **Average propanoic acid concentration with increasing length**

	0	1a/b	1	2a/b	2	3a/b	3	4a/b	4	5a/b	5
Date	0	4	8	12	16	20	24	28	32	36	40
07-Feb	0.04	0.02	0.00	0.00	0.00	0.00	0.00	0.00	0.00	0.00	0.00
08-Feb	0.00	0.00	0.00	0.00	0.00	0.00	0.00	0.00	0.00	0.00	0.00
09-Feb	0.00	0.00	0.00	0.00	0.00	0.00	0.00	0.00	0.00	0.00	0.00
10-Feb	0.00	0.00	0.00	0.00	0.00	0.00	0.00	0.00	0.00	0.00	0.00
11-Feb	0.21	0.04	0.00	0.00	0.00	0.00	0.00	0.00	0.00	0.00	0.00
01-Mar	0.00	0.05	0.00	0.13	0.10	0.00	0.00	0.06	0.00	0.00	0.00
02-Mar	0.00	0.00	0.00	0.00	0.00	0.00	0.00	0.00	0.00	0.00	0.00
03-Mar	0.00	0.00	0.00	0.00	0.00	0.00	0.00	0.00	0.00	0.00	0.00
04-Mar	0.11	0.09	0.08	0.05	0.10	0.08	0.04	0.03	0.07	0.04	0.03
07-Mar	0.00	0.09	0.07	0.06	0.05	0.05	0.05	0.02	0.04	0.02	0.06
08-Mar	0.00	0.12	0.12	0.11	0.09	0.09	0.07	0.06	0.05	0.05	0.03
09-Mar	0.00	0.06	0.05	0.06	0.06	0.03	0.03	0.02	0.01	0.02	0.00
10-Mar	0.00	0.15	0.16	0.15	0.14	0.10	0.00	0.07	0.07	0.04	0.03
11-Mar	0.00	0.08	0.04	0.12	0.08	0.09	0.04	0.03	0.04	0.06	0.05
14-Mar	0.00	0.04	0.05	0.06	0.05	0.09	0.07	0.03	0.00	0.05	0.07
15-Mar	0.00	0.00	0.07	0.02	0.11	0.06	0.04	0.07	0.00	0.00	0.00
16-Mar	0.04	0.06	0.08	0.00	0.00	0.00	0.00	0.00	0.00	0.00	0.00
17-Mar	0.00	0.00	0.00	0.00	0.00	0.00	0.11	0.04	0.09	0.01	0.00
18-Mar	0.00	0.00	0.00	0.00	0.15	0.05	0.00	0.00	0.00	0.11	0.00
Average	0.02	0.04	0.04	0.04	0.05	0.03	0.02	0.02	0.02	0.02	0.01
tm	0	21.468	42.936	64.404	85.872	107.34	128.808	150.276	171.744	193.212	214.68

Appendix TTT. **Average butyric acid concentration with increasing length**

	0	1a/b	1	2a/b	2	3a/b	3	4a/b	4	5a/b	5
Date	0	4	8	12	16	20	24	28	32	36	40
07-Feb	0.00	0.00	0.00	0.00	0.00	0.00	0.00	0.00	0.00	0.00	0.00
08-Feb	0.00	0.00	0.00	0.00	0.00	0.00	0.00	0.00	0.00	0.00	0.00
09-Feb	0.00	0.00	0.00	0.00	0.00	0.00	0.00	0.00	0.00	0.00	0.00
10-Feb	0.00	0.00	0.00	0.00	0.00	0.00	0.00	0.00	0.00	0.00	0.00
11-Feb	0.03	0.00	0.00	0.00	0.00	0.00	0.00	0.00	0.00	0.00	0.00
01-Mar	0.00	0.00	0.00	0.00	0.00	0.00	0.00	0.00	0.00	0.00	0.00
02-Mar	0.00	0.00	0.00	0.00	0.00	0.00	0.00	0.00	0.00	0.00	0.00
03-Mar	0.00	0.00	0.00	0.00	0.00	0.00	0.00	0.00	0.00	0.00	0.00
04-Mar	0.05	0.06	0.05	0.02	0.04	0.02	0.00	0.01	0.00	0.00	0.00
07-Mar	0.00	0.05	0.03	0.02	0.02	0.01	0.00	0.01	0.00	0.00	0.04
08-Mar	0.00	0.06	0.05	0.04	0.02	0.00	0.00	0.00	0.00	0.00	0.00
09-Mar	0.00	0.02	0.02	0.02	0.00	0.00	0.00	0.00	0.00	0.00	0.00
10-Mar	0.00	0.41	0.36	0.32	0.28	0.18	0.00	0.10	0.06	0.03	0.02
11-Mar	0.00	0.05	0.02	0.10	0.05	0.04	0.00	0.00	0.00	0.00	0.00
14-Mar	0.00	0.00	0.05	0.05	0.00	0.00	0.00	0.00	0.00	0.00	0.04
15-Mar	0.00	0.00	0.00	0.01	0.05	0.01	0.00	0.00	0.00	0.00	0.00
16-Mar	0.04	0.05	0.05	0.00	0.02	0.01	0.00	0.00	0.00	0.00	0.00
17-Mar	0.00	0.00	0.00	0.00	0.00	0.00	0.04	0.02	0.02	0.00	0.00
18-Mar	0.00	0.00	0.00	0.00	0.00	0.00	0.00	0.00	0.00	0.00	0.00
Average	0.0059	0.0366	0.0341	0.0299	0.0244	0.0150	0.0019	0.0069	0.0046	0.0018	0.0049
tm	0	21.468	42.936	64.404	85.872	107.34	128.808	150.276	171.744	193.212	214.68

Appendix UUU. **Average sodium concentration with increasing length**

	0	1a/b	1	2a/b	2	3a/b	3	4a/b	4	5a/b	5
Date	0	4	8	12	16	20	24	28	32	36	40
07-Feb	17.03	32.82	24.68	24.64	47.19	33.97	41.56	27.05	32.33	34.11	41.86
08-Feb	10.03	15.38	12.22	21.20	35.81	30.12	36.33	24.49	26.48	34.90	33.92
09-Feb	10.30	14.34	19.77	31.47	49.12	35.74	34.98	39.60	32.49	36.42	44.70
10-Feb	20.98	14.38	18.81	20.34	48.39	35.08	47.84	32.37	32.53	38.26	33.30
11-Feb	19.62	12.74	17.16	19.69	27.73	18.56	46.36	37.82	29.30	37.16	13.17
01-Mar	32.87	46.90	47.68	76.12	81.33	58.81	53.80	35.71	32.10	30.82	26.38
02-Mar	28.32	41.38	53.13	70.73	35.41	53.40	53.43	30.60	27.08	16.12	27.53
03-Mar	20.82	15.74	16.60	24.85	57.07	34.80	36.68	18.81	12.86	21.38	12.81
04-Mar	25.30	18.93	15.10	39.50	48.20	37.52	42.39	26.68	12.03	19.83	21.38
07-Mar	19.87	24.70	27.74	45.86	39.98	41.50	31.19	31.99	21.72	19.94	25.73
08-Mar	28.10	20.70	23.50	47.30	51.30	41.70	71.60	28.00	26.20	17.70	25.90
09-Mar	22.50	14.20	16.20	35.00	41.30	31.65	43.80	24.55	21.50	20.02	22.70
10-Mar	20.18	28.39	18.22	32.93	37.82	57.14	45.74	24.54	28.17	23.79	21.77
11-Mar	28.50	13.27	27.78	21.66	12.40	31.94	18.94	23.44	43.93	13.64	29.26
14-Mar	8.91	8.18	6.71	8.10	15.01	10.09	13.92	19.57	11.64	18.99	9.75
15-Mar	15.59	21.49	6.99	8.52	19.70	17.14	29.69	33.70	42.37	50.23	40.28
16-Mar	16.91	14.97	15.33	13.67	22.30	12.95	50.64	18.95	31.32	23.35	34.37
17-Mar	12.90	27.10	17.27	23.80	26.12	24.21	22.43	25.38	31.19	39.91	41.80
18-Mar	30.26	21.54	19.12	19.69	23.42	18.79	26.53	27.52	26.83	29.65	27.09
Average	20.47316	21.42579	21.26368	30.79026	37.87368	32.89789	39.36053	27.93368	27.47737	27.69421	28.08947
tm	0	21.468	42.936	64.404	85.872	107.34	128.808	150.276	171.744	193.212	214.68

Appendix VVV. **Average potassium concentration with increasing length**

	0	1a/b	1	2a/b	2	3a/b	3	4a/b	4	5a/b	5
Date	0.00	4.00	8.00	12.00	16.00	20.00	24.00	28.00	32.00	36.00	40.00
07-Feb	38.70	46.90	58.10	29.65	35.70	28.20	34.60	28.10	34.80	31.00	34.10
08-Feb	46.59	46.98	34.43	42.37	35.48	29.60	32.49	25.02	30.71	33.87	33.45
09-Feb	37.31	39.00	52.55	52.27	51.54	34.34	29.00	34.89	29.40	35.42	29.13
10-Feb	64.89	39.18	55.81	47.54	59.91	46.77	50.34	28.16	27.76	43.80	33.24
11-Feb	56.80	33.42	50.15	53.79	63.06	38.53	65.96	35.89	29.63	35.46	30.85
01-Mar	215.00	171.00	168.00	126.50	116.00	120.50	120.00	85.03	71.65	58.45	52.05
02-Mar	145.00	151.00	207.00	126.00	62.80	103.88	130.00	60.85	60.30	31.28	62.10
03-Mar	96.50	55.25	66.30	43.38	92.05	65.65	84.10	37.58	26.65	28.78	22.30
04-Mar	138.00	65.95	58.98	59.92	71.34	64.09	93.34	50.46	17.31	27.27	28.55
07-Mar	120.00	101.48	107.00	68.75	59.40	78.60	71.40	71.10	53.40	34.10	49.20
08-Mar	155.00	91.60	116.00	131.05	88.70	62.10	143.00	58.95	53.30	33.45	48.40
09-Mar	118.00	64.30	77.10	81.40	61.60	54.83	84.50	48.10	40.60	38.25	42.50
10-Mar	110.00	68.50	86.65	121.50	78.00	79.38	64.50	59.60	60.40	44.48	43.15
11-Mar	143.00	69.73	140.00	120.00	68.50	110.13	42.80	40.84	73.75	32.88	69.20
14-Mar	45.20	49.23	81.60	74.03	152.00	73.08	61.10	43.53	41.70	55.23	36.10
15-Mar	42.95	74.05	29.15	34.90	102.00	83.78	132.00	103.35	102.00	88.40	125.00
16-Mar	66.95	48.63	43.06	34.88	76.75	64.40	93.15	103.28	73.95	51.03	82.55
17-Mar	74.00	115.40	83.10	91.33	94.65	97.63	91.75	129.00	154.00	177.00	164.00
18-Mar	35.22	26.71	23.63	24.43	24.81	18.10	21.34	22.96	20.16	22.34	22.52
Average	92.06	71.49	80.98	71.77	73.38	65.98	76.07	56.14	52.71	47.50	53.07
tm	0.00	21.47	42.94	64.40	85.87	107.34	128.81	150.28	171.74	193.21	214.68

Appendix WWW. **Average COD with increasing length**

	0	1	2	3	4	5
Date	0.00	8.00	16.00	24.00	32.00	40.00
07-Feb	570.00	500.00	25.00	0.00	70.00	35.00
08-Feb	1230.00	645.00	175.00	195.00	0.00	0.00
09-Feb	1680.00	920.00	430.00	55.00	20.00	50.00
10-Feb	2440.00	1870.00	705.00	170.00	125.00	0.00
11-Feb	2400.00	1630.00	1200.00	530.00	0.00	0.00
01-Mar	7000.00	4315.00	620.00	530.00	25.00	25.00
02-Mar	3635.00	2880.00	270.00	290.00	20.00	55.00
03-Mar	2125.00	1360.00	555.00	90.00	70.00	20.00
07-Mar	740.00	125.00	45.00	0.00	0.00	50.00
08-Mar	860.00	485.00	0.00	0.00	0.00	0.00
09-Mar	815.00	220.00	20.00	10.00	30.00	10.00
10-Mar	1855.00	1315.00	265.00	110.00	100.00	115.00
11-Mar	1735.00	1365.00	405.00	15.00	0.00	0.00
15-Mar	765.00	490.00	205.00	30.00	125.00	0.00
16-Mar	515.00	90.00	70.00	110.00	35.00	55.00
17-Mar	1030.00	655.00	445.00	355.00	105.00	120.00
18-Mar	2795.00	2755.00	1985.00	1175.00	470.00	780.00
Average	1893.53	1271.76	436.47	215.59	70.29	77.35
tm	0.00	42.94	85.87	128.81	171.74	214.68

Appendix XXX. **Daily flow into the CW**

Date	Flow / m^3/day	Meter Reading / m^3	Average
02 February 2005		19.62	
03 February 2005	4.85	24.47	2.29
04 February 2005	2.44	26.91	2.29
05 February 2005	1.98	28.89	2.29
06 February 2005	1.68		2.29
07 February 2005	1.68	32.25	2.29
08 February 2005	1.42	33.67	2.29
09 February 2005	1.88	35.55	2.29
10 February 2005	1.65	37.20	2.29
11 February 2005	2.77	39.97	2.29
12 February 2005	0.41		2.29
13 February 2005	0.41		2.29
14 February 2005	0.41	41.20	2.29
15 February 2005	2.37	43.57	2.29
16 February 2005	5.03		2.29
17 February 2005	5.03	53.63	2.29
18 February 2005	2.84	56.47	2.29
19 February 2005	2.03	58.50	2.29
20 February 2005	1.02		2.29
21 February 2005	1.02	60.53	2.29
22 February 2005	0.04	60.57	2.29
23 February 2005	0.00	60.57	2.29
24 February 2005	2.28	62.85	2.29
25 February 2005	3.39	66.24	2.29
26 February 2005	0.75		2.29
27 February 2005	0.75		2.29
28 February 2005	0.75	68.48	2.29
01 March 2005	2.12	70.60	2.29
02 March 2005	0.04	70.64	2.29
03 March 2005	0.36	71.00	2.29
04 March 2005	0.17	71.17	2.29
05 March 2005	0.01		2.29
06 March 2005	0.01		2.29
07 March 2005	0.01	71.21	2.29
08 March 2005	1.93	73.14	2.29
09 March 2005	0.01	73.15	2.29
10 March 2005	3.53	76.68	2.29
11 March 2005	1.82	78.50	2.29
12 March 2005	0.99		2.29
13 March 2005	0.99		2.29
14 March 2005	0.99	81.47	2.29
15 March 2005	4.73		2.29
16 March 2005	4.73		2.29
17 March 2005	4.73	95.65	2.29
18 March 2005	9.20	104.85	2.29
19 March 2005	3.76		2.29
20 March 2005	3.76		2.29
21 March 2005	3.76		2.29
22 March 2005	3.76	119.87	2.29
23 March 2005	5.53	125.40	2.29
24 March 2005	4.20	129.60	2.29
25 March 2005	2.73		2.29
26 March 2005	2.73		2.29
27 March 2005	2.73		2.29
28 March 2005	2.73		2.29
29 March 2005	2.73	143.26	2.29
30 March 2005	5.07	148.33	2.29
31 March 2005	1.94	150.27	2.29
Total Flow	130.65	130.65	130.65
Average for Data		2.30	

Appendix YYY. **Determination of ethanol rate constant from RTD**

k-Value Determination - for 1-X=0.99							
kt	exp(-kt)	exp(-kt)*E*delt t)	Sum(exp(-kt)*E*dt	Real Ca/Cao	Theta	Theta Length	Concentration
0.00	1.00	0.00000000	0.00	1.00	0.00	0.00	0.90
0.67	0.51	0.00000000	0.00	0.51	0.05	1.96	0.46
1.53	0.22	0.00016287	0.00	0.22	0.11	4.46	0.20
2.33	0.10	0.00508639	0.01	0.10	0.17	6.81	0.09
3.22	0.04	0.00317123	0.01	0.05	0.23	9.39	0.04
4.05	0.02	0.00087413	0.01	0.03	0.30	11.81	0.02
4.58	0.01	0.00036112	0.01	0.02	0.33	13.38	0.02
5.36	0.00	0.00024101	0.01	0.01	0.39	15.65	0.01
7.18	0.00	0.00008649	0.01	0.01	0.52	20.97	0.01
8.78	0.00	0.00001291	0.01	0.01	0.64	25.62	0.01
10.36	0.00	0.00000218	0.01	0.01	0.76	30.24	0.01
12.06	0.00	0.00000033	0.01	0.01	0.88	35.21	0.01
13.69	0.00	0.00000005	0.01	0.01	1.00	39.98	0.01
15.07	0.00	0.00000001	0.01	0.01	1.10	44.01	0.01
16.35	0.00	0.00000000	0.01	0.01	1.19	47.72	
18.62	0.00	0.00000000	0.01	0.01	1.36	54.38	
21.17	0.00	0.00000000	0.01	0.01	1.55	61.81	
24.87	0.00	0.00000000	0.01	0.01	1.82	72.60	
28.89	0.00	0.00000000	0.01	0.01	2.11	84.34	
32.22	0.00	0.00000000	0.01	0.01	2.35	94.08	
34.34	0.00	0.00000000	0.01	0.01	2.51	100.26	
37.60	0.00	0.00000000	0.01	0.01	2.74	109.77	
51.72	0.00	0.00000000	0.01	0.01	3.77	151.00	
267.23	0.00	0.00000000	0.01	0.01	19.51	780.22	
401.01	0.00	0.00000000	0.01	0.01	29.27	1170.82	
536.07	0.00	0.00000000	0.01	0.01			
	sum	0.0099987	=1-X				
k	0.8039		0.99				
	Ca=	0.900000					

Appendix ZZZ. **Finding conversion for average ethanol feed using RTD**

For average Co=0.9mL/L						
Ca	Integral of E(theta)	Theta	(theta)	k.theta	exp(-ktheta)	e-ktheta.E(theta).Delta Theta
0.90		0.00	0.00	0.00	1.00	0.0000
0.90	0.00	0.05	0.00	0.44	0.64	0.0000
0.90	0.00	0.11	0.01	1.00	0.37	0.0003
0.90	0.05	0.17	0.89	1.53	0.22	0.0113
0.89	0.08	0.23	1.22	2.11	0.12	0.0096
0.89	0.05	0.30	0.82	2.66	0.07	0.0035
0.89	0.04	0.33	0.90	3.01	0.05	0.0017
0.89	0.05	0.39	0.90	3.52	0.03	0.0015
0.89	0.11	0.52	0.86	4.72	0.01	0.0010
0.89	0.08	0.64	0.72	5.77	0.00	0.0003
0.89	0.07	0.76	0.59	6.80	0.00	0.0001
0.89	0.06	0.88	0.45	7.92	0.00	0.0000
0.89	0.04	1.00	0.38	9.00	0.00	0.0000
0.89	0.04	1.10	0.37	9.90	0.00	0.0000
0.89	0.03	1.19	0.32	10.74	0.00	0.0000
0.89	0.05	1.36	0.31	12.23	0.00	0.0000
0.89	0.03	1.55	0.18	13.91	0.00	0.0000
0.89	0.05	1.82	0.19	16.34	0.00	0.0000
0.89	0.07	2.11	0.25	18.98	0.00	0.0000
0.89	0.04	2.35	0.15	21.17	0.00	0.0000
0.89	0.03	2.51	0.20	22.56	0.00	0.0000
0.89	0.02	2.74	0.10	24.70	0.00	0.0000
0.89	0.00	3.77	0.00	33.97	0.00	0.0000
0.89	0.00	19.51	0.00	175.55	0.00	0.0000
0.89	0.00	29.27	0.00	263.44	0.00	0.0000
			0.00		sum	0.0293
					k	9.00000
	1.00				1-X	0.03
					X	97.07%

Appendix AAAA. **Scaling RTD of Port 5 to the 4m location within the reactor for ethanol degradation**

Scaled to length = 4m						
Length = 4m		Theta	(theta)	k.theta	exp(-kt	e-ktheta.E(theta).Delta Theta
E(Theta/Tau=11.61)		0.00	0.00	0.00	1.00	0.0000
tau	11.61	0.07	0.00	0.07	0.93	0.0000
		0.16	0.01	0.17	0.85	0.0006
	1.55	0.25	0.61	0.26	0.77	0.0405
		0.34	0.83	0.35	0.70	0.0556
		0.43	0.56	0.44	0.64	0.0321
		0.49	0.61	0.50	0.61	0.0214
		0.57	0.62	0.59	0.56	0.0285
		0.77	0.58	0.79	0.46	0.0518
		0.94	0.49	0.96	0.38	0.0320
		1.11	0.40	1.14	0.32	0.0220
		1.29	0.31	1.32	0.27	0.0150
		1.47	0.26	1.50	0.22	0.0100
		1.61	0.25	1.65	0.19	0.0072
		1.75	0.22	1.79	0.17	0.0049
		2.00	0.21	2.04	0.13	0.0067
		2.27	0.12	2.32	0.10	0.0033
		2.66	0.13	2.73	0.07	0.0033
		3.10	0.17	3.17	0.04	0.0030
		3.45	0.10	3.53	0.03	0.0010
		3.68	0.14	3.76	0.02	0.0007
		4.03	0.07	4.12	0.02	0.0004
		5.54	0.00	5.67	0.00	0.0000
		28.63	0.00	29.29	0.00	0.0000
		42.97	0.00	43.95	0.00	0.0000
					sum	0.3400
					k	1.02294
					1-X	0.34
					X	65.63%

Appendix BBBB. **Scaling RTD of Port 5 to the 8m location within the reactor for ethanol degradation**

Scaled to length = 8m							
Length = 8m		Theta	E(theta)	k.theta	exp(-kthe	e-ktheta.E	Integral
E((Theta/Tau)=16.37		0.00	0.00	0.00	1.00	0.0000	
tau	16.37	0.05	0.00	0.20	0.82	0.0000	0.00
		0.12	0.01	0.45	0.64	0.0005	0.00
		0.18	0.86	0.68	0.51	0.0264	0.05
		0.24	1.18	0.94	0.39	0.0308	0.08
		0.31	0.79	1.18	0.31	0.0153	0.05
		0.35	0.87	1.34	0.26	0.0092	0.04
		0.41	0.87	1.57	0.21	0.0107	0.05
		0.55	0.82	2.10	0.12	0.0139	0.11
		0.67	0.69	2.57	0.08	0.0064	0.08
		0.79	0.57	3.03	0.05	0.0033	0.07
		0.92	0.43	3.53	0.03	0.0016	0.06
		1.04	0.36	4.01	0.02	0.0008	0.04
		1.15	0.36	4.41	0.01	0.0005	0.04
		1.24	0.31	4.79	0.01	0.0002	0.03
		1.42	0.30	5.45	0.00	0.0002	0.05
		1.61	0.17	6.20	0.00	0.0001	0.03
		1.89	0.18	7.28	0.00	0.0000	0.05
		2.20	0.24	8.46	0.00	0.0000	0.07
		2.45	0.14	9.44	0.00	0.0000	0.04
		2.61	0.19	10.06	0.00	0.0000	0.03
		2.86	0.09	11.01	0.00	0.0000	0.02
		3.93	0.00	15.15	0.00	0.0000	0.00
		20.31	0.00	78.26	0.00	0.0000	0.00
		30.47	0.00	117.44	0.00	0.0000	0.00
					sum	0.1200	1.00
					k	3.85393	
					1-X	0.12	
					X	88.19%	

Appendix CCCC. **Scaling RTD of Port 5 to the 12m location within the reactor for ethanol degradation**

Scaled to length = 12m							
Length = 12m		Theta	E(theta)	k.theta	exp(-kthe	e-ktheta.E	Integral
E((Theta/Tau)=21.14		0.00	0.00	0.00	1.00	0.0000	
tau	21.14	0.04	0.00	0.38	0.68	0.0000	0.00
		0.09	0.01	0.87	0.42	0.0003	0.00
		0.14	1.11	1.32	0.27	0.0140	0.05
		0.19	1.52	1.82	0.16	0.0128	0.08
		0.24	1.02	2.29	0.10	0.0050	0.05
		0.27	1.12	2.60	0.07	0.0026	0.04
		0.32	1.12	3.04	0.05	0.0025	0.05
		0.42	1.06	4.07	0.02	0.0019	0.11
		0.52	0.89	4.97	0.01	0.0006	0.08
		0.61	0.74	5.87	0.00	0.0002	0.07
		0.71	0.56	6.83	0.00	0.0001	0.06
		0.81	0.47	7.76	0.00	0.0000	0.04
		0.89	0.46	8.54	0.00	0.0000	0.04
		0.96	0.40	9.26	0.00	0.0000	0.03
		1.10	0.39	10.55	0.00	0.0000	0.05
		1.25	0.22	12.00	0.00	0.0000	0.03
		1.46	0.23	14.09	0.00	0.0000	0.05
		1.70	0.31	16.37	0.00	0.0000	0.07
		1.90	0.18	18.26	0.00	0.0000	0.04
		2.02	0.25	19.46	0.00	0.0000	0.03
		2.21	0.12	21.31	0.00	0.0000	0.02
		3.04	0.00	29.31	0.00	0.0000	0.00
		15.72	0.00	151.44	0.00	0.0000	0.00
		23.60	0.00	227.25	0.00	0.0000	0.00
					sum	0.0400	1.00
					k	9.63063	
					1-X	0.04	
					X	95.94%	

Appendix DDDD. **Scaling RTD of Port 5 to the 16m location within the reactor for ethanol degradation**

Scaled to length = 16m							
Length = 16m		Theta	E(theta)	k.theta	exp(-kthe	e-ktheta.E	Integral
E((Theta/Tau)=25.90)		0.00	0.00	0.00	1.00	0.0000	
tau	25.90	0.03	0.00	0.03	0.97	0.0000	0.00
		0.07	0.02	0.07	0.93	0.0007	0.00
		0.11	1.36	0.11	0.89	0.0468	0.05
		0.15	1.86	0.15	0.86	0.0677	0.08
		0.19	1.25	0.19	0.82	0.0412	0.05
		0.22	1.37	0.22	0.80	0.0283	0.04
		0.26	1.37	0.26	0.77	0.0396	0.05
		0.34	1.30	0.34	0.71	0.0806	0.11
		0.42	1.09	0.42	0.66	0.0549	0.08
		0.50	0.90	0.50	0.61	0.0417	0.07
		0.58	0.69	0.58	0.56	0.0315	0.06
		0.66	0.57	0.66	0.52	0.0232	0.04
		0.72	0.57	0.72	0.48	0.0183	0.04
		0.78	0.49	0.78	0.46	0.0135	0.03
		0.89	0.47	0.89	0.41	0.0211	0.05
		1.02	0.27	1.02	0.36	0.0120	0.03
		1.19	0.29	1.19	0.30	0.0153	0.05
		1.39	0.37	1.39	0.25	0.0180	0.07
		1.55	0.22	1.55	0.21	0.0076	0.04
		1.65	0.30	1.65	0.19	0.0059	0.03
		1.81	0.15	1.81	0.16	0.0038	0.02
		2.48	0.00	2.48	0.08	0.0000	0.00
		12.83	0.00	12.83	0.00	0.0000	0.00
		19.26	0.00	19.26	0.00	0.0000	0.00
					sum	0.5717	1.00
					k	1.00000	
					1-X	0.04	
					X	95.94%	

Appendix EEEE. **Reactor equation comparison for ethanol degradation**

CSTR Model

N	1.89
k	0.088

Tau	Cout	Average	Delta square Function
0	0.9	0.90111	1.23625E-06
21.468	0.12117	0.17277	0.00266285
42.936	0.04682	0.17901	0.017474528
64.404	0.02494	0.0314	4.16667E-05
85.872	0.01557	0.00137	0.000201452
100	0.01205		0.020381733
150	0.00598		
200	0.00359		
215	0.00315		

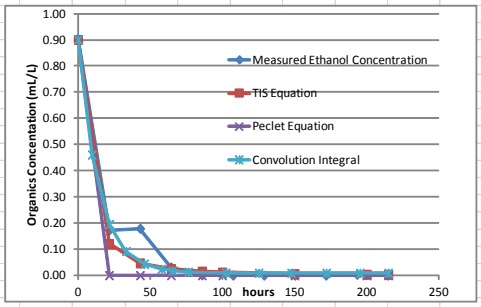
Peclet Model

q	Pe	Da	k
	2.3	0	7.85

Tau	Da	q	Cout	Average	Delta square Function
0	0	1	0.9	0.90111	1.23625E-06
21.468	168.524	17.1489	7.74205E-09	0.17277	0.029848732
42.936	337.048	24.2316	2.24642E-12	0.17901	0.032043975
64.404	505.571	29.6691	4.32308E-15	0.0314	0.000985823
85.872	674.095	34.254	2.21762E-17	0.00137	1.88442E-06
100	785	36.9624	9.84557E-19		0.06288165
150	1177.5	45.264	7.0325E-23		
200	1570	52.2631	2.24623E-26		
215	1687.75	54.1869	2.45845E-27		

Cin 0.9

Case as found



Convolution Integral

Theta	Concentration	Time
0.00	0.90	0.00
0.05	0.46	9.56
0.11	0.20	21.79
0.17	0.09	33.25
0.23	0.04	45.87
0.30	0.02	57.72
0.33	0.02	65.36
0.39	0.01	76.45
0.52	0.01	102.44
0.64	0.01	125.18
0.76	0.01	147.73
0.88	0.01	172.00
1.00	0.01	195.32
1.10	0.01	215.00
k=0.8039		

CSTR Model

N	1.42464
k	0.088

Tau	Cout	Average	Delta square Function
0	0.9	0.90111	1.23625E-06
21.468	0.19852	0.17277	0.000663171
42.936	0.09694	0.17901	0.006734793
64.404	0.06031	0.0314	0.000835902
85.872	0.04227	0.00137	0.001672647
100	0.03484		0.00990775
150	0.02054		
200	0.01398		
215	0.01268		

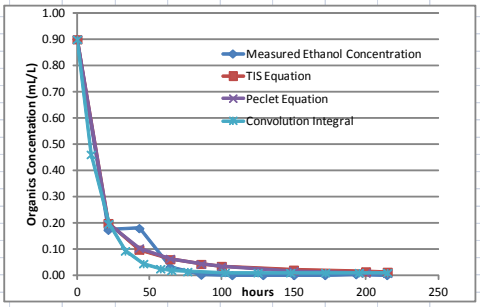
Peclet Model

q	Pe	Da	k
	0.01405	0	7.85

Tau	Da	q	Cout	Average	Delta square Function
0	0	1	0.9	0.90111	1.23625E-06
21.468	168.524	219.059	0.194566077	0.17277	0.000475162
42.936	337.048	309.795	0.102868841	0.17901	0.005797218
64.404	505.571	379.419	0.063081195	0.0314	0.001003836
85.872	674.095	438.115	0.041768776	0.00137	0.00163184
100	785	472.783	0.032741472		0.008909293
150	1177.5	579.038	0.015522928		
200	1570	668.616	0.008274159		
215	1687.75	693.235	0.006960219		

Cin 0.9

CSTR Optimised for N
Peclet Optimised for Pe
Convolution Integral
Rates as found



Convolution Integral

Theta	Concentration	Time
0.00	0.90	0.00
0.05	0.46	9.56
0.11	0.20	21.79
0.17	0.09	33.25
0.23	0.04	45.87
0.30	0.02	57.72
0.33	0.02	65.36
0.39	0.01	76.45
0.52	0.01	102.44
0.64	0.01	125.18
0.76	0.01	147.73
0.88	0.01	172.00
1.00	0.01	195.32
1.10	0.01	215.00
k=0.8039		

CSTR Model

N	0.60548
k	0.8039

Tau	Cout	Average	Delta square Function
0	0.9	0.90111	1.23625E-06
21.468	0.15505	0.17277	0.000314051
42.936	0.10363	0.17901	0.005681483
64.404	0.08154	0.0314	0.002513988
85.872	0.0687	0.00137	0.004533001
100	0.06272		0.01304376
150	0.04919		
200	0.04138		
215	0.03962		
		D	71.1854

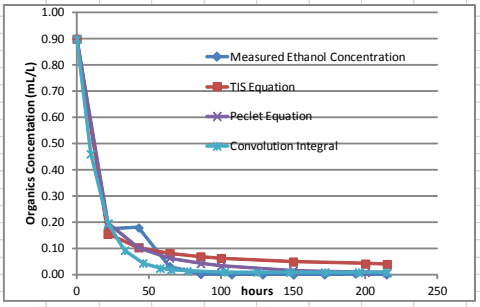
Peclet Model

q	Pe	Da	k
	0.01405	0	0.8039

Tau	Da	q	Cout	Average	Delta square Function
0	0	1	0.9	0.90111	1.23625E-06
21.468	168.524	219.059	0.19456505	0.17277	0.000475117
42.936	337.048	309.795	0.102868072	0.17901	0.005797336
64.404	505.571	379.419	0.063080617	0.0314	0.0010038
85.872	674.095	438.115	0.041768334	0.00137	0.001631804
100	785	472.783	0.032741098		0.008909293
150	1177.5	579.038	0.015522711		
200	1570	668.616	0.008274025		
215	1687.75	693.235	0.006960102		

Cin 0.9

N and Pe optimised with convolution integral k



Convolution Integral

Theta	Concentration	Time
0.00	0.90	0.00
0.05	0.46	9.56
0.11	0.20	21.79
0.17	0.09	33.25
0.23	0.04	45.87
0.30	0.02	57.72
0.33	0.02	65.36
0.39	0.01	76.45
0.52	0.01	102.44
0.64	0.01	125.18
0.76	0.01	147.73
0.88	0.01	172.00
1.00	0.01	195.32
1.10	0.01	215.00
k=0.8039		

Appendix FFFF. **Determination of potassium rate constant from RTD and scaling for various lengths**

k-Value Determination - for 1-X=0.58

kt	exp(-kt)	exp(-kt)*E*delt t)	Sum(exp(-kt)*E*dt	Real Ca/Cao	Theta	Theta Length	C of Potassium
0.00	1.00	0.00000000	0.00	1.00	0.00	0.00	92.06
0.03	0.97	0.00000000	0.00	0.97	0.05	1.96	92.06
0.07	0.93	0.00069872	0.00	0.93	0.11	4.46	92.00
0.11	0.90	0.04696292	0.05	0.94	0.17	6.81	87.68
0.15	0.86	0.06803596	0.12	0.98	0.23	9.39	81.71
0.19	0.83	0.04140598	0.16	0.99	0.30	11.81	78.33
0.21	0.81	0.02851341	0.19	0.99	0.33	13.38	76.09
0.25	0.78	0.03992323	0.23	1.00	0.39	15.65	73.06
0.33	0.72	0.08140980	0.31	1.02	0.52	20.97	67.11
0.41	0.66	0.05557006	0.36	1.03	0.64	25.62	63.38
0.48	0.62	0.04231174	0.40	1.02	0.76	30.24	60.70
0.56	0.57	0.03204233	0.44	1.01	0.88	35.21	58.75
0.64	0.53	0.02371756	0.46	0.99	1.00	39.98	57.36
0.70	0.50	0.01869055	0.48	0.98	1.10	44.01	56.29
0.76	0.47	0.01385888	0.49	0.96	1.19	47.72	55.51
0.87	0.42	0.02171717	0.51	0.94	1.36	54.38	54.30
0.99	0.37	0.01237726	0.53	0.90	1.55	61.81	53.63
1.16	0.31	0.01591323	0.54	0.86	1.82	72.60	52.78
1.34	0.26	0.01882511	0.56	0.82	2.11	84.34	51.78
1.50	0.22	0.00796570	0.57	0.79	2.35	94.08	51.37
1.60	0.20	0.00623810	0.58	0.78	2.51	100.26	51.05
1.75	0.17	0.00397365	0.58	0.75	2.74	109.77	50.85
2.41	0.09	0.00000000	0.58	0.67	3.77	151.00	50.85
12.44	0.00	0.00000000	0.58	0.58	19.51	780.22	50.85
18.67	0.00	0.00000000	0.58	0.58	29.27	1170.82	50.85
24.95	0.00	0.00000000	0.58	0.58			
	sum	0.5801514	=1-X				
k	0.0374		0.58				
	Ca=	92.060000					
	X	0.42					

Appendix GGGG. **Reactor equation comparison for ethanol degradation**

CSTR Model

N	1.89
k	0.00485

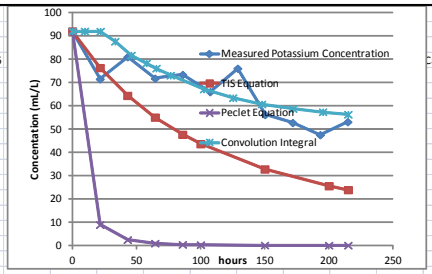
Tau	Cout	Average	Delta square Function
0	92.06	92.0584	2.49307E-06
21.468	76.34319935	71.4876	23.57653839
42.936	64.38751685	80.9795	275.2930315
64.404	55.07458134	71.7711	278.7721537
85.872	47.67423024	73.3837	660.9760235
100	43.60215688	65.9758	500.5794355
150	32.76052438	76.0721	1875.893039
200	25.55817286	56.14	935.2481512
215	23.86515208	52.7089	831.9645264
			5382.302901

Cin 92.06

Peclet Model

q	Pe	Da	k
	2.3	0	0.22

Tau	Da	q	Cout	Average	Delta square Function
0	0	1	92.06	92.0584	2.49307E-06
21.468	4.72296	3.03543	8.861308911	71.4876	3922.056291
42.936	9.44592	4.17465	2.390721483	80.9795	6176.191973
64.404	14.16888	5.06375	0.859961083	71.7711	5028.382905
85.872	18.89184	5.81854	0.361000073	73.3837	5332.312399
100	22	6.26585	0.215825223	65.9758	4324.372898
150	33	7.64142	0.044369951	76.0721	5780.216537
200	44	8.80464	0.01164476	56.14	3150.392262
215	47.3	9.12474	0.008058645	52.7089	2777.383672
					36491.30894



Case as found

Convolution Integral

Theta	Concentration	Time
0.00	92.06	0.00
0.05	92.06	9.56
0.11	92.00	21.79
0.17	87.68	33.25
0.23	81.71	45.87
0.30	78.33	57.72
0.33	76.09	65.36
0.39	73.06	76.45
0.52	67.11	102.44
0.64	63.38	125.18
0.76	60.70	147.73
0.88	58.75	172.00
1.00	57.36	195.32
1.10	56.29	215.00

k=0.0374

CSTR Model

N	0.699124844
k	0.00485

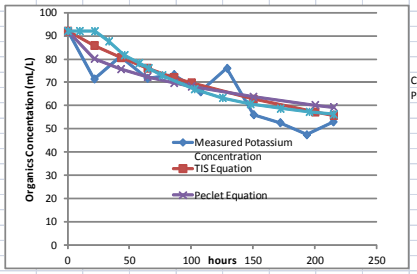
Tau	Cout	Average	Delta square Function
0	92.06	92.0584	2.49307E-06
21.468	85.90081371	71.4876	207.7398192
42.936	80.65582195	80.9795	0.104750444
64.404	76.12675797	71.7711	18.97216896
85.872	72.16990971	73.3837	1.473248537
100	69.82528877	65.9758	14.81864483
150	62.81828986	76.0721	175.6636227
200	57.30629303	56.14	1.360239423
215	55.87168946	52.7089	10.00293755
			430.1354341

Cin 92.06

Peclet Model

q	Pe	Da	k
	0.00411624	0	0.22

Tau	Da	q	Cout	Average	Delta square Function
0	0	1	92.06	92.0584	2.49307E-06
21.468	4.72296	67.7539	80.2424816	71.4876	76.64739897
42.936	9.44592	95.8132	75.73978295	80.9795	27.45435901
64.404	14.16888	117.345	72.45671534	71.7711	0.470133344
85.872	18.89184	135.497	69.79973867	73.3837	12.84466561
100	22	146.218	68.27640595	65.9758	5.292836162
150	33	179.078	63.81151564	76.0721	150.3220578
200	44	206.781	60.27504236	56.14	17.09857528
215	47.3	214.395	59.33787073	52.7089	43.94262489
					334.0726536



CSTR Optimised for N
Peclet Optimised for Pe

Rates as found

Convolution Integral

Theta	Concentration	Time
0.00	92.06	0.00
0.05	92.06	9.56
0.11	92.00	21.79
0.17	87.68	33.25
0.23	81.71	45.87
0.30	78.33	57.72
0.33	76.09	65.36
0.39	73.06	76.45
0.52	67.11	102.44
0.64	63.38	125.18
0.76	60.70	147.73
0.88	58.75	172.00
1.00	57.36	195.32
1.10	56.29	215.00

k=0.8039

CSTR Model

N	0.196372659
k	0.0374

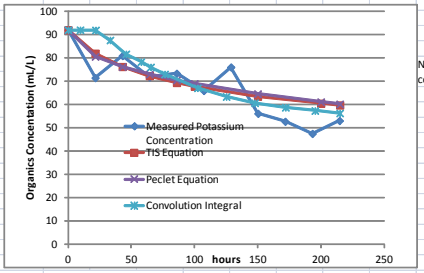
Tau	Cout	Average	Delta square Function
0	92.06	92.0584	2.49307E-06
21.468	81.99832628	71.4876	110.4747031
42.936	76.27659629	80.9795	22.11705574
64.404	72.35771692	71.7711	0.344174991
85.872	69.41388796	73.3837	15.75928227
100	67.82137347	65.9758	3.406180301
150	63.5339459	76.0721	157.2054402
200	60.50056191	56.14	19.01450018
215	59.74426185	52.7089	49.49564987
			377.8169891
		D	251.524

Cin 92.06

Peclet Model

q	Pe	Da	k
	0.003975771	0	0.0374

Tau	Da	q	Cout	Average	Delta square Function
0	0	1	92.06	92.0584	2.49307E-06
21.468	4.72296	67.7539	80.61957486	71.4876	83.39238803
42.936	9.44592	95.8132	76.24582811	80.9795	22.40740046
64.404	14.16888	117.345	73.05121286	71.7711	1.638810214
85.872	18.89184	135.497	70.46221089	73.3837	8.535006392
100	22	146.218	68.97634068	65.9758	9.00330757
150	33	179.078	64.61463249	76.0721	131.2736824
200	44	206.781	61.15251771	56.14	25.12533377
215	47.3	214.395	60.23390493	52.7089	56.62498633
					338.0009177



N and Pe Optimised with conv integral k

Convoltuion Integral

Theta	Concentration	Time
0.00	92.06	0.00
0.05	92.06	9.56
0.11	92.00	21.79
0.17	87.68	33.25
0.23	81.71	45.87
0.30	78.33	57.72
0.33	76.09	65.36
0.39	73.06	76.45
0.52	67.11	102.44
0.64	63.38	125.18
0.76	60.70	147.73
0.88	58.75	172.00
1.00	57.36	195.32
1.10	56.29	215.00

k=0.8039

Exit is only real E(t)
reaction is short term, use Et for long term to get best constant.
Long term Et for all three models, get the ks and fit data.

Appendix HHHH. **Proceedings of the 12th International Conference on Environmental Science and Technology, Rhodes, 8-10 September 2011**